Understanding Complex CI-Combustion Strategies: An Experimental Investigation

By

Antonis D. Michailidis

A Doctoral Thesis

Submitted in partial fulfilment of the

requirements for the award for

Doctor of Philosophy of Loughborough University

August 2012

LOUGHBOROUGH UNIVERSITY

Thesis Access Form

Copy No: …….. **Location:** ……...

Author: Antonis D. Michailidis

Title: Understanding Complex CI Combustion Strategies: An Experimental Investigation

Status of access: OPEN

Moratorium Period: Zero years

Conditions of access approved by……

Supervisor: R. K. Stobart

School of: Dept. of Aeronautical and Automotive Engineering

Author's Declaration: *I agree the following conditions:*

Open access work shall be made available (in the University and externally) and reproduced as necessary at the discretion of the University Librarian or Dean of School. It may also be digitized by the British Library and made freely available on the Internet to registered users of the EThOS service subject to the EThOS supply agreements.

*The statement itself shall apply to **ALL** copies including electronic copies:*

This copy has been supplied on the understanding that it is copyright material and that no quotation from the thesis may be published without proper acknowledgement.

Restricted/confidential work: All access and any photocopying shall be strictly subject to written permission from the University Dean of School and any external sponsor, if any.

Author's signature…….…….. Date……

Loughborough University

CERTIFICATE OF ORIGINALITY

This is to certify that I am responsible for the work submitted in this thesis, that the original work is my own except as specified in acknowledgments or in footnotes, and that neither the thesis nor the original work contained therein has been submitted to this or any other institution for a degree.

……

……

Abstract

Within this body of work several series of experiments will investigate the nature of complex combustion in an experimental single-cylinder engine emulating a modern passenger car size compression-ignition (CI) engine. Regimes of single, piloted single and piloted split-main injections will be tested and compared in terms of combustion characteristics, specific emission output and cyclic behaviour to determine how increased injection complexity affects the emissions and output of the modern CI engine. Through these tests, the effect of fuel-line stationary waves will be demonstrated and investigated, showing conclusively that optimised engine calibration is essential to account for injector-generated waves in any multiple injection scenario. This data will then be confirmed with a dedicated analysis using an injector rate measuring tube.

The tests will then be expanded to include examination into the behaviour of injector needle-lift standard deviation over its operating cycle, in-cylinder pressure standard deviation behaviour and trends over the combustion cycle as well as IMEP variability. Through these tests a novel method to detect start of combustion will be proposed and compared to conventional methods.

Low temperature combustion (LTC) will be tested under incremental injection complexity. Tests will be optimised for combustion phasing and injection pressure, with a view to analysis of emissions, output and cyclic behaviour to establish whether the knowledge gained about conventional combustion holds true under LTC. Optimization of engine parameters will be shown to result in easier to implement LTC regimes with superior emissions characteristics.

Finally, LTC tests will be expanded to include 30% and 50% by volume gas-to-liquid fuel (GTL) blends in order to determine whether fuel characteristics further influence emissions, output and cyclic behaviour in LTC through complex injection regimes. How GTL-blend ratio affects trends in emissions and cyclic behaviour will also be examined and compared to conventional diesel fuel.

Acknowledgements

Looking back at the time I took in researching, investigating, and writing up this body of work I can't help feeling that the creation of a thesis is more an act of tutelage and apprenticeship than outright learning. For that reason I owe my most significant acknowledgement to my supervisors, tutors and mentors: Prof. Richard Stobart and Dr. Gordon McTaggart-Cowan. You both went above and beyond the call of duty to help me. Without your support, guidance and seemingly endless patience I would have neither had the persistence nor the capability to pursue research to the degree that I did. I also would like to thank all the engineers whom I consulted throughout my work and who offered guidance even when they didn't have to: Richard Atkins, Graham Wigley, Prof. Colin Garner, Prof. Rob Thring, Ed Winward, and Jugraj Atawal.

Thanks and acknowledgements also are extended to the large network working tirelessly behind the scenes of the department of Aeronautical and Automotive department; be it the technicians that keep our labs in order (and repair them when we inevitably destroy them) or the secretarial staff that process our paperwork, there would be no research without that infrastructure.

My warmest thanks to my research group's two close colleagues and friends: Dr. Shenghui Cong and Dr. Asish Sarangi. It seems only a few days ago when we first met in a joint meeting, wondering who each other was and why we had to collaborate; the journey of discovery has been a long and interesting one, and it wouldn't have been the same without you. I look forward to working with you both in the future.

My love and thanks finally, but most significantly, go to my family: My parents Dimitri and Eleni for listening to my woes and triumphs, supporting me throughout my research, never judging me and always offering a warm bed when the holidays permitted it. My partner Katerina for putting up with my daily grind, the atypical hours a researcher keeps and the consequent experimental cooking. I wouldn't have been able to do this without you all.

Contents

List of Acronyms

ATDC = After Top Dead Centre

BTDC = Before Top Dead Centre

CA = Crank Angle

CA50 = Crank Angle at which 50% Burn occurs

CHR = Cumulative Heat Release

CI = Compression-Ignition

CO = Carbon Monoxide

CO_2 = Carbon Dioxide

DOC = Diesel Oxidation Catalyst

DPF = Diesel Particulate Filter

ECU = Engine Control Unit

EGR = Exhaust Gas Recirculation

FAME = Fatty-Acid Methyl Ester

FC = Fuel Consumption

FSN = Filter Smoke Number

F-T = Fischer-Tropsch

G30 = 30/70% GTL/Diesel Blend fuel

G50 = 50/50% GTL/Diesel Blend fuel

GTL = Gas-To-Liquid Fuel

HCCI = Homogeneous Charge Compression-Ignition

HFID = Hydrogen Flame Ionization Detection

HGV = Heavy Goods Vehicle

HR = Heat Release

HRR = Heat Release Rate

ICE = Internal Combustion Engine

ICP = In-cylinder Pressure

ICP-SD = Standard Deviation of In-cylinder Pressure

IMEP = Indicated Mean Effective Pressure

IMEP-CoV = Covariance of Indicated Mean Effective Pressure

ISFC = Indicated Specific Fuel Consumption

LNT = Lean NO_x Trap

LTC = Low Temperature Combustion

NL = Needle Lift

NL-SD = Standard Deviation of Needle Lift

NO_x = Oxides of Nitrogen

NVH = Noise-Vibration-Harshness

PM = Particulate Matter

PSOI = Pilot Start of Injection

RME = Rapeseed Methyl Ester

RPM = Revolutions Per Minute

SCR = Selective Catalytic Reduction

SI = Spark Ignition

SoC = Start of Combustion

SOF = Soluble Organic Fraction

SOI = Start of Injection

TDC = Top Dead Centre

THC =Total Hydro-Carbons

$\Delta P/\Delta \Theta$ = Rate of Change of Pressure Over Crank Angle

List of Figures

List of Tables

List of Equations

1 Introduction

1.1 Background of modern compression-ignition engines

Internal combustion engines (ICE) have been central to global economic growth for over a century. Nowhere is this more obvious than in their application to on-road transportation, where they are the nearly exclusive provider of motive power for everything from personal transportation to goods movement, from motorcycles to HGVs and earth-moving machinery. The growing number of ICEs used in transportation around the world is leading to increasing demand for the raw materials used to fuel these engines as well as increasing the impact of their emissions on their surroundings. As a result, governments and regulators around the world are imposing ever more stringent regulations on fuel consumption and emissions from all sizes of vehicles (AVL 2007, Delphi 2010). To address these concerns, new fuels and new modes of combustion are being developed. This thesis investigates several aspects of these considerations, including the use of new, non-crude oil based fuels, and their application to combustion techniques designed to dramatically reduce emissions without impairing efficiency.

The modern diesel engine is a forerunner of combustion technology. Not only is the level of control over its operation superior to that of spark-ignition engines but it is also arguably more apt to making gains in both efficiency and emission cleanliness (Heywood 1988, Stone 1999).

In the last decade between 40% and 51% of all new car sales within the European Union have been running diesel engines and commercial vehicles, heavy goods vehicles and earth-moving machinery are almost exclusively powered by diesel combustion. There are numerous reasons that have resulted in this level of dominance of compression-ignition (CI) engines: not necessitating running at a specific ratio of fuel to air, the diesel engine is not equipped with a restriction in the air intake, meaning a significant saving on pumping losses which is magnified at low load when less air ingested would be desirable in a SI engine. As a consequence of

this relatively leaner combustion, diesel engines generally tend to emit fewer unburnt hydrocarbons (tHC) and carbon monoxide (CO), both of which are often associated with incomplete combustion. SI engines on the other hand have to resort to very tight control over their combustion process and three-way catalysts in order to achieve similar results.

Having significantly higher torque at low engine speeds compared to equivalent size petrol engines also makes diesel the natural choice for any high-torque application. Exceptional efficiency as a generator is one of the most fundamental reasons they are indispensable to earth-moving machinery and off-highway vehicles as their power-train often serves a dual role as both transportation and generator.

Current automotive research is mostly driven by emissions regulations, more so than it ever has been in the past (Johnson 2011). Highly stringent regulation on both oxides of Nitrogen (NO_x) and particulate matter (PM) both have become rising challenges to be addressed by compression-ignition engines. Reducing these emissions to near-zero levels has been proven possible under low-temperature combustion (LTC) conditions (Ogawa et al. 2007). Being able to transverse from conventional diesel combustion into LTC for even brief periods of time would dramatically improve an engine's overall output in an emissions test, potentially negating or at least drastically reducing the need for weight-intensive after-treatment systems like urea catalysts, lean-NO_x traps (LNT) and de-NO_x-ifiers. All these devices are highly complex and expensive, often requiring very specific maintenance regimes and a lot of space to function correctly (Johnson, 2011).

1.2 Modern diesel after-treatment methods

Several devices are commonly used to reduce diesel-engine emissions, sometimes in tandem. Most commonly, diesel particulate filters (DPF), which trap carbonaceous deposits from the exhaust and oxidise them later-on into carbon dioxide (CO_2) Selective catalytic reduction (SCR) devices which use a chemical (most commonly urea) to convert NO_x emissions into molecular nitrogen plus oxygen. And lean-NO_x

traps (LNT), which also reduce NO_x emissions, but not in as efficient a manner as SCRs, but have a higher ease of implementation.

Though significant progress has and is still being made in the efficiency, operating envelope and affordability of all these devices, it is preferable not to generate the harmful emissions in the first place than to rely on expensive and cumbersome after-treatment devices to clean the engine-out emissions.

1.3 Evolution of modern injection regimes

Since diesel combustion evolved past mechanically driven injection into high pressure fuel rail injection there has been a marked change in the development and understanding of the combustion event. As control machinery has continued to develop over the years it has become increasingly popular to inject multiple times per engine cycle in order to more tightly control the combustion event and subsequent emissions. Commonly the type of injection regime will alter several times as the load and engine speed changes, with up to two pilots helping control exact start of combustion points and one or more post-injections in order to limit smoke in the exhaust emissions by promoting soot oxidation late in the cycle. Thanks to the modern need for downsizing, higher specific output has caused rate of pressure rise to increase to levels which would be unacceptable from a noise/vibration/harshness (NVH) perspective. Separating the main injection into two or more smaller, pulsed injections helps keep the overall fuel quantity delivered high but reduces the rate of pressure rise as it prolongs the combustion duration and minimizes the amount of fuel combusted in diffusion burning as opposed to premixed burning.

1.4 Alternative fuels

As part of the current trend in sustainability and energy security alternative fuels have been very high on the priority list of every research institute in the last few decades. Being naturally more tolerant of variations in fuel composition and physical as well as chemical characteristics the diesel engine has proven to be an ideal starting point to investigate whether the future lies in a new fuel. Not taking into

account gas-fuelled CI engines, alternative fuels to diesel can be said to fall into two broad categories based on provenance: First and Second generation bio-fuels. First generation bio-fuels are deemed those derived from sources such as starch, sugar, animal fats or vegetable oil. While they definitely are of a more environmentally friendly source than petroleum-derived conventional diesel, there are significant moral and ethical issues undermining their validity as wide-spread alternatives to diesel: It can be shown that in order to generate a significant enough volume of crop to supplant fossil-fuel such vast areas of land need to be cultivated. Given the volume of land, the cost would have to be such that the only economically feasible locations for this to occur are third world countries and the Amazon delta. Both of these choices carry significant ecological, sociological and moral implications (National Geographic October 2007). There is also consideration about tying food prices to fuel/energy prices, thus potentially impoverishing under-developed countries further. Many crops are ill-suited to ecologically produce bio-fuel; corn and corn maize have both been shown to be of very small net energy benefit when accounting for fertilization and the energy requirement to germinate them. Finally crop-based fuels introduce the fluctuating factor of weather to energy prices, a volatility from which no economy will benefit. Current sugar-cane farms in Argentina and Brazil which are harvested for Bio-diesel generation have been reported by National Geographic (October 2007) to be torched before harvesting in order to purge them of venomous snakes and vegetation in order to facilitate the harvesting process, still done by hand. It was demonstrated that a brush-fire of those proportions generated a larger volume of CO_2 to the total amount generated by the combustion of the fuel itself, effectively more than doubling the fuel's carbon footprint.

Second generation bio-fuels are manufactured from lignocellulosic crops. Their implementation has several advantages when compared with first generation bio-fuels, mostly related to their reduced dependency on food crops and lower dependence on subsidies which are not commercially as competitive as conventional fossil fuels (DEPD 2010)

Several methods exist to manufacture second generation bio-fuel, the primary being gasification of feedstock, organic matter/waste or even crude oil. Gasification usually results in an intermediate product which is then further used to synthesize gas-to-liquid fuel via the Fischer-Tropsch method. Pyrolysis is also capable of breaking down organic matter into bio-fuel. Aside from GTL, other second generation bio-fuels include synthetic di-methyl ester, bio-methanol and others.

1.5 Project aim

Broadly, the aim of the project is to further the understanding of advanced compression-ignition combustion. Utilising the understanding gained in previous projects in advanced combustion the research's goal is to better the scientific interpretation and overall understanding of the in-cylinder conditions during modern, technically complex (in both physical and chemical terms) combustion. With this in mind, the following research objectives were designed:

1.6 Research objectives

The overall goal of this body of work is to establish a better understanding of the workings of complex compression-ignition combustion regimes. To question certain aspects of combustion that are traditionally taken for granted (such as cyclic variability, and the ease of implementation of multiple injection strategies) and review them with a critical eye from the viewpoint of advanced complex combustion. To determine how a more complete understanding of the combustion process can lead to optimization of advanced combustion modes in terms of output and emissions, and in what ways that optimization differs between modes. In more detail, several factors will be investigated:

- How is injector behaviour affected by the implementation of complex injection strategies? How accurately are injectors performing the operations requested of them? How do closely-spaced injection events affect each other?

- How do modern complex injection strategies affect repeatability and the combustion stability of the diesel engine? Is there knowledge within the cyclic behaviour of in-cylinder pressure? Does cyclic behaviour change with incremental injection complexity? Even if the cyclic variability of IMEP remains acceptable, can more information be gained from the cyclic behaviour of in-cylinder pressure?

- How can conventional combustion be optimised in terms of emissions, output and stability via finely-tuned injection regimes and parameters?

- How does the implementation of low-temperature combustion (LTC) respond to injection regime optimization and fine control? Do LTC regimes behave differently in terms of cyclic behaviour and emission/output optimization? How can complex injection strategies simplify and optimize the implementation of LTC?

- Does the substitution of diesel with gas-to-liquid (GTL) fuel blends alter the nature of LTC? Does the knowledge gained in previous chapters about LTC hold throughout a high percentage of fuel substitution? Can an increase in GTL blend ratio simplify the implementation of LTC?

1.7 Research contributions

Several aspects of the research are novel: Firstly, the existence fuel-line resonance is proven and demonstrated. Secondly, with accurate control over it subsequent tests of single, piloted single and piloted split-main injection are evaluated in terms of emissions, output and combustion stability on a crank-angle basis. A novel marker for start of combustion is identified and compared with conventional markers. Tightly controlled low-temperature combustion is examined with three injection regimes (single injection and two types of 50-50 split injection) and evaluated in terms of emissions, stability and combustion behaviour with a novel approach. This knowledge is then expanded to include gas-to-liquid/diesel blends under similar low-

temperature combustion conditions, and the effect of fuel characteristics examined to determine how the fuel composition affects the behaviour observed in diesel.

1.8 Thesis structure

In the following chapter (2) a comprehensive investigation of the surrounding knowledge pertaining to the work within will be investigated. Particular emphasis will be given to diesel engine emissions, their formation and their characteristics, modern diesel engine architecture and after-treatment systems, as well as multiple injection strategies and their implementation. Some discussion will also cover alternative fuels and advanced combustion regimes.

Chapter 3 will cover the majority of methods and the setup used in carrying out the experiments discussed, as well as analysing the resultant data. All equipment used in data gathering or experimentation will be documented, as will any analytical tools.

Chapter 4,

Injection Complexity and Resonance begins by covering a specific series of experiments designed to conclusively prove the existence and behaviour of fuel-line resonance arising from large fuel injection events. Two series of experiments are covered in this chapter, one in-engine and one on a purpose-built injector flow-rig. Following those experiments, in 4.4 conventional diesel combustion will be examined under three increasingly complex injection regimes to determine behavioural differences between single, piloted single and piloted split-main combustion. This series of experiments will look into emissions, fuel efficiency, mean-effective pressure variability as well as atypical factors such as the standard-deviation of injector needle-lift, the cyclic behaviour of in-cylinder pressure on a crank-angle basis.

Through this research a potentially novel method of determining start of combustion will arise, and will be investigated further in chapter 5. Current accepted start of combustion tools will be examined and compared to the novel method suggested, through a series of experiments designed to highlight the differences in implementation and ease of use of each method presented.

Capitalising on the knowledge gained, Chapter 6 will analyse a similar series of tests to chapter 4. In this instance incremental injection complexity under low-temperature combustion will be examined so as to compare the behavioural differences between the two combustion types. One series of single and two types of split injection will be investigated, once again focusing on emissions, efficiency and cyclic behaviour of in-cylinder pressure. The tests will then be replicated in chapter 7 using two new fuels, 30% and 50% by volume gas-to-liquid/diesel blends. In this chapter the emphasis of investigation will be with a view to determine how behavioural patterns observed in the preceding chapter change with an increasing blend ratio of gas-to-liquid fuel.

The work will then finalise with a conclusions chapter (8) summarising the knowledge gained through the experiments performed and suggesting future avenues of research arising from this work.

References used throughout the work and an appendix with any data and graphs from experiments too extensive to include in the main body will be attached at the end.

1.9 Publications arising from this Research

A. D. Michailidis, R. K. Stobart, G. P. McTaggart-Cowan, “Fuel Line Stationary Waves and Variability in CI Combustion During Complex Injection Strategies”, Proceedings of the ASME 2010 International Combustion Engine Division Fall Technical Conference ICEF201-35069, 2010

A. D. Michailidis, R. K. Stobart, G. P. McTaggart-Cowan, “Low Temperature Combustion (LTC) Optimization and Cycle-By-Cycle Variability Through Injection Optimization and Gas-To-Liquid (GTL) Fuel-Blend Ratio”, Proceedings of the ASME 2012 International Combustion Engine Division Fall Technical Conference ICEF2012-92060, 2012

2 Literature Review

In view of the complexities faced by ever-more stringent emissions regulations, tied to the necessity of increased fuel efficiency a more complete understanding of the workings of compression-ignition is in order. In this chapter the author will endeavour to introduce the current state of knowledge on low-temperature combustion (LTC), complex injection strategies, and determination of start-of-combustion (SoC).

2.1 Conventional compression-ignition combustion

The four-stroke compression-ignition engine has a combustion cycle characterized by three distinct phases (Kuo 2005. Heywood 1988.) As soon as fuel begins to be delivered into the combustion chamber, the ignition delay starts; during this phase the fuel expands rapidly and atomizes thanks to its very high pressure and disperses within the combustion chamber. Ambient air flow causes it to spin and tumble within the chamber. Local temperatures, oxygen concentration, fuel droplet size as well as fuel physical and chemical characteristics combine with chamber geometry and air motion to determine when this phase ends and the next phase begins: That of premixed combustion. During premixed combustion the highest rate of heat-release is observed as the reaction speed is quite fast. After it is over, the combustion settles into the third, and final phase commences: Mixing-controlled combustion. According to Hsu (2002) this phase is divided into two distinct periods: Diffusion burning and post-burning. Diffusion burning occurs when the injector delivers fuel into the already combusting flame mass of volatile gasses left from the premixed combustion. Post-burning occurs slightly later, nearer the end of the fuel injection. By the time post-burning settles in the engine's cycle is significantly past top-dead centre and therefore the cylinder volume is starting to rapidly expand. The expansion leads to a gradually reduced cylinder pressure and this contributes to a significantly lower combustion rate. It has been suggested that during this phase the low local and mean temperature is the main contributor of bulk quenching (Han et al. 2009. Mendez et al. 2009). The low rate of heat release during this phase also may lead to

reduced local temperatures, which may be too low to oxidize CO, tHC and PM, resulting in higher emissions than would be otherwise observed.

2.2 Compression-ignition combustion emissions

The health and environmental impacts of diesel exhaust are well known; in fact, the California Air Resources Board has classified diesel exhaust as an 'air toxic' because of its substantial health implications. In most jurisdictions with some form of clean-air laws, specific species in the exhaust gases from a compression-ignition engine are regulated. The most significant of compression-ignition engine's regulated engine-out emissions are the following:

- Oxides of Nitrogen, mostly comprising NO and NO_2, referred to as NO_x.
- Particulate Matter (PM), which constitutes primarily carbonaceous particles of various sizes, some of which have adsorbed organic molecules they have come into contact with during the combustion process. Some PM may also be formed by volatile species that condense in the post-combustion environment.
- Carbon Dioxide (CO_2), a natural product of any combustion, CO_2 emissions from compression-ignition are significant and will be the focus of engine research in the future thanks to highly stringent emissions targets with a view to minimizing global warming.
- Carbon Monoxide (CO), a by-product of incomplete combustion. CO is in general terms less of a problem in compression-ignition thanks to a frequent abundance of oxygen, particularly when running at low load. It becomes increasingly more problematic, however, at certain oxygen-starved conditions.
- Unburnt Hydrocarbons, referred to as "total hydrocarbons" (tHC), mostly comprising of partially-burnt or unburnt fuel, tHC only become a serious problem when very low fuel-efficiency is observed. Some portion of tHC may also be contributed by lubricating oil which has found its way into the combustion chamber and taken part in the ensuing combustion. tHC is unique

as an emission as it is not a specific chemical species but rather made up of a wide range of chemical species.

- Combustion Noise, commonly referred to as part of the “noise-vibration-harshness” triumvirate (NVH), noise is generally correlated with high rates of pressure rise within the cylinder. Noise is directly and indirectly a pollutant, directly as it contributes to ambient noise levels and indirectly as increased noise signifies increased internal stress on the engine components, which in turn mandates stronger, heavier structures which make for worse fuel economy. Noise will become a serious point of research in compression-ignition in the future thanks to downsizing mandating higher peak pressures.

2.2.1 Carbon Dioxide (CO_2)

CO_2 is a product of the combustion of organic matter and has been identified as one of the major contributors of climate change (IPCC, 2007). In the EU road-going transport accounts for approximately a quarter of the man-made CO_2 emissions, and in a bid to limit its effect on the earth’s climate the European Parliament has set a fleet average target of 120 g/km and 95 g/km by 2015 and 2020 respectively to automotive manufacturers (EU, 2009).

As a natural product of combustion, CO_2 is intrinsically linked with fuel consumption for the majority of conventional fuels, so any targets attempting to limit CO_2 production are tantamount to an increase in fuel efficiency. Due to certain design characteristics the compression-ignition engine is naturally higher in efficiency to an equivalent spark-ignition unit; the lack of pumping losses due to low-load intake throttling and higher thermodynamic efficiency thanks to increased compression ratio naturally grant it lower fuel consumption for similar or better tractive capability. This puts compression-ignition at an advantageous position in the effort to reduce automotive CO_2 output. Johnson (2011) claims the diesel engine is at a 20% advantage compared to a petrol equivalent engine in terms of CO_2.

2.2.2 Nitrous Oxides (NO_x)

NO_x formation is a very heavily researched area of combustion chemistry. Understanding NO_x formation mechanisms gives fundamental insight into the workings of the combustion of energetic materials, as nitrogen is universally present in such materials. The first mechanism to produce NO_x was identified by Zel'Dovich (1946) and is named after him. The Zel'Dovich mechanism is the predominant method of NO_x production and is considered the de-facto "thermal" mechanism due to its requirement of a high activation temperature (Kuo, 2005). There is also the Prompt NO_x mechanism, discovered by Fenimore (also named after him) which accounts for oxides formed at the front of the combustion. The Fenimore mechanism conventionally produces less NO_x than the Zel'Dovich mechanism but remains a significant percentage of overall generation.

2.2.2.1 The Zel'Dovich NO_x formation mechanism

The Zel'Dovich formation mechanism accounts for the majority of nitrous-oxide formation during combustion and has three principal reactions:

- $N_2 + O \leftrightarrow NO + N$
- $N + O_2 \leftrightarrow NO + N$
- $N + OH \leftrightarrow NO + H$

The first two reactions are complementary, in that they are considered to be of a chain nature, such that their sum is essentially:

- $N_2 + O_2 \leftrightarrow 2NO$

Key in understanding this mechanism is the observation that the first reaction is the determinant in this mechanism: The activation energy required to dissociate the nitrogen molecule is 946 kJ/mol (Heywood, 1988) thanks to its triple bond. It is generally accepted that the prevalence of the Zel'Dovich mechanism of NO production does not come into effect below temperatures of 1800 K, and even so the

reverse reaction does not majorly affect the outcome as its rate of propagation is very slow.

While this mechanism is coupled to the chemistry of the fuel combustion, the rate of its reactions (in particularly the first) is very slow in comparison. Zel'Dovich therefore suggested the NO formation reactions can be considered uncoupled from the oxidation of the fuel.

Practically, the determining factors in this mechanism are the ambient temperature and the concentration of oxygen, as well as the time the high-temperature environment remains. It is commonly held that these conditions are prime in the post-flame gases (Kitamura et al., 2005). When post-flame gases reach an equivalence ratio of between 0.8 and 1.0 peak combustion temperature is observed, and therefore highest NO thermal formation rate.

2.2.2.2 The Prompt (Fenimore) NO_x formation mechanism

Observations made by Fenimore (1970, 1979) and Miller & Bowman (1989) noted that a portion of NO was formed in the flame zone of laminar premixed flames at a time that preceded the slow thermal mechanism outlined by Zel'Dovich. It is understood that these oxides are mostly formed when various hydrocarbon radicals (CH, CH_2, C_2, C_2H, C) react with molecular nitrogen, within hydrocarbon flames and form amines or hydrocyanic acid (HCN). Subsequently, these reagents form NO. It follows that the Fenimore mechanism is only relevant to hydrocarbon fuels such as diesel and become increasingly more prevalent at conditions with higher fuelling (or more specifically, lower air-to-fuel ratios), as they are less likely to produce the high-temperature environment that the Zel'Dovich mechanism requires to initiate.

By association, the Prompt NO formation mechanism is the prevalent method of NO production during low-temperature combustion: Firstly, by its very definition LTC is at low temperature (< 2000 K) and therefore does not initiate significant NO formation via the Zel'Dovich mechanism. Secondly, LTC is characterized by a low abundance of oxygen, which in turn means a higher air-to-fuel ratio, burdened further by the low

specific fuel efficiency. The overly rich and relatively cold combustion environment makes the Prompt NO formation mechanism much favoured compared to the Zel'Dovich mechanism during LTC (Kuo, 2005).

2.2.2.3 NO production from fuel-bound nitrogen

Kuo suggests there may be a further source of NO from nitrogen atoms bound in the fuel. Obviously the prevalence of this effect is dependent primarily on the level of nitrogen compounds in the fuel as well as the local combustion environment (air-to-fuel ratio, temperature, fuel atomization, pressure). The onset of this reaction begins with the rapid conversion of the fuel's nitrogen compounds to ammonia and hydrogen cyanide (NH_3 and HCN), Fuel-rich conditions enhance the conversion of these molecules into NO. It should be noted, however, that conventional Type-2 diesel will contain insignificant amounts of nitrogen compounds and therefore NO production from this mechanism can be ignored when combusting diesel or near-zero nitrogen fuels.

2.2.3 The nitrous oxides – particulate matter (NO_x-PM) balance

Almost universally NO_x and smoke generation in compression-ignition combustion are opposed. In broad terms, when thermodynamic efficiency increases smoke generation drops, but correspondingly peak temperature rises and with it NO_x generation. Any alteration in operating conditions which results in lower cylinder temperature, like late injection or EGR has a negative effect on the late-cycle oxidation of particulate matter. Conversely, PM can be reduced by implementing early injection, which promotes a higher percentage of premixed combustion and a longer oxidation later in the cycle.

High local equivalence ratio is known to be correlated with increased smoke due to the increase in local rich pockets of fuel within the cylinder. The easiest way to control this is with increased injection pressure; fuel pressurised higher atomises better when sprayed, maximizing the surface area of the fuel in contact with air and therefore oxygen, minimizing local rich pockets and reducing smoke generation.

Higher atomization however may result in faster, more violent combustion which in turn increases NO_x generation (Fang et al., 2010, Fischer et al. 2009, Lee et al., 2004). It may also increase spray penetration and result in increased wall-wetting and increased local equivalence in subsequent cycles when the wet fuel is scraped-off the wall by the piston ring.

Conventional diesel combustion has long been known to demonstrate a consistent trade-off between NO_x and PM over a wide range of parameters, including EGR and injection timing (the two key levers for controlling engine-out NO_x).

2.2.4 Hydrocarbons and Carbon Monoxide (tHC and CO)

Total hydrocarbons (tHC) are a by-product of incomplete combustion due to local flame extinction in the fuel during combustion. They are composed mostly of either partially reacted hydrocarbon oxide species or volatile components of the fuel which did not participate in the combustion process. Warnatz et al. (1999) suggests two mechanisms of formation of tHC: Flame extinction by strain and flame extinction at the walls or crevices. Within compression-ignition engines, bulk quenching and wall quenching are the primary sources of tHC emissions (Mendez et al., 2009). These effects are exacerbated by poor air-to-fuel mixing which enforces quenching effects: Localized under-mixing results in fuel-rich pockets within the combustion chamber which when met with the flame are oxygen-starved, leading to excessive tHC generation. Over-mixing doesn't improve tHC formation either; excessive air-to-fuel mixing may result in an overly-stratified charge with an overall lean ratio that may be leaner than necessary. Consequently, over-mixed charges may suffer from early flame-propagation termination (Heywood 1988, Mendez et al., 2009).

In high equivalence ratio combustion regimes, it is frequently common to advance the injection events significantly in order to benefit from additional mixing in order to maximise oxygen utilisation. With earlier injection phasing comes greater spray-penetration, however. Fuel spray approaching the cylinder walls risks cooling due to proximity and may be sufficient to quench subsequent combustion before it has had time to complete. Decreased global temperatures enhance this effect and make late-

cycle oxidation even less likely. Parts of the spray that do actually reach the wall and find their way into the crevice volume also account for high tHC and CO emissions (Heywood, 1988, Ekoto et al., 2009)

CO is largely, like tHC, a by-product of incomplete combustion. Control of CO emissions in internal combustion is primarily done by the fuel-air equivalence ratio. Under conventional compression-ignition, CO emissions are trivial, as the mixture is always fuel-lean, and the CO will normally be nearly fully oxidized in the post-combustion gases. However, under certain specific combustion regimes, especially those with high equivalence ratios (like high-EGR LTC or HCCI) there may not be sufficient free oxygen, or a sufficiently high temperature to fully oxidize CO into CO_2 leading to significant CO emissions.

Koci et al. (2009) suggest a small amount of fuel in the sac volume of the injector nozzle is a potential source of partially oxidized fuel. He claims the oxidation rate in this specific part of the injector charge is low as it leaves the injector late in the combustion process during the expansion stroke. Low ambient oxygen and ever-decreasing temperature make complete oxidation of this segment of the fuel charge a particularly strong source of tHC and CO (Ekoto et al., 2009 and Mendez et al., 2009). This does depend on the volume of fluid contained in the nozzle sac; modern injection systems tend to minimize this volume to avoid this source of emissions.

Specifically in low temperature combustion, Musculus et al. (2007) suggests that unburnt hydrocarbons are generated a few millimetres downstream of the injector. He demonstrates that shortly after the end of injection the area immediately after the injector tip has a particularly high equivalence ratio. This is due to the end of injection region being exceptionally poor in oxygen content, resulting in particularly high equivalence ratios and a much higher likelihood of partial combustion. Early onset of combustion in this region, either shortly before the end of injection or immediately after it, results in incomplete combustion and resultant increase in total hydrocarbon emissions.

2.2.5 Engine Noise

Engine noise is an increasingly critical limiting factor of engine design; there are three principal sources of engine noise: gear-train noise, the various types of piston slap and combustion noise (Kanda et al. 1990, Heywood 1988), with gear-train accounting for less than 20% of the overall noise and slap plus combustion making up the rest. As the first two types of noise generations mostly relate to the physical design of the engine this body of work will not focus on their behaviour.

Combustion noise is a significant part of the overall vehicle noise-vibration-harshness (NVH) according to Costa et al. (2009). The structure of modern CI engines is such that their low attenuation coefficient to high-frequency vibrations encourages the radiation of high-frequency noise produced during the combustion (Ge-qun et al. 2005). Compression-ignition engines naturally generate a higher amount of combustion noise than spark-ignition due to their higher compression ratios and consequent higher rate of pressure rise when combustion commences. The highest rate of pressure rise is what generates “diesel knock”, an audible sound that is generated by a strong excitation which causes the cylinder charge to oscillate. Designing engines which can withstand such forces is a significant design constraint for modern diesel engines (Yun et al. 2008).

The rate of pressure rise during the start of compression-ignition combustion as well as the peak pressure reached during the combustion cycle may be controlled via modulation of the fuel mixing through adjustment of the ignition delay (Heywood, 1988). The implementation of complex injection regimes such as pilot injection and late-cycle injection can also alleviate engine noise, reducing ignition delay and promoting smoother running with reduced combustion noise (Badami et al., 2003).

2.3 Modern engine architecture

2.3.1 Exhaust-gas recirculation

Exhaust-gas recirculation (EGR) is a method employed to help control emissions of NO_x. EGR can be effected in multiple ways, including internally (by using novel valve design to ensure a specific amount of exhaust is retained after the exhaust stroke is over) or most commonly in compression-ignition, with an external recirculation circuit. External EGR most commonly draws exhaust gas from the exhaust upstream of any after-treatment devices installed and channels it back to the intake. Most modern compression-ignition engines will introduce a heat-exchanger to lower the temperature of the EGR before it is delivered (Heywood 1988, Stone 2005, Van Basshuysen et al. 2004).

The introduction of EGR to the combustion chamber lowers local temperatures as well as slowing the combustion's rate because it replaces oxygen-rich air with oxygen-poor exhaust-gas. Work by Ladomatos et al. (2000) used an optical engine to prove the adiabatic flame temperature dropped due to the reduced oxygen concentration in the trapped charge. They also noted there is an additional small cooling effect as the increase in carbon dioxide and water in the cylinder means a lower in-cylinder temperature after the compression stroke (as CO_2 requires more energy to be compressed). The consequent advent of low localized temperatures results in reduced NO_x emissions and was the main reason EGR was adopted en masse to begin with, albeit at the expense of PM which increased due to the only partial oxidation of the particulates in the latter stages of post-burning. Recently it has been shown that in excessively high substitution rates of above 50% this increase in PM can be reversed as the combustion shifts from conventional to low-temperature combustion, who's low temperature and excessive ignition delay period enable near-zero PM and NO_x.

Ladommatos et al. (2000) extensively examined EGR systems; in CI engines, implementing EGR causes an adverse effect called thermal throttling whereby the low-density, hot exhaust gas displaces high-density cool air in the cylinder, causing a

drop in volumetric efficiency. This is in addition to the reduced volumetric efficiency accounted for by the reduced concentration of oxygen (*the dilution effect*). In addition, the existence of water vapour and carbon dioxide in the exhaust causes a so-called *chemical effect*, as the dissociation of these two species at high temperature generates reactants that can take part in both NO_x and PM oxidation mechanisms. As a consequence of the CO_2 and H_2O concentration in EGR the engine's inlet charge specific heat capacity rises marginally; this effect is named the *thermal effect*. Finally, by supplementing hot exhaust gas to the cool inlet air the inlet charge temperature increases. Aside from the thermal throttling mentioned previously, this also raises the cylinder gas temperature at the end of the compression and subsequently during the combustion. This is known as the *inlet temperature effect*.

2.3.2 Development of fuel supply systems in compression-ignition

Compression-ignition fuel supply has a more complex arrangement than spark ignition; several mechanical setups are available including the vane-type supply pump, the tandem fuel pump and the locking-vane pump. Most of these are either driven by the drive shaft or the camshaft. Largely they operate by drawing fuel from the tank, compressing it to a suitable pressure and delivering it to the injector via some form of governor to provide control over pressure and quantity delivered. Invariably all mechanical fuel supply systems have a return line back to the fuel tank.

An inherent drawback of mechanical pump-driven fuel supply is inconsistent pump output; the pump-line nozzle system was developed to cater for this. Instead of one pump feeding all the injectors, the pump-line system has one smaller pump per injector so as to ensure more consistent quantity delivered per injector.

Subsequent development introduced electronic control and the implementation of the unit injector where the fuel filter fed into a tandem pump which is controlled by a control unit. The unit injector system also allowed for fine adjustments to cater for varying fuel temperature (Bosch Automotive Handbook, p.607-612, 8th ed. 2011). However, injection pressures were still limited by the need to compress the fuel

within the injector body, leading to significant pressure variations over the duration of the injection event.

2.3.3 Modern injection systems and ancillaries

Modern compression-ignition engines have a lot more flexibility than their older mechanically-driven pump predecessors; powerful engine control units (ECUs) can command several injections per engine cycle for each cylinder at exacting pressures at very specific timings. The development and understanding of complex combustion models would not be possible were it not for high-pressure fuel rail injection systems and their controllers.

Current compression-ignition engines almost exclusively run common rail fuel delivery systems. In the common rail, after the low-pressure pump has drawn fuel through the tank and fuel filter it is then piped to a high-pressure pump which will compress it to a much higher pressure. The fuel is then fed into a common rail from which all the engine's injectors draw. (Bosch Automotive Handbook, p.606, 8th ed. 2011). Rail pressures exceeding 2000 bar are being researched for their potential emissions and performance-enhancing capabilities (Ganser, 2000).

This system enables much higher pressure fuel to be delivered to the cylinder, which in turn causes better atomization, thereby maximizing the surface area of the fuel in contact with air (Deng, 2010, Nishida, 1990). Fuel rail arrangements also enable a wider spectrum of operating pressure. This is primarily because the operation of pressurizing the fuel and that of delivering it is performed by two separate systems: the pump and the injector. The rail performs the role of pressure accumulator (Bosch Automotive Handbook, 8th ed. p.612, 2011).

Two types of injector are used in fuel-rail setups: Solenoid-valve injectors and piezo-inline injectors. In solenoid-valve injectors a complex hydraulic arrangement enables fine control of the injector output: the injector open command lifts a solenoid-actuated plunger which in turn causes a small drain of fuel to the return pipeline from a valve-control chamber. This in turn generates a pressure differential between it and

the injector nozzle chamber and a subsequent force lifting the injector needle. The fuel quantity delivered is proportional to the length of time the injector is opened. The response of the injector depends on the hydraulic system and the actuator, and tends to be slower than equivalent piezo-based actuators; however large needle lifts are achievable with relatively small actuators. In a piezo-inline injector a servo valve controlled by a piezo actuator directly lifts the needle and enables fuel flow out of the injector. Piezo injectors are naturally more hydraulically efficient than solenoid injectors as there are no leak points between high and low pressure circuits. They also actuate faster and have the ability to open and hold a specific height of needle-lift, though they are substantially more expensive and require a much higher driving voltage. (Skiba, 2012, Smith, 2011, Bosch Automotive Handbook, 8th ed. p.616-620). As well, to achieve high lifts, either a displacement amplifier is needed or a large piezo stack must be used, adding to the cost and complexity of the system.

Work carried out by Skiba and Melbert (2012) suggests both solenoid and piezo type injectors offer comparable derivation in the quantity of fuel they deliver in linear operation, though solenoid injectors improve with increased fuel temperatures. Likewise piezo injectors seem unaffected by variance in temperature. The authors propose a closed-loop control system to adjust solenoid injector delivery deviance to below 1 mg, effectively matching the accuracy of piezo injectors at a fraction of the component cost.

Zhong et al. (2000) compiled a study on cycle-to-cycle repeatability of injector performance in a fuel-rail system, concluding that there was significant variation in cyclic performance of the injector's fuel delivery. Running a fuel rail at pressures of 600, 800 and 1000 bar and engine speeds of 1500 and 2000 RPM up to 23% variances in fuel delivery cycle by cycle were recorded, and attributed to variations in injection pressure in the injector's pressure chamber up to 9%.

Chen et al. (2000), Mizuno et al. (2001, 2002) suggest that large injection events set in motion a stationary wave within the fuel line that reaches the fuel rail. Huhtala and Vilenius (2001) note that specific injection settings may generate self-amplifying oscillations within the fuel rail depending on fuel line length. They also note the wave

effect is diminished when the supply line of the fuel rail is situated at the end of the rail and the injector in the middle, compared to a setup with the supply line in the middle and the injector at the end of the rail. This suggests that positioning of both supply line and fuel lines is significant in diminishing the oscillations.

2.4 Aftertreatment systems

Several after-treatment systems exist to minimize diesel engine emissions; the most prevalent are presented here.

2.4.1 Diesel particulate filter (DPF)

DPFs are designed to remove the carbonaceous component of particulate matter from the exhaust. They work with a simple principle: the gas flows through a tight cell structure, trapping the soot particles within the pores of the ceramic filters. At certain times in the operating cycle, the DPF is regenerated to oxidise the carbon deposits into CO_2 in order to clean out the filter. Regeneration typically removes up to 98% of the carbon deposits. Backpressure in the exhaust from partial obstruction of the DPF has been reported to be from a delta of 5 to 60 kPa depending on soot loading and exhaust flow rate (Boger et al., 2008), leading to increased pumping load for the engine.

Current typical regeneration strategies are mostly active; Very-late post fuel injection, or even injection directly into the exhaust manifold forces DPF regeneration by increasing exhaust gas temperature to a sufficiently high level to initiate oxidation. Increased NO_2 flow through the exhaust also promotes oxidation. (Gardner et al., 2009). There are also passive methods which enable oxidation, though these are typically most effective at low soot-loading and mandate specific engine duty-cycles to function effectively.

Most recent advances in DPF technology centre around their regeneration. Recent work by Southward et al (2010) shows promising results using a complex ceria

material which provides the oxygen necessary for oxidation rather than relying on gaseous oxygen from the exhaust gas.

In terms of outright catalyst efficiency, specific DPF filters that perform at high efficiency at high load (showing more robust construction and a 30% reduction in back pressure) and at low load (showing 15% better NO_x emissions at cold start) are being developed (Johnson, 2011). This suggests the future of DPF will be in purpose-built specialised filters, designed to be optimal for a given operating cycle and service requirement.

2.4.2 Diesel Oxidation Catalyst (DOC)

Diesel oxidation catalysts are commonly paired with DPFs in a bid to further improve the particulate filter's efficiency both in terms of temperature and composition of exhaust gasses (Johnson 2011). The DOC functions by oxidising tHC and CO emissions into water and CO_2, at an efficiency of approximately 80%, as well as reducing soluble organic fraction by about 60%. As a by-product of the oxidation NO_2 is formed, which subsequently reacts with trapped particulates within the DPF and reacts with them to form CO_2 and NO, offering a minor regenerative effect.

2.4.3 Selective catalytic reduction (SCR)

SCR is the most prominent NO_x reducing technology in heavy and light duty diesel engines. They function by using a wash-coated or homogeneous extruded catalyst plus reagent to convert NO_x from the exhaust into molecular nitrogen and oxygen (Muench et al., 2008, Johnson, 2011). In most cases the chemical of choice is a urea solution. Conventional SCR technology has the capacity to reduce NO_x by 75%-90%, though is limited by the low efficiency at low operating temperatures. To overcome this, recent SCR developments include urea hydrolysis catalysts, catalysts where the urea is sprayed directly onto a heated catalyst, or the use of gaseous ammonia instead of urea (Johnson, 2011). Longevity and durability is an issue with SCR devices; necessary regeneration cycles of DPFs have caused durability

problems in the US and Japan leading to certain types of SCR not being usable in those markets.

Conversely, in a bid to minimise space, advances are being made on the integration of SCR and DPF devices. Research has shown that by pairing the SCR catalyst to the DPF filter a NO_x improvement of 60% can be shown with little difference in functionality (Johnson, 2011).

2.4.4 Lean NOx Traps (LNT)

LNTs function by trapping NO_x while under lean engine operating conditions, reducing it under rich conditions with a precious metal substrate. CO and tHC are used as reactants to convert NO_x into molecular nitrogen, CO_2 and water.

LNTs are typically implemented in small, lean-burn engines: diesel passenger and direct-injection gasoline passenger engines. They are mostly considered where there is limited space availability or for some reason urea usage is hindered. Their NO_x reduction efficiency is approximately 70%, much lower than the 90-95% possible with modern SCR systems, and they have a high level of precious metal usage. Current development in LNT is focused around minimising the precious metal content, and increasing their efficiency (Johnson, 2011).

2.5 Start of combustion determination

Start of Combustion is not a factor commonly investigated in compression-ignition; nonetheless, there are several proposed methods worth examining. Originally, the highest gradient of rate of pressure rise was believed to be the marker of start of combustion (Xia et al. 1987, Wong et al. 1982), but this method is somewhat antiquated and reliant on a specific model of combustion to be accurate. Later on a criterion was determined which was the point at which the pressure inside the cylinder (corrected to remove the effect of the compression stroke sans combustion) recovers from the cooling effect of the fuel vaporization (Kobori et al. 2000, Assanis et al. 2003). This method, while more accurate still suffers from being a few degrees

off, as evidently, some form of heat release took place before the gradient recovered the lost heat from the spray vapourisation. This is particularly true of very high fuel pressures, when smaller droplets maximize fuel surface area and therefore its cooling effect. Katrašnik (2006) also poses that this method introduces additional computation and the necessity for computation of a reference state which introduces error. While not strictly untrue, whether or not the additional computational burden is even worth mentioning is debateable. The level of inaccuracy induced by mathematic estimation of the cylinders volume (and therefore pressure due to geometry) at any given crank angle is also worthy of debate: Minor discrepancies induced by small amounts of blow-by and even by late intake-valve closing early in the compression will differ from the theoretic calculated ambient cylinder pressure. While it may not be absolutely the same as taking a pressure-reading of the cylinder while skip-firing to compare, it is a close approximation.

Some tools used for determination are evolutions of methods used to detect knock in spark-ignition engines, due to the high degree of similarity between spark-ignition knock and compression-ignition combustion. Ando et al. (1989) and Michael et al. (1996) propose the use of 2^{nd} order derivative of heat release with respect to crank angle, while Heywood (1988) and Assanis et al. (2003) the 2^{nd} order derivative of pressure with respect to crank angle. While there is a definite correlation between them, neither is ultimately suitable. This is because while they are excellent at determining the existence of the knock-like event, they aren't very apt at accurately placing its exact timing (Ando et al. 1989, Michael et al. 1996, Checkel et al. 1986 and Barton et al. 1970). Ando et al. (1989) and Michael et al. (1996) even go on to suggest these markers predict start of combustion with delay, which is proven later on by Katrašnik (2006). Katrašnik also demonstrates how the third order derivative of pressure with respect to crank angle is the least erroneous method, but still not perfect. He proposes a specific type of filtration of high-resolution data before performing the differentiation, however, which is undisclosed as part of proprietary code. This is understandable, as very high sample rates of in-cylinder pressure result in local ringing effects interfering with the signal and resulting in a less coarse but noisier pressure-trace. The obvious caveat for this analysis, of course, being that

over-filtration dilutes the trace so much that evaluating the start of combustion accurately becomes impossible. It is also questionable whether this knowledge really contributes to the scientific community as it can only be accessed and evaluated given the proprietary code which is not made public.

Other non-specific to start of combustion published papers sometimes erroneously use the 5% burn point as start of combustion, but this method is highly inaccurate as it fails to operate correctly in the case of pilot injection and/or low load, as well as clearly ignores the fact that the preceding 5% of the heat release was emitted by an exothermal reaction which must have occurred after the actual start of combustion. 5%HR as a marker displays the same flaws as the 2^{nd} order derivative of heat release or corrected pressure, but just like them is a moderately useful and simple tool to use in comparing similar injection strategy combustion experiments, or to evaluate broadly similar tests in terms of ignition delay.

2.6 Multiple Injection Strategies

Thanks to the wide-spread adoption of fuel rail technology it is now commonly possible to implement very tightly controlled injection events at very specific timings up to several times per cycle.

In essence, there are three possible types of additional injection: Pilot injection, split injection and post injection.

2.6.1 Pilot Injection

Pilot injections are small injection events implemented in advance of the main injection event, typically 15° to 25°CA before the main injection event. The purpose of pilot injections is to combust early (far in advance of the power stroke) and provide a volatile in-cylinder environment for the subsequent injection events to combust in. In broad terms, pilot injection events shorten ignition delay, prolong combustion duration, minimise rate of pressure rise and shift combustion slightly towards diffusion-controlled rather than premixed combustion. The shortening of ignition

delay coupled to the subsequent lower rate of pressure rise usually results in reduced NO_x emissions, as peak pressure and temperature are reduced (Chen 2000,). Jung et al. (2011) suggests this is mostly due to combustion phasing rather than the combustion of the pilot itself. Ishida et al. (1994) note that NO_x improvement from pilot injection is particularly apparent in low-load conditions and superior to any similar improvement that may be had from simply retarding single injection. There is also evidence that when the quantity of the pilot becomes sufficiently large its combustion may account for a significant amount of the overall NO_x production. Pilot injection significantly reduces acoustic ringing in the engine and noise-vibration-harshness (NVH); this is in fact the main reason for using pilot injections in most modern commercial diesel engines.

Whether the implementation of pilot injection increases or decreases smoke largely depends on how optimised the injection and engine settings are. Theoretically, the shift towards diffusion-controlled combustion should result in increased smoke emissions as the main charge does not have sufficient time to mix and local rich pockets do not have time to disperse. Increases in smoke, however are easy to mitigate by either post injection or split injection as will be shown.

Optical experimentation conducted by Husberg et al. (2008) demonstrates that piloted single injection regimes form more soot at the beginning of the combustion of the main injection, but as less total fuel is burnt during the main combustion the soot formation ends at an earlier crank-angle phasing compared to single injection and net soot oxidation commences earlier. It is also possible a portion of the liquid fuel of the main injection may interact with a pilot combustion that has not yet fully quenched and generate additional soot (Merkel et al. 2008)

Given that pilot injections are in principle delivered quite a few degrees BTDC their contribution to the power stroke is mostly in the slight rise in in-cylinder pressure rather than as outright thrust during the expansion stroke; it would therefore be logical to assume their use would come with a slight penalty in fuel efficiency, though this is proven to not be the case: Jung et al. (2011), Shayler et al. (2005) Minami et

al. (1995) and Ishida et al. (1994) show that fuel efficiency increases for piloted injection in comparison to single injection.

Husberg et al. (2008) state that pilot injections igniting before their charge has sufficiently mixed may result in non-optimal NO_x and PM emissions. They claim significant heat release prior to the main injection must be prevented, and conclude that high EGR is the only way to ensure notably low NO_x and PM emissions when implementing piloted single injection. This is a result of requiring a long ignition delay to maximize mixing, which is achieved through the use of high levels of cooled EGR.

Ishida et al. (1994) notes that pilot injection reduces ignition delay equally as effectively for low Cetane fuels as for high ones. This is particularly interesting because it suggests that injection regimes with a pilot are still optimal when running lower consistency or lower quality fuel.

Chen (2000) states that for small diesel engines pilot injection quantity needs to be as small as possible, less than 1.0 mg, while noting that increasing the distance between the pilot and the main injection reduces NO_x but increases smoke.

2.6.2 Post Injection

Post injections are implemented after main injections with some retard and are used almost exclusively to control smoke emissions. It has been shown that post injections are of a particular benefit in conditions where fuel mixing is difficult, like high EGR or when injecting at low pressures (Payri et al. 2002, Husberg et al, 2008, Dronniou et al. 2005). Work carried out by Payiri et al. (2002) on a large-bore engine demonstrated that at high load a 10% and at low load a 20% mass substitution as post injection would result in reductions of smoke as much as 45% when running high EGR. It transpires the actual amount of fuel in question is nearly identical, suggesting that optimal post-injection quantity doesn't vary significantly with engine load or total fuel delivered. It was also demonstrated that specific timing of post injection did not significantly influence the NO_x or BSFC.

2.6.3 Split Injection

Split injection is a method whereby the main fuel delivery is segmented into two smaller parts with a small amount of delay between them, called a dwell. The most common split is the 50%-50%, but there has been research performed up to 10%-90% which bears similarities in behaviour to very late piloted single injection. It is possible to implement more than two injection events but there is little incentive to do so mostly due to time limitations; adding a few crank-angles worth of dwell in an injection event increases its duration and doing so twice makes for a particularly long combustion duration with the disadvantages associated with early start and late end.

Separating the main delivery of the fuel into multiple smaller quantities has numerous effects. Firstly, by inserting a minor delay between the events it effectively lengthens the combustion duration. It also lowers the peak pressure rise by as much as 45% (Nehmer et al. 1994) and the rate of pressure rise, limiting acoustic ringing and NVH. This occurs as during the early stages of combustion the fuel available is less and the fuel/air mixture is less rich. Montgomery et al. (2001) suggest split injection as a method to improve air utilization; the superior mixing possible with its implementation allows for lower air-to-fuel ratios (through higher EGR) and consequently less free oxygen in the cylinder. This in turn drops the temperature during premixed burn phase. This, plus lower peak pressures (due to longer combustion duration and slower rate of combustion) and therefore temperatures reduce NO_x with minimal impact on smoke. The longer combustion duration allows the combustion to continue later into the cycle without the adverse effects of late conventional combustion; simply delaying a single injection would result in the same late combustion but tends to generate more smoke than a similar split-injection that endures as late.

Work carried out by Shayler et al. (2005) suggests that equivalence ratio and actual phasing of the combustion event is more critical in determining emission optimization than the ratio of fuel delivered and their dwell-time. Research they carried out demonstrated the emissions showed very little fluctuation when dwell-time was altered or the ratio of fuel delivered between the first and second part of the split.

Regardless, the split-main tests they examined showed a universal improvement in NO_x-PM trade-off, as has been the case for Nehmer et al. (1994), Pierpont et al. (1995) and Montgomery & Reitz (2001) and Tow et al. (1994).

Pierpont et al. (1995) demonstrate the effect of a triple injection, comparing it to an equivalent single and double injection. Their conclusions are not entirely clear; in some situations the NO_x-PM trade-off is slightly improved and in some it is slightly worse with a triple injection than with a double. They are clear that it is superior to a single however; rather than conclude what most other researchers come to, that split injection achieves comparable smoke while reducing NO_x they state comparable NO_x while reducing smoke. This may suggest a slightly different combustion phasing, but the fundamental point of importance is that their NO_x-PM trade-off is comparable to other researchers. The triple injection is shown to be potentially useful for low-load cases, as the control it offers over the amount of premixed burn can be critical in emission optimization.

They also suggest that in general, later phasing offers an improved reduction in smoke compared to earlier phasings. Of interest, they also note that BSFC is not altered between the three injection types, though when dwell-times increase substantially there is a penalty of circa 4%, an understandable loss given an ever-increasing amount of fuel is combusted at a less-than-optimal cylinder position.

Earlier work performed by Tow et al. (1994) showed an even more dramatic decrease in smoke with similar NO_x results to the baseline when implementing split injection in a heavy-duty engine. They note that split injection can be implemented to increase the rate of particulate oxidation in late-combustion, this effect in particular they suggest is sensitive to dwell time. It could be argued these tests are bordering on a main with a large quantity of PM-controlling post-injection rather than split injection.

More significantly, they suggest that conventional heat release analysis yields similar results between single and split-injections, suggesting that local rather than global effects are responsible for changes in particulate emissions.

It has also been demonstrated (Merkel et al. 2008) that implementing split injection benefits soot emissions by simultaneously reducing the soot formed in the early stages of combustion and increasing its oxidation later in the cycle.

Determining the optimal ratio of fuel for each part of a split is not easy to establish; Montgomery & Reitz (2001) state it is a function of engine load required; low load proved to be optimal with a larger first split while mid load showed preference to a 60%-40% ratio. High load was deemed to prefer a 55%-45% ratio and a moderately large dwell-time of 9°CA, though their work was on a heavy-duty single cylinder engine of 2.44 L capacity and may not be indicative of optimal settings for passenger car-size engines. Han et al. (1996) state that for small diesel engines a 75%-25% split significantly reduces smoke with comparable NO_x, while simultaneously allowing for a later combustion phasing, resulting in reduced NO_x as well.

Several researchers note that multiple injection scenaria like split injection and piloted split injection respond more favourably to increased EGR than conventional single injection does. Chen (2001), Montgomery & Reitz (2001) and Mendez & Thirouard (2008) in particular demonstrate that increased EGR shows beneficial effects when implementing such injection regimes, giving a superior NO_x-PM trade-off throughout the operating regime.

Later work performed by Mendez & Thirouard (2008) shows that an optimally timed split injection in which the second segment starts spraying just after the heat release of the primary injection reduces the overall peak heat-release by supplementing a cooling effect due to the latent heat of vaporization of the liquid fuel. The consequent lowering in peak heat release (and heat release rate) prompts a significant decrease in combustion noise without losing overall heat release; the overall energy is comparable as the combustion duration is merely prolonged.

The various injection strategies reviewed have indicated that multiple injections can provide significant benefits to conventional diesel combustion. As common rail fuel systems and diesel injectors increase in speed and complexity, a larger number of injections will likely become necessary rather than possible. Another area where

multiple injections are potentially of significant interest is in advanced combustion – specifically, strategies such as HCCI where charge preparation is more important than in a fundamentally non-premixed diesel combustion event.

2.7 Homogeneous charge compression ignition (HCCI)

Homogeneous charge compression-ignition (HCCI) is a method of combustion primarily designed to eliminate the problematic generation of engine-out NOx and PM emissions. In HCCI the fuel/air mixture is either of an equivalence ratio of less than 0.45 or a higher equivalence ratio with a large amount of EGR occupying a percentage of the cylinder. The result is a charge that burns at a relatively lower temperature, typically below 2000K. The combination of good fuel mixing and atomization keeps soot formation low and the low overall temperature and absence of hot-spots prevents most NOx formation (Christensen et al. 1998, Dec 2009. Sjöberg et al. 2008, Zhao et al. 2003, Juttu et al. 2007). Understanding how HCCI relates to conventional combustion (and low-temperature combustion) is much simpler thanks to the modified φ-T map demonstrated by Neely (2005), Figure 2-1.

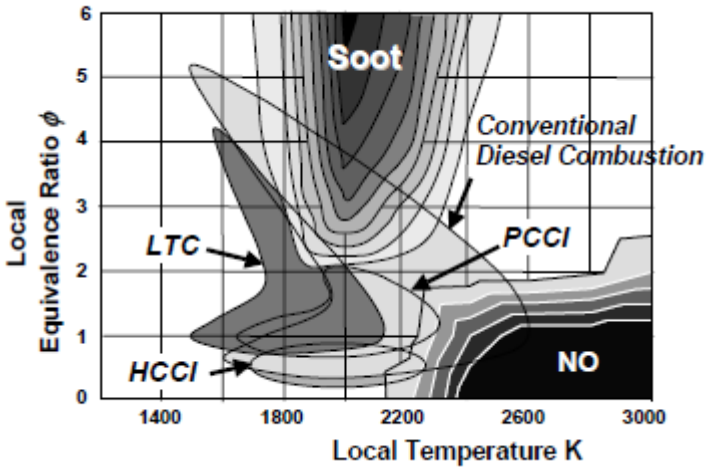

Figure 2-1: Soot and NO_x contour plots on local equivalence ratio vs. local temperature graph, reprinted with permission from SAE Paper No. 2005-01-1091 © 2005 SAE International.

While in theory HCCI is a near-ideal combustion regime in practice there are several issues preventing it from being a truly viable one. The operating range HCCI can

function at is very narrow, as high-load produces an unrealistically high rate of pressure rise. By its very nature the homogeneous charge combusts very rapidly once critical pressure is reached and the resulting acoustic knock would generate pressure rise rates in excess of 9 bar/CA at equivalence ratios above 0.3 (Eng 2002, Dec 2006). The resultant excessive mechanical stress on the engine prevents HCCI from being usable in high-load operation. At low-load, HCCI suffers from low combustion efficiency: As load drops EGR must increase in order to prevent over-leaning of the fuel, but with an equivalence ratio of below 0.2 at low RPM CO emissions increase dramatically, as do hydrocarbon emissions. Dec (2003) showed that at a typical idling condition in HCCI approximately 60% of the fuel's Carbon molecules are converted to CO and exhausted and combustion efficiency was recorded at 62%. It is suggested that this is mostly due to extremely low combustion temperatures, typically below 1500 K, a side-effect of excessively lean charge, low load and very high EGR rates. At this low temperature the bulk reactions that convert CO to CO_2 cannot propagate to completion before being quenched during expansion.

Aside from the limited operational range, there are also issues with the control of transient states between HCCI and conventional combustion. Being able to seamlessly switch from normal CI to HCCI without navigating through a combustion regime of extremely high NO_x or PM emission is crucial in the commercialization of HCCI. The load limitations and control challenges for HCCI have thus far prevented its widespread application in automotive diesel engines. However, other strategies have been developed that try to achieve many of the benefits of HCCI while overcoming some of these challenges.

2.8 Low temperature combustion (LTC)

In order to maximize the range of HCCI-like combustion LTC was developed; LTC operates at a much richer level fuelling than HCCI, with a local equivalence ratio (φ) of up to 4 (in lieu of <0.45 for HCCI). This is commonly achieved by very high rates

of EGR, typically up to 55% and 65% by volume (Sarangi et al. 2012, Cong et al. 2010, Mizuno et al. 2002, Alrikson et al. 2006).

LTC has several advantages over HCCI, not least of which its broader range of operating equivalence ratios and lower temperature range (as low as 1500 K). It does not necessitate the extensive, often impossible mixing HCCI demands and therefore has higher local equivalence ratios. Ideally, HCCI generates no NO_x as there is an absence of a propagating flame, however in practice this is hard to reliably replicate. Unlike HCCI, LTC is not designed to spontaneously combust throughout its whole fuel charge, and as a consequence can have lower peak temperatures, generating less NO_x than non-ideal HCCI.

There is currently no consensus on what exact factors constitute LTC, short of operating conditions which prohibit high in-cylinder temperatures combined with LTC-like emission output. Broadly, characterisation of a combustion regime as low-temperature combustion (LTC) can be done in one of the following ways: Firstly, the observation of a cool-flame reaction in the heat release curve of the combustion, whereby a small amount of heat is released and then seems to be quenched, only to be followed by the rapid rise in heat release of the main combustion. Secondly, a peak adiabatic flame temperature of under 2000 K, though this method mandates computational modelling or measuring equipment which is not wide-spread in its use. Or, lastly, an experimental string in which a trend in particulate emissions is demonstrated to increase and then decrease dramatically to near-zero levels. This non-linearity correlates with trends that traverse the high-smoke “island” in the local equivalence ratio vs. flame temperature graph (known also as the φ/T map) (Akihama, 2001) and signifies the transition from conventional compression-ignition to low-temperature combustion. It should be noted that not always is the cool-flame reaction visible from the pressure trace, as its later stage of declining gradient may be masked by the early onset of the main combustion event. It is also harder to distinguish in low-load LTC.

Chemically, the first part of the LTC reaction sequence is the cool-flame reaction which is a limited exothermic reaction occurring when a small part of the fuel is

converted at a temperature between 700 K and 900 K. It is understood the heat released from this reaction enhances vaporization of the remaining fuel, and the amount of heat released is dependent on temperature (Yamada 2006).

LTC's weakness compared to HCCI is potential for smoke formation; not having the extensive mixing time and consequent homogeneity non-optimal LTC suffers from increased smoke due to local rich pockets in its fuel distribution. To oppose this, a post-injection is often implemented to assist in oxidizing the particulate matter. Yun et al. (2005, 2007) demonstrates that a small, accurately placed injection of fuel late in the cycle can significantly impact PM emission without notably influencing NO_x. Timing is critical if this method is employed, however, as phasing too late will only result in increased tHC emissions due to only partial or non-combustion of the post charge. Likewise, injecting too early could result in the post fuel charge being injected before the main combustion initiates, in which case it may transpire that the post is in fact behaving as part of a split-main injection.

Regardless, post-injection for PM-control is a viable method to employ during LTC, but is most useful at relatively high-load LTC. Even with minimal post injection quantities, low-load LTC would suffer a non-trivial impact in fuel efficiency with the introduction of a post injection. This is because the post does not contribute to useful power production, and relative to the total quantity of fuel delivered it represents a larger percentile increase for low-load LTC than it does for mid- and high-load LTC. Post injection in LTC is also inherently a low-efficiency operation with limited scope; the extremely high levels of EGR imply that what little oxygen there is available will be mostly used by the preceding combustion, making the oxidation of the post-injection harder to implement.

Alternatively, increasing EGR rate even higher can effectively throttle PM emissions, as demonstrated by Cong (2011). The obvious caveat being that increasing EGR has a degrading effect on combustion efficiency, forming a trade-off between PM and tHC/CO. CO and tHC emissions in LTC are always excessive, particularly at high load, even without excessively high EGR, as such LTC necessitates the

existence of some form of after-treatment in order to bring exhaust emissions back to acceptable regulated levels.

2.9 Alternative Fuels

European legislation allows diesel fuel to be sold with up to 5% bio-diesel content without additional notification and without alteration to consumer statutory rights or legal stance. By extrapolation this implies that passenger car manufacturers are obliged to honour warranties on vehicles running up to 5% bio-diesel blends (Standard EN590).

EU strategy on bio-fuels (Communication from the Commission - an EU Strategy for Biofuels [SEC (2006) p.142]) states very strong intent to construct, support and ensure viability for a bio-fuel infrastructure both in economic and environmental terms. Named specifically are points such as “ensuring environmental benefits”, “stimulating demand” and “enhancing trade opportunities” of bio-fuels. The directive also discusses the possibility of a different tax regime on bio-fuels. Since this strategy has been in place, the availability of bio-fuel pumps has risen steadily in central Europe. Several countries sell bio-fuels at prices lower than diesel.

2.9.1 First-generation bio-fuels

First generation bio-fuels are those derived from lignocellulosic crops such as sugars, starches, animal fats or vegetable oils. Bio-diesel is most commonly produced via transesterification and chemically classified as Fatty Acid Methyl Ester (FAME).

Suitability of bio-diesels in terms of their effect on the mechanicals of the diesel engine has been examined from numerous perspectives but largely focuses on the side-effects of first-generation fuels particularly those that derivative of soy bean and rapeseed as engines tend to be least tolerant of them. Fuel filter blockages, accelerated injector pump wear, injector blockages and possible corrosion to certain plastics including elastomers used for sealing are all considerations worth noting,

though for the most part are not proven to be as severe as first anticipated (Terry et al. 2006).

2.9.2 Gas-to-Liquid fuel (GTL)

Gas-to-liquid fuel (GTL), a fuel manufactured with the Fischer-Tropsch (F-T) method is currently the forerunner of 2nd generation bio-fuels. First discovered by German research in 1923, the F-T method of GTL synthesis was essentially the hydrogenation of CO. Later the process was commercialized using coal as the base material (Nishina 1999). Currently it is understood that GTL can be synthesized by liquefying natural gas or similar fuel-gasses.

There are numerous advantages to the combustion of GTL in CI engines, not least of which almost undetectably low levels of sulphur, relatively lower soot emissions, higher power density and specific power output with respect to diesel (Mitsuharu et al. 2002, 2004, Schaberg et al. 2005). In physical terms GTL is a liquid fuel at ambient pressure and temperature. This makes it highly suitable as both a choice for a fuel blend and a fuel in and of its self. It has a high Cetane number, generally higher than that of diesel. It is practically sulphur-free and has no aromatics in it further strengthening its case for emissions compliance.

Chemically, GTL in general terms is slightly less dense than diesel (between 9 and 13% less dense) and has a higher Cetane number, typically between 78 and 88. When used in a compression-ignition engine, GTL notably decreases soot emissions (Oguma 2004, 2002 & 2002, Moon 2010, Nishina 1999, Hassaneen, 2012). Factors that influence this include GTL's lower density which allows it better atomization and therefore lower incidence of local rich pockets in the chamber; the low aromatic is also understood to prevent significant soot formation. This effect has a higher prevalence on soot formation than its higher Cetane number, which commonly correlates with shorter ignition delay, and therefore less premixed burn and higher smoke emissions.

The fact that GTL reduces soot is generally well recognized. Particles generated from GTL combustion tend to range between 30 and 200 nm (Hassaneen 2012). Schaeberg et al. (2005) conducted tests with neat GTL and GTL blends of 20% and 50% with diesel on a 2.2 lit Mercedes Benz passenger-car engine running a standard production ECU and map and found PM reductions to be in the range of 30% for the 50-50 blend and 60% for the neat GTL. Of note, when running with the 20% GTL blend they noted soot reduction ranging from 5% to 35%, which would signify that the presence of the GTL was in certain cases contributing to more soot reduction than simple substitution would account for. How GTL contributes exactly to lower soot count is not fully understood, though several factors are identified. Heywood (1988) proposes that aromatic hydrocarbons follow a direct route to soot formation at low temperatures (below 1700 K). Work done by Azetsu (2003) demonstrates a correlation between soot formation in a diesel-type flame and total aromatic content of the fuel. Earlier work by Natarajan (2001) established a linear relationship between the ratio of Hydrogen to Carbon molecules in the fuel atom and PM emissions for non-oxygenated fuels.

GTL has a slightly higher heating value, enough so as to grant it a marginally higher power density than diesel despite its lower volumetric density. As a result, it can be used nearly interchangeably with conventional diesel.

Being manufactured from natural gas GTL theoretically has a zero sulphur content. This is particularly favourable as certain after-treatment devices such as Diesel Particulate Filters (DPF) and NO_x oxidation catalysts are coming into increasingly wide-spread use and their internal surfaces can be poisoned and damaged by any sulphur contamination.

GTL has several disadvantages when compared to diesel: There is a definite issue with its lubricity which is notably decreased; the lack of polar constituent molecules and the absence of sulphur make it poor as a lubricant. This can be seen as an increase in wear rate in sliding metal parts that come into contact with the fuel, notably the fuel injection system. Research has shown that the injection pump's plunger and the injector needle are particularly susceptible to damage (Oguma 2004.

Fukumoto 2003). While several types of lubricity improver are commonly used when combusting GTL, the wear acceleration is not considered severe enough to warrant its use on low percentages of diesel substitution blends. However, if high concentrations of GTL were used, then these lubricity additives would be needed.

GTL's lack of aromatics may also causes issues with sealing; the effectiveness of rubber seal materials is severely reduced when sealing zero-aromatic fluids as the rubber may not swell sufficiently to provide a perfect seal. Subsequent leaks could result in high-pressure fuel leaks or entrainment of air into the fuel system. Work carried out by Oguma et al. in 2004 does not conclusively demonstrate that GTL's inferior seal swelling results in such entrainment but does establish that it is slightly inferior compared to low-sulphur diesel and diesel in this respect. Whether the way GTL affects used rubber seals differently is not examined.

High pour-point is a problem when using GTL in low-temperature environments. Depending on composition, GTL ranges from 10 to 30 K lower pour-point than regular diesel and therefore has problematic flowability at low ambient temperatures. While it does not wax as diesel does, it goes 'gel' or harden. This can be easily mitigated, however, with a standard similar to diesel grades (Oguma 2004, Moon 2010). In much the same way that diesel specifications vary in pour-point throughout the calendar year GTL must be altered to suit the ambient environment it is used in so as to not seize-up in low-temperature environments.

2.10 Fuel blends in low temperature combustion

Recent research has attempted to ameliorate low temperature combustion by using alternative fuels to diesel. Work done by Northrop et al. (2009, 2011) examined LTC with various blends (as well as neat) soy-based methyl ester biodiesel. They note that there appear to be artefacts relating to the ignition region of biodiesel which consequently make the conventional evaluation of start of injection to 50% burn point unusable in fuel comparisons. They note that comparing tests by combustion phasing is an optimal choice when examining LTC so as to avoid discrepancies in pressure and combustion phasing. Of note, small variations in injection pressure

(±200 bar) appeared to have less of an effect than a 2°CA variance in combustion phasing.

Also worth noting, they found that tHC emissions for ultra-low aromatic biodiesel (after normalization for phasing and lower heating value) were lower than the reference diesel tested, though for unexpected reasons. While the low-aromatic fuel had lower soot generation, the particle size distribution suggested a higher soluble organic fraction (due to post-combustion agglomeration) resulting in a comparable FSN. This finding is particularly significant as many biofuels aside from the ones the authors tested are very low in aromatic content and may suffer similarly poor PM emissions.

Later experimentation by the same group focused on PM emissions during LTC combusting biofuels and noted that while the 100% biofuel produced lower soot emissions than the reference diesel the engine-out PM was higher by an order of magnitude, as unburnt methyl-esters from the fuel were converting to particulates when diluted. The same body of work demonstrated that a DOC was adequate to convert these species however back to comparable amounts of soot to the reference diesel.

2.11 Opportunity to fill gap in knowledge

There is a wealth of knowledge available in advanced diesel combustion currently, with many impressive research groups pursuing specific directions with a view to improve efficiency and emissions with as little a complexity and cost increase as possible. One aspect that has not been looked into centres around aspects of compression-ignition traditionally taken for granted: In principle, fundamental compression-ignition is highly repeatable; it is taken for granted that whatever injection is requested will be delivered. This is an assumption which may not hold given modern complex injection strategies, and how exactly the fuel supply systems respond to their much more complex and precise demands.

There is also a lack in research combining multiple innovative approaches: while there is research on how GTL behaves in diesel blends in conventional combustion, and how LTC is different to conventional combustion, there appears to be no literature on how GTL behaves in LTC, particularly when employing optimised complex injection strategies.

Current start of combustion determination methods are neither perfect nor fool-proof; they can be difficult to use accurately in atypical engine conditions and do not function well in distinguishing the start of multiple separate injection events. It would help the understanding of the modern combustion process if an efficient tool was developed to determine each individual injection event's start of combustion.

3 General experimental methodology

In this chapter descriptions of the equipment used throughout this body of work will be detailed. The hardware as well as the data acquisition system will be explained, as will the hi-speed and low-speed data gathered during experimentation.

In certain chapters additional experimental methodology which specifically pertains to their experiments will be supplemented where appropriate.

3.1 Experimental rig

Experiments were carried out on a fully-instrumented AVL 5402 single-cylinder research engine designed to mirror a single piston of a typical automotive 2.0 L four-cylinder light-duty high speed direct injection engine. Details of the engine are described in Table 1. A four-valve double over-head camshaft (DOHC) head provided aspiration while a 1st order mass balancing system maintained oscillations at a manageable level.

The engine was controlled with an ETAS engine controller using INCA software to enable user-defined injection regimes. Tests were carried-out on user-specified single, piloted single, and piloted split-main combustions, in order to determine if more complex fuel delivery resulted in a change in variability.

Aspiration on the rig was of a switchable setup: A bypass-valve allowed natural aspiration through a filter element directly into the intake resonance tank, installed immediately prior to the intake plenum of 25 L capacity. An identical tank was installed downstream of the exhaust manifold. The tanks were designed to damp out the pulsations generated by the intake and exhaust events and hence make the engine aspiration more closely represent what would be expected in a turbocharged multi-cylinder engine (Cong 2011). Switching the valve, an external boost supply was connected. The external boost rig consists of an electric motor driving a centrifugal compressor supplied air via the same filter element used in the natural aspiration setting. The boost rig allows fine control over the volume of displaced air as well as

its pressure, up to a maximum of approximately 2.1 bar gauge pressure and approx. 1000 lit/min, equating to 4000 RPM. In both boosted and natural aspiration the intake charge is passed through a flow-straightener prior to the resonance tank, of 2 m length and 5.0 cm internal diameter. Coupled between the flow-straightener and the tank is a EPI 8712MPNH thermal mass flow meter. In the middle of the flow-straightener is an external heating element, controlled by software and able to stabilize the intake air to within ±2°C. More details on the boost system are available from Sarangi (2012).

Bore x Stroke (mm x mm)	85 x 90
Swept volume (cm^3)	510.7
Chamber geometry	Re-entrant bowl
Compression Ratio	17.1:1
Nominal Swirl Ratio	1.78
Induction	Externally boosted
Fuel Injection System	Bosch CP3 Common Rail
Engine Management System	AVL RPEMS, Bosch ETK7
Intake Open	8°CA BGTDC
Intake Close	226°CA AGTDC
Exhaust Open	128°CA ATDC
Exhaust Close	18°CA AGTDC
Max Cylinder Pressure (MPa)	17

Table 1: Engine Specification

The engine was equipped with a back-pressure valve in the exhaust stream to simulate the back pressure normally encountered by a turbocharged engine. A second surge tank upstream of the back-pressure valve was used to damp out

pulsations. The backpressure valve was also used to generate the pressure differential needed to drive exhaust gas through the EGR system. Although it varied slightly from mode to mode, the back pressure was generally maintained 10 kPa above the intake manifold pressure.

Injector Model	CP3 (VCO)
Nozzle	DSLA 142P
Max. Injection Pressure	135 MPa
Holes/Diameter	5/0.18 mm
Spray Angle	142°
Max. Needle Lift	0.2mm
Max. Flow Rate	750 ml/min
Min. Dwell	200 µs

Table 2: Injector specification

The fuelling system for the engine included an automotive belt-driven fuel pump providing fuel at up to 1400 bar to a Bosch CP3 common rail. The high-pressure rail was of an equivalent length and volume to that used in a four-cylinder automotive size diesel engine. The fuel was supplied to the injector through a thick-walled fuel line of approximately 40 cm length with an internal diameter of 2.75 mm. The only difference from a multi-cylinder engine was that the common rail supplied only this single line; all other fittings and controls were the same as for a multi-cylinder engine. The fuel line fed into a five-hole valve covered orifice injector. Details of the injector are shown in Table 2.

The EGR system (designed by Cong, 2011) allows for control of exhaust back pressure and EGR rate, as well as EGR temperature. An electronically controlled PID controlled butterfly valve enabled accurate control of backpressure and coupled with a throttle valve enabled precise levels of EGR. A separate controller throttled

the supply of cooling water to the EGR cooler, allowing for modulated EGR temperature.

The fuel injection event was controlled by the engine control system mentioned above. This system allowed control of the timing and quantity of up to four injections per cycle. The timing is set in terms of crank-angle phasing, and is not modified by the controller. However, the injection quantity command (in mg) is converted into an injection opening duration (pulse-width), based on a performance map from the engine supplier. This map adjusts the commanded duration on the basis of speed and fuel rail pressure only; it does not account for injection timing. However, in the case of multiple injections that are commanded to occur too closely together, the controller will reduce the injection duration of the first injection to ensure that the minimum required injector dwell time (0.2 ms) is maintained.

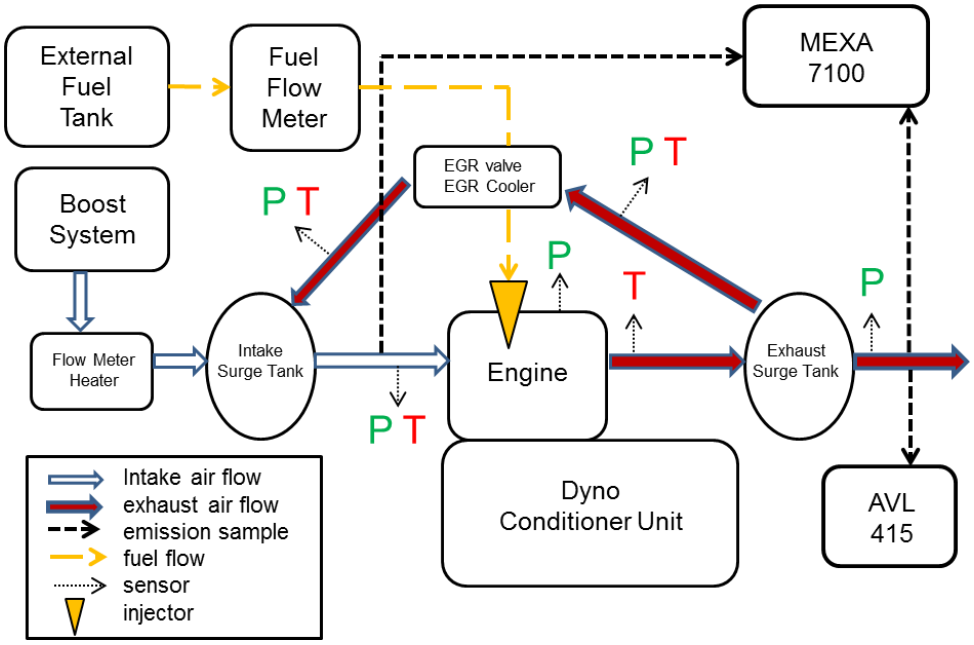

Figure 3-1: Schematic of the test-cell setup

Whenever non-diesel fuel was used a splice was performed at the fuel-to and fuel-return hose upstream of the AVL fuel meter. These two hoses were then connected to a temporary tank full of the fuel required which was located at a higher shelf than the engine and the flow meter. The tank was connected to a high-pressure feed so as to initiate fuel flow from the tank to the flow meter, but after that the high-pressure

feed was removed, and the pumps under-pressure drew the fuel out of the tank. A schematic diagram of the test-cell setup can be seen in Figure 3-1.

3.1.1 High-frequency data collection

Needle lift (NL), fuel line and in-cylinder pressure (ICP) were all recorded over 200 cycles at 0.5°crank angle (°CA) resolution. This data allowed a high degree of accuracy in calibration as well as a comprehensive evaluation of the engine performance and was of crucial importance in the investigation of multiple injection tests.

Intake manifold pressure was also measured at high-frequency via a Kistler 4045A5 0-500 kPa piezo-resistive pressure transducer. The signal was amplified and converted by a Kistler 4618A2 amplifier.

The in-cylinder pressure was measured using a water-cooled flush-mounted AVL QC 34-C quartz piezoelectric pressure transducer. This signal was amplified and converted by a Kistler 5007 charge amplifier at a filtering frequency of 200 kHz. The pressure in the fuel line connecting the common rail to the injector was measured using a high-speed AVL SL 31-D2000 transducer, installed in the fuel line approximately 10 cm upstream from the inlet to the injector matted to an AVL 3009A04 amplifier at a frequency of 100 kHz.

All data was collected through a National Instruments cDAQ 9172 and USB6125 system. Two programs to collate data were written in LabVIEW™ V8.5, one for high-frequency acquisition of a specified number of cycles and one for low-frequency data acquisition at a rate of approximately 1 Hz (Cong 2011). The data acquisition hardware comprised seven modules: An NI 9215 was used for in-cylinder pressure, intake manifold pressure, fuel rail pressure, injector current and injector needle lift. An index pulse and a 0.5°CA resolution pulse were imported to the digital NI 9401 I/O module as trigger and clock functions. Two NI 9211 were solely dedicated to the various thermocouples arranged over the engine and ancillaries A NI 9205 module acquired fuel flow rate, exhaust pressure and supercharger inlet air flow rate. A NI

9217 acquired only inlet temperature and finally a NI 9203 acquired inlet pressure and air flow rate. Data from the Horiba MEXA 7100HEGR and AVL 415 opacimeter analysers was fed in through a NI 9203.

The in-cylinder pressure is used to calculate the indicated work, which is then used to calculate the mean effective pressure (IMEP) shown in Equation 2. This work reports the net IMEP, which includes the work done during the exhaust and intake strokes as well as the compression and power strokes (Heywood 1988).

$$Work\ per\ cycle = \frac{Pn_R}{N}$$

Equation 1: Work per cycle

$$IMEP(kPa) = \frac{P(kW)n_R * 10^3}{V_{d(dm^3)} * N(rpm)}$$

Equation 2: IMEP calculation for SI units

Where P is the net indicated power (integral of the P-V curve), V_d is the displacement volume of the engine, n_R is the number of crank revolutions per power stroke per cylinder (in this case 2 for a 4-stroke single-cylinder engine), and N is the engine speed.

The in cylinder pressure is also used to calculate the apparent heat release rate, using Equation 3 (Heywood, 1988):

$$\frac{dQ_n}{d\theta} = \frac{\gamma}{\gamma - 1} p \frac{dV}{d\theta} + \frac{1}{\gamma - 1} V \frac{dp}{d\theta}$$

Equation 3: Heat release rate equation

Where p is the cylinder pressure, V is the volume, θ is the crank angle and γ is the specific heat ratio (C_p/C_v, presumed to be constant at 1.33).The exact value of γ depends on the charge composition and temperature and does not vary significantly

over the compression and power stroke. In general terms, it is between 1.26 and 1.35 and is commonly assumed to be constant (Heywood 1988). The integral of the heat release rate provides the cumulative heat release (CHR), which represents the total amount of heat released up to a given point in the combustion process.

3.1.2 Sample size evaluation

A preliminary test was run to ensure the sample size of 200 was adequate, comparing the results of mean in-cylinder pressure and its standard deviation between the same engine conditions recorded over a 200 cycle sample and a 600 cycle sample.

Seven test-points were selected including tests with multiple injections per cycle and low amounts of EGR. The test-point with the highest degree of disparity is tabulated in Figure 3-2. Shown are mean in-cylinder pressure (ICP) and in-cylinder pressure's standard deviation (ICP-SD) across 200 and 600 consecutive cycles. For clarity, the delta between the 200 and the 600 sample is also displayed.

While slightly increased noise can be observed for ICP-SD, mean ICP is nearly indistinguishable. The general profile and behaviour of ICP-SD is not significantly altered between the two sample sizes. Indicatively, the test represents a piloted split-main injection at 650 bar rail pressure and 1500 RPM engine speed, of approximately 2.7 bar IMEP.

For most of the other test-points examined, both in-cylinder pressure and in-cylinder pressure standard deviation were practically identical and the differences between them were comparable to the difference between repeat-tests of the same point. Subsequently all tests presented in this body of work are processed from hi-speed samples of 200 consecutive cycles.

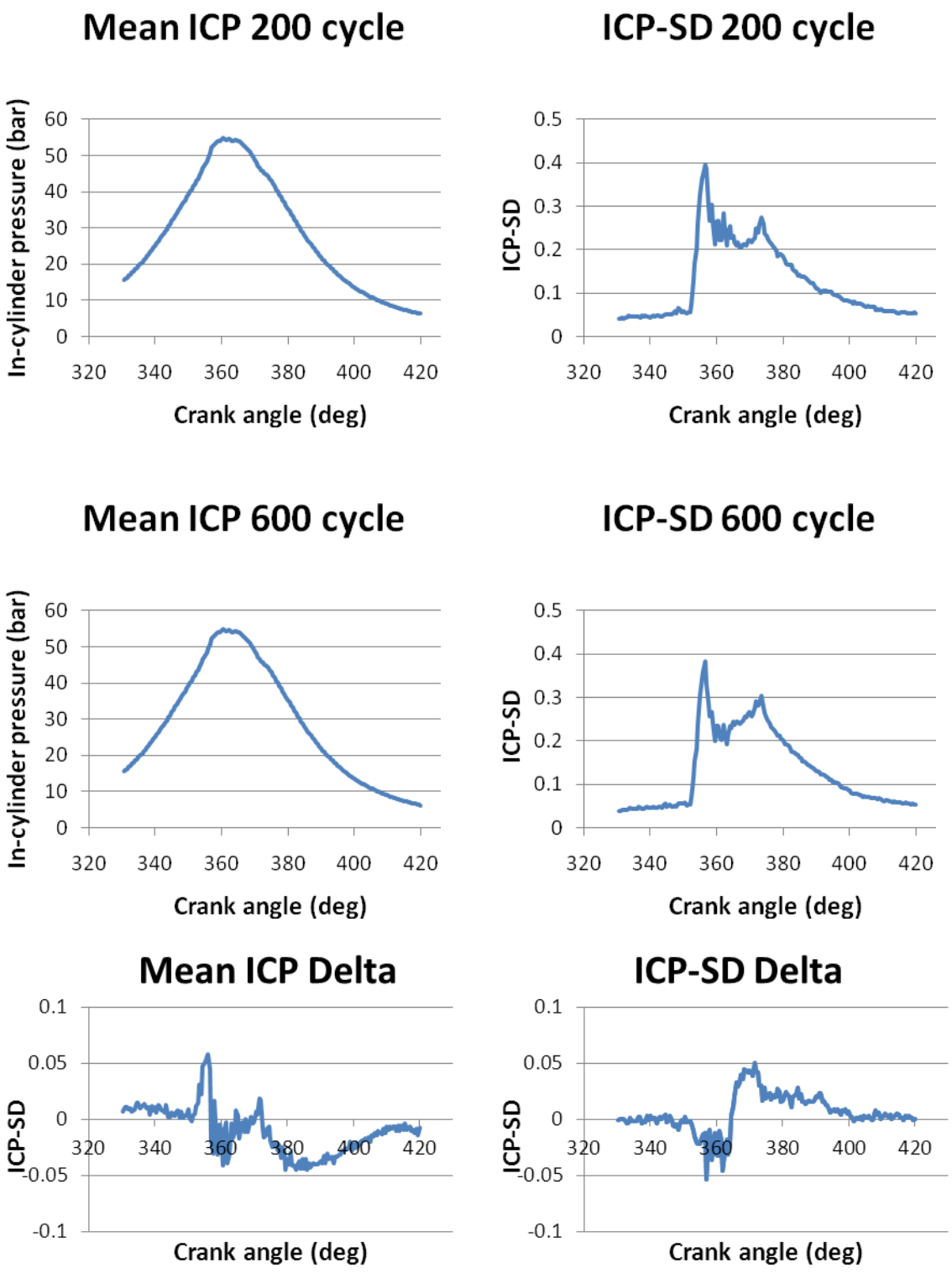

Figure 3-2: Mean in-cylinder pressure (ICP) and in-cylinder pressure standard deviation (ICP-SD) comparison of 200 and 600 consecutive engine cycles and the delta between them.

3.1.3 Low-frequency data collection

Aside from the in-cylinder pressure, engine performance parameters were sampled at a lower frequency. These parameters included various temperatures as well as temperature and pressure in the intake stream and the EGR line and fuel consumption (FC). FC was measured using an AVL 733 Dynamic Fuel Meter; its values stripped of statistical irregularities via Chauvenet's criterion (Holman 1998) and averaged over a 2-minute period per setting, following a 5-minute stabilizing time. Chauvenet's criterion was employed as the samples tended to have one or two excessively large spikes, often more than twenty times the value of the mean, attributed to electrical noise. The method removes any values that diverge from the mean by more than a factor of 2.81 times the standard deviation; this is adequate for tests containing between 50 and 100 samples. As an indication, between zero and two values per test-point were removed from each data set, out of a total of around 90 points per sample.

Emissions were drawn downstream of the exhaust surge tank via a heated sampling line set at 191°C of 4 mm internal diameter and 6m length. It could be argued that this allowed for some nominal ageing of the exhaust gas, however earlier testing showed that drawing exhaust directly out of the exhaust port generates sample biasing due to pressure pulsations and inhomogeneity in the sample (Cong 2011). Raw undiluted exhaust gas was tested with a Horiba MEXA 7100HEGR analyser which tested for concentration of CO, CO_2, NO_x and tHC. This analyser also sampled CO_2 concentration from the intake, downstream of the intake surge tank and prior to the intake manifold. A relative comparison of CO_2 concentration between exhaust and intake allowed for accurate EGR estimation. Smoke was measured with an ALV 415 opacimeter drawing raw, undiluted sample at the same junction as the MEXA 7100 The 415 unlike any other sensor in this test sampled at a maximum rate of one per 15 sec.

3.2 Emission measurement

CO, CO_2, NO_x and tHC are all measured via the Horiba MEXA 7100HEGR. As was mentioned above the analyser draws raw exhaust through a heated sample line. The sample line is designed specifically to avoid absorption of NO_2 by the humidity in the exhaust gas, and to avoid eventual build-up of fouling by unburnt gases or high boiling-point hydrocarbons adhering to the inner walls of the sample pipes.

The analyser comprises of an internal oil catcher, several filters and a heat exchanger for the removal of oil vapour, dust and water from the sample downstream of the hydrogen flame ionization detector (HFID). The dehumidified dry samples are then fed through separate analyser channels to determine their dry concentration of each measured pollutant, and retroactively converted to wet PPM when accounting for the lost humidity.

CO and CO_2 concentration are measured by passing the gasses through a non-dispersive infrared detector. The dehumidified sample is passed through a chamber and the difference in infrared light detected by the sensor is used against a calibrated baseline to determine how much of each species was present in the sample (Horiba manual 2001).

NO_x concentration needs to be routed through a converter device, which dissociates the NO_x species into NO. This is then made to react with ozone to create activated nitrogen dioxide (NO_2*) which emits a specific wavelength photon when it reverts to its normal stable state. A chemiluminescence detection method determines the concentration of NO. The ozone is generated via electrical discharge into low pressure oxygen (Horiba manual 2001).

Total hydrocarbons are measured via hydrogen flame ionization detection. The sample is passed over a hydrogen flame situated inside an electric field. Hydrocarbons combusting generate an ionization current that is proportional to the number of carbon atoms present. The comparison is based on the theory that the current response of a propane molecule is three times more than a molecule containing a single-carbon atom (Horiba manual 2001).

Smoke is sampled through the AVL 415 opacimeter. An unheated silicone supply line draws the exhaust gas through a filter-paper. Subsequent darkening of the paper's opacity is attributed to elemental carbon, or smoke particles trapped within the paper. The relative darkening of the paper is used to give an indication of the soot content in FSN (AVL 415 manual, 2005).

EGR estimation, while not strictly an emission in its self, was via the same hardware. As was detailed above, the concentration of CO_2 in both intake and exhaust was measured and used to determine the exact EGR percentage with the following equation (Equation 4) which relates EGR from the intake, exhaust and ambient CO_2 concentration:

$$EGR = \frac{CO_2^{int} - CO_2^{amb}}{CO_2^{exh} - CO_2^{amb}}$$

Equation 4: EGR calculation

Ambient concentration was fixed at 0.038% by volume. Work done by Cong et al. (2009) suggests that trapped residual gases from preceding cycles may contribute to an increase in effective EGR rate. This in turn would increase the charge temperature, resulting in altered emissions and operating characteristics under both conventional and LTC modes of combustion. Research showed that with large backpressures of around 200 kPA up to 10% residual gas fraction was possible, however in this body of work the EGR calculation does not account for residual gas fraction as the pressure differential between intake and exhaust was less very small (typically below 20 kPA).

All emissions mentioned (with the exception of smoke) were measured in either PPM or percentage by volume. These values were converted to Exhaust Index notation, which is specific to fuel consumption (g/kg of fuel) as the raw data can be misleading particularly when operating at high levels of EGR. The formula used was:

$$EI_a = \frac{\dot{m}_a}{\dot{m}_f}$$

Equation 5: Exhaust index calculation

Where EI_a is the exhaust index of pollutant "a", m_a is the mass flow of said pollutant (in g/hr, normalised against total exhaust flow rate), and m_f the mass flow of fuel (in g/hr) at that operating point. Mass flow rates for a given emission are given by:

$$\dot{m}_a = \frac{\dot{m}_{exh}}{MW_{exh}} * \frac{a}{10^3} * MW_a$$

Equation 6: Emission mass flow rate calculation

Where MW_{exh} is the molecular mass of exhaust calculated as the mole fraction average of the component molecular masses. Specifically in the case of NO_x, the molecular mass of NO_2 was used as per emission legislation guidelines outlined by Stone (2009), and CH_4 was used for normalizing tHC emissions as the output from the analyser was recorded as PPM of C_1 (Horiba manual 2001). Smoke was not normalised as the device cannot account for soluble organic fraction (SOF) in the exhaust species. Therefore, at high EGR levels it would be normal for a significant amount of SOF to contribute to the total smoke emission, meaning the FSN value for smoke cannot be used to infer the soot concentration in the exhaust.

3.3 Error estimation

As in all experiments, perfection in measurement is not possible, regardless of the complexity of the devices used or the rigour of the methods employed. Wherever possible, regular calibration and zero-resetting prevented systematic errors arising from drift, fouling and ageing minimised systematic error introduction. Despite this, several sources of random error still exist within the system. Uncertainty levels of the instruments used throughout this test have been tabulated below in Table 3.

Parameter	Uncertainty	Contributing factors
ISFC (g/kWh)	3.0%	Power calculation, fuel flow rate
Smoke (FSN)	3.5%	Smoke meter inherent inaccuracy
CO (g/kg fuel)	3.5%	CO/CO_2 analyser, air flow rate, fuel flow rate
NOx (g/kg fuel), tHC (g/kg fuel)	9.0%	Emissions analyser, air flow rate, fuel flow rate

Table 3: Estimated uncertainty factors

3.4 Fuel types and preparation

Three fuels are reported in this body of work. The first being pump-grade low-sulphur type-2 diesel equivalent to what is commonly available throughout the UK at the time of writing. As per legislation, the pump-grade fuel may contain up to 5% bio-fuel. This fuel is supplied in bulk and stored in an under-ground tank.

In chapter 7 some tests are performed using blends of type-2 diesel and gas-to-liquid (GTL) fuel. These blends were made a few days before experimentation. Blending was done volumetrically with an accuracy of circa 2% to ensure a near-perfect 30% and 50% by volume blend. The GTL was supplied in sealed steel drums which were then blended with diesel and stored in sealed jerry-cans, filled so as to minimize the area of fuel open to residual air in the can. When not in use the jerry-cans of fuel blends were kept indoors at an ambient temperature of approximately 15°C. To evaluate degradation over time, a repeat of certain key test-points was performed a week after collecting data and was found to be indistinguishable in both pressure-trace and emissions characteristics. This indicated that, as expected, the GTL blend had not significantly aged over the week of storage, and that therefore it can be assumed that GTL blends are stable for the time between their preparation and use in the tests (typically less than three days).

Whenever a switch in fuel type was performed the engine was run for half an hour at approximately 4 bar load and 1800 RPM to ensure any remaining fuel was flushed out. The can used during this time was then removed and disposed of as the fuel return-line would by then have diluted the blend with the residual fuel left over from the previous running. At that point the system was flushed again and a new can of identical blend was connected and experiments run. Naturally, a small quantity of diluted original fuel will have been left within the system, but having purged the system and already diluted the first residual with over 5 L of fuel once before it was re-purged and connected to a further 5 L of fuel ensured the contamination was minimal. Even so, in order to further minimize impact, tests of low-percentage fuel blend were performed before tests of high-percentage. This way, trends across an increase of fuel blend would be impacted the least.

When performing tests of fuel blends the fuelling system was short-circuited to bypass the fuel conditioning unit. This was done for two reasons: Firstly, the fuel conditioning unit has a capacity of approximately six litres and is problematic to purge manually as tilting it causes hardware malfunctions, and secondly there were concerns about its longevity when used with GTL. Regardless, fuel temperature was measured immediately prior to entry into the low-pressure pump (a point which would naturally be downstream of the fuel conditioning unit) and was found to be approximately 2°C higher than the conditioning unit's output, with a minor fluctuation of ±1.5°C (whereas the conditioning unit usually outputs ±1.0°C). The bypassing of the fuel conditioning unit made the process of alternating fuels a lot faster, decreased cross-contamination of the fuel and ensured safe running of the conditioner unit.

Chemical characteristics of the pump-grade diesel, 30% GTL-diesel blend and 50% GTL-diesel blend are tabulated in Table 4 . The samples were sent to an outside lab (Intertek - ITS Testing Services (UK) Ltd. for analysis. The fuel blend analysis was considered important as many of the fuel properties do not scale linearly with composition. In particular, the Cetane number of the G30 and G50 blends are nearly identical. This is not unusual; Cetane number indicates a fuel's propensity to auto-

ignite, therefore in fuel blends whose components exhibit large differences in their nominal Cetane number it does not interpolate the value: Rather, the more readily ignitable fuel acts as a pilot and initiates the ignition of the remaining, lower Cetane fuel. This explains why the Cetane number of 30% and 50% blends is nearly identical. In all cases, standard analytical processes were used by the external laboratory to measure these parameters.

Analysis type	100% type-2 Diesel	30% GTL / 70% Diesel	50% GTL / 50% Diesel
Density at 15°C (kg/l)	**0.8312**	**0.8178**	**0.8101**
Cetane Number (CN)	**59.6**	**68.7**	**68.5**
Calculated Cetane Index	**57.5**	**66.2**	**71.6**
Evaporated Vol. @ 250°C (%)	24.3	22.1	18.9
Recovered Vol. @ 250°C (%)	24.1	20.8	17.7
Evaporated Vol. @ 350°C (%)	97.0	96.2	96.2
Recovered Vol. @ 350°C (%)	96.8	94.9	95.0
Initial Boiling Point (°C)	169.7	183.2	193.8
50% Recovery Point (°C)	280.7	285.8	288.2
Final Boiling Point (°C)	354.1	355.4	354.4
PMC Flash Point (°C)	70	75	79
Kinematic Viscosity @ 40 °C	3.035	3.199	3.269

Table 4: Chemical characteristics of fuels tested

3.5 Injection Notation

Throughout this body of work several injection types will be examined: When a single injection event will be responsible for the power produced in the combustion stroke it

will be referred to as “single injection”. When this injection event is segmented into two separate injections with a small dwell-time between them, it will be referred to as “split-main injection”. All split injections tested aim to achieve a 50%-50% split between the two segments, which as will be demonstrated frequently necessitates different opening durations. In both injection cases, there may be a small injection event preceding the single or split-main injection. When this is the case, the injection will be referred to as “piloted single injection” or “piloted split-main injection”. In both cases, the pilot injection will be of a minor quantity in comparison to the overall injection amount and will typically be between 15° and 20° in advance of the injection event(s) responsible for the engine’s torque output. A typical diagram of injector signal comparing the three regimes is shown in Figure 3-3

It should also be noted that the ECU control software rounds any adjustment to the injector phasing and duration to the nearest $1/8^{th}$ of a °CA, or 0.125°CA. in all instances where applicable the data has been processed to that accuracy, but for clarity in this body of work accuracy will be reported to the nearest 1^{st} decimal place to avoid inadvertently insinuating higher accuracy than was achievable.

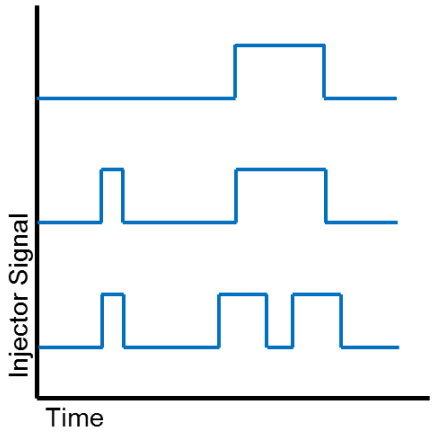

Figure 3-3: Comparison of injector signal for single, piloted single and piloted split-main injection regime.

4 Injection Complexity and Resonance

Sections of this chapter have been presented in ICEF2010-35069 by Michailidis et al., 2010.

As discussed in the previous chapters, modern diesel engines are making more and more use of multiple injections to control emissions, engine noise, and to enable new combustion strategies. In order to better comprehend the consequences of high-complexity injection regimes and the discrepancy between fuel command and fuel delivery it was necessary to investigate into what occurs when modern complex injection is requested by the ECU.

To this end a series of experiments was designed: Firstly a string of tests with a 50-50 split-main piloted injection were conducted, which proved a decaying sinusoidal trend with respect to total fuel quantity delivered. This warranted further investigation, so a subsequent, more accurate series of experiments was run using the same fuel delivery system but injecting into a bespoke rate tube rather than the engine so as to better understand the effect of fuel-rail resonance on fuel delivery.

Following these two experiments, a baseline string of engine tests were conducted in three injection regimes of increasing complexity; a simple single injection, a piloted single injection and a piloted split-main injection were investigated, of varying phasing. These tests were all conducted at the same engine speed and at two fuel-rail pressures, with each regime tested at several timings so as to demonstrate an emission and efficiency curve through its timing in the engine cycle. During multiple-injection events, the quantity of fuel delivered was trimmed to account for fuel-line resonance, so as to ensure a consistent fuel delivery quantity throughout.

After preliminary investigation in power-delivery trends and emission trends through the tests, attention was given to the cyclic behaviour of in-cylinder pressure and needle-lift events. How injection complexity related to their variability was considered and analysed.

4.1 Analysis of experiments

4.1.1 How Resonance was investigated and demonstrated

These tests were conducted at 750 RPM and 1500 RPM, with a pilot injection of 1.8 mg(commanded) starting at 20°BTDC and a main injection of 9.25 mg(commanded) starting at 7°BTDC. Injection pressures were 500 bar at 750 RPM and 500 and 700 bar at 1500 RPM. These conditions were selected primarily as representative of typical 3 bar IMEP low-load driving and had a direct comparison to a standardized running condition from the engine's default map. The 750 RPM case was selected to establish whether the fuel-rail wave frequency would double. For all three conditions, the timing of the second main injection, of 9.25 mg(commanded), was adjusted between 1°CA and 31°CA after the first injection in 2° increments. The sampling order of the test-points at each speed/injection pressure point was randomized.

4.1.2 Effects of Resonance in fuel delivery

In this chapter it will be demonstrated that a large injection delivery event induces a stationary wave within the fuel line, which possibly extends to the fuel rail itself. This wave seriously affects the pressure of the fuel delivered in subsequent injection events in the same cycle, resulting in a discrepancy between the amount of fuel expected to be delivered according to the injector opening duration and the actual fuel delivery.

Displaying injector needle-lift on the same graph (Figure 4-1) as fuel-line pressure shows the following three effects clearly: Firstly, that there is a low-frequency periodical corrected sine-wave oscillation, which is not altered (on a crank-angle basis) by engine speed; this is the output of the common rail pressure-control pump and is visible even on cycles with no injection event. Despite being less than perfect, it is nonetheless extremely reliable and its variance is in the region of +2% to -3% of the commanded rail pressure. Secondly, whenever there is a large injection event there is a sharp drop in pressure for the duration of the event. In magnitude, it may reach -10% of commanded rail pressure. This sets in motion the third effect; a high

frequency oscillation overlapping the first, low frequency one with significantly higher amplitude. This high-frequency disturbance is of no consequence in conventional injection regimes as it decays completely or at least enough so as to be inconsequential by the time the next injection will take place. This means the resonance effect will not affect single-injection regimes, and will only in a minor way influence piloted-single events, as the pilot quantity's delivery is so small the disturbance caused by the fuel-line pressure drop is comparable to the naturally occurring background pressure oscillation in amplitude. In the case of a larger quantity injection event the oscillation can and does affect delivery of subsequent injection events.

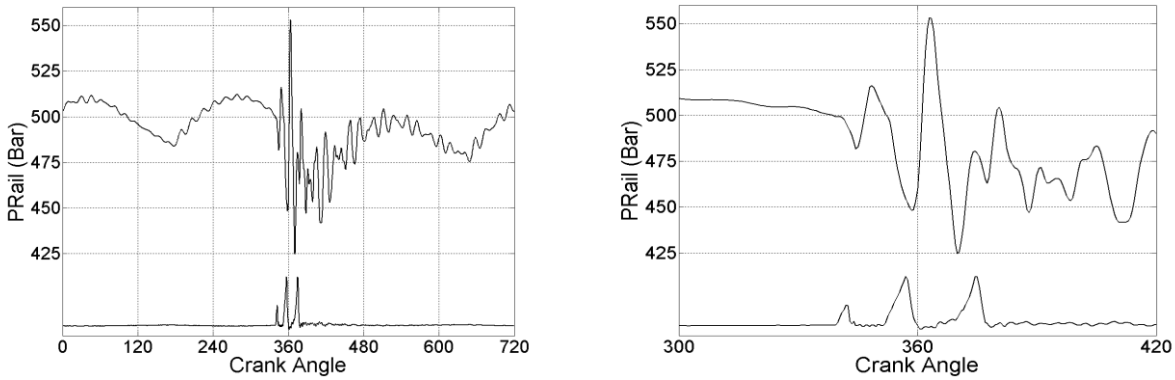

Figure 4-1: Mean fuel line pressure against crank angle over complete engine cycle with injector needle lift illustration, 1500 RPM and 500 bar rail pressure. Needle lift not to scale.

In Figure 4-1 it can clearly be seen in the magnified graph that the oscillation caused by the first part of the split results in the second part drawing fuel at a lower pressure. However, the pilot's effect on the subsequent fuel deliveries can be seen to be negligible; it is therefore clear that the quantity of fuel delivered affects the subsequent resonation wave.

The effects of the fuel line pressure pulsations (shown in Figure 4-1) on the fuel consumption varied with secondary main timing; these are shown in Figure 4-2. The fuel consumption of an identical cycle without a secondary main is 266, 563 and 601 g/hr for the 500 bar/750 RPM, 500 bar/1500 RPM and 700 bar/1500 RPM case

respectively. It can be clearly seen the total fuel injected is exhibiting sinusoidal behaviour, with an amplitude that decays with later injection second-main injections.

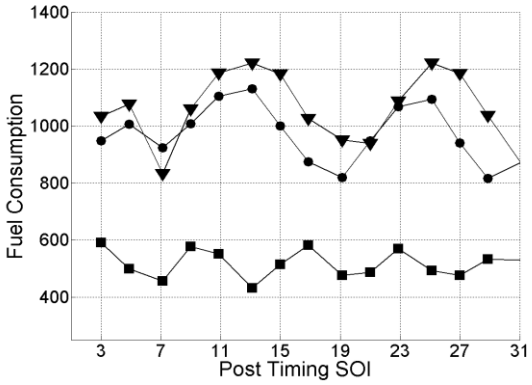

Figure 4-2: Fuel consumption against secondary main timing start of injection. . X-axis is in °CA after the start of the main first injection. Symbols - Squares: 750 RPM / 500 bar, Circles: 1500 RPM / 500 bar, Triangles: 1500 RPM / 700 bar

The results shown in Figure 4-1 suggest that the frequency of the observed oscillation in fuel consumption is halved when the speed is doubled. This agrees with the hypothesis that these are a result of the waves in the fuel line, as a wave's speed (speed of sound in the fuel medium) is unaffected by engine speed, but the time per cycle is halved. It is less clear whether the increased pressure in the 700 bar test affected the standing wave. It appears as though the whole wave is translated towards later timings, but that may be an artefact of the changing injection condition: The higher rail pressure meant the ECU selected a shorter injection duration (in °CA) for both injections, and as the duration of the injector opening is comparable to the wavelength of the standing wave (as will be demonstrated later) it may mean the results are effectively producing a physical rounding error.

The relative amplitude in the apparent fuel consumption 'wave' is consistent through all three tests and seems unaffected by either engine speed or rail pressure. For all three cases, it fluctuates by circa 20% around its mean value.

It is not clear whether the stationary wave's effect on fuel line pressure is the only factor in the dramatic variation in fuel consumption, though they seem to correlate well. Figure 4-3, which provides a magnification of the fuel line pressure combined

with the injection timing, demonstrates the difference in line pressure that occurs between high (875 g/hr) and low (556 g/hr) fuel consumption conditions. Both these points are from the same test-series of 1500 RPM/500 bar. It is particularly notable that the timing of the secondary main injection for these two cases is just 4°CA apart. For the low fuel consumption case, the pulse draws from the lowest observed pressure, dropping it even further; in the high fuel consumption case, it draws from the highest pressure, limiting its total rise. More significantly, injection events that coincide with the low pressure deliver less fuel than commanded and those that coincide with high pressure deliver a higher flow rate than commanded. This also suggests that given the correct frequency of injection events, the disturbance set in motion from each subsequent event could purposely either amplify (if drawn at a trough) or diminish (if drawn at a peak) the stationary wave.

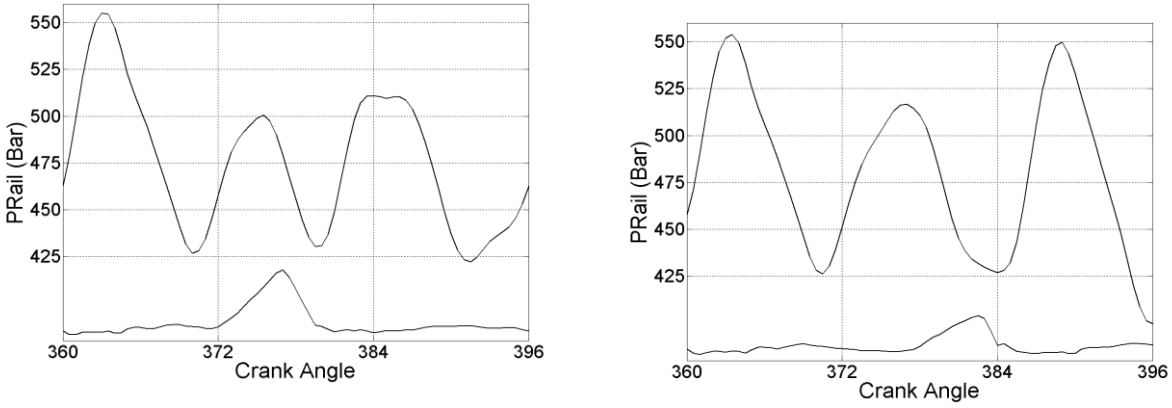

Figure 4-3: Magnification of fuel rail pressure versus crank angle overlaid with injector needle lift in a high (left) fuel consumption and low (right) fuel consumption test-point. Both at 500 bar rail pressure and 1500 RPM. Start-of-injection timing for the first part of the split injection (not shown) is 13°BTDC in both cases. The secondary main pulse is 12°ATDC (left) and 16°ATDC (right).

It is worth noting the effect of the secondary main's draw on the fuel line's pressure after it: in the first case the pulsation has acted against the wave, limiting the rise of pressure after it, while in the second case its pulsation has effectively tuned-in with the already existing pulse and resulted in a much higher peak after it.

It can also be seen that the rate of injector needle lift opening is lower in the low fuel consumption case, suggesting that the lower fuel pressure impeded the injector's performance. It is not clear whether this is the determining effect in the observed changes in the fuel delivery quantity or whether it is merely a symptom of the lower fuel line pressure, though it is highly likely to be a significant factor.

A higher resolution of fuel-line pressure trace coupled to a range of injectors could yield more insight into the exact interaction and behaviour between the injection event and the non-linear pressure within the fuel when injecting during a wave. Knock-on effects to spray pattern and vaporisation would provide valuable insight and be worth quantifying.

Further investigation via Fourier transform could yield a complete and separate image for the two pressure waves present in the fuel line: The output from the high-pressure pump could be subtracted from the overall trace and in doing so would isolate the pressure pulsation effect to give a clearer image. Then an exact correlation between the rail pressure, the speed of sound in the fuel and the density of the fuel could be established with a higher degree of scientific accuracy. Through this type of analysis it could be demonstrated with a higher degree of certainty that engine settings do not affect fuel line resonation.

Investigating the interaction between fuel pressure inside the injector (or even pressure inside the injector sac) and needle-lift opening amplitude and fuel delivery is beyond the scope of this body of work; a fluid thermodynamics simulation would be ideal to shed some light onto the specific workings of the injector needle, and answer the question of whether the pressure or the opening of the needle accounts for the discrepancy in delivered fuel. One key question is whether variability in the injector performance is leading to the observed variations in fuel flow rate. This was evaluated by observing the variability in the performance of the instrumented injector and will be shown to be trivial in Ch.4.4.4.2.

4.2 Confirmation of results with rate-tube experimentation

4.2.1 Experimental methodology of rate tube tests

In order to better quantify the discrepancy in fuel delivery a second series of experiments was conducted in which the injector was removed from the engine and the fuel line (pipeline downstream of fuel rail, upstream of injector) with the injector attached were rotated without being bent. The injector was then connected via a specially made coupling to a diesel spray rate tube rig. The rig has been designed as an evolution of a similar rig originally designed by W. Bosch in 1966. An AVL GM12D miniature pressure transducer downstream of the injector tip measured pressure over the injection cycle. A bleed-off valve was regulated during testing to ensure as close a pressure as possible to that of an engine's combustion chamber during injection, while staying within the safety limits of the rig's maximum pressure. An average of 28 bar backpressure was maintained throughout the tests. As a comparison, 28 bar is about the same as the pressure in the cylinder at 15°CA BTDC, while running at atmospheric pressure intake, with a peak pressure 50 bar at TDC. The maximum operating limit of the rig was 30 bar, however, so that high a pressure was not achievable. The engine was set to run at 750 RPM, to imitate the test performed previously and a speed beyond 1000 RPM was not possible due to hardware limitations of the rate tube. The injection regime was one injection of 6.0 mg(commanded) followed by another injection of 6.0 mg(commanded) of varying phasing, with the second one starting from 6° to 33°CA after the start of the first injection in 1° increments. Naturally, commanding a quantity delivery of the ECU does not necessarily translate to an actual delivery of the quantity requested; the ECU translates the quantity requested into an injector opening duration depending on rail pressure from a pre-designed map. The injector settings were chosen so as to mirror the engine tests as closely as possible, albeit at half the engine speed, and to a much higher resolution. Test order was randomized and repeated to ensure clarity, and the pressure output of the rate tube was recorded, as well as the injector signal. At the same time, data output from the gravimetric AVL fuel gauge was also

recorded to correlate the results. A schematic diagram of the rate-tube is shown in Figure 4-4.

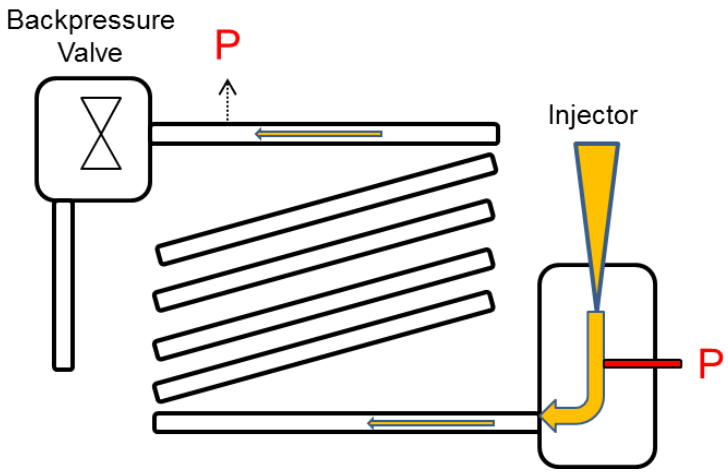

Figure 4-4: Schematic of rate-tube setup

4.2.2 Processing the rate-tube data

A typical output from the rate tube test rig for a split injection is demonstrated in Figure 4-5 and represents the pressure reading from downstream of the injector. Indicatively, time is zeroed at engine TDC. The rig records pressure at a rate of 10^5 signals per second (2.2 samples per °CA at 750 RPM). For this case, the commanded start-of-injection phasing was 358°CA, and the apparent fuel delivery starts approx. 0.5°CA later. As can be seen, there is a notable “bounce” after the initial pressure wave of the fuel delivery, where the pressure transducer output first becomes negative and then rises again before stabilizing near zero (between 362^oCA and 364^oCA ATDC). This is deemed to be an artefact and is normal for this level of back pressure. Evidently, it does not represent fuel that went back into the injector, so in order to filter the erroneous data out only the volume of the pressure curve that was positive was used to calculate the actual fuel flow. The subsequent “bounce” after the depression also does not represent positive flow, as by this time the injector has closed and is merely a legacy of the preceding artefact.

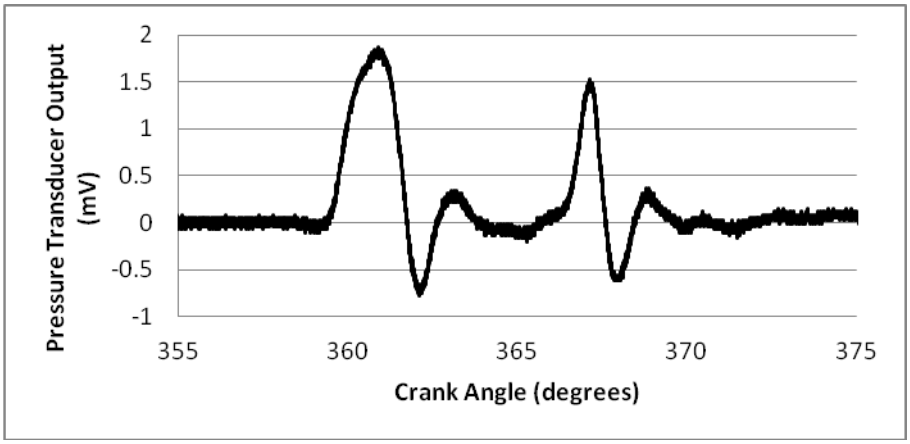

Figure 4-5: Typical pressure output of Rate Tube

The pressure rig used was originally designed to effect experiments on gasoline direct injection and as such was intended to handle fuel pressures of up to 200 bar and is therefore not an optimal length for diesel injection pressures in the order of 700 bar as evaluated here. Even in tests at 200 bar, the “bounce” is still evident, however rather than visibly complete several periods it only displays one peak and then becomes indistinguishable from the background noise. Regardless, as the artefact appears after the event in question and its duration does not extend into the next cycle it is of no consequence to the experiment and is ignored. The total volume delivered per injection event is calculated based on the volume under the initial positive part of the pressure curve. The injector rate tube comprises of a long steel pipe of constant diameter which is filled with fuel and the injector sprays into it a few millimetres above a pressure transducer. The shape of the pressure wave as measured is directly in proportion to the injection rate of the injector and can be evaluated by using Equation 7.

$$q = \frac{p \times A \times 10^5}{6 \times n \times \rho \times a}$$

Equation 7: Pressure within rate tube

Where “A” is the internal area of the tube in mm, “p” is the density of the fluid in kg/L, “n” is the cam speed (half the engine speed) in RPM and “a” the velocity of sound in the fuel in m/s. A subsequent multiplying factor is also included to account for the

specific trim setting of the amplifier circuit which was in-line between the pressure transducer and the data recording equipment. The value of the factor depends on the specific settings of the signal amplifiers and is confirmed by running a calibration test to correlate the data with a known test-point.

4.3 Rate tube data analysis

The corrected pressure wave output at each test-point was integrated and subsequently the fuel quantity delivered per cycle was estimated. This was then converted to fuel consumption per hour and tabulated in Figure 4-6 alongside a graph of the same fuel flow data from the AVL gravimetric fuel gauge, taken during the exact same tests. Indicatively, the AVL gauge was measured for a period of 150 sec for each test-point and the values then corrected using Chauvenet's criterion.

The AVL gauge is known to be accurate to within 4% however despite this moderate error the data aligns very closely in all but some minor outliers. This confirms the existence of the stationary wave (and by association demonstrates it is not an artefact of inadequate or faulty fuel flow measurement). It also demonstrates the wave is of a sinusoidal pattern with decaying amplitude and a constant period (6°CA) which is exactly that of the period observed in the 750 RPM engine tests, when measuring peak-to-peak.

Worthy of noting is the actual commanded fuel delivery: Given the command was for two injections of 3 mg each, ideally, 0.27 kg/hour of fuel should have been delivered. With the exception of the 9°CA dwell-time which surpasses it, only the peaks of the waveform reach the commanded delivery quantity suggesting that fuel-line resonance is only likely to result in an over-delivering effect if the affected injection event occurs at the first peak of the wave.

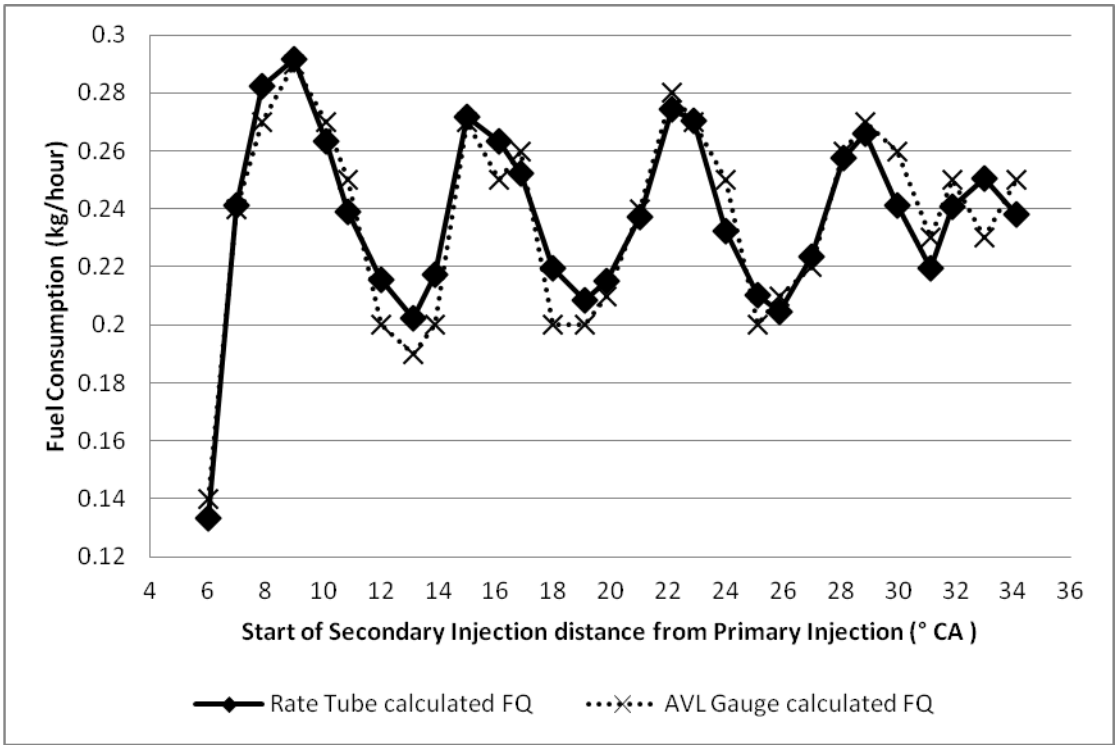

Figure 4-6: Fuel consumption versus secondary injection start of injection delta from primary.

Single injection cycles are not affected by pressure pulsations, and as such the measured accuracy is within the range of errors induced by the measuring equipment and the range of uncertainty in the engine calibration tables. By inference, the first injection event of any multiple injection cycle should therefore have a similar level of accuracy. For the multiple injection cases presented here, the first injection is commanded to deliver 3 mg; this quantity was verified to be identical throughout all tests. As such, and given the measured total fuel quantity, it is possible to infer the secondary has varied from as little as 1.22 mg to as high as 3.45 mg (from a total fuelling between 4.22 and 6.45 mg/cycle). This correlates well with empirical evidence: when trying to correctly calibrate an engine setting to account for fuel-line resonance, an over-pressurised second split is simpler to adjust for than an under-pressurised one, as the latter may require a particularly long duration to compensate which may result in spray being delivered too late to be of meaningful use.

The extremely low first data point can be easily explained by ECU boundary: as has been explained earlier, there is a minimum threshold to how close in time the end of an injection event can be to the beginning of a subsequent injection event.

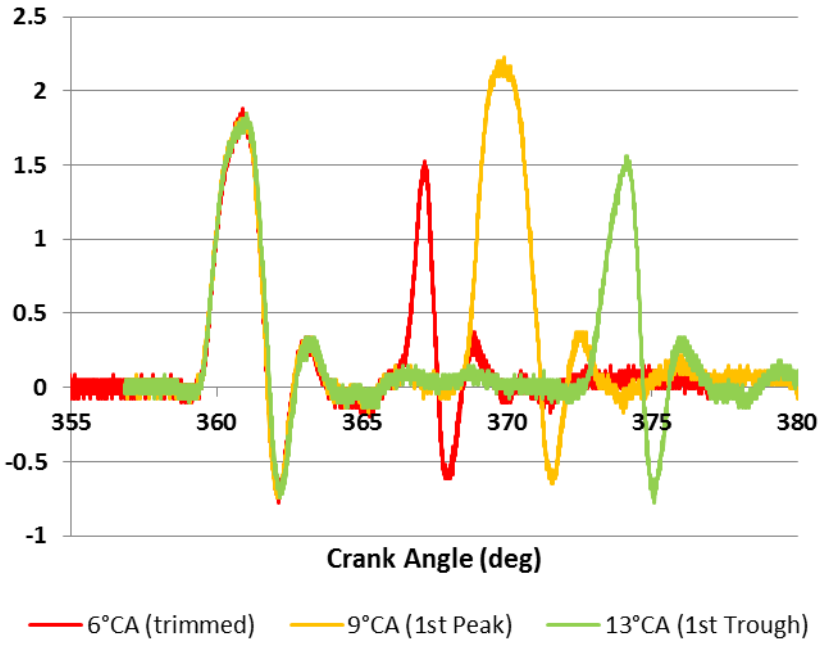

Figure 4-7: Pressure output comparison of 6°CA , 9°CA and 13°CA test-points, showing the trimmed first point, and the two points with the highest disparity between results.

In this case the test-points were suitably close that the ECU was forced to trim the duration of the second injection event, resulting in noticeably reduced primary injection duration (red line “6°CA(trimmed)” in Figure 4-7), and therefore is not representative of the effects of fuel-line resonance as the injector could not perform the requested operation. A graph including this trimmed point, the first peak and the first trough (the couple with the largest degree of disparity) is demonstrated In Figure 4-7. Two things are immediately apparent: Comparing the yellow (9°CA “1st peak”) and green (13°CA ”1st trough”) it can clearly be seen there is a significantly larger fuel delivery event in the “peak” than the “trough”. This is the largest disparity recorded. The second thing immediately visible is that the earliest point (in red, 6°CA “trimmed”) is indeed trimmed; this is not exclusively a measurement affected by fuel-line resonance, it is in part attributed to ECU minimum dwell-time limit restriction. As

mentioned in Chapter 3.1, the ECU cannot handle injection events demanded too close together without adjusting the quantity delivered in order to ensure the minimum dwell-time is maintained. This explains the extremely low first point in the fuel consumption graph in Figure 4-6. It should also be noted that the y-axis on Figure 4-7 represents pressure but is not to scale; the exact magnitude of the pressure pulsation could not in this instance be determined, though this measurement is not required to ensure robustness; the same post-processing filter was applied to every test-point and it can be seen that in every instance the first part of the injection (which suffers no effects from resonance) is absolutely identical.

In conclusion, this higher-accuracy test is consistent with the findings about fuel-line resonance so far, indicating pulsations significantly influence fuel delivery during multiple-injection strategies. The influence has been explicitly quantified, and very large variations in excess of 50% in delivered fuel quantity were observed for the second injection in a split-main injection strategy. Although the fuelling quantity can be corrected by adjusting the duration of the second injection event to ensure that the total fuel delivered is correct, the observed significant variation in flow rate through the injector is likely to have a marked effect on the fuel spray after exiting the injector. The influence of this on the combustion event and subsequent emissions needs to be quantified.

A more representative rate-tube (with the capacity for higher back-pressure and higher engine speed) would be invaluable in providing better scientific correlation in future experiments; the naturally high rate of sampling of the spray rig coupled to highly reliable models for correlating spray pressure to mass flow would be invaluable in quantifying the exact relationship between resonance and actual spray delivery. Ideally, an optical setup would be best suited to show changes in the spray behaviour (atomisation, penetration, break-up) but a spray-rig could yield critical information relating rate of injector needle-lift and the gradient of the pressure pulse.

4.4 Incremental complexity tests

Following the findings of injection resonance a series of experiments was designed to demonstrate the effects of increasing injection complexity on the cyclic behaviour of combustion. All tests were conducted at 1500 RPM, with a boost of 0.2 bar and an EGR rate of circa 13% by volume. In every string of tests, the timing was varied in order to get CA50 as close as possible to TDC for optimal efficiency, without exceeding $\Delta P/\Delta\theta$ of 11 bar/°CA. Points around that optimum were taken in circa 2°CA intervals. Emissions data as well as high-speed data of in-cylinder pressure and injector signal were recorded and analysed. In the cases where relevant, the duration of the last segment of split-injections was trimmed on a case-by-case basis to compensate for fuel-line resonance and thus result in an almost identical fuel consumption figure through each string of tests. The test injection parameters are summarised in Appendix 9.1. CA50 was chosen as a variable (as opposed to start of injection or start of combustion) as it relates directly to thermodynamic efficiency and is independent of ignition delay. Using a different variable to represent phasing would not offer as meaningful a spread of data.

In the tests with pilot injection, the pilot's timing and the main injection quantity had to be adjusted slightly in order to ensure consistent fuel quantity delivered, and to avoid covariance artefacts; it has been noted that when demanding very small quantities of fuel delivered, as for pilot injections, certain specific points in the ECU control may deliver an injection that in an attempt to interpolate between two points alternates odd cycles and even cycles at a 0.125° discrepancy.

In each case test sequence was randomized, and several tests were repeated numerous times at random points during the tests to ensure repeatability.

4.4.1 Piloted split-main test parameter selection

When an injection event includes three components, there are six variables, of which five are essentially independent: timing and quantity of each injection, with the only constraint being the total fuelling quantity which will define one of the injection

quantities. A seventh variable is injection pressure: in the work presented here, two rail pressures of 600 and 700 bar were evaluated. These were selected as being representative of the rail pressures likely to be used at low- to mid-load operating conditions in a commercial diesel engine.

In the case of the piloted split-main injection evaluated here, several factors were constricting the selection of the injection timing and quantity. The initial intent was to replicate the piloted-single injection of the previous series, with a 50-50% split. This volume of split was selected as it would facilitate understanding and provide the opportunity to investigate some interesting results while attempting to balance the fuel quantity of each half of the split. Previous work in the literature, as discussed in 2.6.3, has shown that nearly-equal split injections have interesting combustion characteristics but that the specific quantity of fuel in each split is less important than the fact that the single long injection is split in two.

Pilot injection was mandatory in order to maintain a maximum $\Delta P/\Delta\theta$ of less than 11 bar /°CA. In accordance to the 50-50 brief, the first part of the injection delivery was requested at slightly less than half the commanded injection quantity of the previous series main injection. The quantity supplied for the pilot injection was selected as the minimum value that produced a useful effect of reducing rate of pressure rise. As a result, the remaining fuel was retained for the second half of the main injection; in this case, as shown in Table 5 (Appendix 9.1), the second main injection quantity was comparable to the initial pilot injection, after adjusting to ensure correct total fuel consumption.

Several lengths of dwell-time (crank angle difference between the start of the first and second part of the split injection) were screened, and it was found that for this operating condition dwell-times of over circa 7°CA (irrespective of start of injection) would result in unrealistically high smoke emissions of over 1.5 FSN coupled to high HC emissions, indicating large amounts of unburnt fuel in the exhaust, increasing dramatically with increased dwell-time. This correlates well with the concordant trend of decreased IMEP with increased dwell-time.

These findings suggest that exceedingly long dwell time results in fuel injection that was so late it didn't burn, and thus extremely inefficient and detrimental to emissions and power. Given a fixed first split of 3-3.5 mg commanded injection, dwells of less than 5° would cause interference artefacts, as there is a mandatory minimum time between injector closing and subsequent injector opening event, which if not observed resulted in the ECU auto-trimming the first or second split duration (and therefore quantity).

Indicatively, an example of such behaviour can be seen in the preceding chapter (Figure 2-1, Figure 4-6): the first test-point of the rate-tube series of experiments displays drastically lower total fuel quantity delivered due to such a trimming effect as the ECU attempts to adjust commanded events so as to comply with the minimum dwell-time hard-limit. This is normal for any modern multiple-injection system and is more a limitation on the hardware and its control software than anything else. This is typical of even the most advanced common-rail engines and not a specific issue with the experimental rig.

Thus it was decided that 6°CA dwell between the split would be optimal at this given IMEP, engine speed and rail pressure. The second split quantity in every case had to be trimmed in order to obtain correct total fuel-consumption. As per the previous series of experiments, tests were conducted with the optimal efficiency point of CA50 as close to TDC as possible, limited by $\Delta P/\Delta\theta$. Also as per previous experiments, the test points are phased in CA50 terms as this variable is unaffected by ignition delay and easier to detect, therefore more suitable than start of injection, or start of combustion

4.4.2 Results presentation

For the evaluation of the piloted split-main injection, the results are presented in total, after which the key findings are discussed in detail. This method has been selected as it provides a full overview of the experimental findings while grouping the graphs in a consistent location to enable easier comparison between test conditions.

The relevant figures will then be referred to at the appropriate points in the discussion.

The experiments presented are tabulated in Appendix 9.2 with one string of experiments per page. The graphs demonstrated will be (in order) in-cylinder pressure against CA50, heat-release against CA50, in-cylinder pressure standard deviation against CA50, indicated mean-effective pressure and indicated mean-effective pressure covariance against CA50 and lastly ISFC against CA50. The first graph will also include a tabulation of injector signal below the pressure as an indication of injection events in the temporal domain. Its magnitude is not to scale and should not be considered as it does not relate to anything. The figures are ordered starting with single injection (600 bar Figure 9-1, 700 bar Figure 9-2); piloted single injection (600 bar Figure 9-3, 700 bar Figure 9-4); and finally piloted split-main injection (600 bar Figure 9-5, 700 bar Figure 9-6).

The emissions are all presented on one page to facilitate the visibility of trends through the injection regimes; two graphs for each injection regime showing smoke and NO_x on the left and tHC and CO on the right, with both strings of 600 and 700 bar tests tabulated on the same graph for each case. These are shown in Figure 4-8, while the most important trade-offs are shown in Figure 4-9.

4.4.3 Emission findings through injection regimes

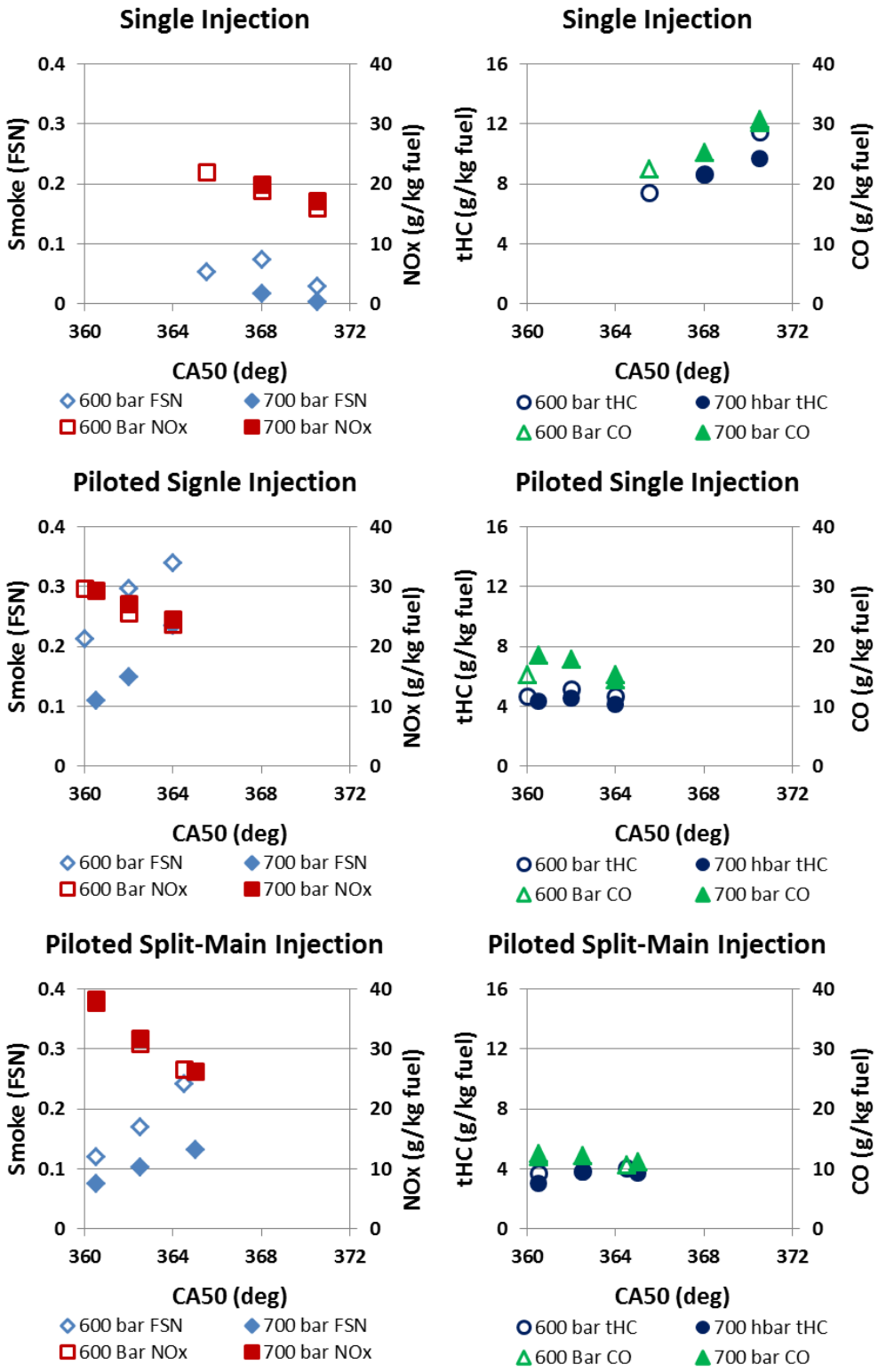

Figure 4-8: NO_x/PM and tHC/CO vs CA50

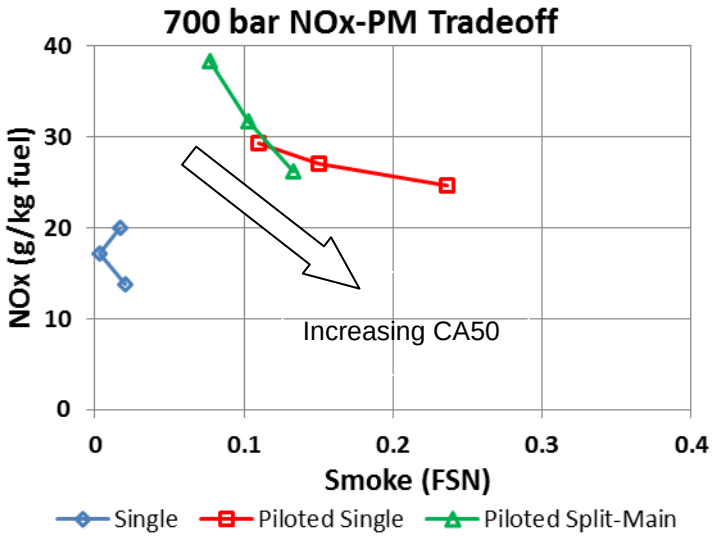

Figure 4-9: NO_x-PM Trade-off

The principal indication of the effects of the multiple injection regimes on the combustion event can be shown from the emissions data, especially of NO_x, PM, tHC, and CO, as these are demonstrative of peak combustion temperature (NO_x), level of mixing (PM), and incompleteness of the combustion event (CO and tHC). As can be seen from the graphs, there are several trends immediately apparent in terms of emissions:

4.4.3.1 Oxides of nitrogen (NO_x)

Nitrogen oxides seem to ignore the transition from 600 to 700 bar rail pressure (Figure 4-8); there's a clear trend with it decreasing as CA50 is later. This correlates well with the corresponding decrease in $\Delta P/\Delta\theta$ and peak pressure which leads to lower peak localized temperatures and therefore lower NO_x formation. This is expected as it is a standard trade-off in compression-ignition.

There is also a somewhat unexpected trend in NO_x: The piloted single cases demonstrate overall lower NO_x across the span of the tests than the piloted split-main cases. This is a side-effect of the CA50 phasing: As the piloted split-main injection's combustion from start to finish lasts a few crank angles longer than the piloted-main's, in order to achieve similar CA50 phasing the pilot injection and the

first charge of the main injection had to be injected slightly more advanced. This implies that both the pilot and the first charge of the piloted split-main start combusting at slightly higher pressures and temperatures than the pilot and the main charge of the piloted single cases. Not only do split-injection regimes start earlier (and therefore have less time to mix) but also last longer, meaning the relatively slow-forming NO molecules have an increased envelope of opportunity to form. There may also be an additional minor effect compounding this: Before the second charge of the split-injection begins a much smaller quantity of fuel has been delivered to the chamber compared to piloted single injection. The relatively higher abundance of oxygen means the first part of the split will burn at a higher temperature, facilitating NO formation, and will result in a hotter cylinder for the second half of the main charge. Also, by “stretching” the combustion with a split-injection there is more time late in the combustion cycle for the second half of the split to form NO via the Zel’Dovich mechanism.

This not only means the temperature is relatively low because not much fuel has been oxidized (therefore keeping the Zel’Dovich-formation NO_x low) but also the relative air-to-fuel ratio is higher, hindering the prompt-formation of NO_x too. By the time the second charge of the split is delivered peak heat-release rate has passed and with it peak temperature, further inhibiting peak slow-NO_x formation.

4.4.3.2 Particulate matter (PM)

Smoke emission appears to be very heavily influenced by rail pressure (Figure 4-8); in every case noted, smoke was decreased notably (less so for single-injection, but as can be seen it was very low to begin with) with higher rail pressure This is well-documented in the literature, with a strong correlation having been established between droplet size and smoke formation, and higher rail pressures produce a finer atomized spray (Badami et al. 1999, Habchi et al. 1997). It is also noteworthy that both piloted single injection and piloted split-main injection clearly show an increase in smoke across their combustion phasing. The presence of the pilot injection causes this in two ways: Firstly, it drastically decreases ignition delay of the main

charge/charges by providing locally hot pockets of volatile gases left over from the combustion of the pilot charge. Decreased ignition delay makes for less mixing time and so the main injection charge/charges have a less uniform dispersion resulting in a higher incidence of locally rich pockets within the chamber, thereby increasing smoke particulate formation. There is also a less pronounced increase from the left-over radicals generated during the pilot's burn, though this is likely to contribute a much smaller portion of the smoke emissions.

With respect to why piloted single injection's overall FSN was higher than piloted split-main injection's, it is more than likely mostly due to smoke-reducing effect of the dwell-time introduced. This reduces the amount of fuel being sprayed into a developing flame which is typically a very smoky part of the combustion process. Introducing the dwell-time allows for some respite in the onset of combustion of the second part of the charge, allowing it to mix better than it would have otherwise and thus reduce the localized richness. There is also a potential minor effect of additional particulate oxidation due to the split-main injection lasting later into the combustion cycle, although more detailed optical analysis or modelling would be needed to evaluate the relative importance of this effect.

Of interest, as can be seen in the NO_x-PM trade-off graphs (Figure 4-9), the trade-off curve is fairly similar between piloted single and piloted split-main cases. This would suggest that there is little difference between the most prevalent NO_x and PM formation (and oxidation) mechanics between these two regimes. There is however a clear trend in PM reduction with a small increase in rail pressure, a trend which will not necessarily hold true in later chapters. Of particular note, however, is the impact of the pilot injection on the NO_x-PM trade-off. Both species are increased by the presence of the pilot, whose only role is to reduce the rate of pressure rise following the initial ignition. As seen in the in-cylinder pressure traces in Figure 9-1 through Figure 9-6, the peak combustion intensity is reduced by a factor of more than 3 (from nearly 1200 to ~400); as the HRR is a function of the rate of change of pressure, this demonstrates that the pressure rise rate has also been substantially reduced. However, these effects come at the expense of significantly increased PM and NO_x

emissions, indicating that further strategies are required to achieve low emissions and acceptable rate of pressure rise (and hence engine NVH).

4.4.3.3 Hydro-carbons and carbon monoxide (tHC & CO)

Total hydro-carbon emissions have two interesting trends. Firstly, they tend to ramp-up quite dramatically as combustion phasing gets very late, as can be seen in the single-injection case, and is clearly indicative of an increased percentage of unburnt fuel as combustion gets later and later in the engine cycle. The second trend visible is the clear improvement in tHC across injection complexity: Single injection tests have significantly higher tHC than piloted single injection tests, which in turn are slightly higher than piloted split-main tests. Carbon monoxide very much follows the trends of tHC, which makes sense as it is often correlated with partial burn, as is the case in the most retarded single injections. This supports the theory that bulk quenching is occurring late in the combustion cycle.

4.4.4 Variability of needle lift and how it affects modern injection regime

Understanding the reliability of the injector is paramount in interpreting the results from a repeatability perspective; if the injector is found to be performing exactly as requested by the ECU it can be safely assumed that any variance in fuel delivery is not due to the injector's lacking behaviour. This analysis aims at determining whether there is any cyclic variation in the behaviour of the injector given a fixed opening signal.

4.4.4.1 Needle-lift experiment-specific methodology

Needle lift was measured via a Hall-effect instrumented injector. The injector had identical specifications to the normal injector for this engine. The injector's measured needle lift was compared to the command signal sent to the injector (measured using a non-intrusive current probe on the injector driver line). The results showed that variations between the command signal and observed needle lift were less than the resolution of the crank angle encoder.

4.4.4.2 Typical needle-lift behaviour

A typical injection event's standard deviation is demonstrated in Figure 4-10 . The injector needle lift standard deviation (NL-SD) is negligible at all points except where the needle begins to close after a large delivery. This is significant as it implies that cycle-to-cycle variance is extremely low, therefore any inconsistent behaviour that is observed is unlikely to be due to poor injector repeatability.

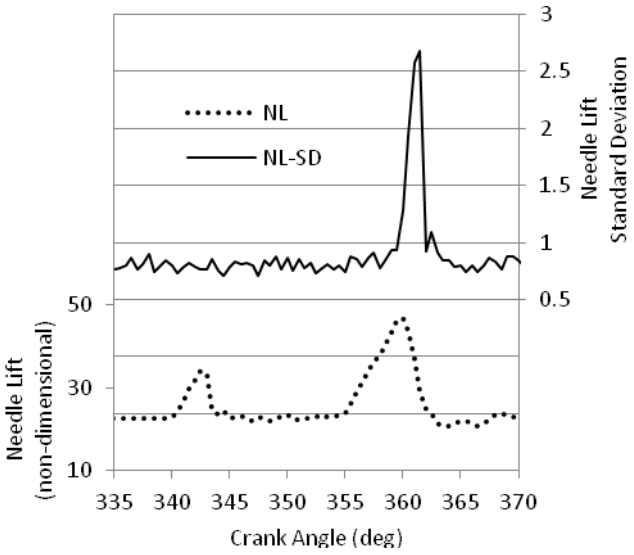

Figure 4-10: Injector needle lift standard deviation against crank angle and injector needle lift against crank angle. Case is piloted-single injection

The spike at start-of-injector-close is visible in all major injection events and is most likely a result of a time-delay discrepancy in the rate of discharge of the needle's coil. This SD spike lasts for most of the closing event, and peaks at values of up to 2.5, though the majority of tests were under 1.6 (indicatively, the needle's peak height was around 50. This is in a non-dimensional representation of height.)

There were no discernible trends that linked this behaviour to injection regime, engine speed or rail pressure. Variation in the opening portion of the injector's performance was not discernible above the background noise in the needle lift (NL) signal. This implies that the part of the NL that's actuated by the coil is extremely repeatable. Coupled to the high repeatability of the output from the fuel-rail's pump

and tightly controlled signal sent to the injector, it is not expected that the actual injection quantity would be changing significantly over the test duration (200 consecutive cycles). It should be noted that the case shown in Figure 4-10 is the most extreme example of non-perfect NL behaviour, in most injection scenaria NL displays next to no variation cycle-to-cycle and when it does display peaks of NL-SD, they are always of the exact same shape as this case, though mostly of a maximum SD below 1.8.

4.4.5 Variability of in-cylinder pressure and relation to injection regime

In-cylinder pressure variability demonstrates some characteristics which are constant throughout the tests: It always rises quite sharply as soon as combustion commences, stays very high for a few crank-angles and then drops just as sharply to a plateau, at which it stays for most of the combustion before petering-off towards the end. In order to understand this behaviour it is necessary to consider what exactly ICP-SD represents: High ICP-SD essentially means a reduced level of repeatability in in-cylinder pressure at that specific crank angle, on a cycle-by-cycle basis. Therefore, it is natural that the onset of combustion displays a sharp rise in instability: Occasionally, a cycle will display an unusually early or late start of combustion compared to the mean. This means that at that specific crank angle, on some cycles the pressure will be identical to the baseline (as combustion may not have started), on some it will be moderately high (as combustion has just started), and on some it will be very high (as combustion will have already started a few degrees ago). This, in part, accounts for the very high spike in ICP-SD around the start-of-combustion point.

This explains, however, only part of the effect; there is also great disparity in repeatability depending on the injection regime implemented: Single injections are a lot less repeatable than injections with pilot. It can be clearly seen that single injections peak at between 1.2 to 1.4 bar for 600 bar rail pressure, and between 1.5 and 1.6 bar for 700 bar rail pressure. This is a very much higher value than the peaks of both piloted-single injection and piloted split-main injection (0.4 to 0.6 bar,

and 0.3 to 0.65 bar for 600 bar rail pressure respectively. 0.4 to 0.8 and 0.3 to 0.9 bar for 700 bar rail pressure respectively). The reason for this effect is clearly the presence of the pilot injection, which provides a very reliable environment which initiates combustion with high repeatability at a very specific point in the cycle. Variability in the pilot ignition timing itself is also observed, with a first peak in ICP-SD for the cases with pilot injection; however this variability does remain below the that seen from the start of the main combustion event, which is normally associated with the highest value of ICP-SD. This relationship between peak values of ICP-SD and start-of-combustion for the fuel injected in various injection pulses will be discussed in more detail in chapter 5.2.2. At this point, suffice to point out that, even with the piloted split-main cases, it is possible to identify three distinct peaks in ICP-SD which appear to relate directly to the combustion of the three separate injection events.

Looking at single injection there is an observable trend linking peak ICP-SD and proximity to top-dead centre: With the exception of the earliest test at 700 bar, the closer the start of combustion is to TDC the lower the peak ICP-SD. This correlates well with what is expected at extremely late injections: Eventually the injections are so late into the cycle that they begin to exhibit misfiring, which would make ICP-SD increase dramatically. The further away from TDC the combustion event is phased, the less repeatable it becomes, eventually not even reliably occurring.

In the cases of piloted-split main there appears to be an odd trend: Advancing CA50 seems to simultaneously increase the ICP-SD of the first half of the split-main injection's combustion, but lower the ICP-SD of the second half of the split main's combustion. It is not clear why this is so, in fact it is counter-intuitive: It stands to reason that a higher instability in the first half's combustion would lead to a more irregular environment at the time of the second half's injection, and therefore a less-repeatable combustion of the second half.

There may be some incidental correlation between ICP-SD and rate of pressure rise ($\Delta P/\Delta\theta$), though this is not really a finding as a coincidence: Highest rate of pressure rise occurs at or shortly after start of combustion, which is also where highest ICP-

SD occurs. For a combustion regime with naturally high ΔP/Δθ any disparity in start of combustion amplifies the magnitude of ICP-SD, as there's a possible rapid increase in pressure, rather than a possible less noticeable increase in pressure. To wit, a very rapid combustion may increase at a peak rate of 10 bar per crank angle, while a much smoother one may increase at a peak rate of 3 bar per crank angle. Assume the mean starts combusting at an ambient pressure of 50 bar. Assuming that one in ten cycles ignites one crank angle earlier than the mean (say 360° instead of 361°), for the more volatile experiment the value of pressure at 361° would 60 bar (instead of the mean of 50) while the pressure at 361° would be 53 bar (instead of 50) for the smoother experiment. In turn, the volatile test would return a higher ICP-SD value at that crank angle, even though in both cases only one-in-ten tests started to combust only one degree earlier than the mean.

It is possible to discriminate between how much of the ICP-SD magnitude is caused by actual discrepancy in cycle-by-cycle behaviour of the combustion and how much is caused by discrepancy in cycle-by-cycle behaviour of purely the in-cylinder pressure by examining ICP-SD of a non-injecting cycle. Subtracting the ambient ICP-SD from the observed ICP-SD it is possible to accurately compare the characteristics of in-cylinder pressure repeatability between engines. In general, the background ICP-SD is very low (less than 0.2 bar) and hence the spikes observed at the start of the combustion event can be seen to clearly define the start-of-combustion phasing. However, the gradual reduction in ICP-SD as the combustion progresses makes it impossible to use this measure as a reliable indicator of end-of-combustion phasing or combustion duration.

4.4.6 Indicated mean effective presure (IMEP) and indicated specific fuel consumption (ISFC) findings through Injection Regimes

Overall IMEP was very consistent throughout the tests, there does not seem to be any trend developing in IMEP-CoV. In some strings of tests increased rail pressure increases IMEP-CoV and in some it decreases it, though it is not clear why. It could be argued that with the exception of the 700 bar rail pressure piloted single injection,

the existence of a pilot has slightly decreased IMEP-CoV compared to single injection tests, but there isn't enough evidence to support this, nor is it certain it isn't simply an artefact of the much earlier combustion phasing achievable in the cases with pilot.

Irrespective of the lack of correlation between findings and IMEP-CoV values, IMEP-CoV remains decidedly low overall: Barring the 700 bar piloted single injection all tests displayed an IMEP-CoV of below 2% which indicates smooth running and consistent power output cycle-by-cycle. Plots of the IMEP and IMEP-CoV are plotted in Figure 4-11. This is within the limits expected of automotive diesel engines (Zarling et al. 1993). This is an important finding because it suggests that the introduction of complex injection strategies has not significantly impacted the torque output variation. Heywood (1988) suggests that an IMEP-CoV of above 10% would result in drivability issues, though this information is neither quantified nor explained further.

There does not appear to be any correlation between ICP-SD and IMEP-CoV. While it might be presumed that there should be at least some connection between cyclic variance of in-cylinder pressure and mean effective pressure, there are no discernible trends in either magnitude of peak, overall shape or phasing of ICP-SD that correspond to similar IMEP-CoV findings. This is logical as IMEP-CoV is measured over the whole cycle and ICP-SD displays flux of a very small magnitude and only over a very small section of the cycle.

If there was correlation between them it would signify that either ICP-SD is highly irregular over a very segment of the cycle, like perhaps if the combustion was borderline not firing, or borderline quenching (whereby some cycles there is combustion and some cycles there is none.) A comparative graph of ISFC against CA50 for all tests can be seen below (Figure 4-12) Hollow markers represent 600 bar rail pressure tests, while solid markers 700 bar rail pressure.

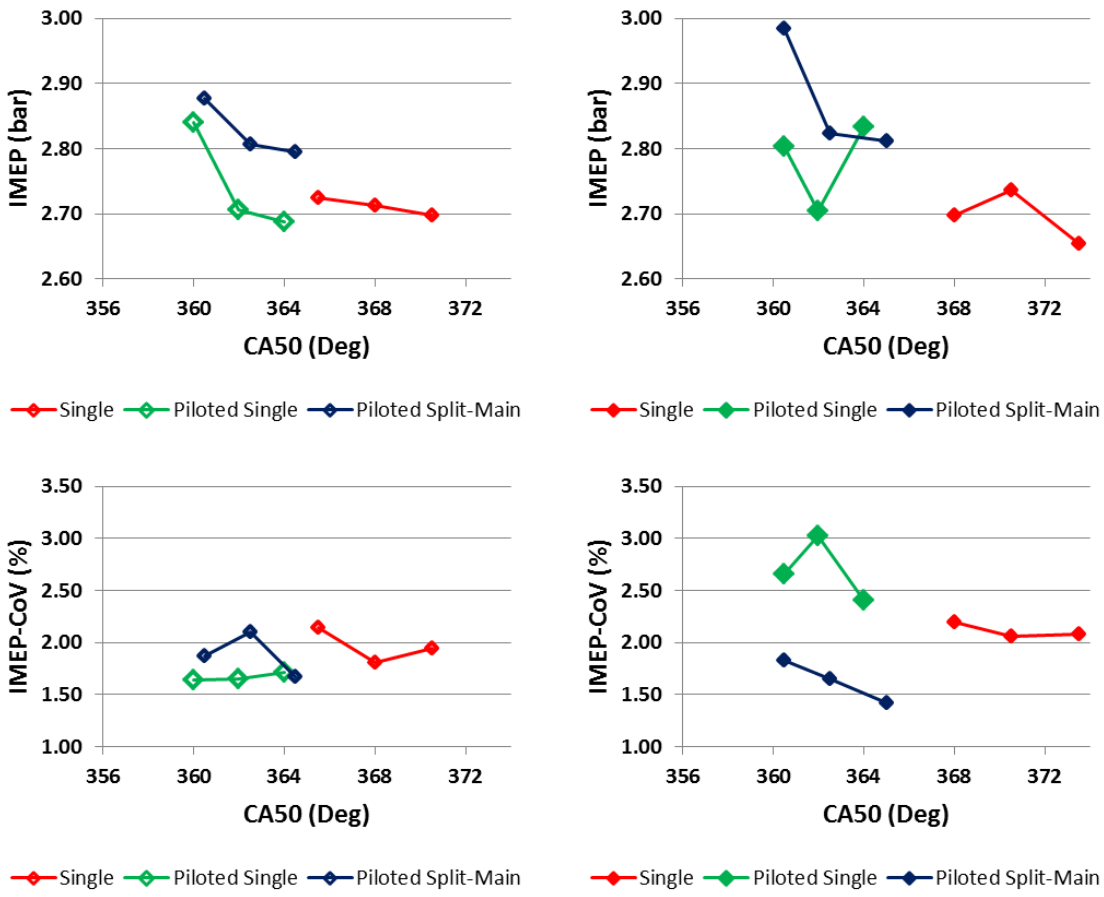

Figure 4-11: IMEP and IMEP-CoV vs. CA50. Left: 600 bar Prail. Right: 700 bar Prail

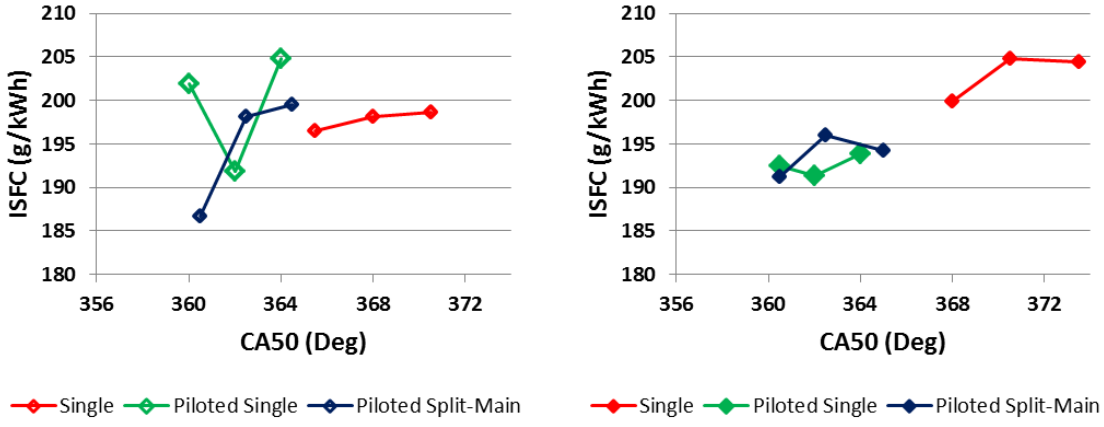

Figure 4-12: ISFC vs. CA50 for all tests. Left: 600 bar Prail. Right: 700 bar Prail

Neither is there any significant trend observable in ISFC; throughout all the tests ISFC varies from a peak of 201 to a trough of 186 with all other values between 191

and 199. Overall this suggests a remarkably consistent, if unimpressive, fuel efficiency. In truth, the main reason the ISFC is tabulated in this chapter is to facilitate comparison with ISFC in subsequent chapters, where its flux will be seen to be a lot more pronounced.

4.5 Summary: How complex injection strategies have changed compression-ignition combustion

The results presented in this chapter have shown the implications of advanced injection strategies on injector performance, combustion and emissions of a light-duty diesel engine operating in part-load conditions. The key findings were:

- Pressure pulsations in the fuel rail caused by injection events severely influence the pressure of the fuel (and therefore the quantity) delivered in subsequent injection events that happen in the same engine cycle. The pulsation effect is too short to affect injection events in different engine cycles, but can seriously impact the combustion of complex multiple-injection strategies

- Minor injections such as pilot injections cause minor or undetectable stationary waves. Large injection events, such as the first part of a split-main injection have a significant influence on later injections.

- Injector actuation repeatability is not correlated with cycle-to-cycle combustion variability. For both single and multiple injection strategies, the phasing of injector opening, injector fully-open and injector closing were extremely repeatable. The only portion where injector performance was less stable was the initiation of injector closing, though this instability disappears before the end of injector closing.

- Rate-tube testing confirms the difference in fuel delivered when the second half of a 50-50 split-main injection is altered in phasing without accounting for the difference in delivery pressure due to fuel-rail resonance. It is also clearly

demonstrated that the fuel-rail stationary wave is a decaying-amplitude sinusoid that is unrelated to engine speed or combustion conditions.

- For all combustion events the ICP-SD generally follows a trend: A brief spike from the start of the charge's combustion which then drops to a plateau that decreases as the combustion advances. This holds true of any large injection/combustion event.

- Pilot injections greatly reduce both peak and plateau magnitude of subsequent injection's ICP-SD. This indicates a pilot injection stabilizes the phasing and reduces the variability of the main injection's start of combustion.

- The introduction of a pilot injection greatly increases the repeatability of the combustion. Having the products of the pilot injections combustion in the cylinder greatly stabilizes the ignition delay of the main charge, whether it is a split injection or a single.

- Supplementing an injection regime with a pilot injection dramatically increases the potential to phase the combustion earlier without excessive cylinder pressure rise. This is due to the effect it has on reducing $\Delta P/\Delta\theta$. It is most likely this earlier phasing that is predominant in reducing tHC and CO emissions rather than the advent of the pilot injection, but regardless, pilot-injected regimes are superior to equivalent regimes without pilot injections.

- Pilot injection has a negative effect on PM emissions, as it reduces ignition delay. Shorter ignition delay leads to less local mixing and therefore more local rich pockets within the chamber when the main charge ignites. Therefore, introducing a pilot to an injection regime will generally increase PM. This effect is partially mitigated by splitting the main injection; the brief dwell between the delivery of the second half of the main injection allows for slightly more mixing time, thereby reducing PM.

- NO_x decreases as Pmax decreases. The earliest-phased test-points were also those with the highest peak pressure. As test-points became

progressively more retarded, NO_x emissions decreased. This is because the later combustion timing results in lower combustion temperatures, and high temperature is the most significant factor in NO_x formation.

- IMEP is highly repeatable throughout tests. The increase of injection complexity did not significantly impact the cycle-by-cycle repeatability of IMEP, nor is there any discernible trend in ICP-SD behaviour and IMEP.

4.6 Novelty of knowledge gained

By looking at how complex injection strategies affect injector performance and therefore combustion characteristics it is clearly visible that complex multiple-injection strategies require an increased level of attention during their design, calibration, and implementation. These experiments looked at several tests of increasing injection complexity in a novel way, investigating atypical factors and attempting to determine the cyclic behaviour of in-cylinder pressure as well as needle-lift and IMEP, in a way which has not been done before. Also, the nature of fuel-line resonation was investigated in a novel way and shown to be a decaying sinusoidal wave following large injection events which can and does significantly affect subsequent injections.

5 Start of combustion investigation

Sections of this chapter have been presented in ICEF2010-35069 by Michailidis et al., 2010.

Investigating the cyclic behaviour of in-cylinder pressure revealed a behavioural trait: there's a discernible trend possibly correlating in-cylinder pressure to start of combustion; Accurate determination of start of combustion is fundamental to correctly understand and interpret ignition delay, and it may be possible the cyclic behaviour of combustion will offer insight into its determination.

5.1 Current Start of combustion determination tools

In order to determine whether ICP-SD is a valid tool in the determination of SoC it is necessary to investigate conventional methods as well as more complex recent ones. Methods of SoC determination are derived through the pressure-trace, the most common being defined as the point in the engine's cycle where the pressure (after accounting for the change in pressure due to any change in volume) rises to the height it had before the injection event, immediately following the small cooling effect the injection had on the cylinder pressure (Aligrot et al., 1997) This viewpoint however is dated and was originally designed to detect SoC in a combustion bomb rather than an engine. It also is inherently less accurate as clearly some amount of heat was released before the indicated point, and therefore there were significant exothermic reactions which preceded the suggested SoC. It is also inaccurate in cases where a pilot injection was employed, as the small amount of heat released from the pilot's combustion more than off-sets the minor cooling effect of the spray vaporization, making it almost impossible to pin-point where the "zero" reference point is. More modern work performed by Assanis et al. (2003) indicates the second-order derivative of HRR may be more accurate and more repeatable than using simple rate-of-pressure rise. More recently Katrašnik et al. (2006) have suggested the third-order derivative of ICP to be a superior indicator, particularly in the case of low engine loads where the second order derivative may display less accuracy.

It should be noted at this point that there is no commonly accepted consensus as to which exact event heralds the "start of combustion". Whether it is the point that the fuel starts to react to form free radicals, or whether it is the first exothermic reaction that occurs, or even the first reaction that involves oxidation. In this case, however, the exact definition isn't significant; the accurate identification of SoC is a lot more useful to the understanding of compression-ignition than its precise definition. The use of SoC is fundamental in determining ignition delay and therefore inferring the level of mixing that took place prior to combustion. It is also fundamental in determining combustion duration (again, depending on the definition of combustion end). As with many such markers, the accurate and objective definition isn't nearly as useful as the consequent understanding that is gained through their use in comparing conditions. What is necessary is that the method used to identify SoC be consistent and repeatable, with a high degree of accuracy, and reliably transferable between engine platforms so as to be a useful tool in the understanding and interpretation of combustion.

5.2 Comparative analysis of Start of combustion determination tools

Understanding exactly when and why each method is superior in determining start of combustion is fundamental in being able to accurately evaluate which is optimal, and under what circumstances.

5.2.1 Specific experimental methodology

In order to compare the SoC determination tools two injection regimes were examined: a single injection and a piloted single injection. The conditions selected were 1500 RPM, 600 bar rail pressure, with 18.5 mg of fuel injected at 355.1°CA after top-dead-centre (ATDC) of the air exchange strokes (4.9° BTDC of the firing cycle). For the pilot injection, an additional 1.8 mg at 340.1°CA ATDC (19.9°CA BTDC) was injected. A higher load than in previous experiments was selected to ensure strong combustion with a high amount of heat release for clarity. Once

stabilized, samples of 200 consecutive cycles were collected and processed. Both test-points were carried out in diesel and a 30-70% GTL-diesel blend by volume to establish whether fuel composition or characteristics affect the validity of each method.

The start-of-combustion methods evaluated here are all based on the in-cylinder pressure. For this work, the average pressure is calculated at 0.5^{o}CA resolution over 200 cycles. This averaged pressure was then used to calculate the heat release using Equation 3: Heat release rate equation (chapter 3.1.1).

By working with heat release instead of raw in-cylinder pressure deviation from the flux of cylinder pressure due to volume change (rather than combustion) is filtered out. The heat release was then differentiated three times, to output the first, second and third order derivatives, corresponding to the three methods of determining SoC.

As has been suggested in the preceding chapter, an alternative method for identifying the start-of-combustion is to look at the cycle-to-cycle variability of the pressure trace. This was done by forming a matrix whose columns each represented the pressure-trace of one engine operating cycle. The standard deviation of each row was then taken to form a column matrix which represented the standard deviation of in-cylinder pressure across the whole operating range. This was then differentiated three times. Figure 5-1 shows the three derivatives plotted for the single injection diesel. Their ambient noise can be seen to be below 0.15 before the start of combustion, and clear inflection points are visible in all three derivatives at 363.0°CA 362.5°CA and 362.0°CA respectively for first, second and third order derivatives. Note that start of injection is denoted by the vertical line at circa 355°CA. as expected, each consecutive derivative shows a slightly earlier inflection point. For ease of viewing the inflection points of each signal are signified by a colour-coordinated circle

The third order derivative represents the “jerk”, or the rate of change of acceleration of the standard deviation; its commencement and subsequent inflection point (which does not necessarily have to be positive) is brought about by the start of a change in

the trend of in-cylinder pressure. Before combustion, each cycle's pressure was practically identical to the previous for any given crank angle. In some cycles we observe early onset of combustion (for whatever reason) and consequently the standard deviation increases sharply to mirror the discrepancy in start of combustion between cycles.

The variation in ICP-SD is a good indicator of SoC as cycle-to-cycle variability exists for all engines; if each cycle the engine ignited at exactly the same point with exactly the same rate of heat release the ICP-SD would be zero throughout the combustion. However, as the combustion varies even slightly each time and especially as the variability (and therefore the likelihood it differs from the mean) is particularly high at the start of combustion due to spatial variations in ignition and the distribution of fuel and air in the cylinder, significant variability is to be expected around the timing the first sustained exothermic reactions commence. Using an average pressure-trace to derive the heat release rate may not accurately resolve the premature initiation of combustion. Therefore it is proposed that the jerk of ICP-SD may indicate start of combustion, or possibly the earliest onset of start of combustion.

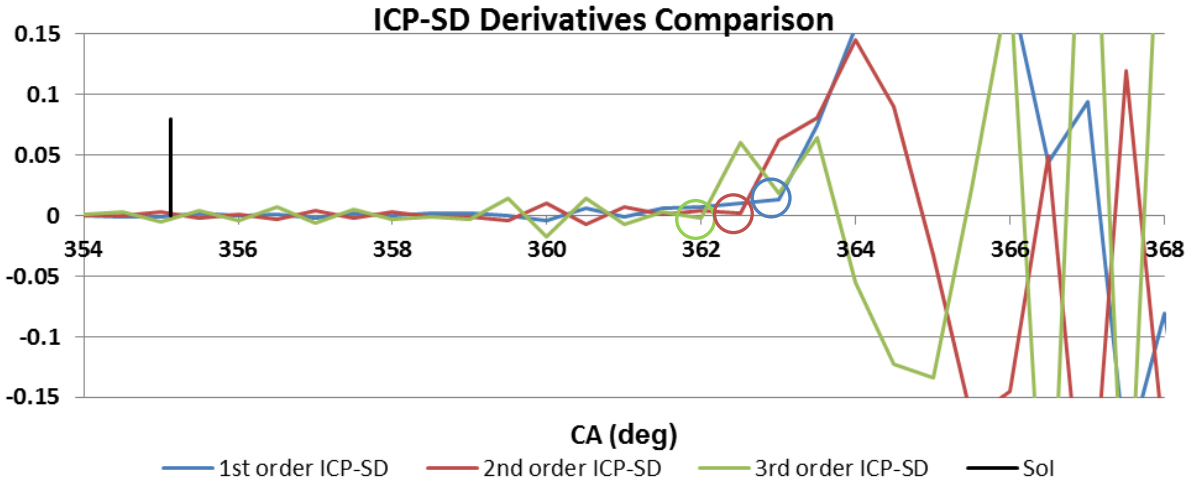

Figure 5-1: Comparison of ICP-SD Derivatives, diesel single injection

A vertical line in black represents the start of injection of the main charge (SoI), while for the piloted-single cases one in red denotes the pilot injection (PSoI). In order to facilitate direct comparison of the methods, when plotted together the 3rd order

derivative of ICP-SD has been multiplied by a factor of 1250 in order to give a good visual comparison. As such, direct comparison of magnitude with HR derivatives is meaningless, as is direct magnitude comparison between HR derivatives. What is significant, is comparing the behaviour of each measuring tool before combustion and after, and noticing the change in behaviour between the two states (clearly not combusting vs. clearly combusting). Most usually a violent inflection point precedes the transition. Note that the inflection point denoting SoC has to be positive in all cases of HR derivatives, representing a sudden increase in rate of heat release (or acceleration of HR, or jerk of HR) while either a positive or negative inflection point in the case of ICP-SD third order may denote deviation from the background pressure.

5.2.2 Comparing the four methods

For this comparison Figure 5-2 and Figure 5-3 will be used: On these graphs, the first, second and third order derivative of heat release will be plotted along with the third order derivative of in-cylinder pressure standard deviation against crank angle. It should be noted that the Y-axis is non-dimensional and does not represent anything. The comparison only relates to behavioural changes in the noise pattern of each marker, as such violent inflection points are much more meaningful than absolute values. In each of these methods, a large spike or gradient change is used to denote start of combustion, therefore to facilitate comparison some have been scaled. The heat-release rate has also been plotted in a dashed-line. This is offset to below the graph in order to minimise interference and is not to scale. While not directly useful in comparing the methods it does give a rough indication of the in-cylinder conditions and facilitates understanding how the heat release relates to each start of combustion indicator. For Figure 5-2 the inflection points have been denoted by colour-coordinated circles, while for Figure 5-3 bright red circles have been used. This is because in the latter figure, high amounts of ambient noise made distinguishing them difficult otherwise.

For single injection with diesel all the methods yield comparable results (Figure 5-2), as was expected in diesel 1st, 2nd and 3rd derivatives of HR yielded consecutively

earlier SoC timings of 363.5°CA, 363.0°CA and 362.5°CA respectively, while the 3rd order derivative of ICP-SD had a clearly visible inflection point at 362°CA. When running the same point in GTL fuel HR derivatives likewise gave a similar output: 362.5°CA, 361.5°CA and 361.0°CA for 1st, 2nd and 3rd respectively. ICP-SD jerk showed an inflection point at 363.0°CA, which is too late in comparison, though had a high magnitude from circa 362.0°CA.

For piloted single injection the results are more atypical. With diesel, though there is a disturbance caused by the combustion of the pilot the magnitude is not such that it significantly impedes the identification of behavioural changes after the injection of the main charge. 1st, 2nd and 3rd order HR derivatives indicate SoC as 360.0°CA, 359.5°CA and 360.5°CA respectively, while the 3rd order ICP-SD derivative indicates 361.5°CA, which is significantly later than all three conventional methods. Importantly, none of the HR based methods clearly identify the start-of-combustion of the pilot separately from that of the main injection. However, the ICP-SD case can be seen to show a significant inflection at 350.0°CA for diesel and 351.0°CA for the GTL blend; this indicates ignition of the pilot. This demonstrates the strength of the ICP-SD method. Heat releases are shown for comparison purposes just below each graph but are not to scale.

With G30 it is easily seen that all three HR derivatives suffer from a high degree of background noise due to the pilot injection (particularly between 342°CA to 348°CA and 352°CA to 360°CA). Thanks to the pilot combustion's high repeatability and consistent cycle-by-cycle behaviour, though it does affect ICP it affects ICP-SD much less, as can be seen in Figure 5-3. In the graph, the variations of all three HR derivatives before and around the main start of injection (355°CA) is so high that identifying the main charge's SoC point from HRR derivatives is impossible. For this test case, SoC appears to be at 361.0°CA according to the 3rd order ICP-SD derivative. HR derivatives suggest 359.0°CA for the 1st order, 360.0°CA for the 2nd and are inconclusive for the 3rd order derivative. As with diesel fuel, the separate ignition of the pilot can be identified (at about 350°CA) with the ICP-SD method but not with any of the HR-based methods.

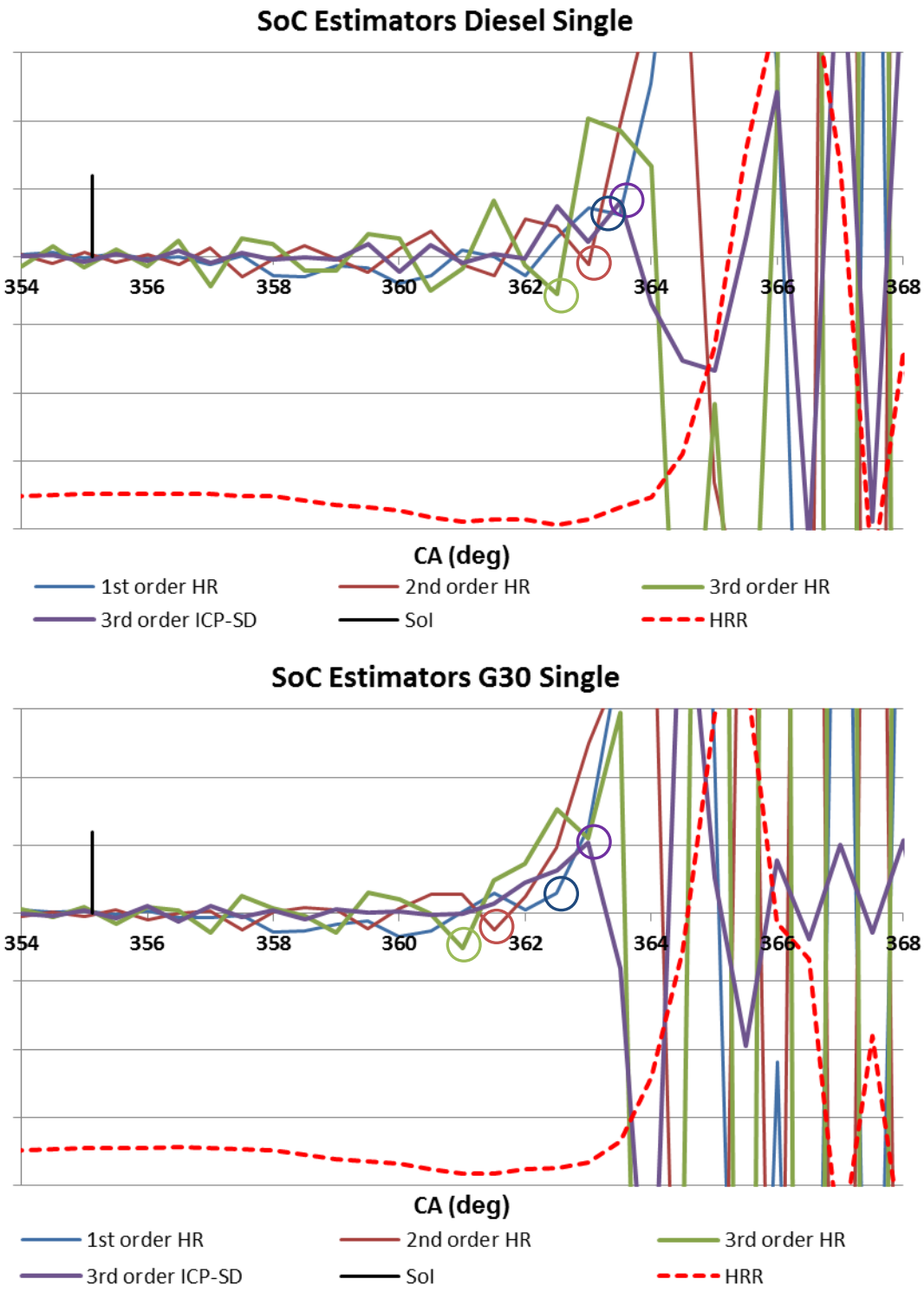

Figure 5-2: SoC estimation methods for single injection with Diesel and G30 fuels. SoC inflection points signified by colour-coordinated circles.

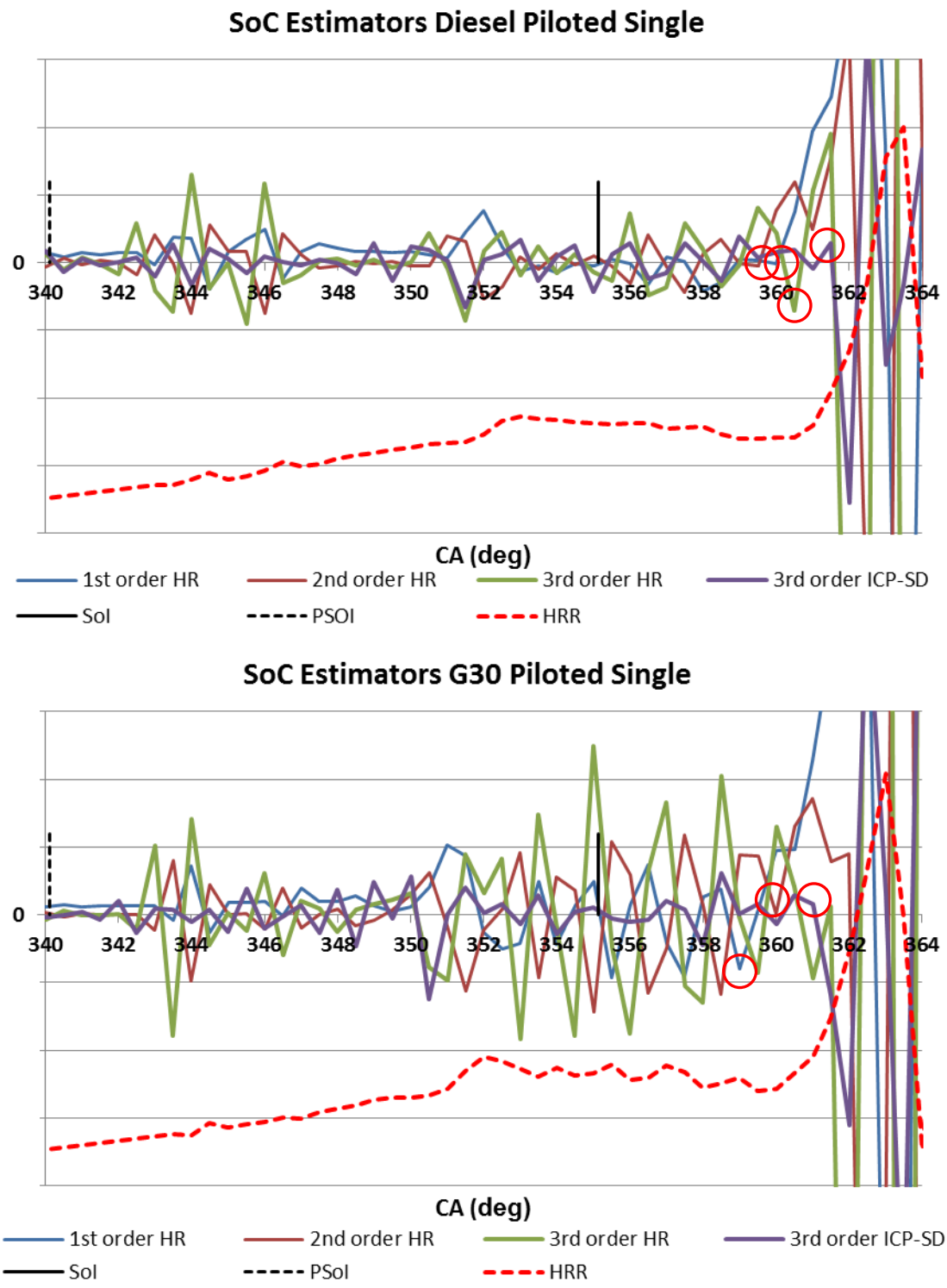

Figure 5-3: SoC estimation methods for piloted injection with Diesel and G30 fuels. SoC inflection points signified by red circles where possible.

An argument could be made that perhaps conditions are such that the main charge ignites immediately as soon as injection starts, however this is not possible: mixing has not occurred, neither has the fuel fully vaporized or heated up, nor could the spray have developed. Also, seeing as the behaviour of all three HR derivatives appears to be unchanged between circa 354°CA and 358°CA that suggests a radical change of state (like the onset of combustion) did not occur.

As was noted by Katrašnik et al. (2006) using a higher sampling frequency of ICP recording results in erroneous data; oscillations that result from cylinder acoustic resonance mar the data as they correlate with the excitation frequency of the gases in the combustion chamber.

Comprehensive singular graphs of the SoC methods are collated in Appendix 9.3 for easier direct comparison.

It is immediately apparent that none of these methods offers simple indicators; in all methods examined, a behavioural change signifies SoC rather than an event or a threshold being reached. With an ideal in-cylinder pressure trace it would be possible to easily derive a SoC marker; if absolutely correct ICP could be obtained, it follows that the heat release trace would have a true-zero value up until the SoC. Given realistic physical constraints (non-perfect ICP signal), with appropriate analysis it may be possible to design a post-processing filter which minimises ICP noise without affecting the HR trace; In scientific terms, this is the absolutely best-case scenario; even with low precision instrumentation it would be simple to subtract the inaccuracy of ICP during the compression stroke. This would result in an HR trace from which the SoC could simply be determined as soon as HR>0.

5.3 Relative validity of each method

Establishing ICP-SD in a complex diesel combustion regime can be challenging; in essence, the 3rd order derivative (jerk) of ICP-SD represents the point at which the first impulse of direction change commences. Heat release derivatives for simple, non-piloted injection regimes are all but ideal for SoC determination, but if there is a

pilot event preceding the combustion it may be difficult to distinguish which inflection point is due to sustained fluctuations in the HRR that result from the pilot combustion several degrees earlier. In this scenario, ICP-SD may prove to be a more reliable indicator, as a spike in 3rd order derivative of ICP-SD represents a sharp change in cycle-to-cycle behaviour, which has been noted to increase significantly immediately at and a little after combustion initiates. By extension, the jerk of ICP-SD from the pilot's combustion will be detectable but dies out very quickly; as a result it is less likely to hinder detection of the start of the main injection's combustion. Although not evaluated in this chapter, it may also be used to differentiate the combustion of the two phases of a split-main injection event. Similarly, ICP-SD jerk may be used with a higher degree of confidence than any HRR derivative to identify pilot injection SoC, a valuable tool for accurate calibration of engine settings.

5.4 Novelty of knowledge gained

Start of combustion is not a well-developed parameter in compression-ignition combustion investigation. Accurately determining the point at which combustion initiates has not proven to be as necessary for the understanding of the workings of conventional diesel combustion until recently. New complex combustion methods however require both ever-more increasing control over the combustion phases and more understanding of when the combustion takes place. Accurately being able to determine when fuel initiates combustion is a fundamental tool to correctly understand modern combustion regimes and its importance will only increase with combustion complexity. Being able to determine SoC in more than one ways may prove to be fundamental in our understanding of multiple-injection regimes, particularly as traditional methods appear to be nearly unusable in piloted injection.

6 The application of multiple injection strategies to low-temperature combustion

Sections of this chapter have been presented in ICEF2012-92060 by Michailidis et al., 2012.

The development of modern common-rail injection systems has led to the capability to introduce multiple injections per cycle, enabling much greater control over the combustion event in a diesel engine. The common-rail systems have resulted in increased control complexity, as discussed in the previous chapters. However, they also offer substantial benefits when combined with advanced combustion strategies, such as LTC. By enabling more precise control over the fuel-air mixture state at any given point in the combustion cycle, multiple injection strategies have the potential to increase performance and reduce emissions from diesel engines operating in LTC.

In this chapter low-temperature combustion will be examined from the critical view-point of investigating how it responds to complex injection strategies in terms of both stability and emissions. Building on the knowledge of the previous chapters, the ways in which LTC differs with conventional diesel combustion will be tested through increasing injection complexity and control The ultimate objective is to evaluate whether multiple injection can reduce harmful emissions or increase combustion stability by tailoring the in-cylinder conditions to provide a better mixture preparation before and during the combustion event.

6.1 Experimental methodology

Barring the possibility of being able to accurately monitor the temperature of the combustion, denoting a combustion point as LTC, as mentioned before (chapter 2.8), has no rigid definition. Several markers denote LTC but their presence is not always apparent; the most readily apparent marker is the existence of a cool-flame reaction in the heat release. The cool-flame reaction manifests as a low-peak rise in heat release at the start of combustion with a small plateau or depression before rising again to the full amplitude of heat release in the main power-producing combustion.

It is not always apparent, particularly at low load conditions, and consequently cannot be insisted upon for every test-point. Furthermore, in some multiple injection strategies, the presence of the low-temperature reactions could be easily confused with combustion of a pilot injection. Finally, identification of this feature on the HRR typically requires visual inspection and hence is subject to observer bias. Another method to ensure LTC conditions is to progress along a series of tests, with a single variable increasing towards a condition correlated with LTC, typically EGR (as increased EGR increases the equivalence ratio when the exhaust gas displaces air) and observe a reversal in smoke emission trend. To wit, for a given test-point, increasing EGR will make FSN emissions increase progressively, until a break-point after which FSN will decrease dramatically. This represents a transition on the φ-T map (Figure 2-1: Soot and NOx contour plots on local equivalence ratio vs. local temperature graph, reprinted with permission from SAE Paper No. 2005-01-1091 © 2005 SAE International.) “over” the high-smoke island and into the LTC region.

Extensive experimentation carried out by Cong and Sarangi (2010, 2012) as well as the present author provided the basis for the test-points examined. All test-points represent combustion regimes which are bordering on the minimum amount of EGR ensuring LTC conditions. This was done as limiting EGR is considered key to enabling LTC to become a commercially viable combustion strategy. The test strings are selected to portray a range of combustion phasing of a given fuelling quantity outputting a net of approximately 3 bar IMEP at 1500 RPM with an intake pressure of 1.20-1.21 bar. This is typical of low-load operating conditions and a prime example of engine conditions which commercially could be converted to run in LTC. It also represents an in-depth investigation into low-load LTC to correlate with work performed by Sarangi (2012) at high load.

6.2 Test-point selection

As per the tests conducted in chapters 4 and 5, it was important to select a representative variety of engine conditions that were of increasing complexity and incorporated as much meaningful variance as possible. Three injection regimes were

selected: A single injection and two split-main injections. The split-main injections were both of a 50%/50% split, and two dwell times were tested, one of 7.1° and one of 10.1°CA between the start of their injection. Testing at a dwell time of longer than 10.1° had serious impacts on ISFC and a correspondingly high rise in tHC and CO emissions as the delivery of the second half of the split so far after the combustion of the first half meant that a large portion of it didn't combust, and therefore a lot of unburnt fuel was being exhausted. Split injection regimes with a dwell of less than 6.9° were shown during screening tests to be bordering on interference artefacts caused by requesting less than the minimum dwell between injections limit of the ECU, so in order to ensure accurate performance a minimum dwell of 7.1° was selected. These findings, while different in detail, are generally consistent with the diesel combustion results shown in 4.4.

Pilot injections were entirely omitted as they don't impact LTC conditions for several reasons: firstly, they were not needed as under high-EGR conditions $\Delta P/\Delta\theta$ is low; secondly, the purpose of a pilot is to reduce ignition delay, whereas in LTC, the objective is to increase the available time for mixing by delaying the ignition; and thirdly the low oxygen concentration in LTC makes it difficult to reliably ignite the pilot injection charge unless the pilot quantity is so large that it is essentially a main injection event. These, combined with the knock-on effect of consuming a part of the available oxygen to combust the pilot results in even more degraded combustion. It was observed during preliminary probing tests that in order to get reliable pilot ignition the quantity of pilot demanded had to be so high it started to compete with the main charge for quantity delivered, and did not produce significant power as it all burnt before the compression stroke was over, resulting in increased ISFC and no benefit in emissions over a simpler split injection.

Preliminary testing also indicated that post injection was ineffective. In conventional combustion post injection is frequently employed in order to control PM emission by implementing a late-cycle combustion event to further oxidize the smoke generated. In LTC there are several factors that inhibit this: Firstly there is very little spare oxygen so post injections mostly end up radically increasing tHC emissions as they

remain unburnt. Secondly, thanks to a large ignition delay under the low in-cylinder temperatures and low oxygen concentrations encountered with LTC, it is difficult to implement a late injection that won't be burnt along with the main charge. Inject the post too early and it becomes a staggered part of the main injection. Inject too late and it isn't burnt at all. In both cases a post injection is very inefficient at reducing PM (which is, ideally, negligible in LTC) and in both cases it impacts ISFC significantly as it is effectively fuel that is emitted virtually unreacted.

As before, engine speed was 1500 RPM, intake pressure was between 1.20 and 1.21 bar, and EGR rate was adjusted for each injection regime so as to maintain LTC but be as conservative as possible. This meant around 57-59% by volume for the single injection tests and between 52 and 54% for the split injection tests. This correlates with the work performed by Sarangi (2012), as it has been demonstrated lower EGR may be used when the fuel delivery is split. In order to determine the effect of rail pressure, all strings of tests were run at 600 bar and 700 bar. Tables of the injection parameters for each condition are collated in Appendix 9.1.

Injection phasing was chosen so as to locate CA50 as close as possible to TDC in order to maximize efficiency; it was then retarded in approximately 2°CA increments for each test-point for the rest of each individual test string. In almost all cases 5 test-points per string are performed and in each case they're ringed by extremes in conditions: the ones latest display very high PM emissions, such that their LTC status is bordering on questionable while the earliest ones have increased NO_x, CO and tHC emissions as well as slightly higher ISFC.

CA50 was once again chosen as a marker rather than SoC, CA05 or start of injection (SoI) as it facilitates understanding of how the injection regime impacts the thermodynamic efficiency of the combustion. When dealing between single and split-main LTC combustion the variation in combustion duration, as well as that in ignition delay can be very large and so it is not as straight-forward to compare test-points with markers that relate to the start of combustion rather than its peak.

6.3 Diesel low temperature combustion analysis

Understanding how diesel LTC differs in emissions, output and cyclic behaviour to conventional combustion is critical to the understanding of LTC. This chapter will attempt to investigate diesel LTC's behaviour and provide a base-line for comparison with subsequent experimentation in LTC with GTL blends.

6.3.1 In-cylinder pressure and heat release rate

Indicatively, the in-cylinder pressure (with corresponding injector drive current) and heat release rate of a single and 7° split injection are shown in Figure 6-1 and Figure 6-2. Comprehensive figures for the cylinder pressure, heat-release rate, ICP-SD, ISFC, and IMEP are shown in detail in Appendix 9.1.

Almost all test-points demonstrate a cool-flame reaction, as expected. Peak heat release is higher for single injection scenaria, as expected since the combustion duration is reduced compared to the split-injection cases. This is a result of more fuel having mixed to a combustible stoichiometry in the case of the single injection, where with the split injection, most of the fuel in the second injection event will not have premixed by the time the combustion reactions begin.

In certain late split-injection cases there appears to be a lower peak heat-release during the combustion of the first half of the charge than of the latter. This could be because of relative timing: the earliest phased test-points have a notably longer ignition delay than the later ones, meaning that relative to the second injection's start the first half of the combustion occurs earlier. Consequently the second half tends less to behave as a staggered combustion and more as a two-stage combustion.

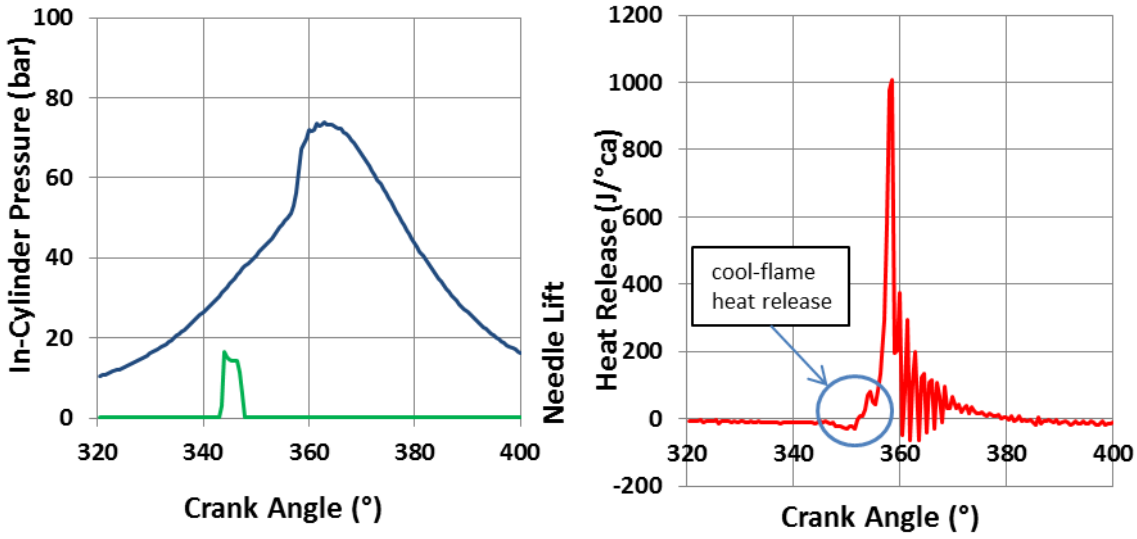

Figure 6-1: ICP and HR for Diesel Single Injection at 600 bar Prail and 357° CA50

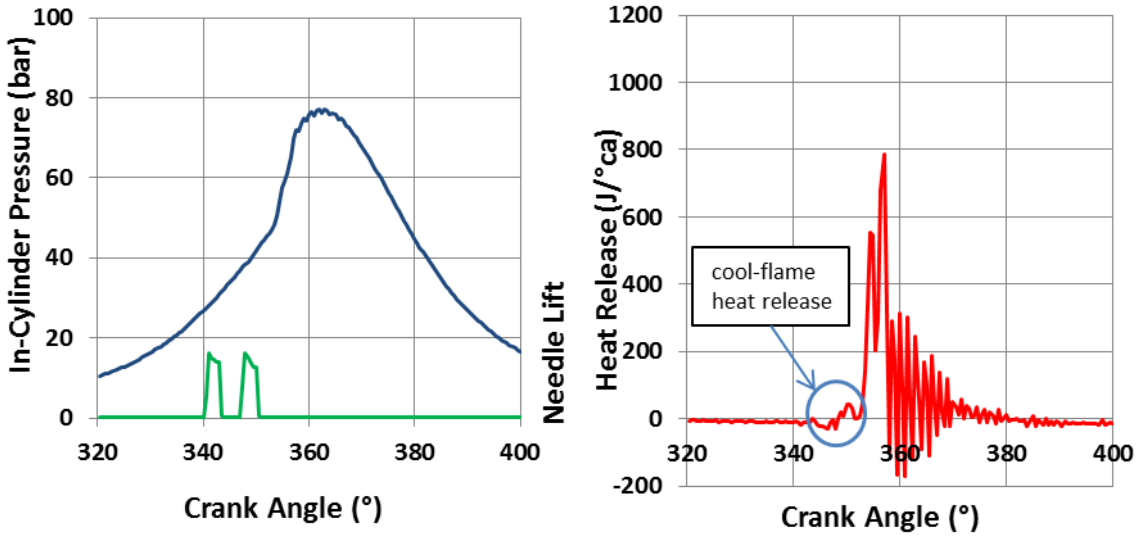

Figure 6-2: ICP and HR for Diesel 7° Split Injection at 700 bar Prail and 355° CA50

6.3.2 Variability of in-cylinder pressure and relation to injection regime

In terms of ICP-SD there appear to be very few global trends. There seems to be a weak correlation between increased rail pressure and increased ICP-SD in that for each test string the 700 bar tests tend to be of slightly higher ICP-SD peaks and means, though there is not enough evidence to be able to conclusively say increased rail pressure means increased ICP instability.

In the single injection scenaria we observe trends similar to those in conventional combustion, that is a sharp increase in ICP-SD as soon as combustion initiates with a following decrease and plateau followed by a gradual decrease. There is nearly no effect on ICP-SD caused by the cool-flame combustion (when apparent) A graph of the ICP-SD of single injection LTC is reproduced in Figure 6-3. When compared to similar tests performed in conventional combustion, single-injection LTC shows a significant decrease in ICP-SD. While single-injection conventional combustion demonstrated peaks of up to 1.6 bar, single-injection LTC has a highest peak test-point of 1.2 bar, with most other points peaking at 0.8, making single injection LTC demonstrate ICP stability comparable to that of piloted injection regimes in conventional combustion.

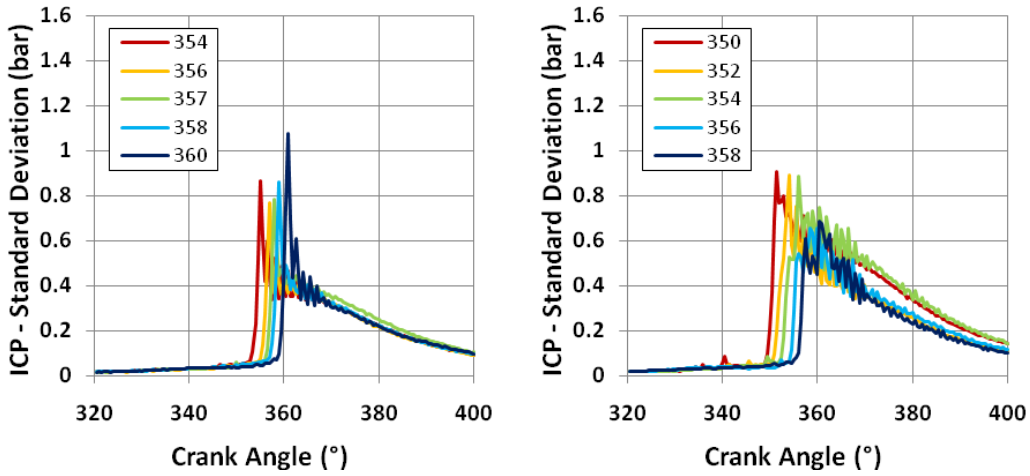

Figure 6-3: ICP-SD for Diesel LTC in single injection at 600 bar Prail (left) and 7° split injection at 600 bar Prail (right)

The trend which was observable in conventional combustion correlating increased ICP-SD peak with CA50 shifting away from TDC is not apparent any more.

Comparing the results of the split injection tests with the piloted split-main tests of conventional combustion shows a slightly higher peak and average throughout, though this is to be expected as the stabilizing effect of the pilot injection is absent. Regardless, the magnitude of ICP-SD in split injection scenaria is comparable to single injection in LTC as can be seen in Figure 6-3. The profile exhibits some

interesting trends: As CA50 progresses later into the cycle, the combustion of the first half of the charge becomes more stable while the latter slightly less stable or unaffected. To a small degree, this mirrors the trend observed in conventional single injection where the cases closest to TDC exhibited higher stability. This effect is most visible in the 10° dwell cases as the instability induced by the second half of the split hasn't masked the increased stability in the first half's combustion as much. 10° split at 700 bar is tabulated in Figure 6-4.

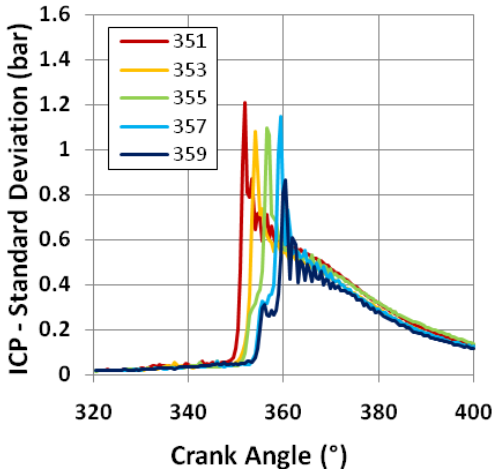

Figure 6-4: ICP-SD of Diesel LTC in 10° dwell split injection at 700 bar Prail

Cases where the split injection phasing is such that the combustion is clearly two-stage (7° dwell @ 600 bar CA50 356 & 358, 7° dwell @ 700 bar CA50 361, 10° dwell @ 600 bar CA50 359) demonstrate overall a much reduced ICP-SD. In Figure 6-3 the 356 and 358 cases on the right graph show a clear change in behaviour. Heat release for two of the most representative cases are displayed magnified in Figure 6-5.

These cases demonstrate low peak heat-release during the first stage of their two-stage combustion. They are also the highest smoke-producing test-points, so much so that they're bordering on being LTC-to-conventional transitory conditions. This makes it unclear whether the increase in stability is due to the bordering combustion-type change or because the phasing is inherently more stable.

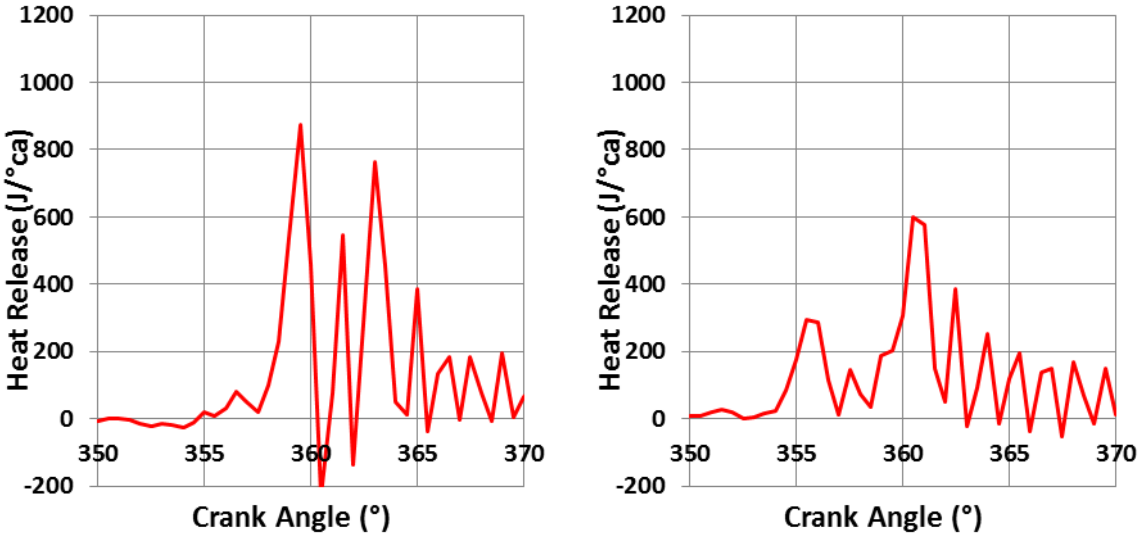

Figure 6-5: Heat Release for Diesel in 7° Dwell @ 700 bar CA50 361 and 10° Dwell @ 600 bar CA50 359

6.3.3 Indicated mean effective pressure (IMEP) and indicated specific fuel consumption (ISFC) findings through Injection Regimes

IMEP was aimed at 3 bar throughout the tests and largely very consistent. Overall IMEP-CoV did not exhibit significant variation. IMEP-CoV seems to be slightly lower in single-injection cases (~1.8% for the singles, ~2.2% for the split cases) but largely IMEP-CoV seems very similar to the values observed in conventional combustion. Figures for each case are tabulated in Appendix 9.1, though collated graphs are shown in Figure 6-6 and Figure 6-7. Repeatability does not seem to have altered in any significant way due to the switch to LTC regime. This result correlates well with the indication provided by the ICP-SD which demonstrated very little evidence of variance through the combustion cycle.

IMEP-CoV being very low also offers an interesting insight into tHC and CO generation: The test-points with the highest tHC and CO do not correlate with those with highest IMEP-CoV. This suggests that the tHC and CO emissions are not due to partial misfires or possible selective “bad” cycles, but rather a generated in a stable consistent fashion from incomplete combustion every cycle. If they were products of partial combustion cycles, IMEP-CoV would be increased at these points.

ISFC doesn't seem to have significant trends with the exception of single injection being almost universally slightly lower than the split injection test strings. This is due to the increased combustion duration; Indicatively, comparing single injection at 600 bar rail pressure with a CA50 of 354 to 7° split injection at the same rail pressure and CA50, the single has a duration of 30°CA while the split 33.5°CA, hence, a relatively larger amount of fuel is burnt further away from the CA50 point and therefore at a lower pressure. This is mirrored in the heat-release graphs, where the single injection tests exhibit much higher peaks than the split injection tests. Peak heat-release correlates with high thermodynamic efficiency, and therefore low ISFC. Graphs of ISFC against CA50 for all test points are tabulated in Figure 6-6.

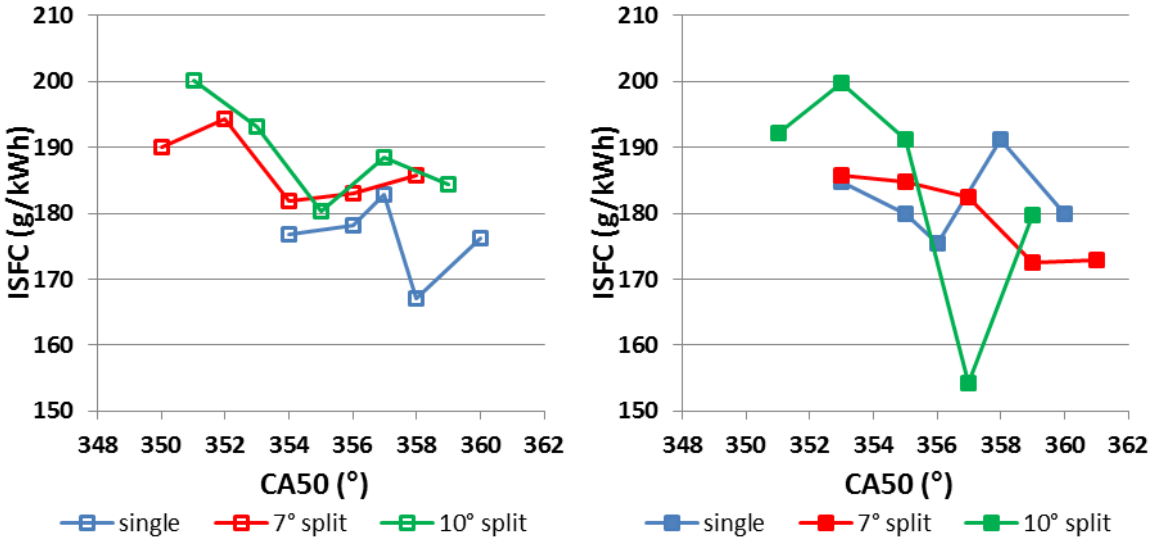

Figure 6-6: ISFC vs. CA50 for Diesel LTC. Left: 600 bar Prail. Right: 700 bar Prail

There appear to be minor trends in some test-strings, like ISFC decreasing across CA50, though this is not apparent in all of the test strings. Bringing CA50 closer to TDC and slightly after increases mechanical efficiency by ensuring a more efficient transferral of force from the piston to the crank shaft. It also minimises the amount of forced the piston receives during the end of the compression stroke which generates negative work as the rotation of the piston opposes it, however slightly.

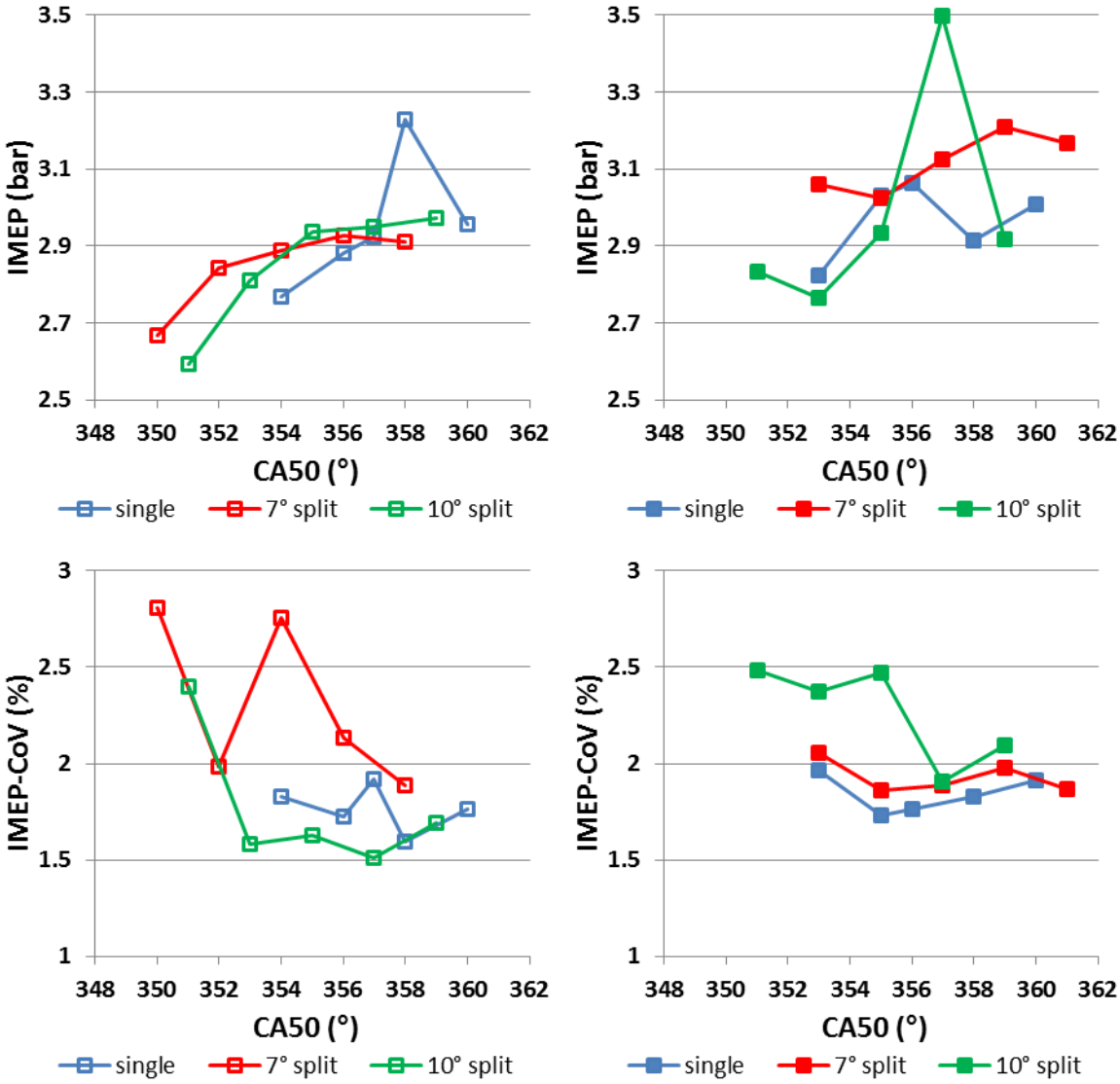

Figure 6-7: IMEP and IMEP-CoV vs. CA50 for Diesel LTC. Left: 600 bar Prail. Right: 700 bar Prail

An overall slight improvement in FC with later CA50 was expected. Also, while some of the ISFC values within test strings appear to be quite disparate, it should be noted that for the low fuel flow measurements recorded the inherent error margin of the gravimetric fuel gauge appears slightly larger than it would at higher flow conditions. With a more accurate fuel-flow measurement device a correlation between fuel consumption and relative location of heat release could be established, taking into account the physical characteristics of the piston/conrod/crankshaft.

6.4 Diesel low temperature combustion emissions analysis

The nature of the combustion, as discussed in the previous sections, has a direct influence on the pollutant formation in LTC. The emissions results from all the tests are shown in Figure 6-8, in terms of FSN, NO_x, tHC, and CO. The trends are presented as a function of CA50, and are subdivided by injection pressure.

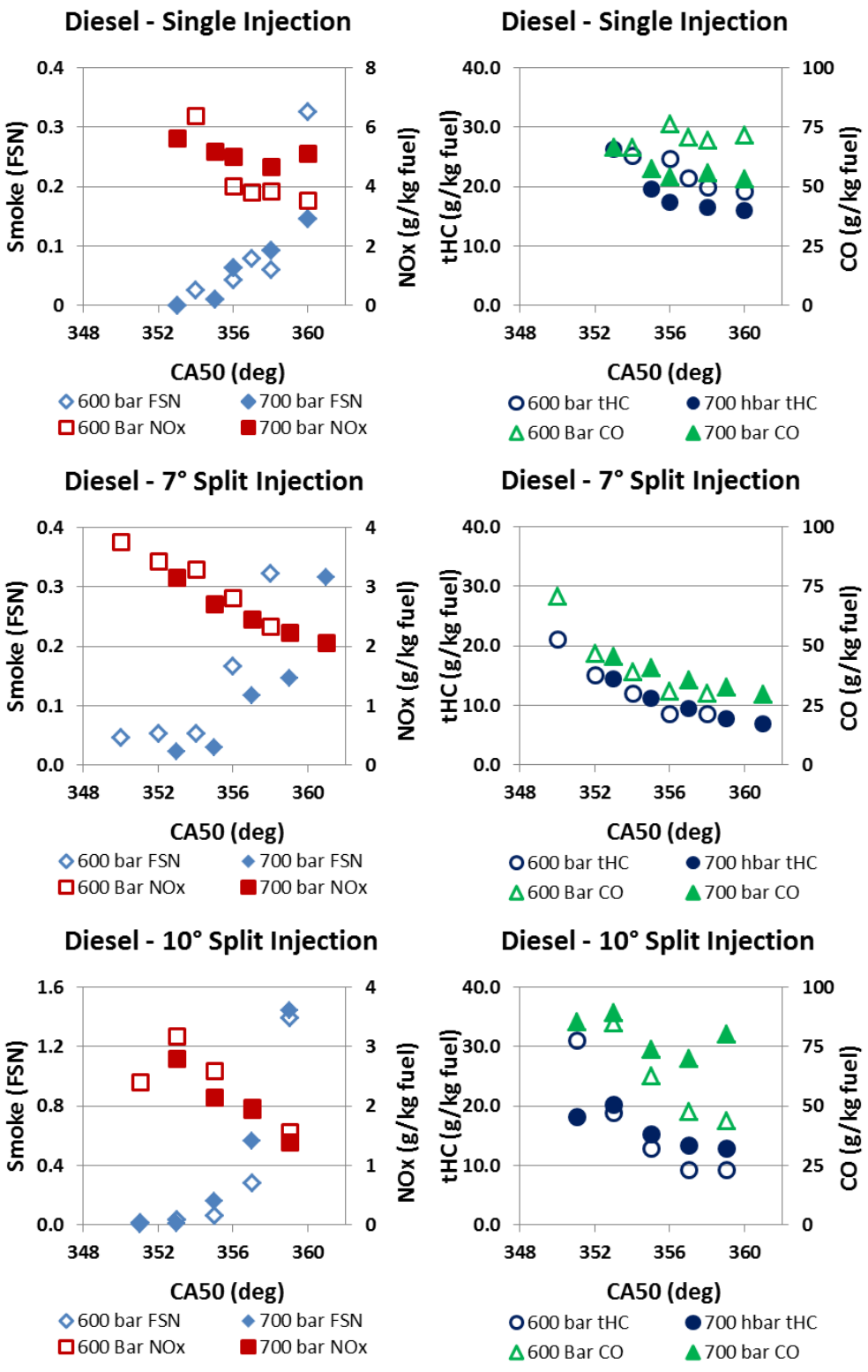

Figure 6-8: NO_x/PM and tHC/CO vs. CA50 graphs for Diesel in LTC for single, 7° dwell and 10° dwell split injection

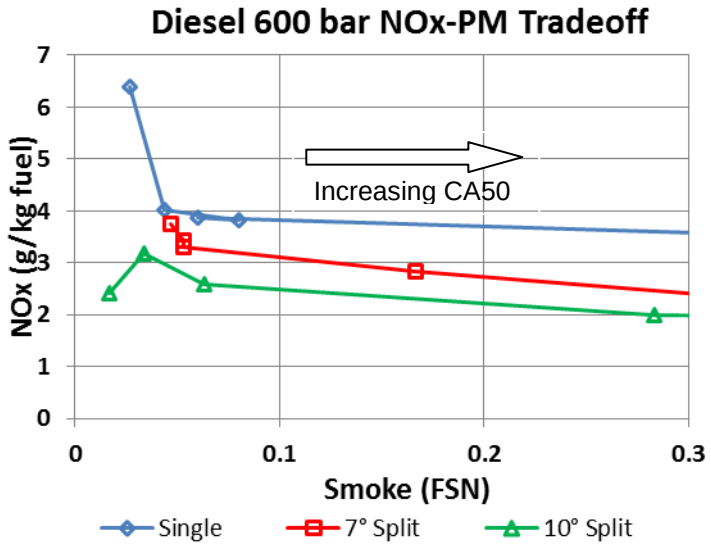

Figure 6-9: NO_x-PM Trade-off for Diesel LTC at 600 bar Prail

6.4.1.1 Nitrous oxides (NO_x)

The LTC regime is characterized by foremost, a temperature well below the 2000 K that enables the Zel'Dovich formation of NO_x. It is also characterized by a very low air to fuel ratio thanks to the high levels of EGR. Both these factors make the Fenimore prompt method of NO_x generation more relevant than in conventional combustion. As expected, NO_x correlates with peak pressure and rate of pressure rise, steadily decreasing as CA50 progresses later into the cycle.

Two trends are interesting to note in terms of NO_x: Firstly, there is overall notably less NO_x in the split-injection scenaria than in the single-injection scenario (note that the scale of NO_x in the single-injection graph is doubled). Secondly, the magnitude of NO_x reduction is more pronounced in the split-injection scenaria. That is, across the CA50 sweep NO_x dropped relatively more in the case of the split injections than in the case of the single injection. All cases showed a significant reduction in NO_x emissions with later phasing.

Another critical reason for the NO_x reduction is the prolonged combustion duration: The staggering of the fuel delivery causes this (indeed, it is often the main reason a fuel delivery is staggered) leading to lower peak heat-release and therefore lower

peak localized temperatures. This would further hinder the Zel'Dovich formation of NO_x, presuming there was a significant amount of it.

Of interest is the magnitude of reduction; in the case of single injection (ignoring the 600-bar first point as an outlier) both for the 600 and 700 bar cases the reduction seems to have been minor across the CA50 span, while for both split injection scenaria the reduction across a similar range of CA50 phasing dropped NO_x by 30-50%. This can probably be attributed to combustion duration and start of combustion. Combustion duration was increased in the 7° dwell tests and even further in the 10° dwell ones. This means a progressively larger portion of fuel was burnt very late in the combustion cycle, at lower pressures and therefore hindered Zel'Dovich formation NO_x. The increased combustion duration compounds this as it decreases peak temperature further.

This correlates with the magnitude of reduction observed when phasing the split-injection tests late: Later phasing means an ever larger percentage of fuel was burnt at a relatively lower pressure/temperature and this explains why the trend of NO_x reduction more closely mimics that of a non-LTC scenario.

Just like in conventional combustion, there is no clear trend between NO_x and rail pressure. This makes sense, as the injection pressure had no significant impact on the combustion event in terms of phasing, duration, or intensity. Larger differences than those evaluated here would be expected to influence these parameters, and hence have a greater impact on the NO_x.

6.4.1.2 Particulate matter (PM)

As expected, PM emissions are one of the limiting factors in LTC. As combustion phasing progresses later and later into the cycle, smoke emissions first increase gradually and then exponentially. In each group of tests combustion phasing was limited on the far side by a drastic increase in PM emission. This is because the late phasing pushes the combustion towards the high-smoke island on the φ-T map (Figure 2-1) and borders on transitioning from LTC to conventional combustion. This

is a result of a shorter ignition delay at later (closer to TDC) timings leading to reduced premixing and higher local equivalence ratios. Early, optimised split injection generates FSN levels similar to those of early single injection cases, despite the lower EGR levels used with split injection.

Split-injection tests did not exhibit improvement in PM emission. In broad terms, the PM emissions of the optimal timings are comparable between all three injection regimes. Naturally the latest timings are increasingly worse as combustion starts to move away from the LTC envelope and into the high-smoke zone of the φ-T map (Figure 2-1). In all cases, CA50 phasings of 352° to 354°CA ATDC were capable of generating FSN levels near-zero.

The correlation between high rail pressure and low smoke which is very prevalent in conventional combustion seems less obvious in LTC. While the 7°-dwell split injection clearly exhibits reduced PM emissions with higher rail pressure the same cannot be decisively said of either the single injection or the 10° dwell split injection.

It is not clear why the improvement in PM via increased rail pressure is visible in the 7° dwell split injection and not in the single injection series. To an extent, the 10° dwell split case does seem to be of slightly lower PM emission at higher pressure, so it could be suggested it follows the same trend as the 7° dwell tests. It has been shown that at higher engine loads a clear trend between rail pressure and PM emission will be much more apparent (Cong 2010).

Of particular interest when considering the FSN and NO_x emissions is their trade-off, as shown in Figure 6-9. Clearly, the use of the split injection strategy significantly reduces smoke at a given NO_x level (or conversely reduces NO_x for a given level of smoke). Additionally, the timing of the split has a further significant impact on the NO_x-FSN trade-off. This demonstrates the potential for significantly reduced emissions by optimizing the split injection event (both by changing the dwell between the two injections, and possibly varying the relative quantity delivered in each of the two parts of the split).

6.4.1.3 Hydrocarbons and carbon monoxide (tHC & CO)

The first immediately apparent trend in tHC & CO is that introducing split-injection at a 7° dwell improves both emissions. This would suggest that less unburnt or partially burnt fuel is being exhausted, and more complete oxidation is taking place. It could be argued for the cases of earlier CA50 that more combustion time spent at useful cylinder pressure results in a better overall combustion efficiency, however even test-points at similar or later CA50 to the single injection cases exhibit much reduced tHC & CO. This also opposes the understanding that longer combustion duration would inherently harm combustion efficiency, as the latter part of the combustion would last longer and therefore be more likely to quench (and only partially oxidize). Also, against this suggestion, almost universally tHC & CO emission decreases with later CA50.

10° dwell split injection exhibits notably worse emissions than 7° dwell, suggesting that perhaps this long a dwell is bordering on too long and a non-trivial amount of fuel is in fact being delivered too late into the cycle. This correlates with the slightly higher ISFC of the 10° dwell test-points (Figure 6-10), almost universally higher than those of the 7° dwell.

Unusual too is the effect of rail pressure: In the single-injection tests it is clear that increasing the rail pressure had a beneficial effect on CO, reducing it from circa 75 to circa 50 g/kg of fuel. This trend is not visible in either the 7° or the 10° dwell split injection tests. In fact, in the 10° dwell series and to a lesser extent in the 7° dwell series, the opposite is observed: increased rail pressure generates higher CO. Given the significantly earlier injection times this perhaps suggests an increased degree of wall-wetting is taking place, and the higher injection pressure is exacerbating this by making the spray penetrate deeper into the cylinder. This correlates with the trend of higher CO emissions with earlier CA50 (and therefore even earlier start of injection).

Both CO and tHC are relatively high compared to conventional diesel combustion. This is a known problem for LTC but is nonetheless an issue which must be addressed. This problem is not alleviated by LTC exhaust gas temperature generally

being either below or perilously close to being below the light-off temperature of Diesel Oxidation Catalysts (DOC) which would eliminate both these emissions.

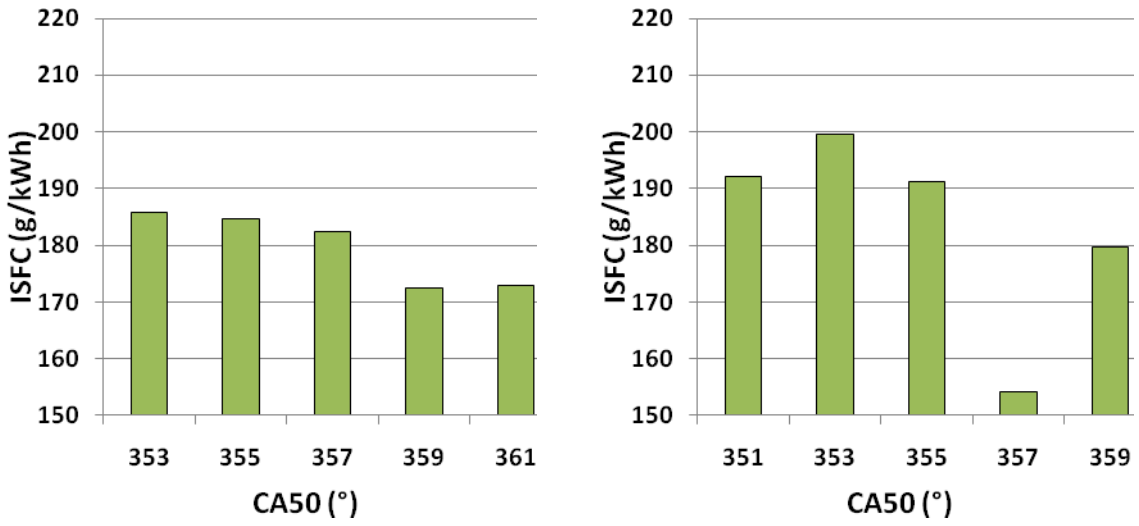

Figure 6-10: Comparison of 7° Dwell (left) and 10° Dwell (right) Diesel ISFC, 700 bar Prail

6.4.2 Summary: How complex injection strategies affect low temperature combustion

- NO_x emissions for a given combustion phasing are reduced by dividing the diesel fuel injection into two halves. Further benefits are achieved by optimizing the phasing as well as the dwell time between the two halves, such that NO_x emissions can be reduced by nearly 1/3 for a given level of FSN production. Retarding the combustion leads to lower NO_x emissions for all injection strategies, but the rate of reduction for a given retardation was greater for the split-injection cases.

- PM emission is the limiting factor in CA50 phasing in LTC. Late injection (and consequent late start of combustion and CA50) causes significant increases in PM. While split-injection regimes do not significantly improve PM they do output comparable amounts of smoke at a reduced EGR rate. The

conventional diesel combustion trend of reduced smoke with higher rail pressure was not apparent, but this may have been a result of the short injection durations at this relatively low IMEP case.

- CO and tHC emissions in LTC while high are improved by swapping from single to short-dwell split injection. Their consequent increase due to spray penetration could be mitigated or eliminated by the use of injectors and swirl valves specifically designed to avoid over-penetration.

- LTC does not appear to be less stable than conventional combustion. Both cycle-average stability, as represented by the CoV of the IMEP, and the instantaneous stability of the combustion, as represented by the, ICP-SD, are similar in LTC regimes to those demonstrated for piloted single injection conventional diesel combustion. There was no indication of unreasonable instability in the combustion event.

- ISFC is slightly reduced by the implementation of split-injection. It is not clear why this is the case.

- Split-main LTC is not significantly different in ICP-SD to single injection. While comparable in magnitude they are different in profile, with split-injection occasionally demonstrating significantly improved ICP-SD during the combustion of the first half of the injection charge.

6.5 Novelty of knowledge gained

An in-depth investigation into how accurately-tuned engine operating parameters optimise LTC was conducted. The method used to investigate the cyclic behaviour offered novel insight into the repeatability characteristics of LTC and how they relate to conventional combustion. An in-depth analysis on the emissions and performance characteristics of LTC with the injection regimes examined established the relationship between emissions optimisation, efficiency and lower EGR requirement possible through the implementation of complex injection regimes.

7 Gas-to-liquid fuel (GTL) blends in low temperature combustion

Sections of this chapter have been presented in ICEF2012-92060 by Michailidis et al., 2012.

As was shown in the previous chapter (6), the use of advanced injection strategies significantly improves performance in LTC, including reducing unwanted emissions and lowering the level of EGR required to achieve low NO_x and low PM levels. However, the work presented earlier, like other work found in the literature, used conventional diesel fuel. The implications of going to an alternative fuel, which is not derived from liquid fossil fuels, has not been evaluated. The current work evaluates the use of synthetic diesel created from natural gas through a gas-to-liquid (GTL) process. This fuel, with virtually no aromatics and a higher Cetane number than conventional diesel, is expected to have a strong influence on LTC combustion stability, phasing, and emissions. The combination of these fuels and the advanced injection strategies introduced in the preceding chapters is also of interest under LTC conditions.

As was discussed in chapter 2, gas-to-liquid conversion using the Fischer-Tropsch process can convert gaseous hydrocarbons into a low-aromatic liquid fuel that has similar behaviour to liquid diesel. While most of the GTL fuels currently in use are derived from fossil natural gas, there is no reason the process could not also be applied to non-fossil gaseous hydrocarbons, for example biogas from farming or waste processing. The applicability of this fuel will to a large extent depend on whether it can be used in an engine in place of diesel fuel with marginal or no impact on the base engine. This chapter aims to evaluate whether relatively high blends of GTL with fossil diesel will have an impact on a diesel engine operating with advanced injection strategies in an LTC regime.

7.1 Fuel Blend selection

Three fuels were selected to test LTC: A type-2 Diesel to provide a base-line, and two GTL-Diesel blends of 30% and 50% GTL by volume. All fuels were supplied by Shell Global Solutions (UK). The ratios of 30% and 50% were selected in order to offer insight into how large substitution rates affect combustion; up to 15% GTL blends are available to the public in several countries already and there is extensive literature examining neat GTL as a fuel as well. Also, maintaining a maximum of 50% GTL ensured a high fuel lubricity level and therefore the safety of the engine and fuel supply systems. More details on the fuels, including the properties of the three fuels were presented in chapter 3.3.

7.2 Experimental Methodology

Similarly to the preceding chapter, strings of test-points will be evaluated with 30% and 50% by volume GTL-diesel blends in LTC conditions. Again, single injection, 7° and 10° degree dwell split injection will be used with a range of CA50 phasings, at 600 and 700 bar rail pressure. Unlike previous chapters, the presentation and discussion of results will be with an additional focus towards the effects of an increasing GTL substitution ratio, rather than direct comparison between injection regimes. Detailed graphs of all the tests can be found in Appendix 9.7.

7.3 Emission findings through gas-to-liquid blend ratio

The figures below (Figure 7-1 to Figure 7-3) are presented together so that comparisons can be drawn between fuels across different injection strategies. Trade-offs between NO_x and FSN, and NO_x and ISFC, as well as ignition delay, are also plotted (Figure 7-5, Figure 7-4). In order to facilitate clarity, the graphs displaying trade-offs only display 600 bar rail pressure tests. Sensitivity to fuel composition at 700 bar was equivalent to the 600 bar cases and hence is not reported here except where appropriate. Also, the NO_x-PM and tHC-CO graphs from chapter 6.4 have been reproduced to enable direct comparison of Diesel and GTL blend fuels.

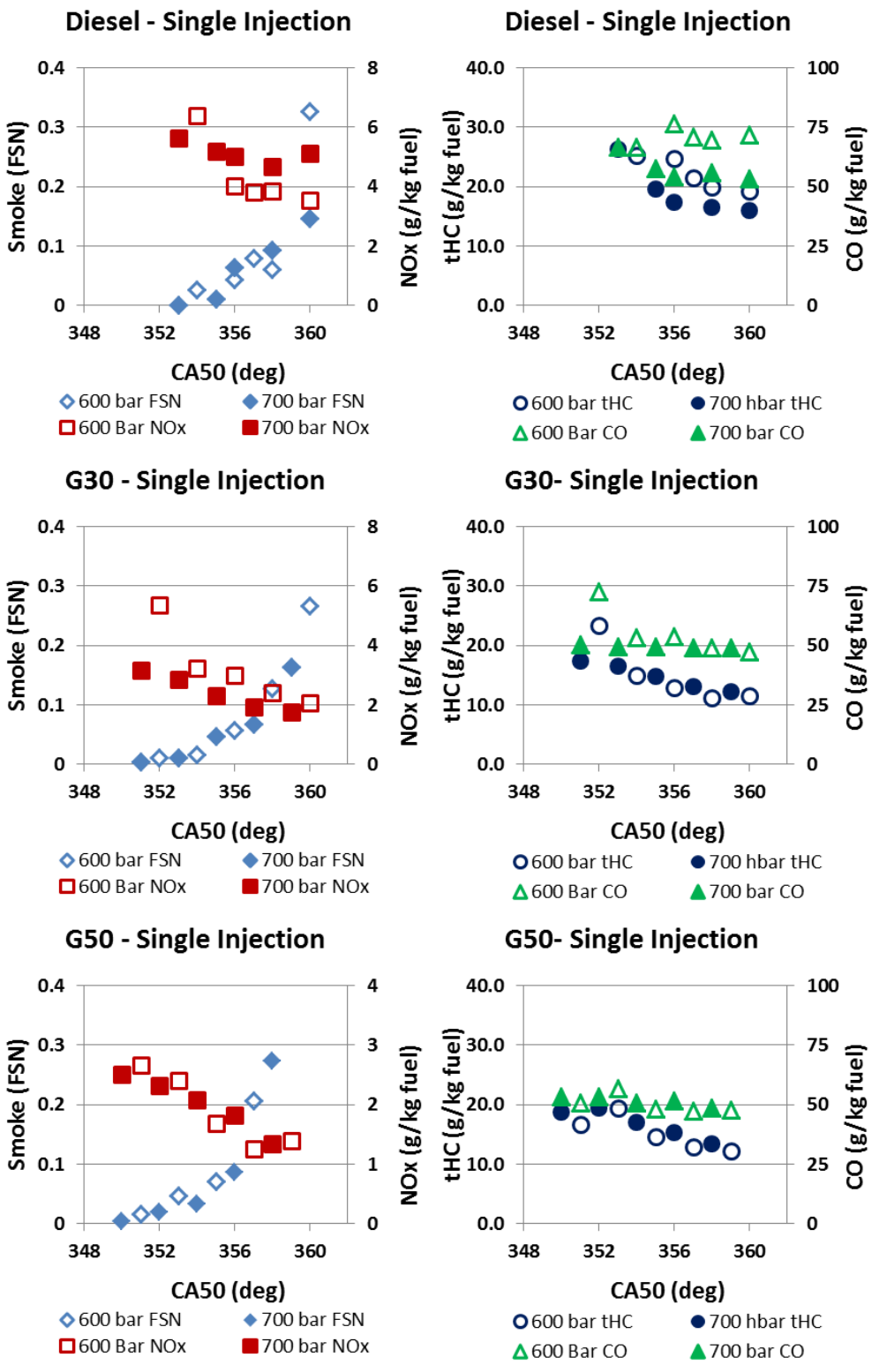

Figure 7-1: NO_x/Smoke and CO/tHC Vs. CA50 for Diesel, G30 & G50 in LTC Single injection

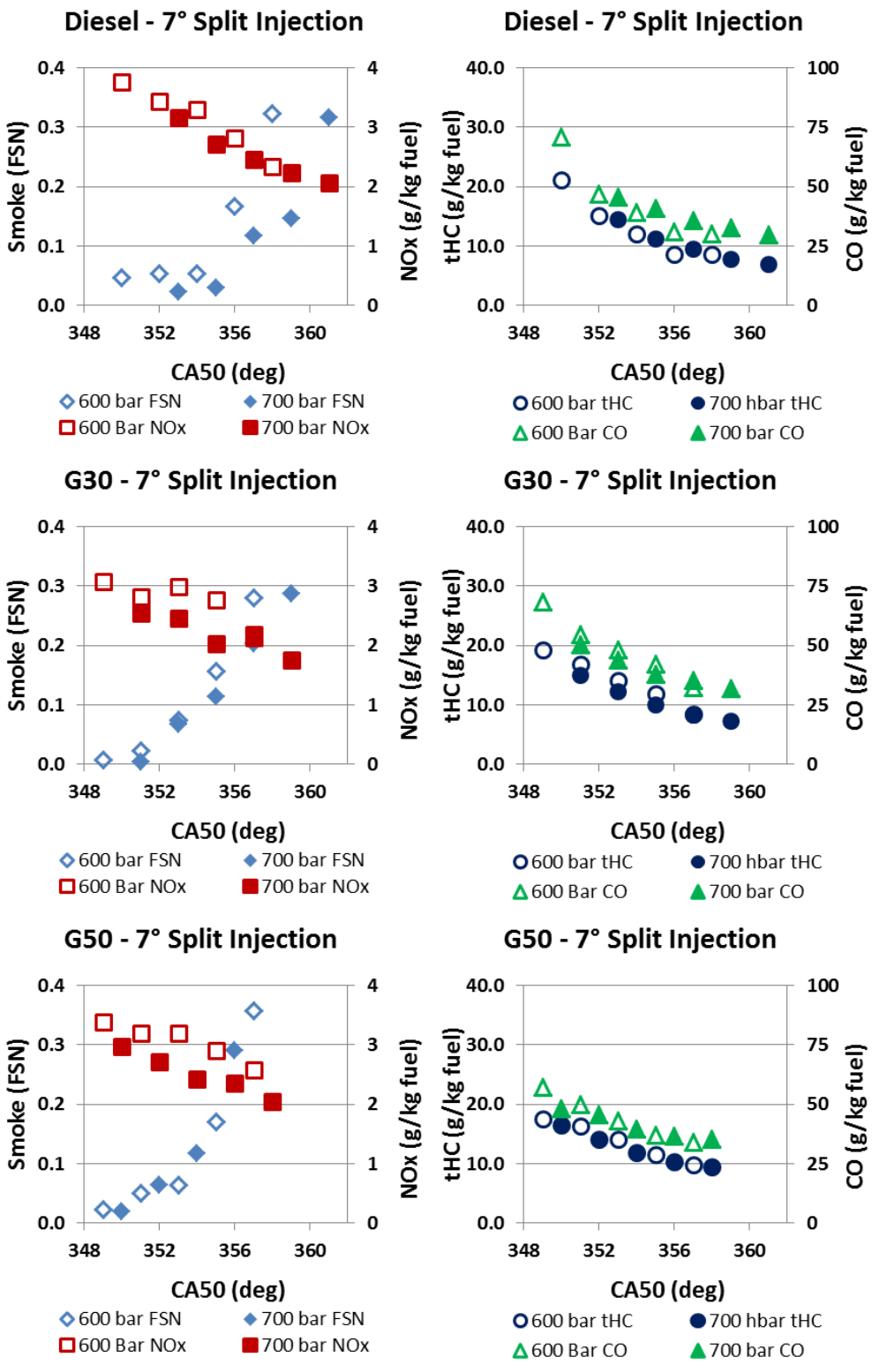

Figure 7-2: NO_x/Smoke and CO/tHC Vs. CA50 for Diesel, G30 & G50 in LTC 7° Dwell injection

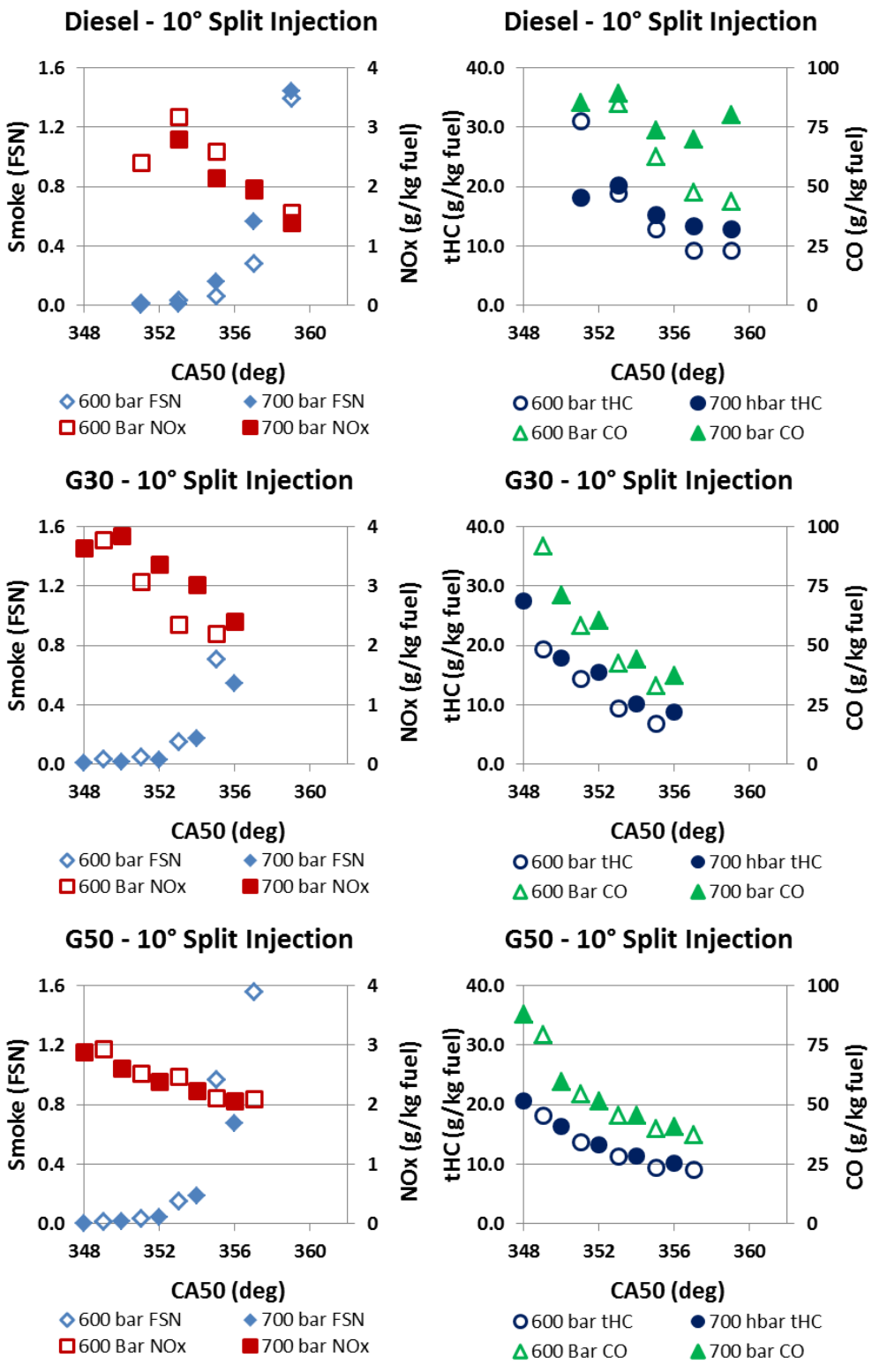

Figure 7-3: NO_x/Smoke and CO/tHC Vs. CA50 for Diesel, G30 & G50 in LTC 10° Dwell injection

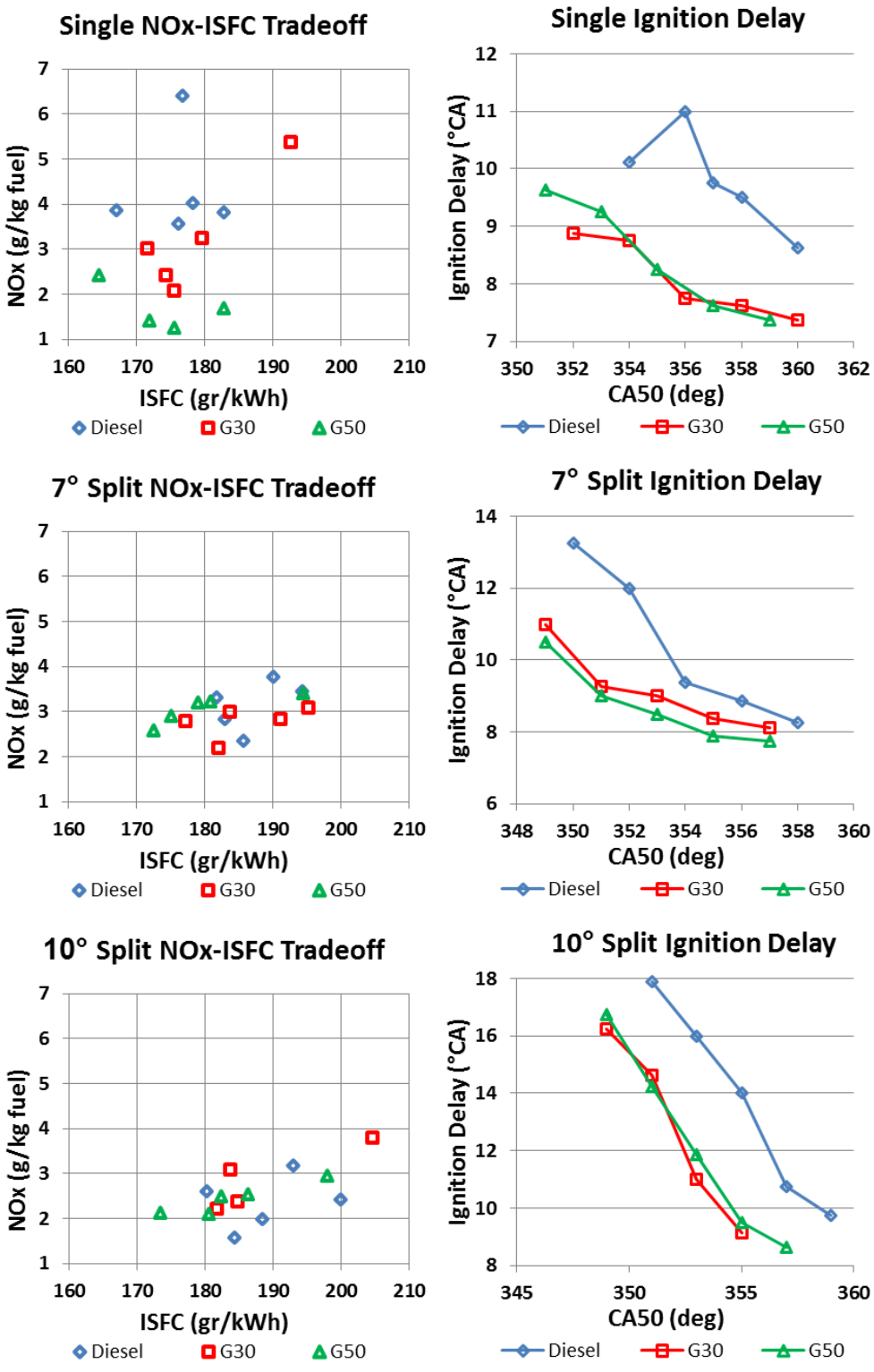

Figure 7-4: NO_x-ISFC Trade-off and Ignition Delay Graphs for Diesel, G30 and G50 in LTC under Single, 7° Dwell and 10° Dwell Injection Regimes. 600 bar Prail only shown.

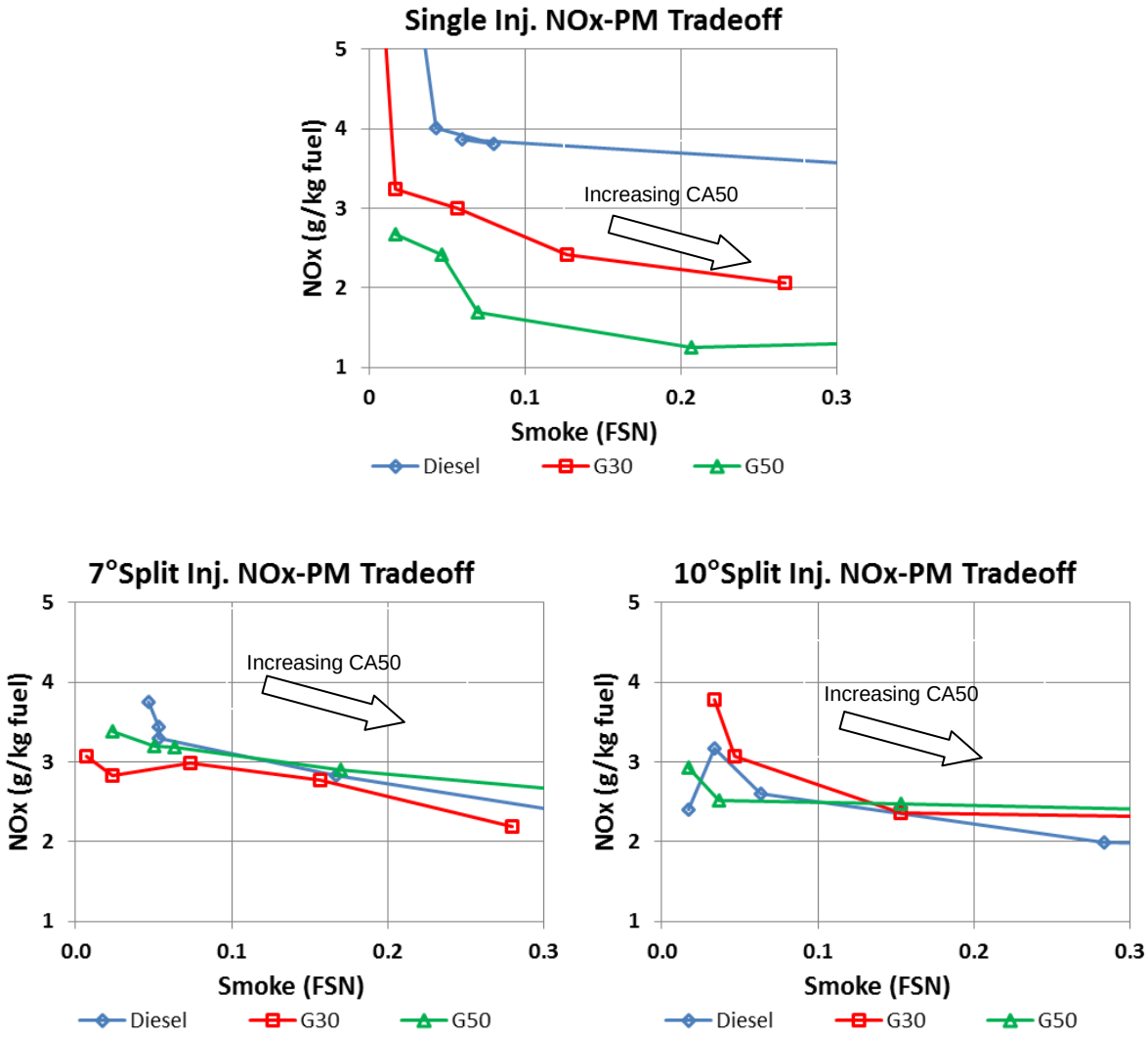

Figure 7-5: NO_x-PM Trade-off Graphs for Diesel, G30 and G50 in LTC under Single, 7° Dwell and 10° Dwell Injection Regimes. 600 bar Prail shown.

The ignition delay plots shown in Figure 7-4 use combustion phasing defined by the 3rd order ICP-SD method described in chapter 5. As such, it represents the time between the commanded start of injection and the first significant variability in the cylinder pressure, which will occur at the start of the low-temperature combustion reactions.

7.3.1 Nitrous Oxides (NO_x)

For single injection LTC NO_x seems notably improved both for the G30 and the G50 fuel (Figure 7-1, note that the NO_x scale in the case of Diesel and G30 single injection is doubled). Optimised Diesel single injection exhibits NO_x emissions of roughly 4 g/kg of fuel, while G30 and G50 exhibit roughly 3 and 2.5 respectively. This shifts the single-injection NO_x-PM trade-off significantly in GTL's favour, as shown in Figure 7-4.

The GTL blends have higher Cetane Numbers and as such exhibit shorter ignition delays and therefore lower mixing times than Diesel (Diesel: 59.6, G30: 68.7, G50: 68.5 as noted in Ch.3.3). The effects of this can be clearly seen in Figure 7-4 where in single-injection scenaria the ignition delay for Diesel is notably longer than either of the GTL blends. Longer mixing time correlates with higher homogeneity, which is known to result in higher peak pressures and peak temperatures, as well as a more intense combustion with a higher peak rate of pressure rise, and therefore higher NO_x emissions (Kitamura et al 2005, Chen 2000, Deng et al 2010). As expected from the similar Cetane numbers of the two GTL-containing blends, there is no significant difference in ignition delay for these two fuels.

Comparatively, the 10° split injection tests have the highest ignition delay; this is not so much a result of the type of injection regime as its early phasing. Despite the long ignition delay, the 10° split tests have the lowest NO_x emissions. This suggests the dwell has lengthened the combustion duration enough to modulate heat release rate and control peak temperature enough to maintain low NO_x emissions. This effect is more significant than the superior mixing effected thanks to the long ignition delay.

A particularly intriguing result is that a dramatic decrease in NO_x emissions with the addition of GTL is only apparent in single-injection scenaria. Comparing the NO_x emissions on (Figure 7-5) it is evident that Diesel, G30 and G50 have a comparable NO_x output throughout the split injection regimes. One possible explanation would involve spray over-penetration; Deng et al (2010) demonstrate how higher density fuels penetrate more than diesel for a given hardware setup.

Being less dense, GTL blends naturally tend to penetrate less than pure diesel (Bobba 2009, Pesant et al 2008, Li et al 2010). Splitting an injection is known to minimize spray penetration (and possible wall-wetting); therefore it stands to reason that the single injection LTC benefits the most, in NO_x terms, from the switch to GTL blends. If this is the case, it would suggest that higher load engine conditions would benefit even greater from a GTL-blended fuel when employing combustion regimes that necessitate very early injection. Reduced spray penetration also results in less premixing. This is particularly relevant in LTC as there is a marked lack of oxygen at high EGR levels, and as such may also result in lower NO_x. This effect also may be less pronounced in split injection as the mixture is already too rich to form significant NO_x, therefore the substitution of GTL – which further reduces penetration – would not significantly affect NO_x formation. Tests carried out by Li et al (2010) between GTL, diesel and rapeseed-methyl ester (RME) conclusively show that GTL has a smaller droplet size than diesel and that it responds to higher pressures by decreasing it further at an increased rate; i.e., higher rail pressure in GTL yields better results (in atomization terms) than diesel.

Work carried out by Borthwick et al (2002) shows that higher injection pressures in large-bore engines alleviate spray over-penetration at speeds of 1500 RPM. This is in opposition to tests performed by Deng et al (2010) which shows a clear trend of increasing penetration with increasing injection pressure in a constant-volume rig. In the tests performed there was no significant differentiation in NO_x output between the 600 and 700 bar tests performed; drawing an inference about spray penetration at such a small delta in injection pressure would be erroneous without further evidence.

7.3.2 Particulate matter (PM)

As shown in 6.4.1.2, PM emissions at early timings are near-zero (just like in diesel combustion) but ramp up sharply with later CA50 phasing (Figure 7-1, Figure 7-2, Figure 7-3). The profiles of the PM trend with CA50 tends to increase at a sharper gradient with higher GTL blend ratio though this just means GTL blends are slightly more sensitive to good timing optimization.

There appears to be no clear correlation between rail pressure and PM trend. Results reveal that as was the case in Diesel LTC, small changes in injection pressure at this engine load have an insignificant effect on PM emission.

It should be noted that while in the 10° split injections the NO_x-PM trade-off is of a comparable value to the 7° split (Figure 7-5), the actual emissions are different (Figure 7-2, Figure 7-3), in the 10° split NO_x is slightly lower throughout the entire range but PM varies from very near 0.00 FSN for early timings, to much higher smoke for later ones. Long dwell-times results in a shorter range of usable combustion phasings, with small reductions in NO_x reflecting a very steep increase in PM. It is however interesting that the trade-off value does not improve, making even longer dwell injection unlikely to yield better results.

The trade-off also suggests there is very little advantage to be had in trading NO_x for PM; with later CA50 phasing PM rises rapidly while NO_x decreases a very small amount irrespective of fuel or injection regime; this is particularly true of the earliest phased test-points where zero or near-zero smoke is recorded: for example in the 7° split 600 bar G30 tests, over 6° CA injection phasing smoke increases from 0.007 to 0.157 while at the same time NO_x drops from 3.08 to 2.77 g/kg of fuel. Smoke emission effectively increases by two orders of magnitude while NO_x decreases by less than 10%. It should be noted, however, that smoke still remains relatively low. This extreme behaviour manifests as the left-most points on the NO_x-PM trade-off graphs (Figure 7-5) which with GTL blends offer improved PM for equivalent NO_x to Diesel. This is a particularly interesting finding for the transition between conventional and low-temperature combustion, which traverses the potentially high-soot region between the two operating regions.

Once again, there appears to be no significant benefit in using G50 in lieu of G30. In fact, G50 appears to have identical or slightly inferior smoke emissions to G30. This correlates with work carried-out by Schaberg et al (2005) where they demonstrate a 50-50 GTL-diesel blend showing approximately a 30% improvement in NO_x-PM trade-off (with both emissions improved to a similar degree) while only a further 5% increase to that for a 100% GTL fuel.

It is not clear why this occurs. It would be expected that the lower aromatic content and lower distillation characteristics of GTL would contribute to significantly lower smoke emissions; Kitano et al (2005) report up to a 70% reduction in smoke under conventional combustion burning GTL fuel. Oguma et al. (2002) similarly report either a significant decrease or a negligible increase in smoke under conventional conditions, running GTL in an unmodified passenger car CI engine.

That the smoke is not reduced in LTC accordingly possibly suggests there is great difference in the formation method, or possibly the soot oxidation method between conventional and low-temperature combustion. Detailed fundamental flame studies and chemical kinetic analysis would be necessary to clarify whether soot formation or oxidation is the prevailing determining factor under these conditions.

Work carried out by Musculus et al (2007) and Bobba et al (2009) suggests that specifically for LTC conditions, soot is formed either just before or shortly after the end of injection. The shape of the mass-profile over time varies notably between regimes with disparate ignition delay. Overall however, under LTC conditions longer ignition delays correlate well with low soot, thanks to the superior mixing possible. It is possible that diesel's lower Cetane number, which led to improved mixing prior to ignition, offset the reduced aromatic content of the diesel-GTL blend fuels. Whether an equivalent result would be seen with an aromatic-free fuel such as pure GTL is unknown but would be worthy of further evaluation.

7.3.3 Hydrocarbons and carbon monoxide (tHC & CO)

tHC and CO emissions through GTL blend show interesting trends: in single injection they're both improved with respect to diesel (Figure 7-1, Figure 7-2, Figure 7-3), with G30 showing a small improvement and G50 more so. In 7°split injection it is not clear whether the GTL blends are either a marginal improvement or practically no different to Diesel, though CO does show a small improvement from G30 to G50.

In the 10° split injections Diesel displays the worst CO and tHC of the three fuels with increasing GTL blend improving the emissions. 10° split as discussed in the previous

chapter is naturally the worst regime for tHC and CO as it represents the regime most likely to exhibit unburnt fuel in the exhaust (thereby raising tHC) and conditions which contribute significant amounts of unburnt fuel to the exhaust generally tend to have a higher fraction of their fuel partially burnt and form CO. GTL appears to behave very well in long-dwell split injection however, reigning in the high tHC and CO emissions of Diesel with the G30 blend while the G50 blend brings the emissions nearly in-line with those observed in the 7° split injection tests. These results suggest GTL has effected notable change, though it is most likely due to the change in ignition delay and combustion propagation characteristics. What is perhaps more interesting is that the changes observed under LTC conditions are not necessarily the same changes we'd anticipate from conventional combustion.

By and large tHC and CO appear to be unaffected by rail pressure with some exceptions; In single injection it is clearly visible that increasing rail pressure by 100 bar reduces CO by circa 30% and tHC by 20-40%. This trend is not visible in either of the GTL blends which are universally superior in both emissions. This perhaps suggests the GTL is assisting in stabilizing the combustion (though IMEP-CoV did not display any visible trend) and promoting burning in particular for test-points which are limited by mixing. This perhaps is why the rise in injection pressure offers benefits to diesel, but not in GTL as further improvement in GTL blends is limited by some different factor.

There appears to be a phenomenon which is visible in the 10° dwell with diesel, where the CO in particular at its latest phasing shows decreased CO with lower injection pressure. It is not clear why this is the case. Perhaps the longer combustion duration and later start of combustion results in higher levels of CO when bulk quenching starts to occur, though this is not clear.

7.3.4 In-cylinder pressure and heat release rate

The substitution of diesel by GTL has not significantly affected the shape of the ICP curve. As an indication, three 7° split tests of CA50 at 355° and 700 bar rail pressure are superimposed in Figure 7-6. The three pressure traces are nearly identical with

the only visible exception being that diesel appears to have a slightly higher profile over the peak of the combustion after a slightly later ignition, as would be expected from the longer ignition delay. The higher pressure also suggests a greater degree of premixing, as suggested above. Once again, there is nearly no difference between G30 and G50 blends, suggesting that the effect is primarily that of ignition phasing (relating to Cetane number) and not a result of the chemical composition of the fuel.

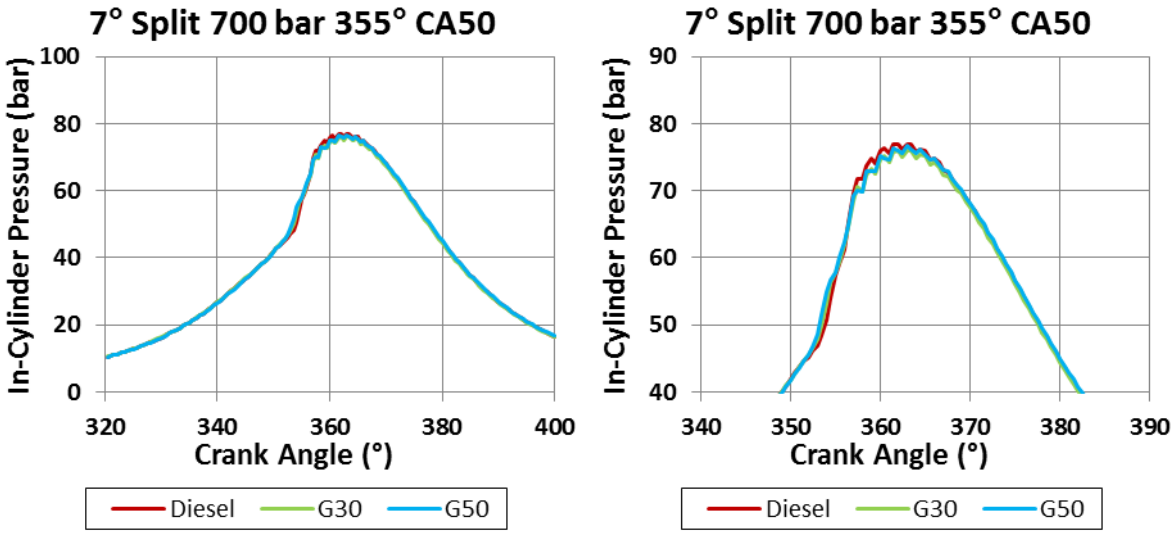

Figure 7-6: ICP Comparison of Diesel, G30 & G50 in 7 Dwell, 700 bar Prail, 355 CA50 LTC

There is no particular trend through GTL blend ratio in heat release, other than a slight increase in the volume of heat released during the cool-flame reaction; GTL tests generally tend to have a marginally more distinguishable cool-flame heat release than diesel. Aside from that, heat-release of GTL blends is roughly in-line with diesel as in Ch.6.3.1. For similar CA50 phasings cool-flame heat release is nearly indistinguishable between the three fuels. A typical example of this is Figure 7-7, where the heat release rate of all fuels at 7° split injection at 700 bar rail pressure with a 357°CA50 is shown. It should be noted the excessive volatility in HRR late in the combustion (circa past 360°CA) is likely due to the pressure oscillations visible around peak cylinder pressure.

Of interest, the cool-flame reaction does not appear to be influenced in the same way as the main combustion, with no distinct change between fuels. Almost

invariably, however, the first peak in heat release is higher in Diesel than it is in G30, which is slightly higher or identical to that of G50. This makes sense, given the lower Cetane number, and hence longer ignition delay and more premixing of the diesel compared to the two GTL blends. Regardless, it is impossible to distinguish between the cool-flame reactions of the three fuels either in phasing or in magnitude of heat release.

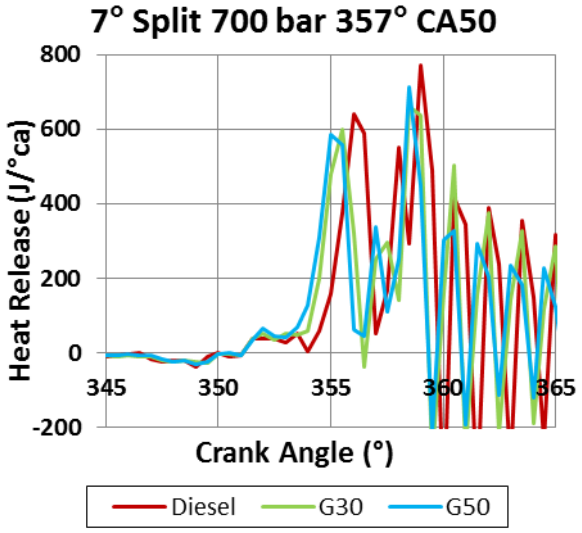

Figure 7-7: Heat Release of Diesel, G30 & G50 at 7° Dwell, 700 bar rail pressure, 357 CA50 LTC

7.4 Variability of in-cylinder pressure through gas-to-liquid fuel blend ratio

Comparing the ICP-SD traces of the GTL blends to the diesel reference tests one interesting trend is apparent: It appears the variability peaks of G30 and G50 are comparable or higher in single injection compared to diesel, yet lower in both types of split injection than diesel. Indicatively, single 600 bar injection yielded an average peak of 0.8 in ICP-SD for diesel, 1.2 for G30 and 0.8 for G50 (Figure 7-8), yet comparing 7° split at 700 bar shows 0.9, 0.6 and 0.6 for diesel, G30 and G50 respectively. Why GTL blends are especially more repeatable than diesel in split injection and not so in single is not clear. Regardless, both peak and mean ICP-SD appears to be universally reduced for G50 compared to G30.

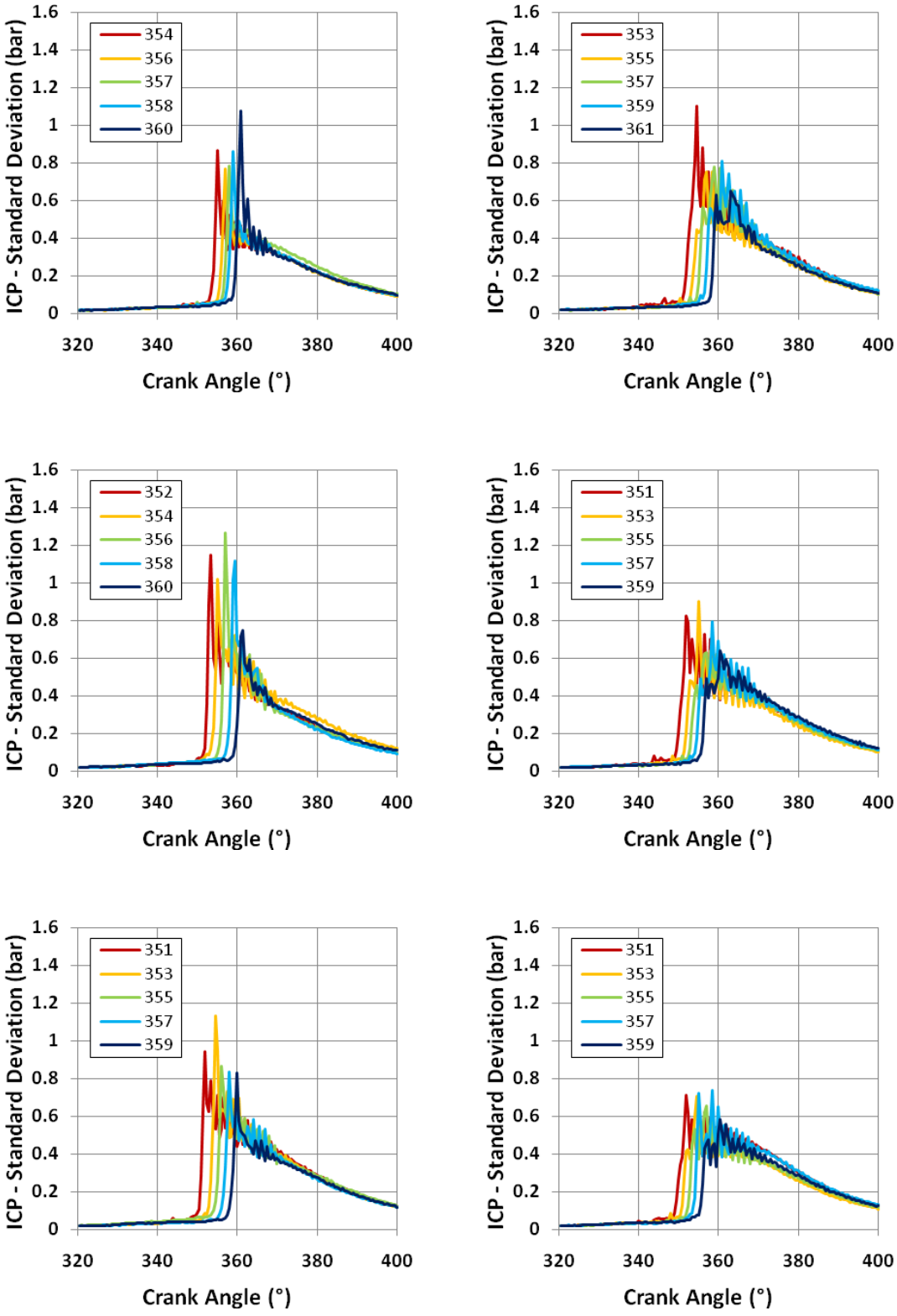

Figure 7-8: ICP-SD comparison. Left side: Single injection 600 bar Prail. Right side: 7° split injection 700 bar Prail. Top: Diesel. Middle: G30. Bottom: G50.

Just like diesel, GTL appears to occasionally display ICP-SD behaviour that may indicate two-stage combustion, with an ICP-SD trace that appears to have two peaks that are staggered (such as the latest phased cases in the 10° split injections displayed on Figure 7-8).

7.4.1 Indicated mean effective pressure (IMEP) and indicated specific fuel consumption (ISFC) findings

As in chapter 6, IMEP was aimed at 3.0 bar and was throughout highly consistent. There does not appear to be a trend in either IMEP or IMEP-CoV through GTL fuel. There is also no clear trend through either factor through rail pressure. Overall, GTL blends exhibited similar behaviour in their cycle-by-cycle power output.

There are likewise few findings in ISFC; largely, G50 tends to exhibit lower fuel consumption by circa 4-7% than G30 in most tests, which in turn is slightly better or identical to diesel. It is not clear why G50 has a notably higher efficiency than both G30 and diesel. This effect is most visible in single injection and short-dwell split at 700 bar rail pressure (Figure 7-9). There is nearly no difference in ISFC between rail pressures, the highest observable difference is in the G50 blend though the improvement is slight (Figure 7-10).

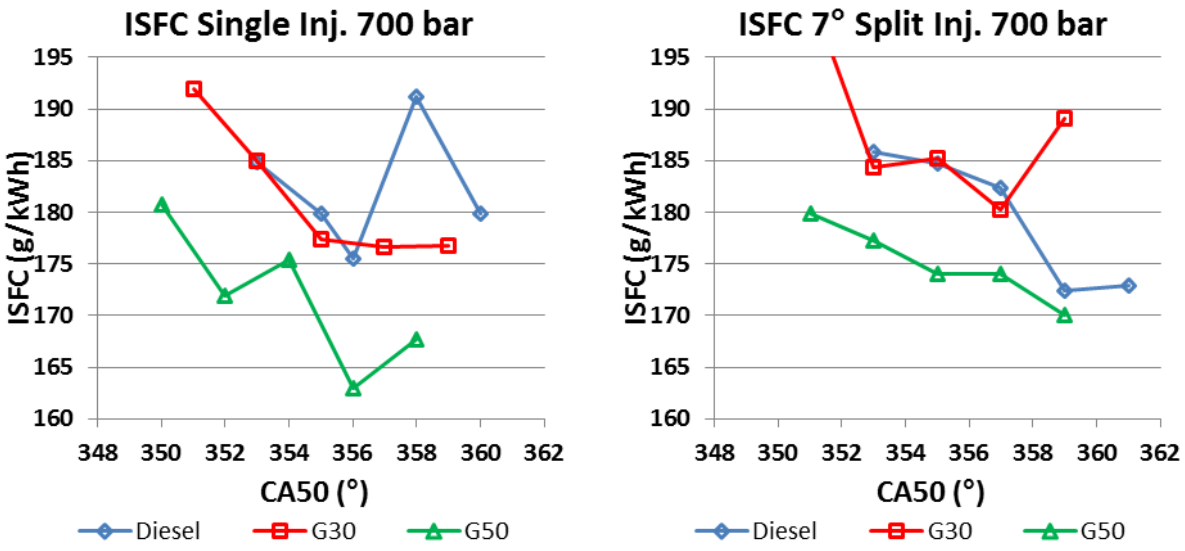

Figure 7-9: ISFC Vs. CA50, Diesel, G30 & G50 in Single and 7° Dwell LTC

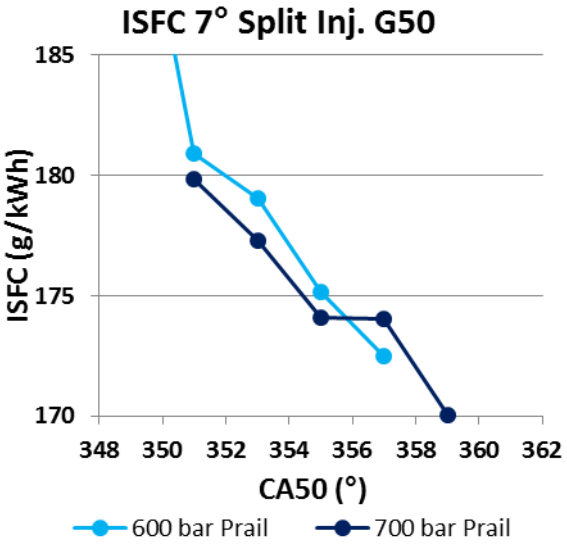

Figure 7-10: ISFC vs. CA50, G50 in 7° Dwell LTC

7.5 Summary: How gas-to-liquid fuel blends affect low temperature combustion

- Using GTL blends influences the combustion and emissions produced during LTC, however the exact way in which it does so depends on injection strategy. This is significant as it implies an engine calibration would have to incorporate adjustments to cater for fuel composition.

- Ignition delay is shortened when burning GTL blends under certain conditions; however the relatively small disparity between G30 and G50 suggests the ignition-promoting effect is non-linear. This agrees with the Cetane Number measurement which showed no significant difference between G30 and G50 but a significant increase relative to diesel.

- NO_x emissions in single injection are reduced with increased GTL blend ratio. However, the presence of GTL in the fuel does not appear to generate any significant reduction in NO_x in the split injection scenaria. It is not clear why this effect is only visible in single injection.

- For single injection cases the NO_x-PM trade-off is superior when combusting GTL blends; for the same near-zero PM emissions as diesel, NO_x is reduced.

- The NO_x-PM trade-off, particularly for later CA50 deteriorates rapidly in smoke. Earlier CA50 offers excellent gains in PM for a very modest relative increase in NO_x, though the trade-off goes to near-infinity as smoke reaches 0.0 FSN. These trends are not affected by the change in fuel type.

- Using GTL blends in LTC does not appear to give any particular benefits in terms of PM emissions compared with mineral diesel. This is surprising given the low aromatic content of the fuel; it suggests PM formation under LTC is notably different from conventional combustion.

- The 50% GTL blend showed lower peak ICP-SD values for every test series evaluated than the 30% GTL. Their variance compared to diesel was not consistent however; results were either slightly inferior or indistinguishable to diesel for single injection, but universally better for both types of split injection.

- Using GTL blends does not affect IMEP-CoV compared with diesel in LTC. GTL blends are equally stable and repeatable as diesel.

- G50 appears to offer a 4-7% benefit in fuel efficiency over G30 and diesel. There is no discernible difference in fuel efficiency between G30 and diesel.

- Rail pressure did not appear to be a significant factor in any of the results; fuel efficiency was unaffected, repeatability and emissions likewise seemed unaffected by changes. This is not surprising given the small range of rail pressures evaluated; however, the results do indicate that the use of GTL blend fuels did not introduce any more sensitivity to rail pressure than for conventional diesel.

- Overall, using GTL blends in LTC showed a useful emission benefit over plain diesel. The combination of lower NOx for nearly identical other emissions and

increased repeatability throughout the tests means that GTL blends constitute a superior fuel choice for LTC scenaria.

7.6 Novelty of knowledge gained

The knowledge gained from the previous chapter (6) was expanded on to establish how the relationships determined respond to a GTL/diesel blend fuel. Several novel observations were noted: an increasing GTL blend ratio appears to offer significant NO_x-PM trade-off benefits in LTC but only in certain injection conditions. The cyclic-behaviour of GTL blends was determined, compared to diesel, and found to show an atypical behaviour. These characteristics have not been investigated and compared before. The results suggest that high percentages of GTL blends could not be used interchangeably with diesel in engines running LTC without recalibration to accommodate the differences in combustion and emission characteristics, though with accurate fine-tuning there may be significant benefits.

8 Conclusions & Future work

Low-temperature combustion and other advanced strategies offer the potential to significantly reduce diesel engine emissions while maintaining efficiency and removing the need for costly and complex PM and NO_x after-treatment systems. However, to date these strategies are not in general use. This project aimed to help make LTC-type combustion strategies viable through a detailed investigation of the fuel system and combustion stability under the different injection and fuelling regimes needed. New beneficial fuelling regimes were also investigated, as was the effect of using these strategies with alternative fuels.

The work reported in this thesis focused on a single-cylinder research engine apparatus. Detailed measurements of pressure in the fuel line were compared to fuel delivery measured both on-engine and in a rate tube to assess the fuel system stability under multiple-injection regimes. In-cylinder pressure data was used to evaluate the stability of the combustion event and its sensitivity to the injection. Tailpipe emissions measurements were used to evaluate the overall impact of the combustion strategies investigated and the impacts of the shift towards alternative fuels.

8.1 Conclusions of research

Broadly, several groups of findings are presented:

- Pressure pulsations following injection events may influence the fuel delivered in subsequent injector events within the same cycle by as much as 50% if not accounted for during calibration.

- Modern complex “conventional” (low EGR) diesel combustion remains highly repeatable with low cycle-to-cycle variability, improving with increased injection complexity

- The behaviour of in-cylinder pressure cyclic variance offers valuable insight into the nature of the combustion and may be used to identify start of combustion

- Split injection regimes are good for reducing the EGR requirement in LTC, making it easier to bring to a commercially acceptable level.

- GTL substitution has no significant impact on combustion stability or emissions in LTC and offers potential benefits when correctly calibrated for.

8.1.1 Fuel line resonance and injector variability

Injector performance is highly repeatable and is not considered a significant source of variability. However, accounting for fuel-line resonance must be done correctly in order to capitalize on advanced injection strategies.

8.1.2 Combustion stability

While compression-ignition's repeatability remains high throughout the tests performed, the behavioural characteristics of the in-cylinder pressure standard deviation can be used to improve our understanding of the combustion process, as well as to anticipate potential spots of lower repeatability within the cycle. Examining the cyclic behaviour of in-cylinder pressure beyond IMEP-CoV may prove helpful in understanding combustion as its complexity increases over time.

8.1.3 Start-of-combustion identification

Being able to accurately determine the start of combustion is critical in the understanding of compression-ignition combustion. The specific advantages and disadvantages of each method need to be well understood so that the optimal method is selected, as not all methods are suitable for detecting all types of combustion event.

8.1.4 Injection strategies in conventional combustion

More complex injection strategies require a significantly higher degree of complexity at the calibration stage; high levels of optimization are necessary and useful as injection complexity increases. Two variables for each injection event added makes for a much broader calibration potential and with it the possibility of further gains in emissions and efficiency.

8.1.5 Injection strategies and Low-temperature combustion

Implementing low-temperature combustion with less extreme requirements is fundamental in enabling the technology to become main-stream. Injection regimes with more than one injection event per cycle are vital in this regard.

8.1.6 Gas-to-liquid fuel blends in low temperature combustion

If correctly calibrated to accept it, a compression-ignition engine running a gas-to-liquid fuel blend can show improvements over a diesel-fuelled one under low-temperature combustion. The fuel's improved chemical and physical characteristics may be contributory to the efficient implementation of low temperature combustion.

8.2 Novelty of knowledge gained

The existence and effects of fuel-line stationary waves are demonstrated to have significant impact on complex injection strategies. The necessity of adjusting subsequent injection event duration is demonstrated in order to compensate for changes in fuel quantity delivered. While these effects are thought to be known in the industry, they tend not to be openly discussed, and are normally avoided through design modifications. The description of the rail pulsations and effects presented here hence fills a gap in the scientific knowledge.

The impact of increasing injection complexity on cycle-by-cycle variation in in-cylinder pressure and mean effective pressure is investigated. This was possible thanks to the understanding of the previously examined fuel-line stationary wave.

The characteristics of in-cylinder pressure variation across the cycle are demonstrated to follow certain patterns and have a typical profile. This specific analysis to definitively determine the nature of the pressure-wave has not been done before.

Changes in emissions as well as fuel consumption are analysed through increasing injection complexity from one to three injections per cycle. These results demonstrated for the first time the importance of understanding the fuel rail pulsations on the subsequent combustion event in multiple-injection combustion.

The use of the variation in in-cylinder pressure on a crank-angle basis to evaluate the combustion event, and in particular the combustion phasing, provides a new technique for evaluating compression-ignition combustion. The evaluation and interpretation of the behaviour and morphology of the in-cylinder pressure standard deviation over the combustion cycle is novel and has not been done before.

Likewise, the same effects are investigated during low temperature combustion; the cyclic behaviour of LTC is compared to conventional combustion, and found to be even more repeatable; this is particularly interesting as it would be reasonable to expect such a high-EGR operating condition to suffer from poor repeatability. Testing LTC with such fine control over injection parameters, and correctly calibrated injection settings to account for fuel-line resonance has not been done before.

Subsequent tests in low temperature combustion using a 30% and 50% by volume GTL blend expanded this knowledge into new territory. How trends in emissions, pressure, fuel consumption and cyclic variability of pressure and mean-effective pressure behave through increased GTL blend ratio and increased injection complexity has not been done before. An unprecedented result that GTL blend ratio increase improves the NO_x-PM trade-off significantly only in single injection LTC but not in split injection LTC is both novel and unexpected.

8.3 Possible avenues of new research

There are several interesting possible avenues of new research arising from this body of work.

8.3.1 Fuel-line resonance

Further research using various types of injector with different sac volumes and fuel-lines of varying length/diameter could investigate whether there's a correlation between the ratio of volume of fuel in the injector to that in the fuel line and the stationary wave.

Alternative designs of fuel lines could be tested to establish whether it is feasible to prevent the stationary wave from propagating in the first place. Baffles in the line, or a varying diameter pipe could be considered.

Further testing on multi-cylinder engines with a view to damping out waves with opposing waves generated from other lines at strategically placed points in the fuel rail could be an alternative, more efficient solution.

Multiple pressure sensors across the fuel line's length as well as some in the fuel rail could help understand whether resonance produced in one injector's line affects the performance of other injectors in multi-cylinder engines.

Control software could be developed to automatically compensate for the difference in fuel pressure after a large injection. With enough refinement it could become a viable piece of engine calibration software. Software could even be calibrated to take advantage of the pulsation effect, adjusting injection timing so as to maximise pressure, increasing spray atomization without the increased losses that come with a higher rail pressure.

8.3.2 Start of combustion

Experimentation to determine how the SoC determination tools perform relative to each other could be expanded to incorporate a broader range of engines and a larger range of operating conditions. It is possible that very high engine speed or load may skew the results in an unexpected direction, or that more or less unstable combustion regimes alter ICP-SD in such a way that its relative merit changes. It may also transpire that lower resolution in-cylinder pressure transducers are less prone to errors with an ICP-SD based method. High resolution tests on multiple engine types could be performed in various combustion regimes to determine more accurately the relative merit of ICP-SD as a marker for start of combustion. Optical experimentation may also yield useful correlating results. The luminosity of early combustion reactants could help cross-check start of combustion markers against a superior (though technically more demanding) indicator.

8.3.3 Injection complexity

By increasing the number of injections per cycle it is possible to exert finer control over emissions, fuel consumption and engine noise. The application of one or two pilot injections, a post injection and a staggered multiple split-main injection can radically improve compression-ignition's potential under certain combustion regimes.

As a sub-set of this research avenue, low-temperature combustion may be further refined by separating the injection into more than two events, or possibly altering the ratios of each delivery. Perhaps three or four injections of varying quantity each time will allow LTC to be implemented at usefully lower EGR rates or with higher fuel efficiency. However, it is expected that increased injection duration and the corresponding reduction in total momentum of each injection pulse (because of the lower mass in each pulse) will likely lead to diminishing returns as the number of injection pulses increases for a given mass of fuel per cycle.

8.3.4 Gas-to-liquid fuel

GTL appears to offer interesting prospects: Further investigation into the particular nature of PM in LTC may show a different PM formation mechanism. There could also be interest in investigating which engine conditions perform at an acceptable level interchangeably between diesel and medium blends (above 15% but below 50%) of GTL-diesel, in anticipation of a possible future increase in the amount of GTL in pump-grade diesel, and subsequent necessity for engines capable of running such a blend with no alteration in calibration.

8.4 Implication of findings for future engine development

Compression-ignition combustion has a wealth of potential thanks to fine control over fuel delivery. Modern injection systems are capable of delivering multiple, highly controlled injections during each engine cycle and thanks to this engine calibrators have greater control over the combustion regime and subsequent emissions generated.

Correctly understanding the effect of fuel-line resonance enables engine developers and calibrators to take advantage of (rather than be hindered by) changes in fuel pressure through the injection cycle. Complex multiple-injection strategies cannot be implemented without adjusting injector opening duration to account for changes in fuel quantity delivered due to the resonance legacy of the preceding injection events.

In the era of mechanical injector units it was understood and accepted that compression-ignition was so repeatable cycle-by-cycle that investigating its cyclical behaviour was uncommon. Knowing that highly complex injection regimes and atypical combustion models do not change this trend ensures any instability is correctly attributed to its cause rather than an artefact of an inherently unstable condition.

Identifying where during the combustion cycle repeatability is lowest and why helps the interpretation and understanding of the chemical kinetics of combustion. It also

helps implement tighter control over the combustion process, as well as identifying specific mechanisms that enhance or worsen stability.

Low temperature combustion is a regime that in its current state is nearly commercially viable. The zero or near-zero NO_x and Smoke emissions achievable through its implementation are highly desirable despite its inability to function at high load. Minimizing the exhaust-gas recirculation required for it is crucial to its commercial application. Using a split-injection regime can usefully reduce the amount required, and by tailoring the injector design and injection strategy to not over-penetrate when very early injection is required it can further be refined to bring significant gains in emissions to low load compression-ignition.

The use of blends of advanced fuels such as GTL can have a modest effect on fuel efficiency, and a significant effect on the combustion which an engine control system could adapt for through the use of advanced injection strategies. In combination, this would allow the compression-ignition engine to continue to offer a low-emission, high-efficiency power plant which can adapt to changes in fuel composition and with a reduced reliance on fossil fuel.

9 Appendix

9.1 Incremental complexity tests injection parameters

Rail Pressure (bar)	**Pilot Injection** (mg@°CA BTDC)	**Main Injection** (mg@°CA BTDC)	**First Split** (mg@°CA BTDC)	**Second Split** (mg@°CA BTDC)
600	-	7.4@3.0	-	-
600	-	7.4@1.1	-	-
600	-	7.7@-1.1	-	-
700	-	8.0@0.4	-	-
700	-	8.0@-1.5	-	-
700	-	8.0@-3.4	-	-
600	1.5@21.0	3.9@7.1	-	-
600	1.5@19.1	3.9@4.9	-	-
600	1.5@16.9	3.9@3.0	-	-
700	1.5@20.6	4.65@6.4	-	-
700	1.5@18.8	4.5@4.2	-	-
700	1.5@16.2	4.85@1.9	-	-
600	1.5@22.1	-	3.2@9.0	1.3@3.0
600	1.5@19.9	-	3.35@7.1	1.3@1.1
600	1.5@18.0	-	3.2@5.3	1.3@-1.1
700	1.5@22.1	-	3.5@9.0	1.4@3.0
700	1.5@19.9	-	3.5@7.1	1.4@1.1
700	1.5@16.9	-	3.3@4.9	1.4@-1.1

Table 5: Incremental complexity tests injection parameters

9.2 Incremental complexity tests graphs

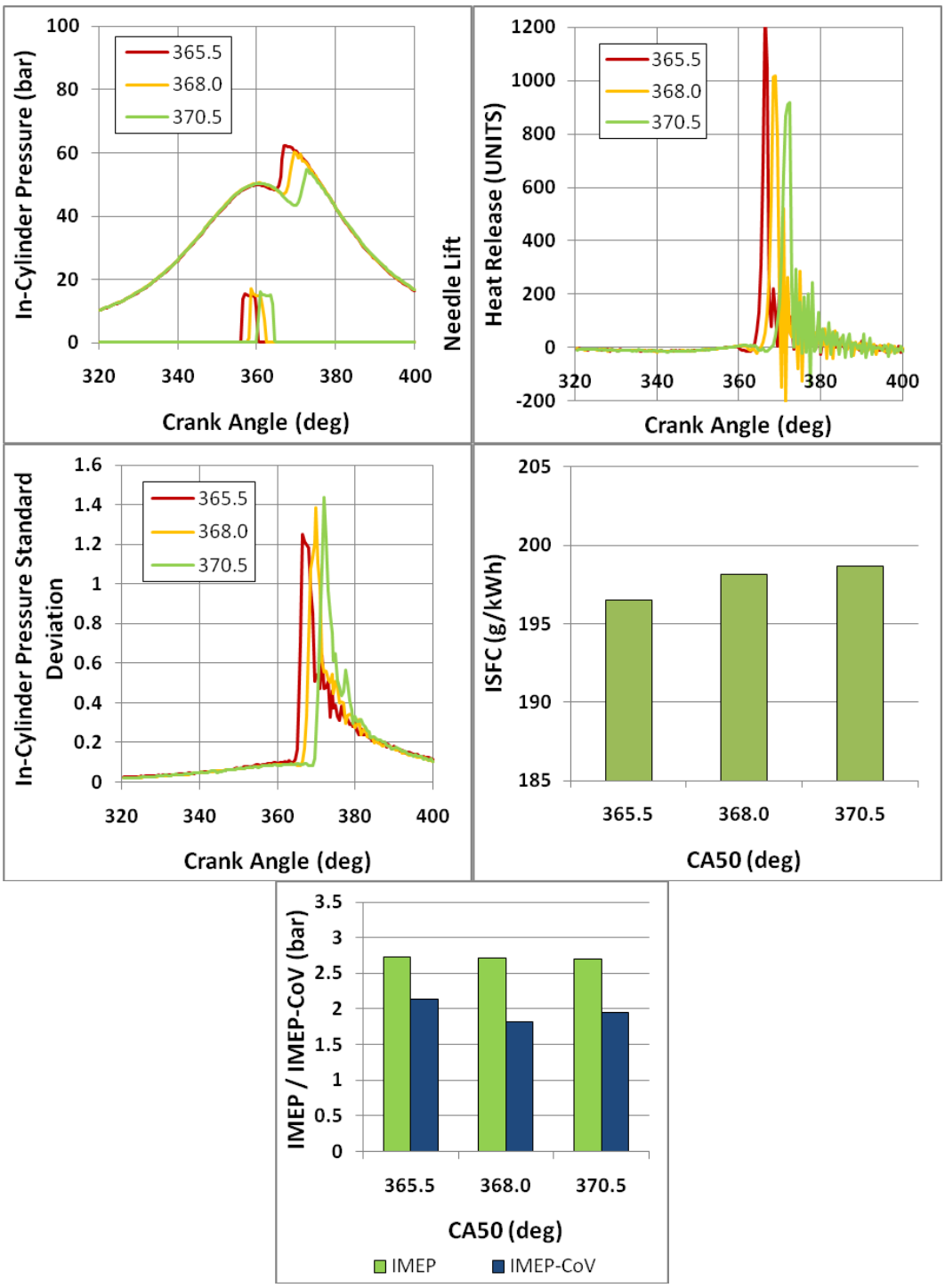

Figure 9-1: Single Injection 600 bar Prail

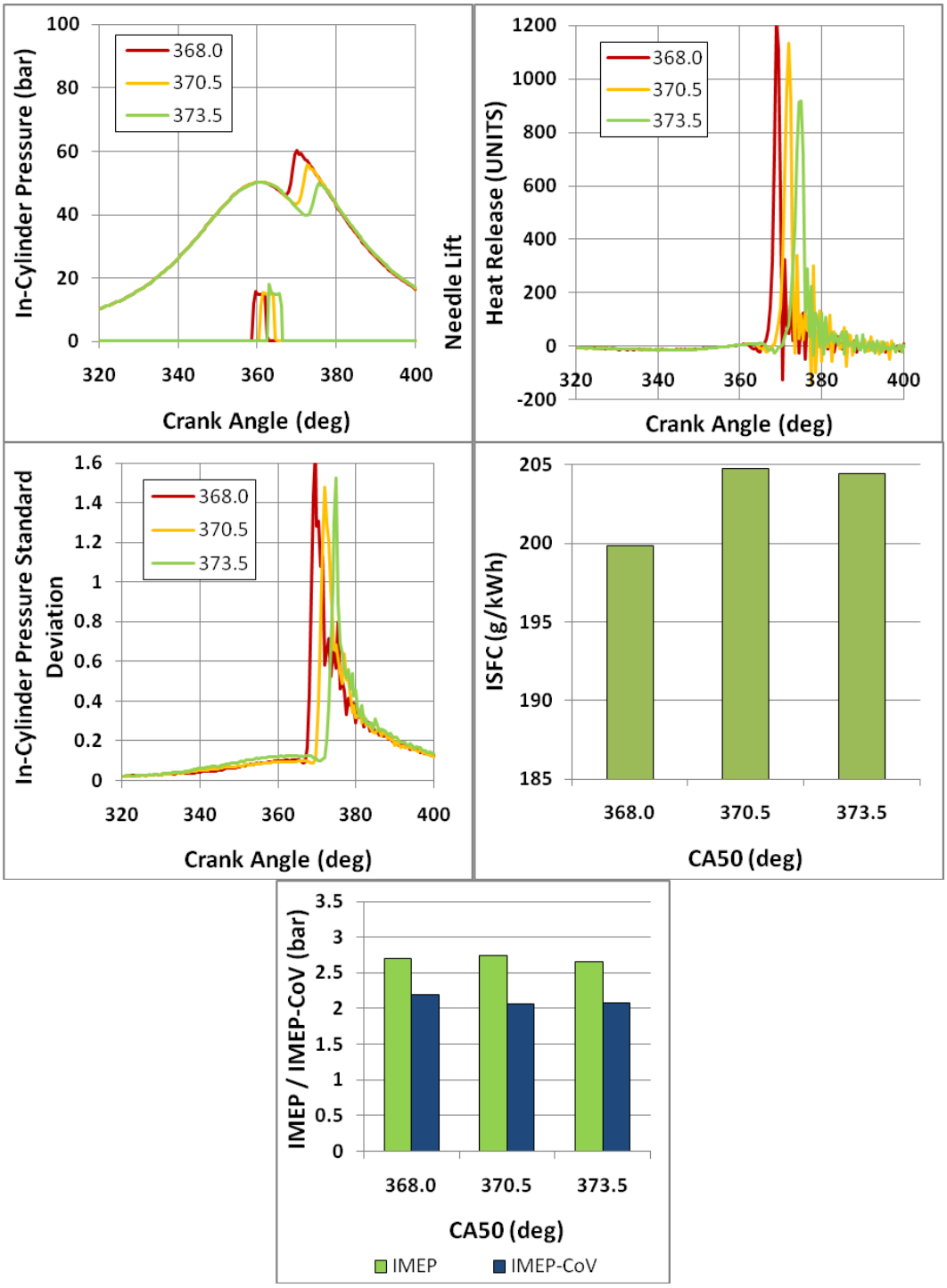

Figure 9-2: Single injection 700 bar Prail

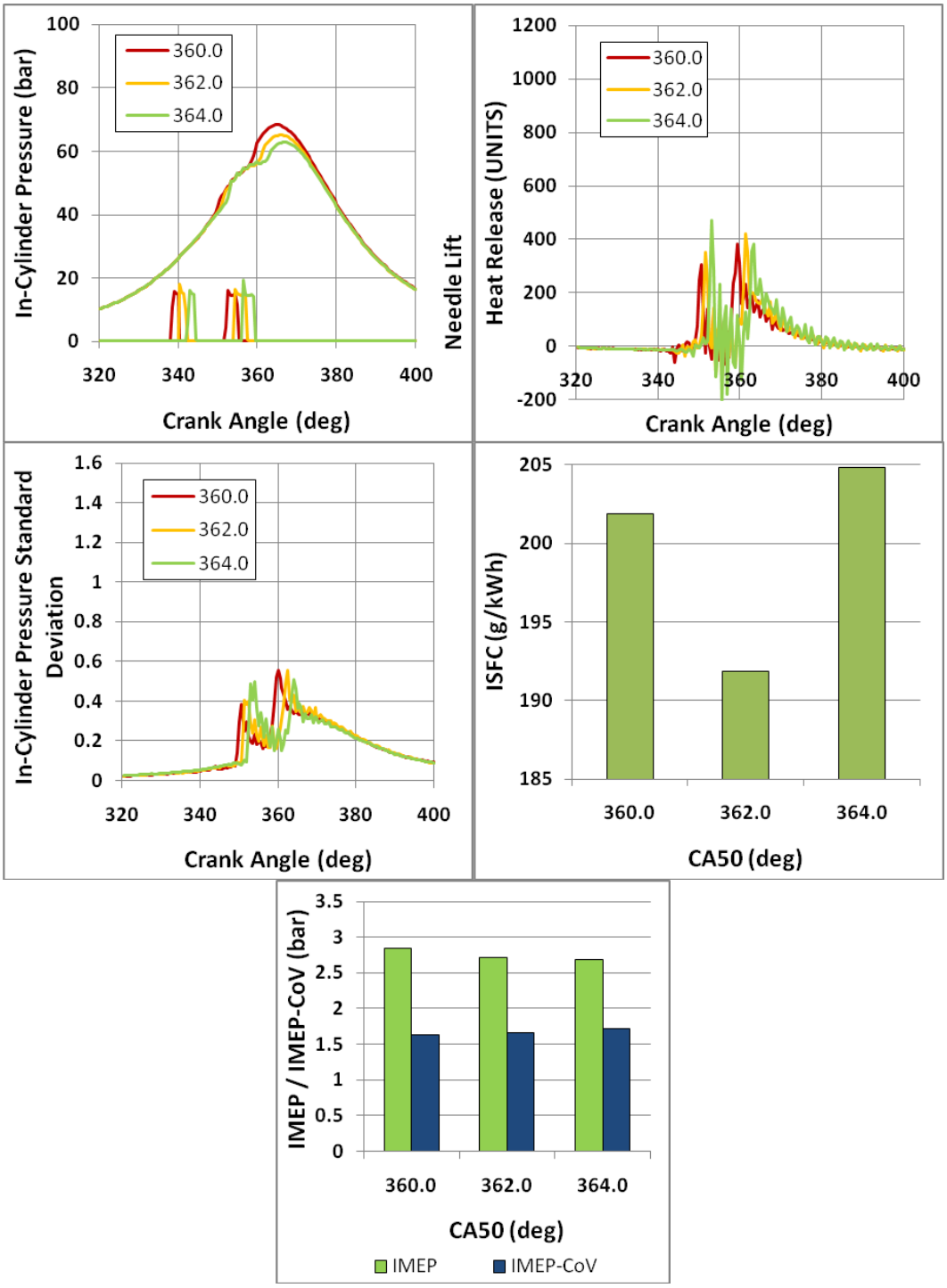

Figure 9-3: Piloted Single injection 600 bar Prail

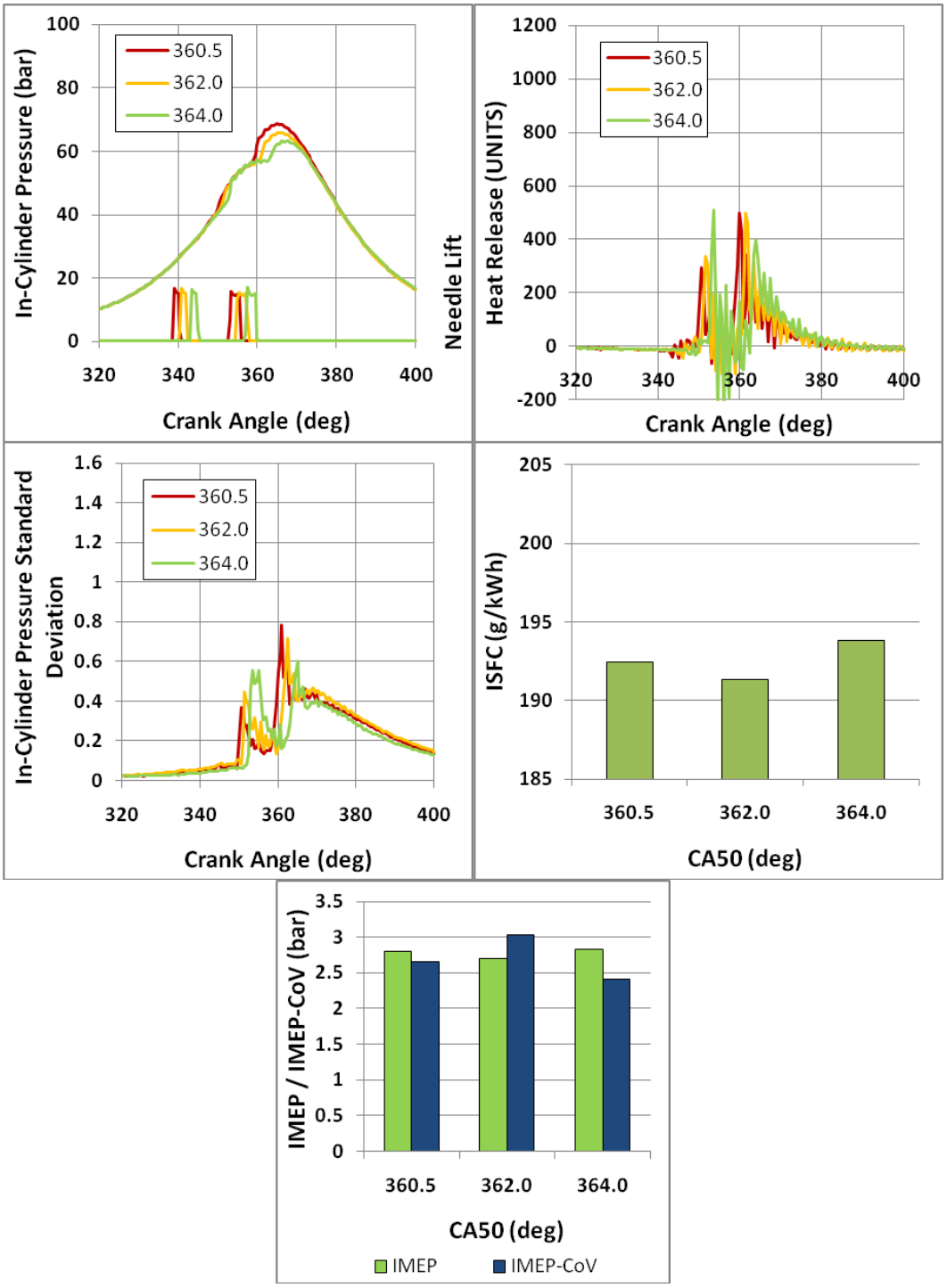

Figure 9-4: Piloted Single injection 700 bar Prail

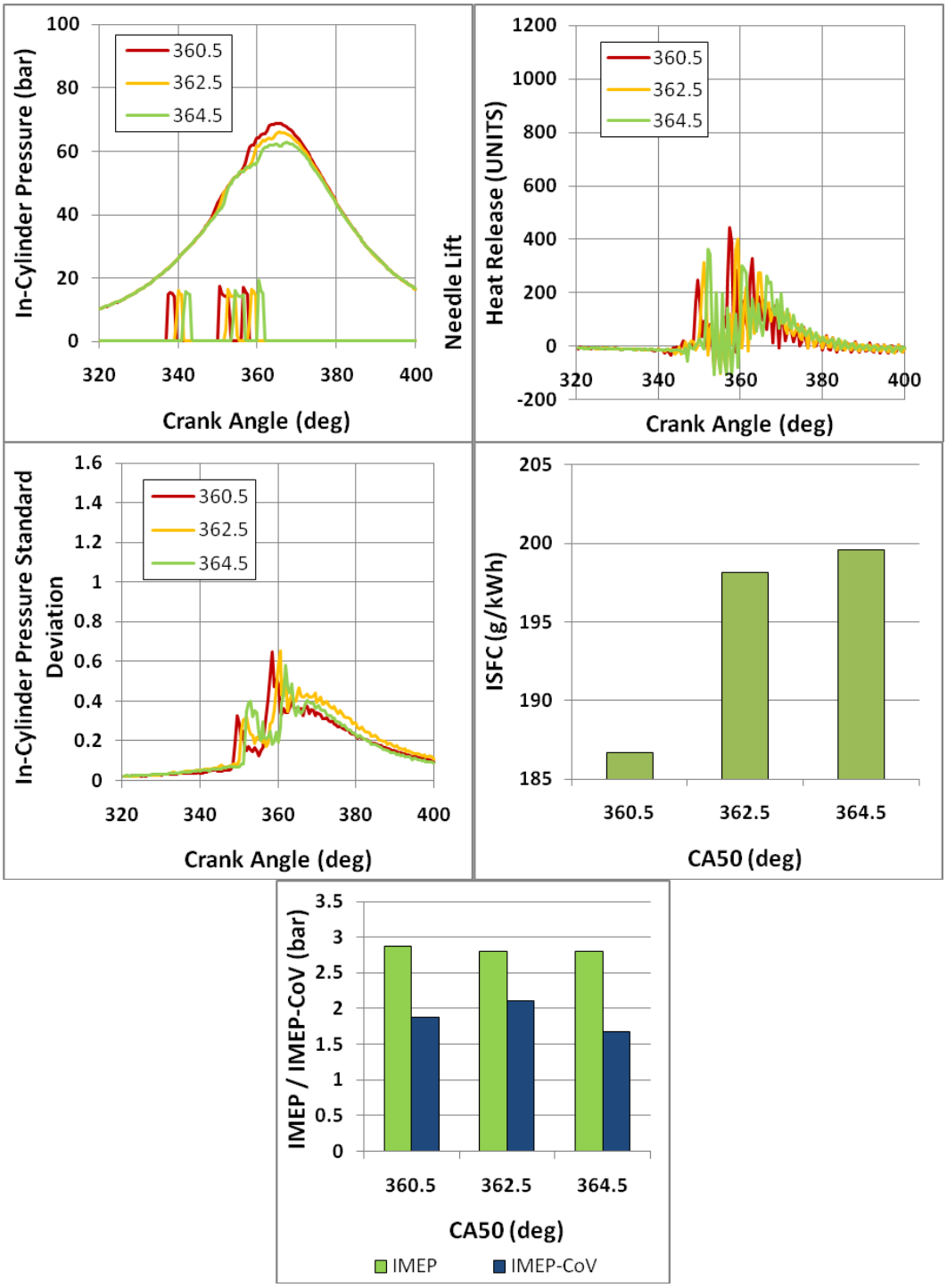

Figure 9-5: Piloted Split-main injection 600 bar Prail

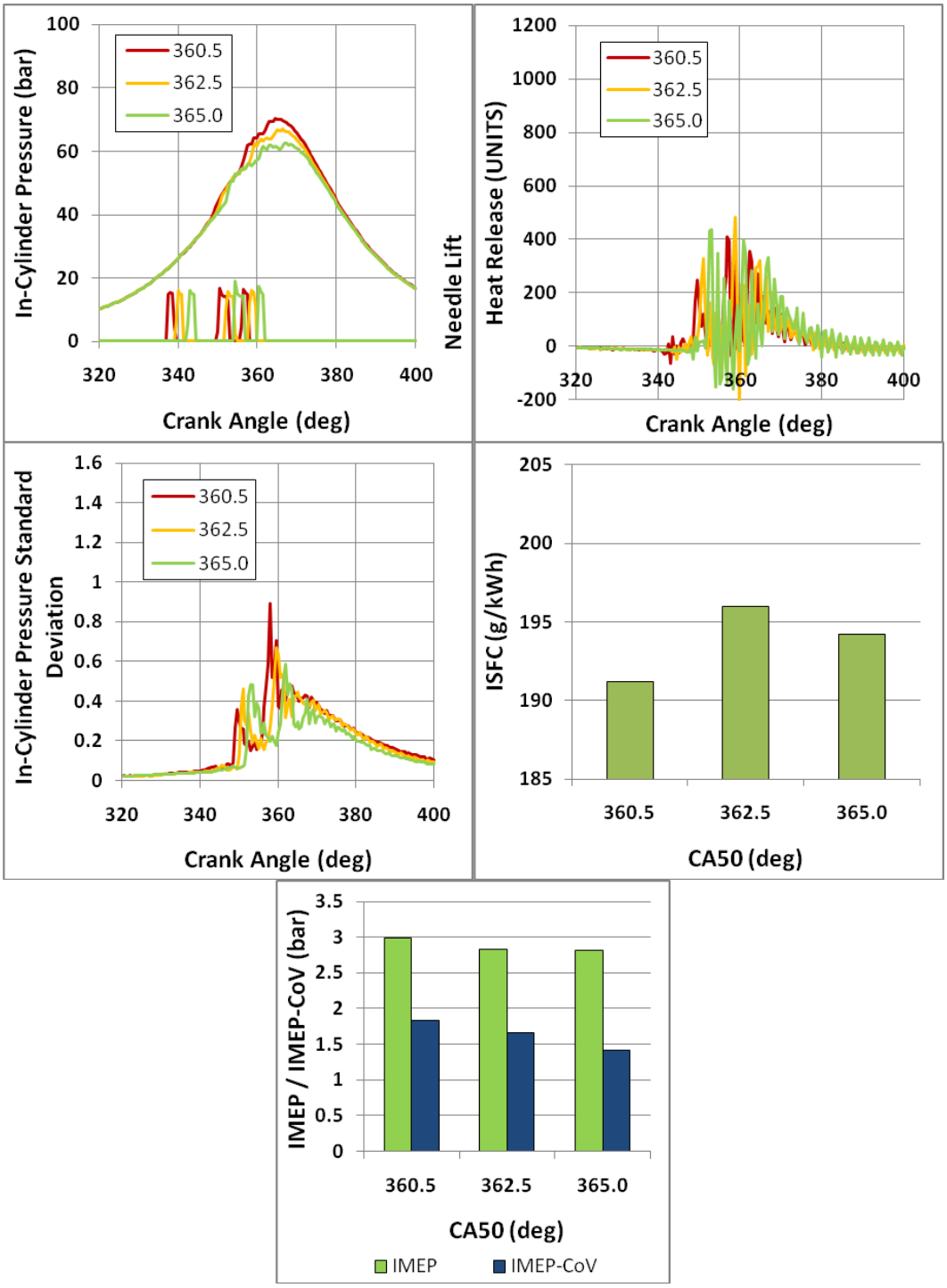

Figure 9-6: Piloted Split-main injection 700 bar Prail

9.3 Start of combustion determination tools comparisson

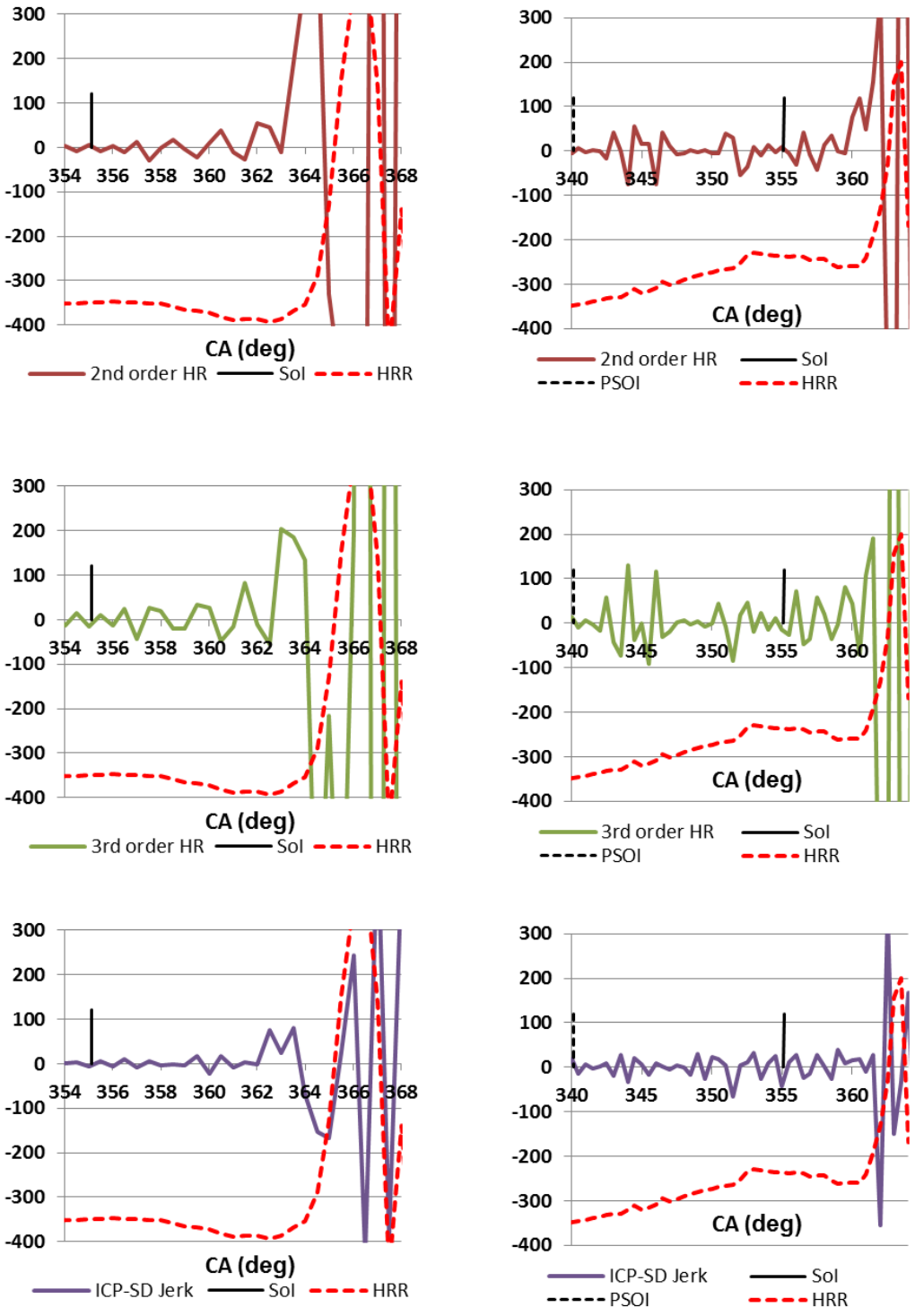

Figure 9-7: SoC tool comparison. Left: Diesel Single. Right: Diesel Piloted.

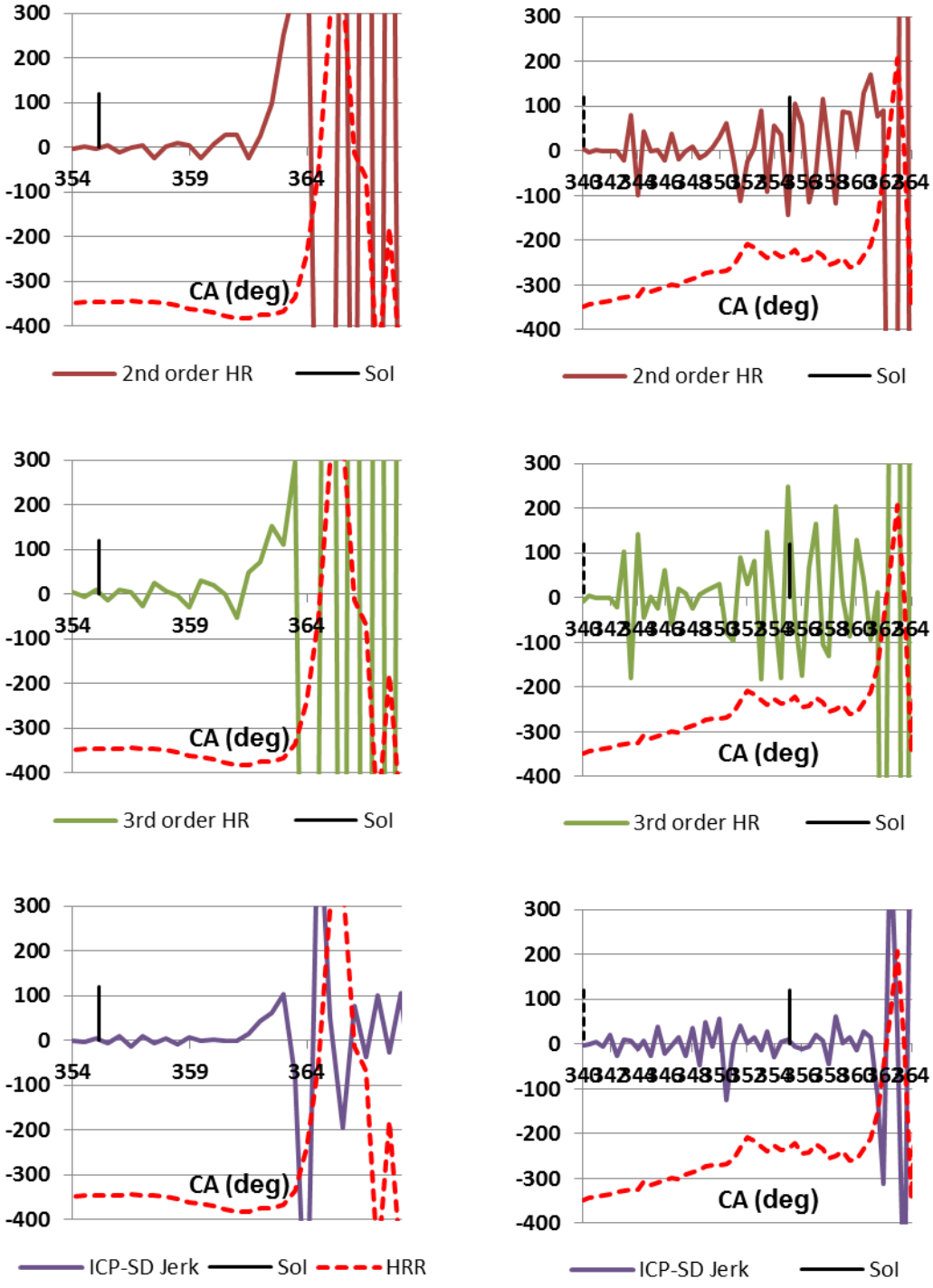

Figure 9-8: SoC tool comparison. Left: G30 Single. Right: G30 Piloted.

9.4 Diesel low temperature combustion injection parameters

CA50 (@°CA)	**Rail Pressure** (bar)	**Main Injection** (mg@°CA BTDC)	**First Split** (mg@°CA BTDC)	**Second Split** (mg@°CA BTDC)
354	600	7.35@19.1	-	-
356	600	7.35@18.0	-	-
357	600	7.35@15.8	-	-
358	600	7.35@15.0	-	-
360	600	7.35@11.6	-	-
353	700	8.2@20.6	-	-
355	700	8.2@16.9	-	-
356	700	8.2@13.5	-	-
358	700	8.2@12.4	-	-
360	700	8.2@10.1	-	-

Table 6: Diesel LTC Single Injection parameters

CA50 (@°CA)	**Rail Pressure** (bar)	**Main Injection** (mg@°CA BTDC)	**First Split** (mg@°CA BTDC)	**Second Split** (mg@°CA BTDC)
350	600	-	3.6@29.3	3.6@22.1
352	600	-	3.6@24.0	3.6@16.9
354	600	-	3.6@19.9	3.6@12.8
356	600	-	3.6@16.9	3.6@9.8
358	600	-	3.6@14.3	3.6@7.1
353	700	-	4.7@22.9	4.7@15.8
355	700	-	4.7@18.8	4.7@11.6
357	700	-	4.7@16.1	4.7@9.0
359	700	-	4.7@13.5	4.7@6.4
361	700	-	4.7@11.2	4.7@4.1

Table 7: Diesel LTC 7° Dwell Split Injection parameters

CA50 (@°CA)	**Rail Pressure** (bar)	**Main Injection** (mg@°CA BTDC)	**First Split** (mg@°CA BTDC)	**Second Split** (mg@°CA BTDC)
351	600	-	2.15@34.9	2.15@24.8
353	600	-	2.15@28.5	2.15@18.4
355	600	-	2.15@23.5	2.15@13.1
357	600	-	2.15@20.3	2.15@10.1
359	600	-	2.15@17.3	2.15@7.1
351	700	-	2.65@31.1	2.65@21
353	700	-	2.65@28.1	2.65@18.0
355	700	-	2.65@22.9	2.65@12.8
357	700	-	2.65@20.3	2.65@10.1
359	700	-	2.65@18.0	2.65@7.9

Table 8: Diesel LTC 10° Dwell Split Injection parameters

9.5 Gas-to-liquid fuel low temperature combustion injection parameters

CA50 (@°CA)	**Rail Pressure** (bar)	**Main Injection** (mg@°CA BTDC)	**First Split** (mg@°CA BTDC)	**Second Split** (mg@°CA BTDC)
352	600	7.35@19.9	-	-
354	600	7.35@17.3	-	-
356	600	7.35@14.3	-	-
358	600	7.35@11.6	-	-
360	600	7.35@9.4	-	-
351	700	8.2@22.1	-	-
353	700	8.2@18.8	-	-
355	700	8.2@15.8	-	-
357	700	8.2@12.8	-	-
359	700	8.2@10.5	-	-

Table 9: G30 LTC Single Injection parameters

CA50 (@°CA)	**Rail Pressure** (bar)	**Main Injection** (mg@°CA BTDC)	**First Split** (mg@°CA BTDC)	**Second Split** (mg@°CA BTDC)
349	600	-	3.7@28.5	3.7@21.4
351	600	-	3.7@24.8	3.7@17.6
353	600	-	3.7@21.0	3.7@13.9
355	600	-	3.7@18.4	3.7@11.3
357	600	-	3.7@16.1	3.7@9.0
351	700	-	4.7@25.1	4.7@18.0
353	700	-	4.7@20.3	4.7@13.1
355	700	-	4.7@18.0	4.7@10.9
357	700	-	4.7@15.8	4.7@8.6
359	700	-	4.7@13.5	4.7@6.4

Table 10: G30 LTC 7° Dwell Split Injection parameters

CA50 (@°CA)	**Rail Pressure** (bar)	**Main Injection** (mg@°CA BTDC)	**First Split** (mg@°CA BTDC)	**Second Split** (mg@°CA BTDC)
349	600	-	2.25@32.3	2.25@22.1
351	600	-	2.25@28.1	2.25@18.0
353	600	-	2.25@24.0	2.25@13.9
355	600	-	2.25@20.6	2.25@10.5
348	700	-	2.8@35.3	2.8@25.1
350	700	-	2.8@29.6	2.8@19.5
352	700	-	2.8@26.3	2.8@16.1
354	700	-	2.8@22.9	2.8@12.8
356	700	-	2.8@19.5	2.8@9.4

Table 11: G30 LTC 10° Dwell Split Injection parameters

CA50 (@°CA)	**Rail Pressure** (bar)	**Main Injection** (mg@°CA BTDC)	**First Split** (mg@°CA BTDC)	**Second Split** (mg@°CA BTDC)
351	600	7.6@22.1	-	-
353	600	7.6@18.8	-	-
355	600	7.6@15.8	-	-
357	600	7.6@13.1	-	-
359	600	7.6@10.9	-	-
350	700	8.4@24.0	-	-
352	700	8.4@19.9	-	-
354	700	8.4@16.9	-	-
356	700	8.4@13.9	-	-
358	700	8.4@11.6	-	-

Table 12: G50 LTC Single Injection parameters

CA50 (@°CA)	**Rail Pressure** (bar)	**Main Injection** (mg@°CA BTDC)	**First Split** (mg@°CA BTDC)	**Second Split** (mg@°CA BTDC)
349	600	-	3.8@28.5	3.8@21.4
351	600	-	3.8@24.0	3.8@16.9
353	600	-	3.8@21.0	3.8@13.9
355	600	-	3.8@18.4	3.8@11.3
357	600	-	3.8@15.8	3.8@8.7
351	700	-	5.2@24.8	5.2@17.6
353	700	-	5.2@21.0	5.2@13.9
355	700	-	5.2@18.0	5.2@10.9
357	700	-	5.2@15.8	5.2@8.7
359	700	-	5.2@13.5	5.2@6.4

Table 13: G50 LTC 7° Dwell Split Injection parameters

CA50 (@°CA)	**Rail Pressure** (bar)	**Main Injection** (mg@°CA BTDC)	**First Split** (mg@°CA BTDC)	**Second Split** (mg@°CA BTDC)
349	600	-	2.5@32.3	2.5@22.1
351	600	-	2.5@27.8	2.5@17.6
353	600	-	2.5@24.4	2.5@14.3
355	600	-	2.5@21.0	2.5@10.9
357	600	-	2.5@19.1	2.5@9.0
348	700	-	3.0@34.1	3.0@24.0
350	700	-	3.0@29.6	3.0@19.5
352	700	-	3.0@22.9	3.0@15.8
354	700	-	3.0@22.9	3.0@12.8
356	700	-	3.0@20.3	3.0@10.1

Table 14: G50 LTC 10° Dwell Split Injection parameters

9.6 Diesel low temperature combustion graphs

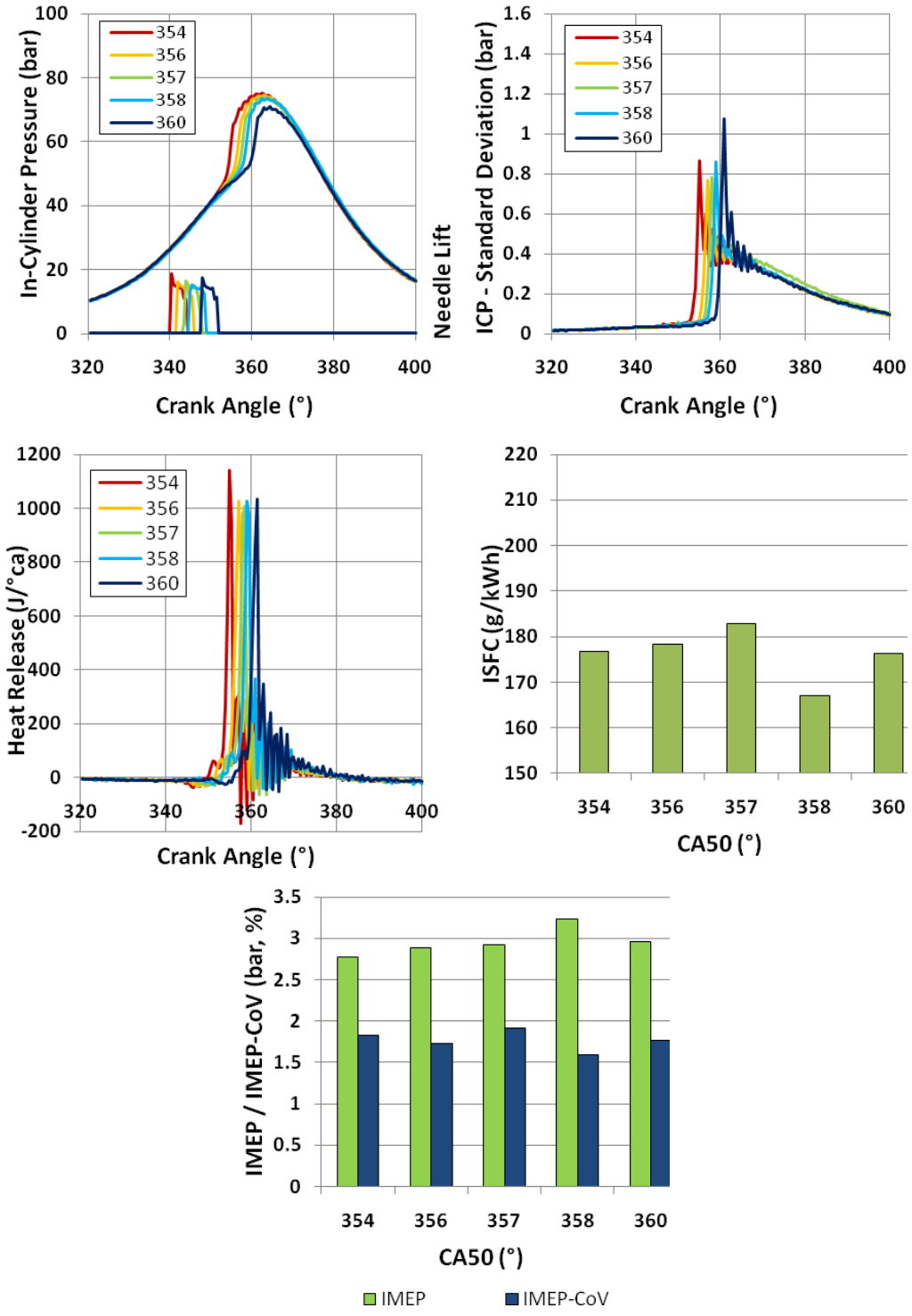

Figure 9-9: Diesel LTC Single injection 600 bar

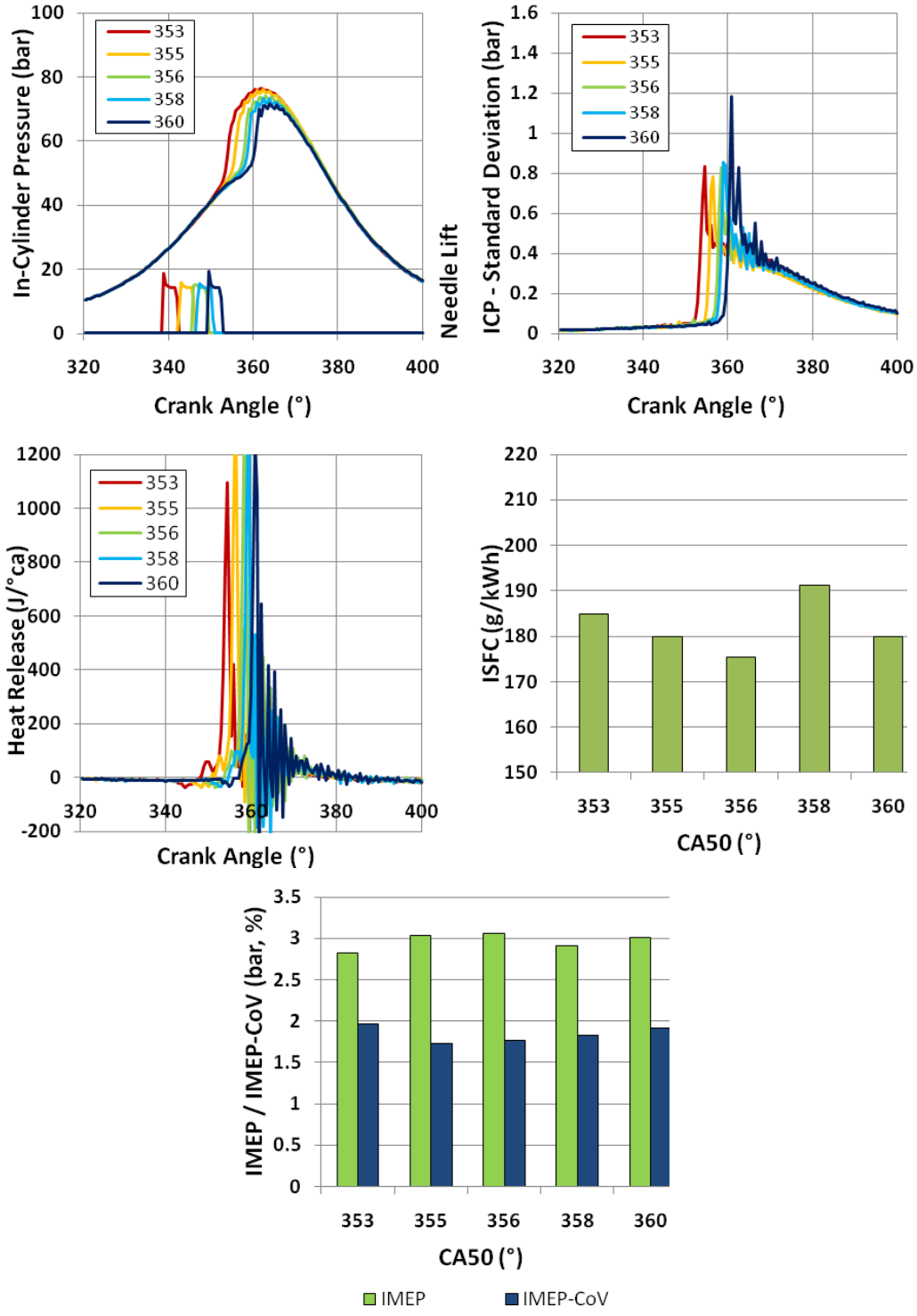

Figure 9-10: Diesel LTC Single injection 700 bar

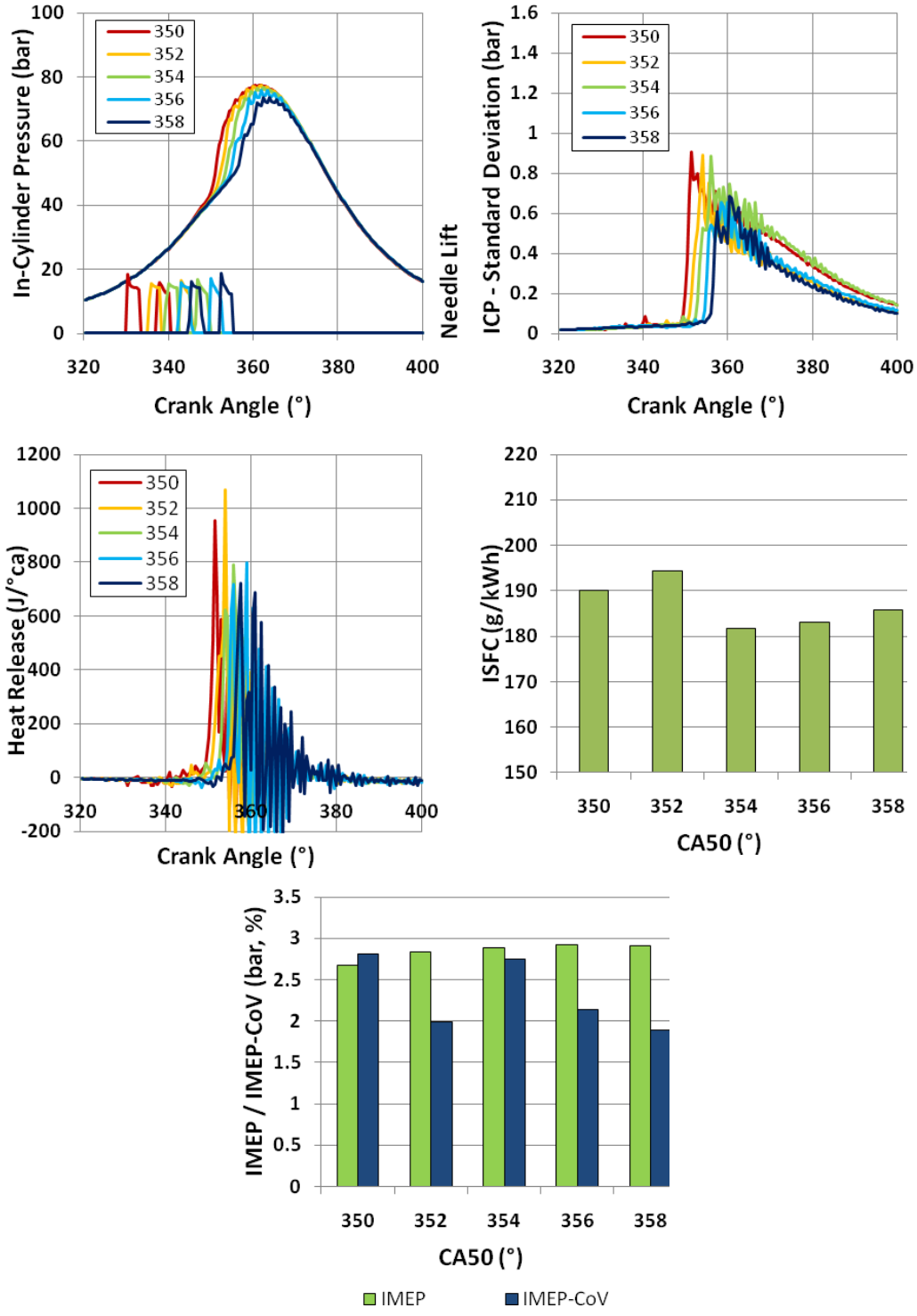

Figure 9-11: Diesel LTC 7° Split injection 600 bar

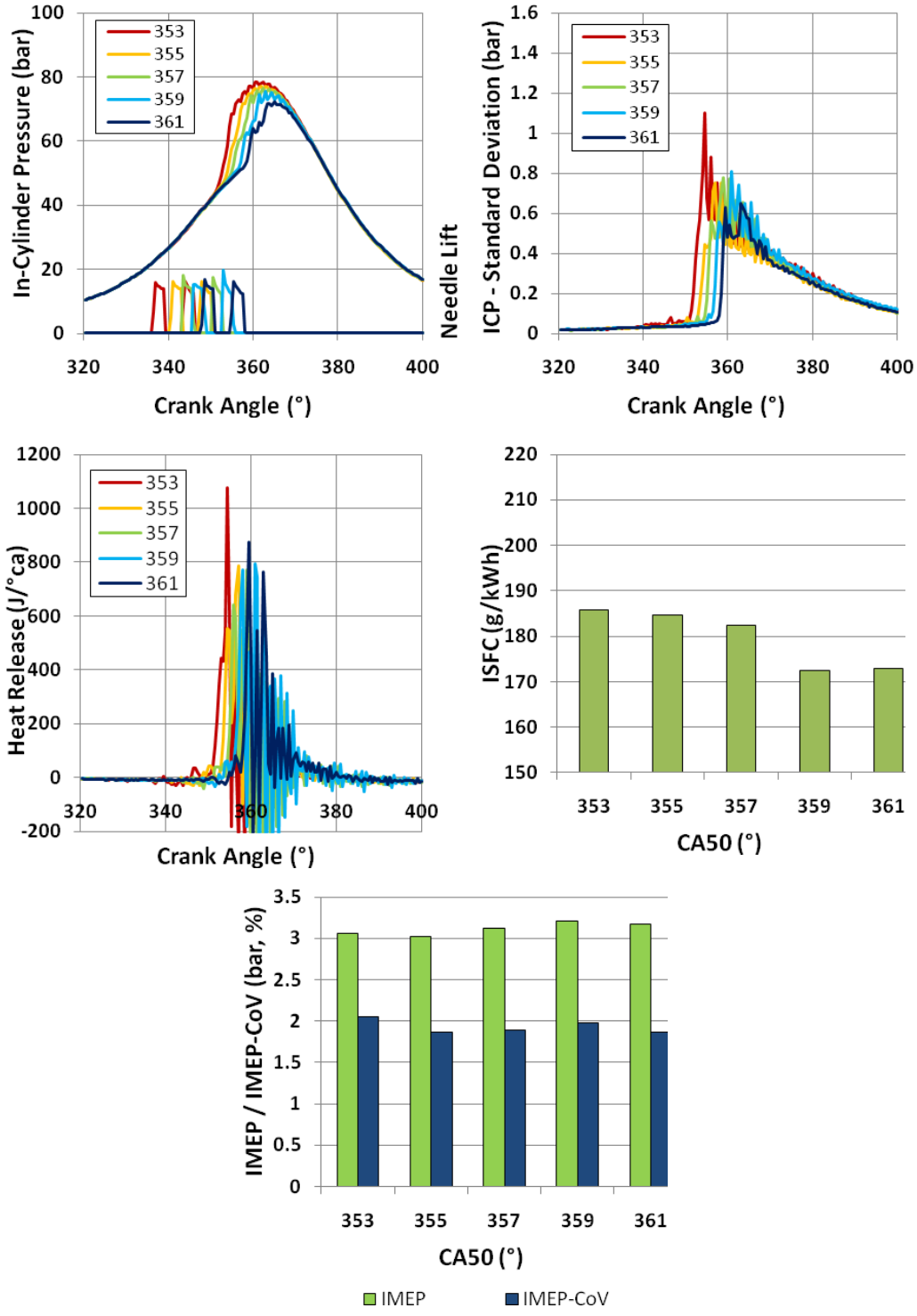

Figure 9-12: Diesel LTC 7° Split injection 700 bar

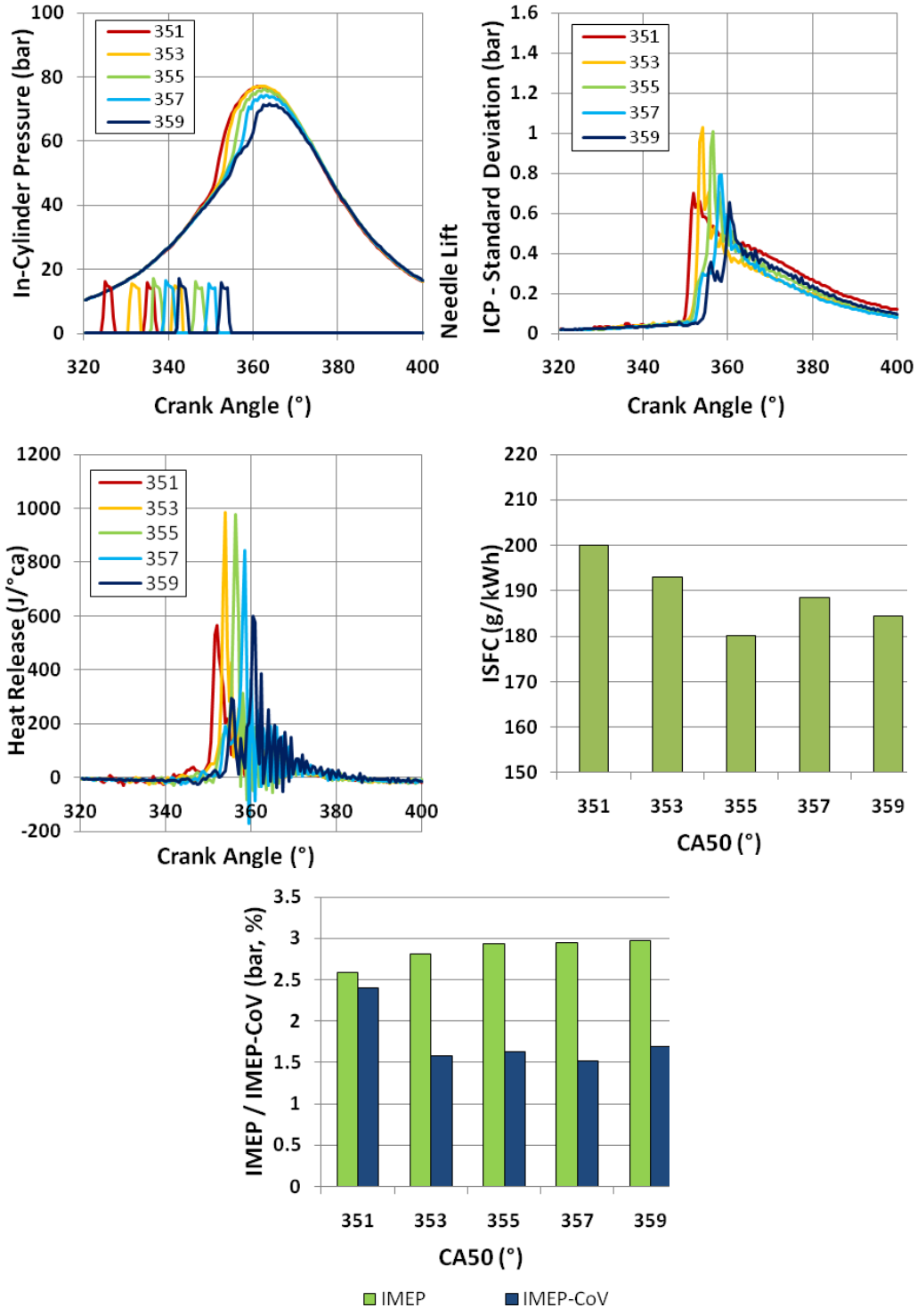

Figure 9-13: Diesel LTC 10° Split injection 600 bar

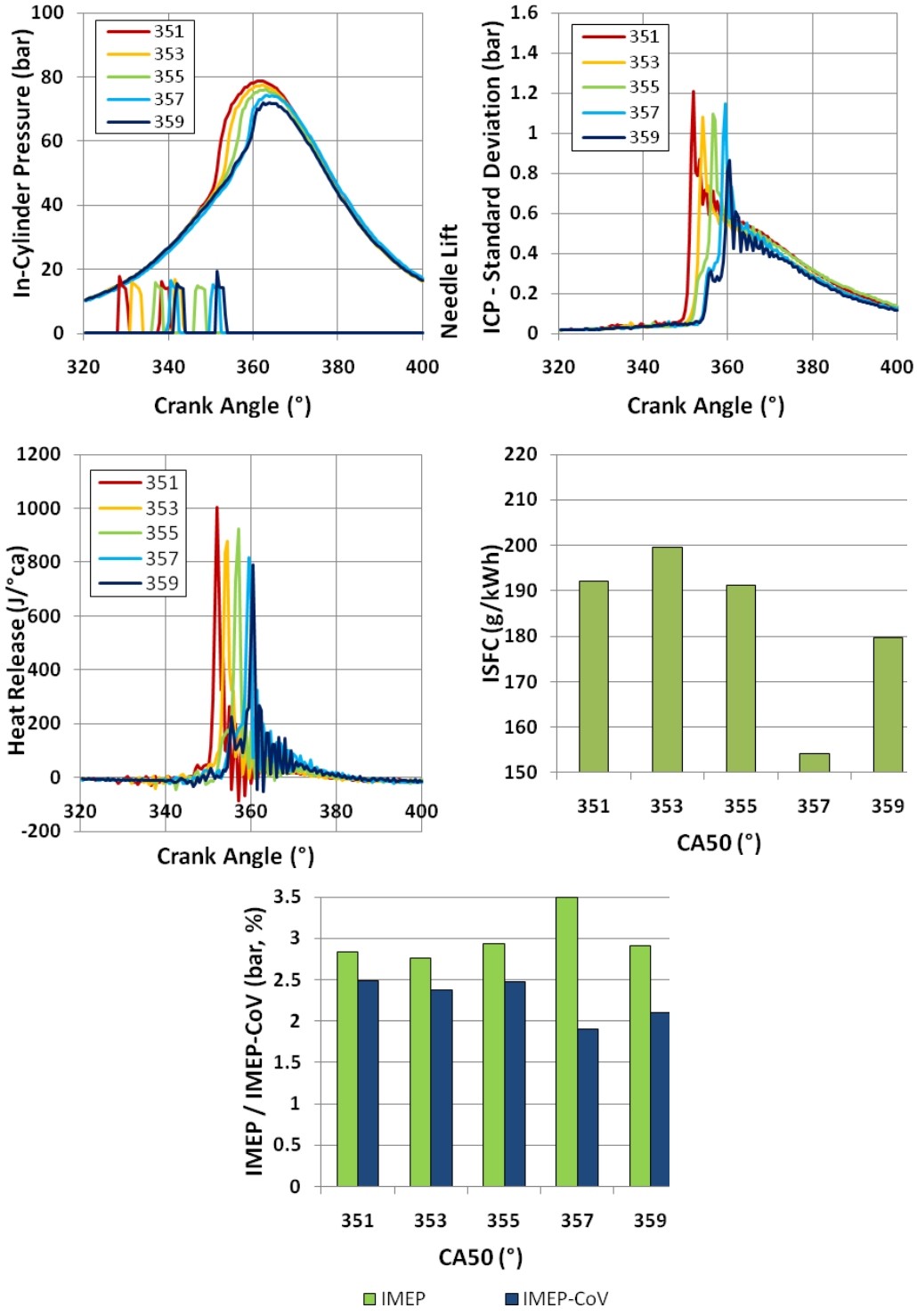

Figure 9-14: Diesel LTC 10° Split injection 700 bar

9.7 Gas-to-liquid fuel low temperature combustion graphs

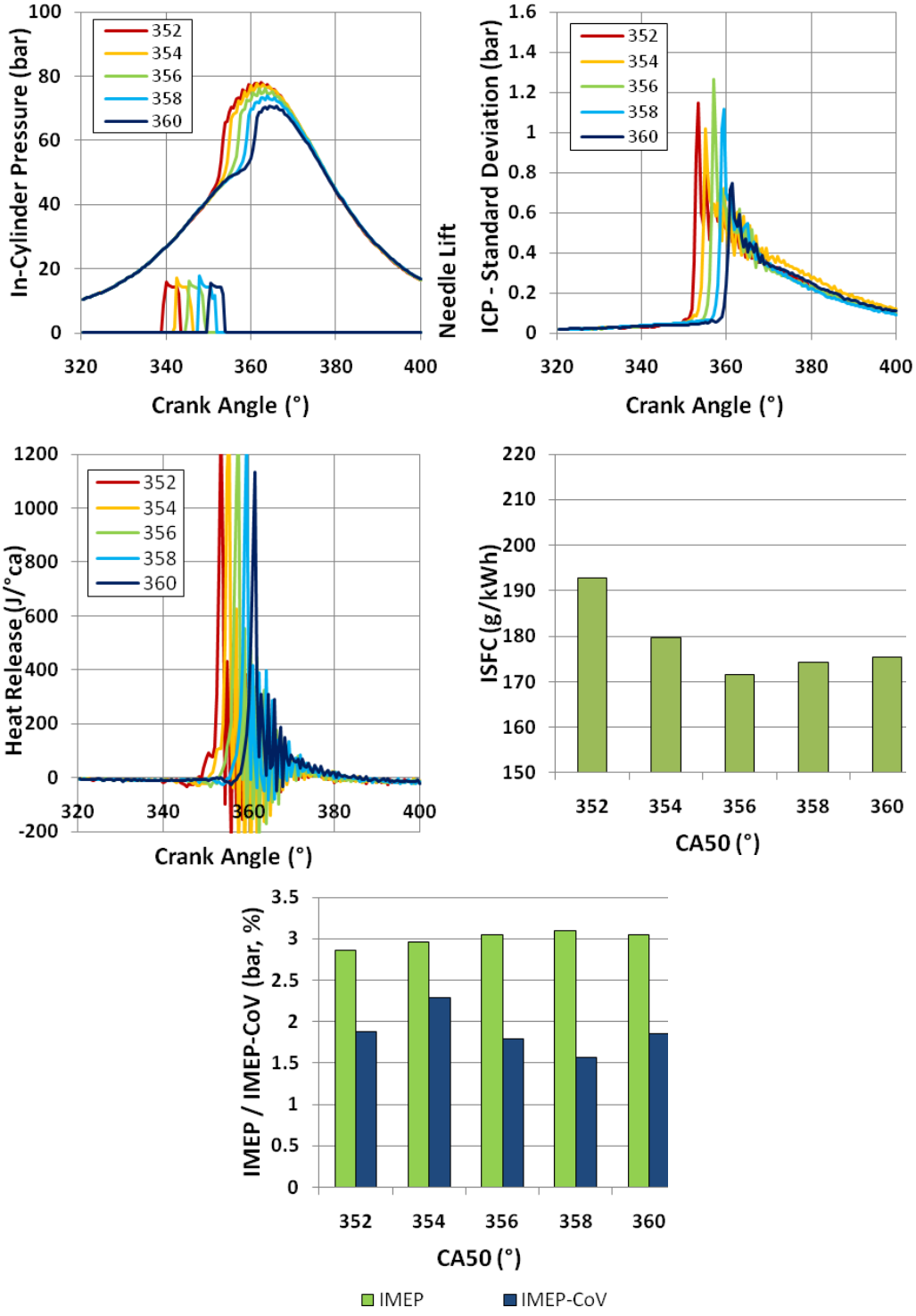

Figure 9-15: G30 LTC Single injection 600 bar

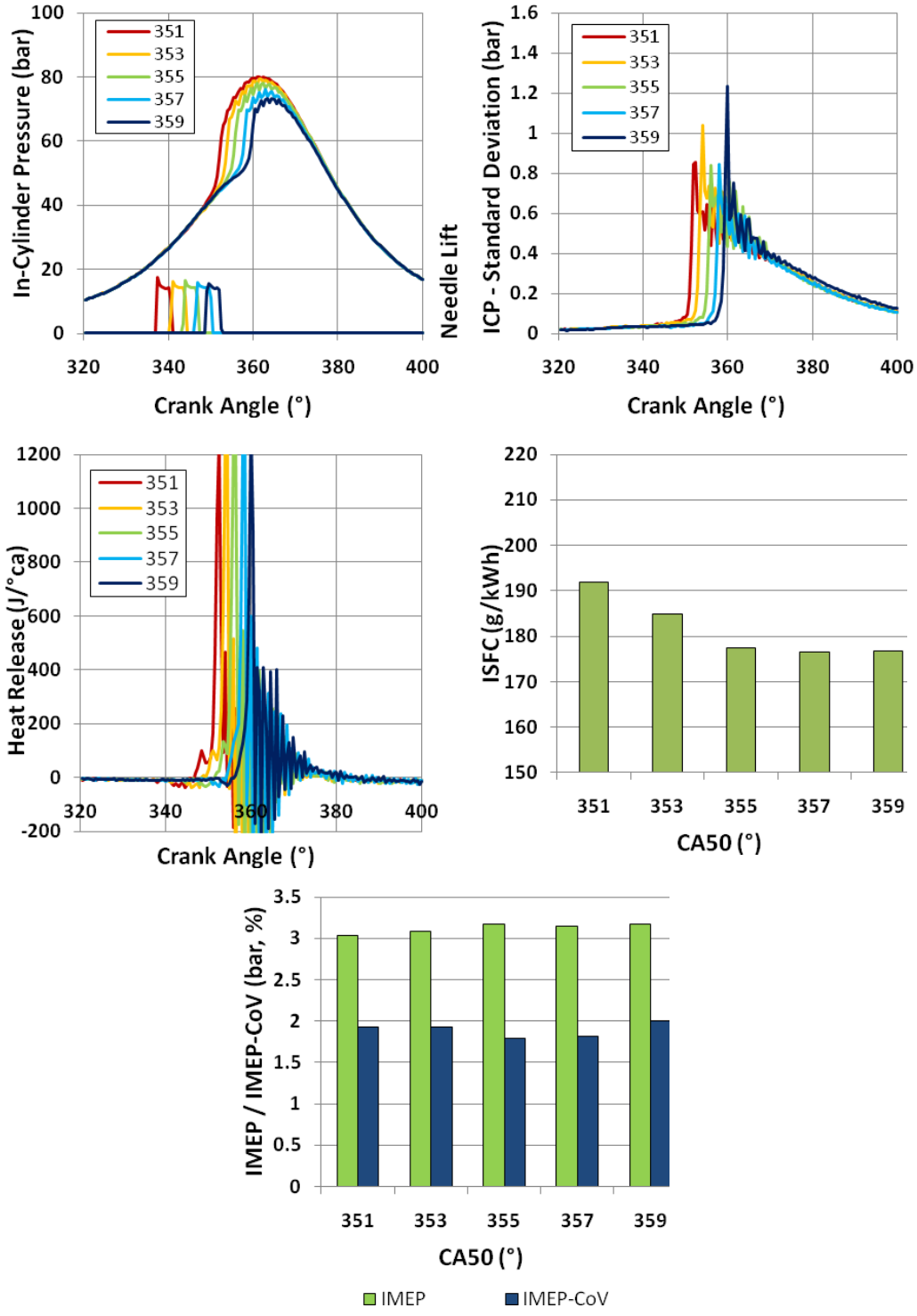

Figure 9-16: G30 LTC Single injection 700 bar

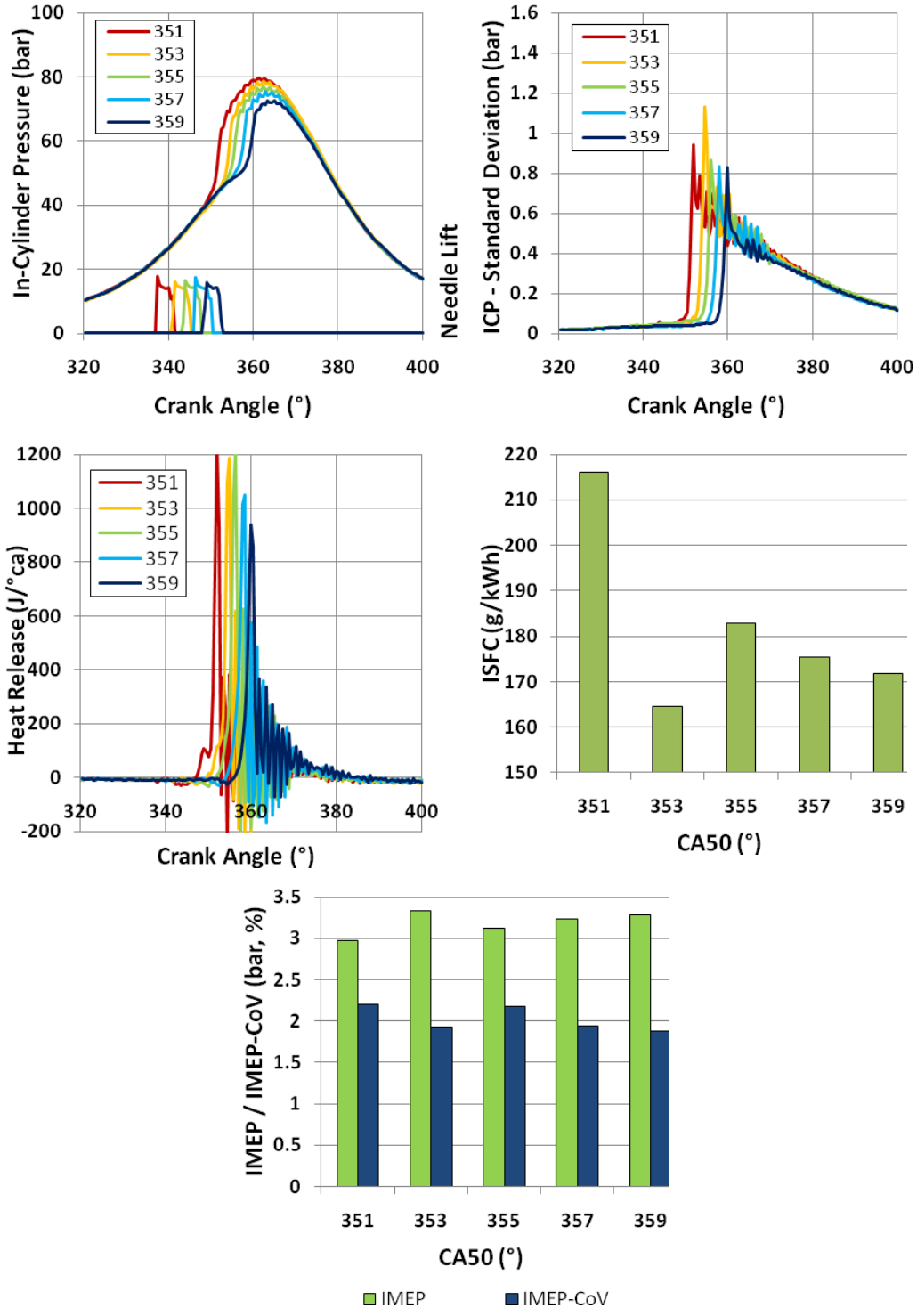

Figure 9-17: G50 LTC Single injection 600 bar

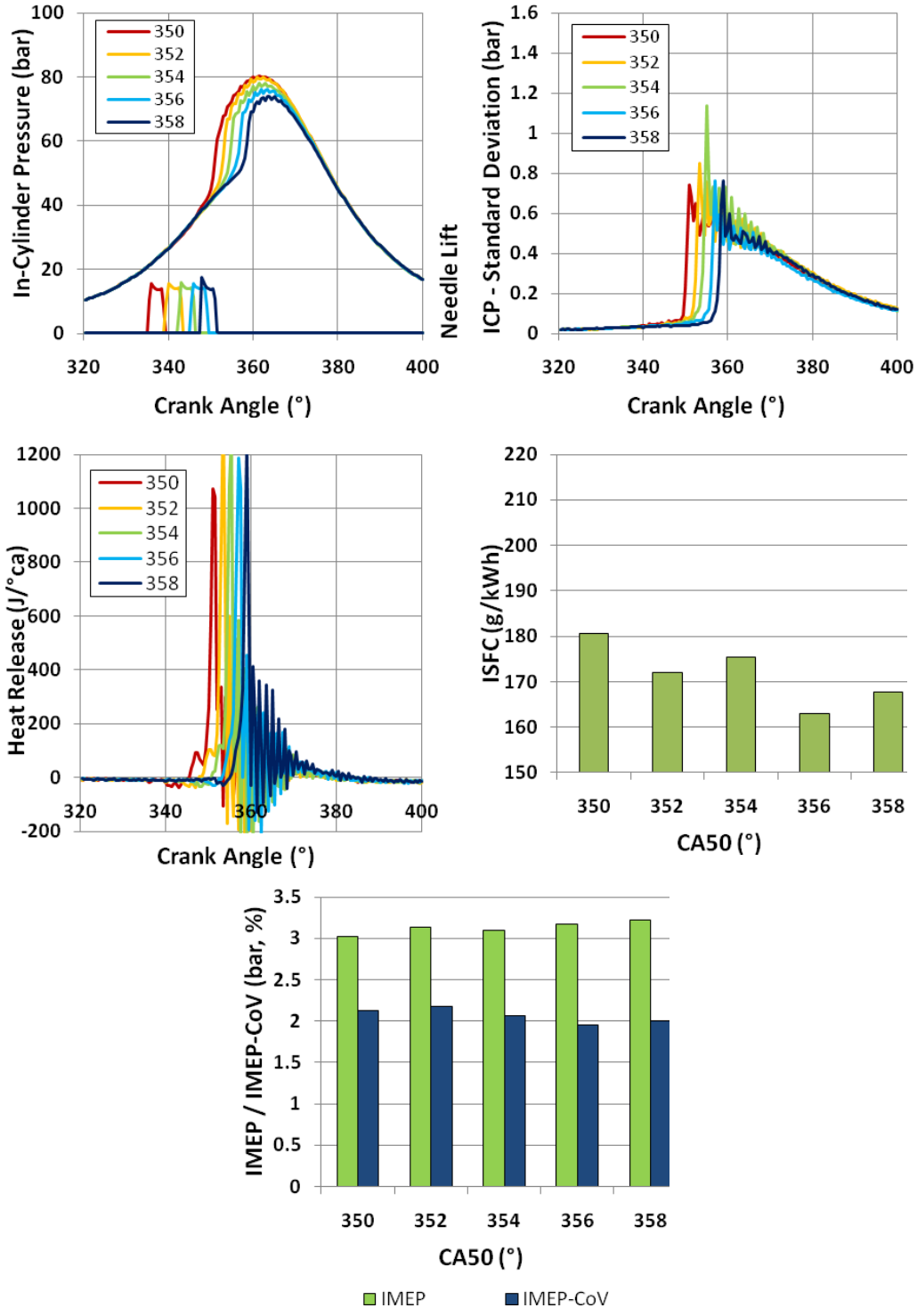

Figure 9-18: G50 LTC Single injection 700 bar

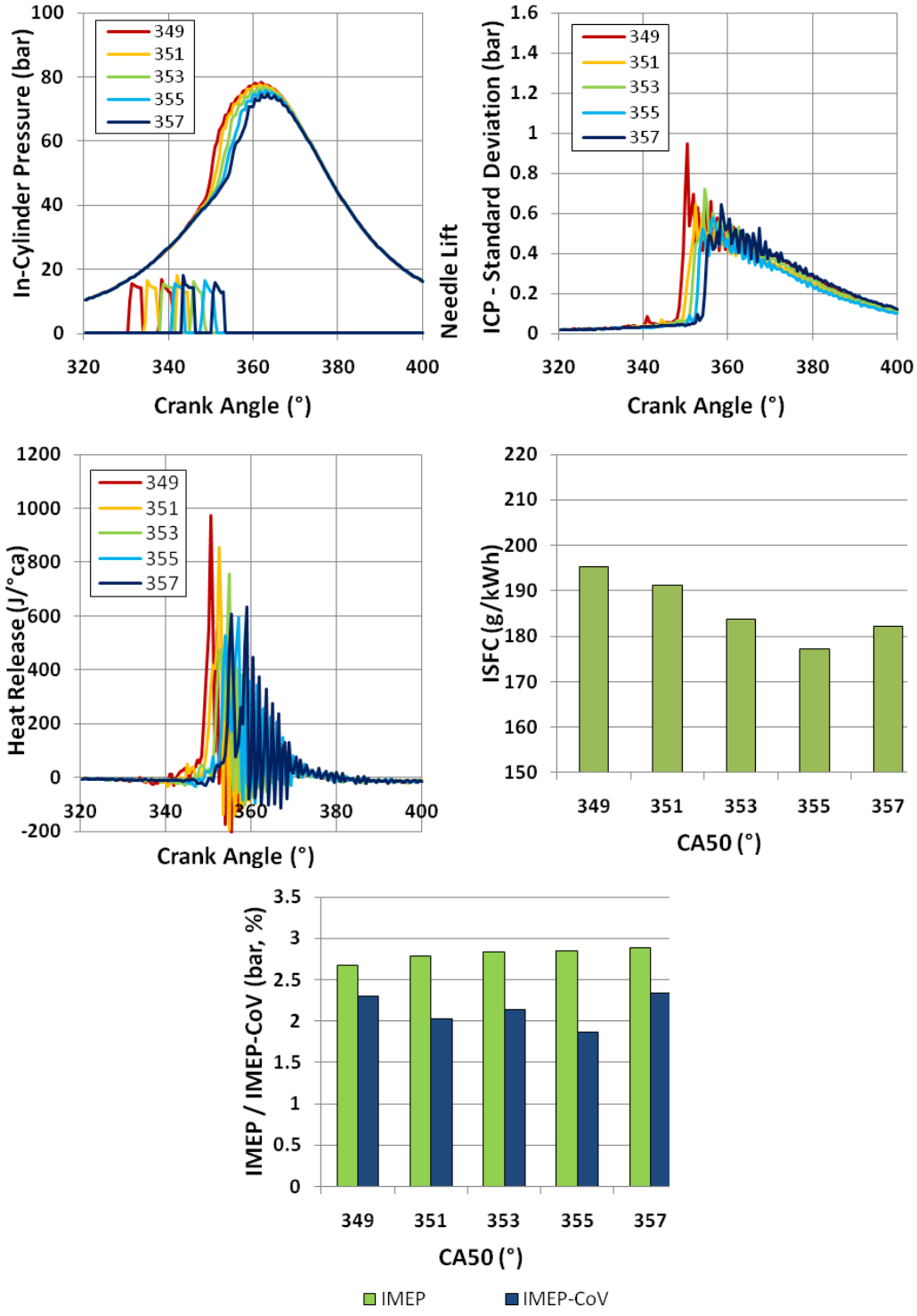

Figure 9-19: G30 LTC 7° Split injection 600 bar

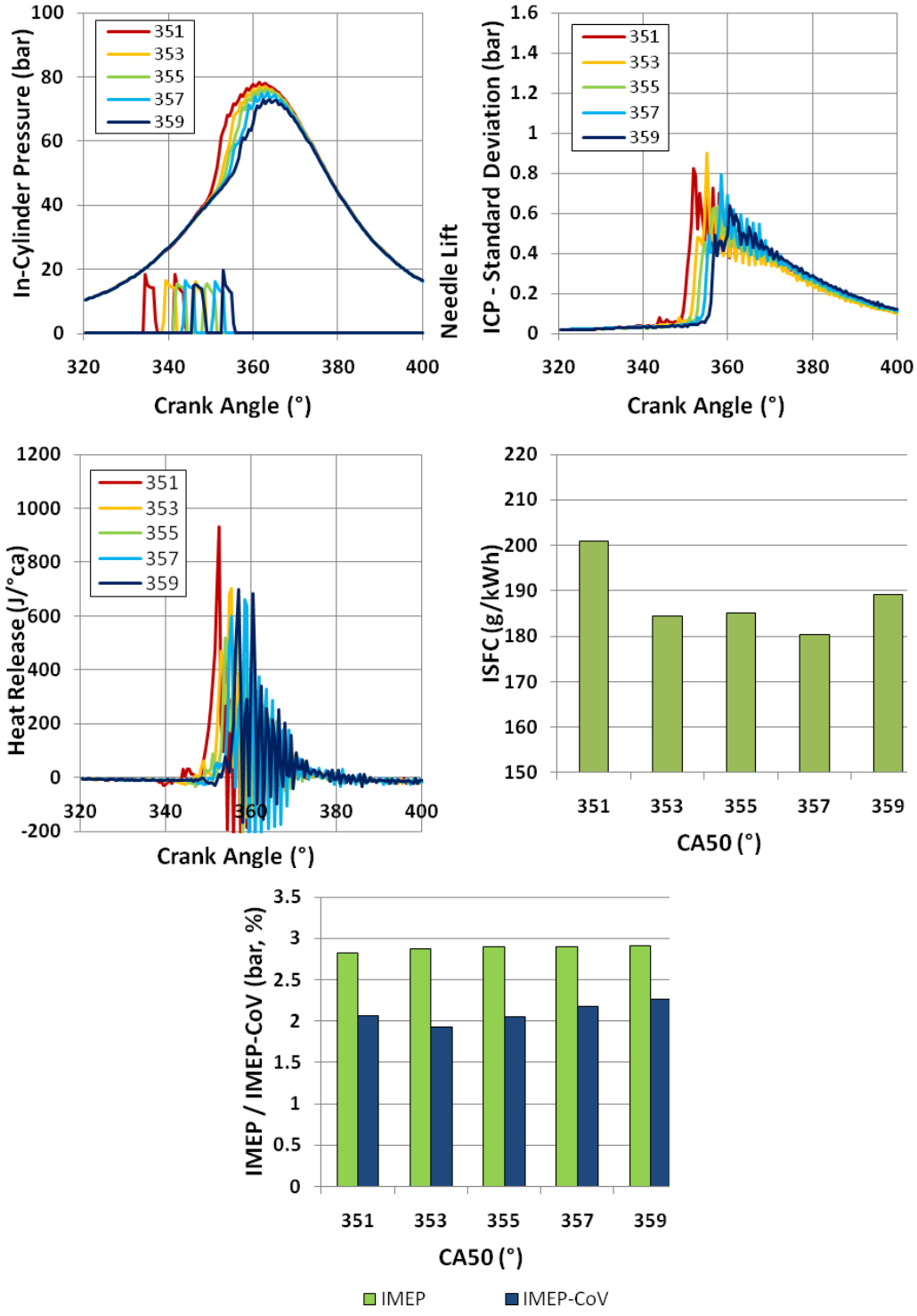

Figure 9-20: G30 LTC 7° Split injection 700 bar

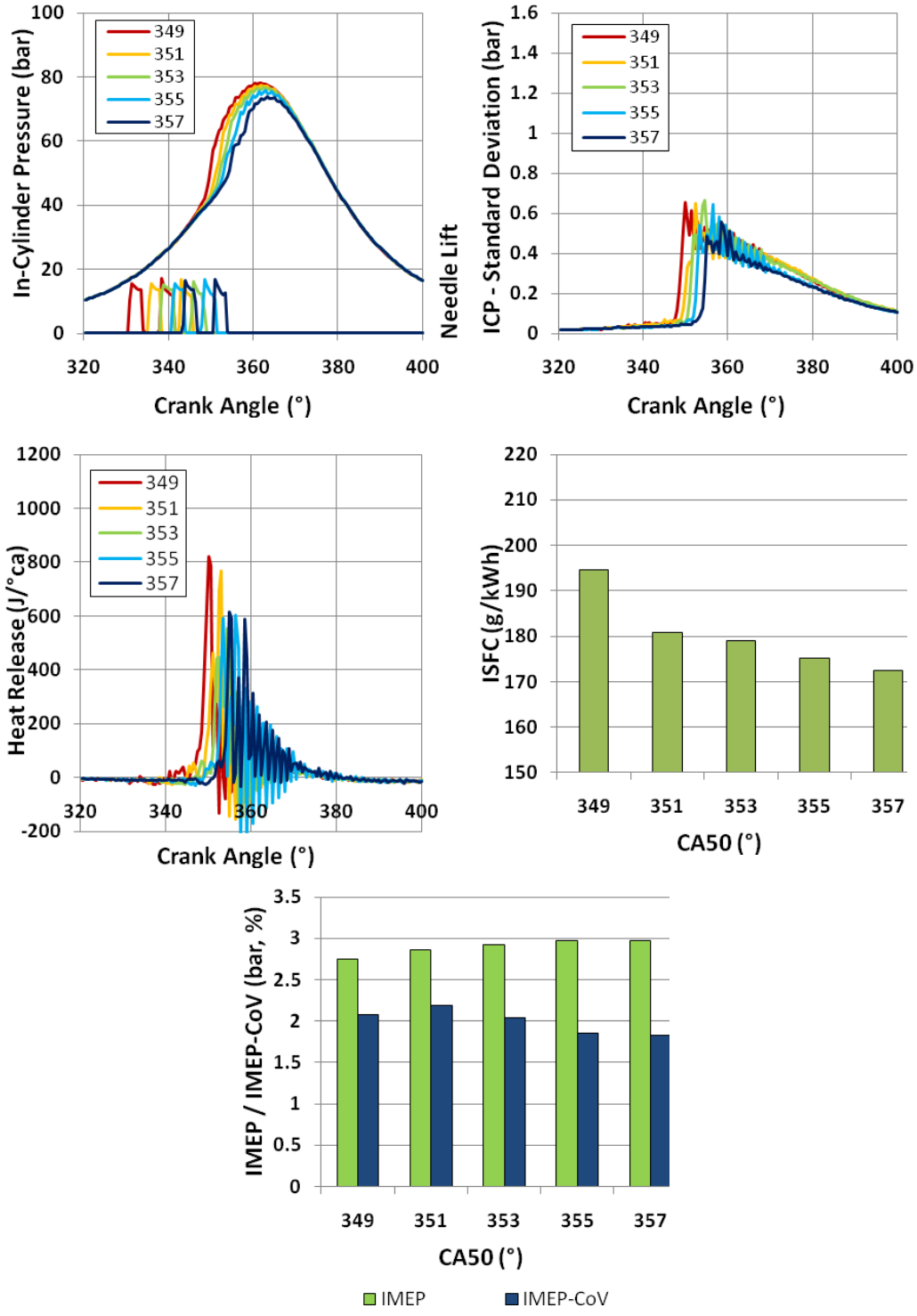

Figure 9-21: G50 LTC 7° Split injection 600 bar

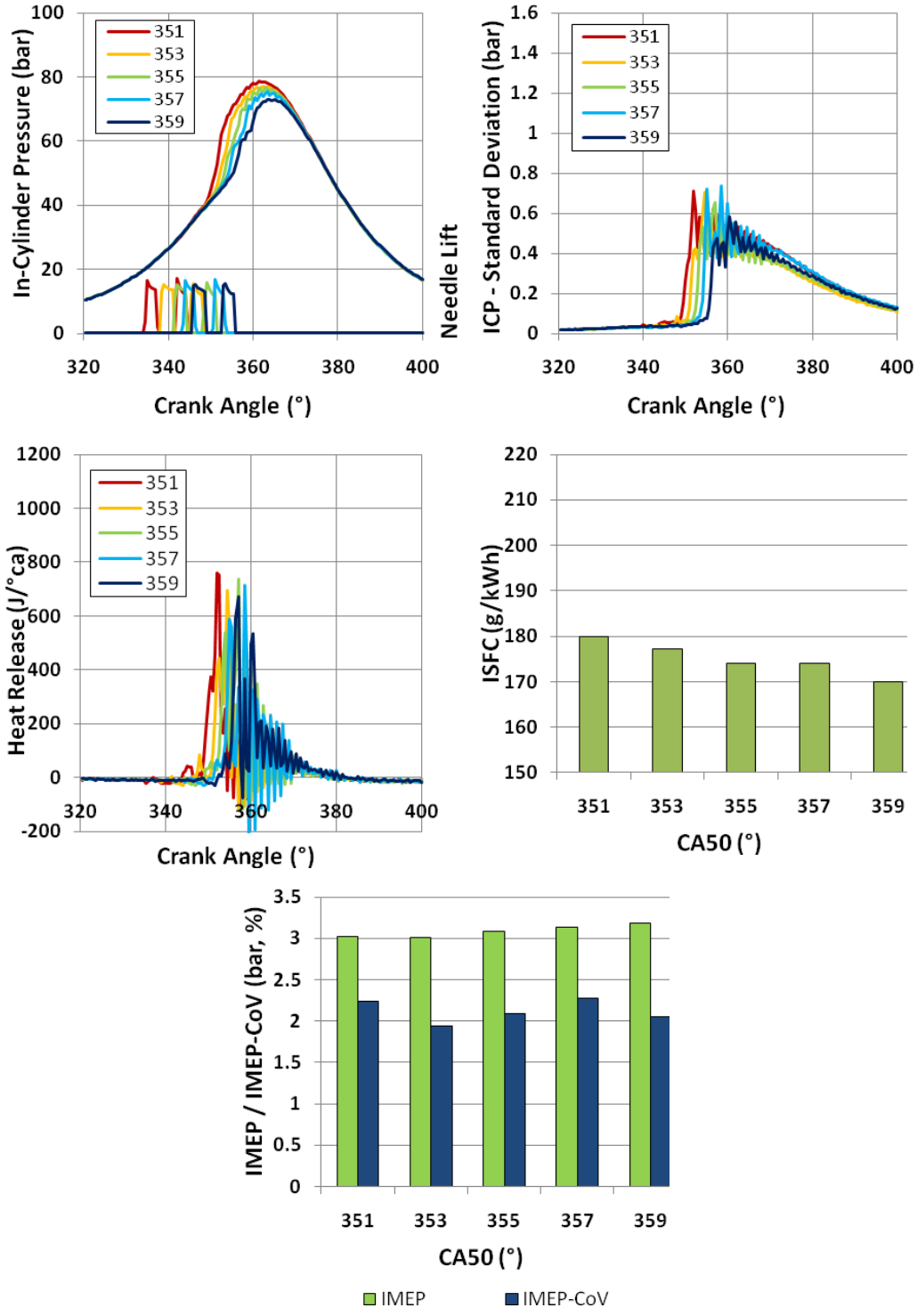

Figure 9-22: G50 LTC 7° Split injection 700 bar

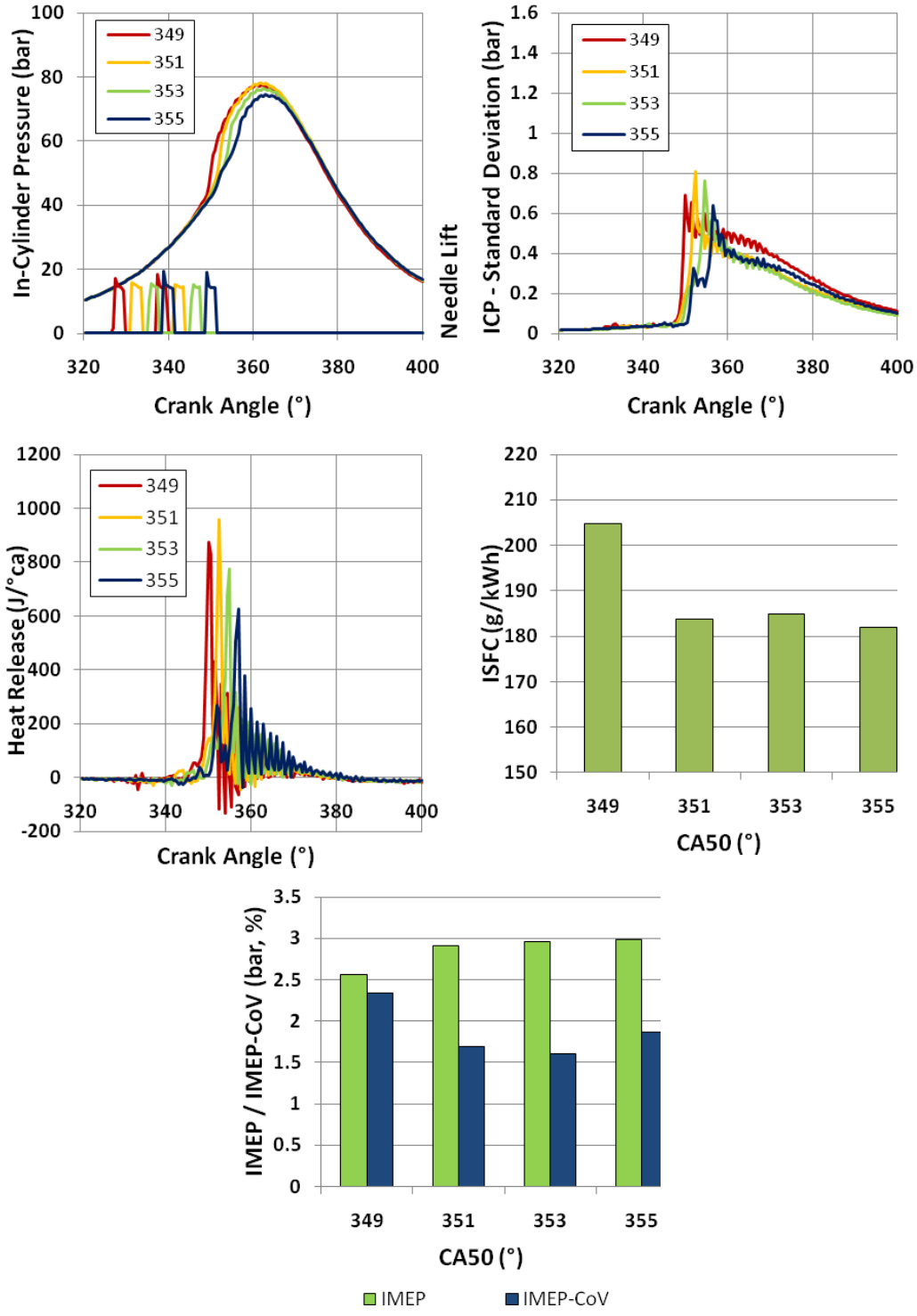

Figure 9-23: G30 LTC 10° Split injection 600 bar

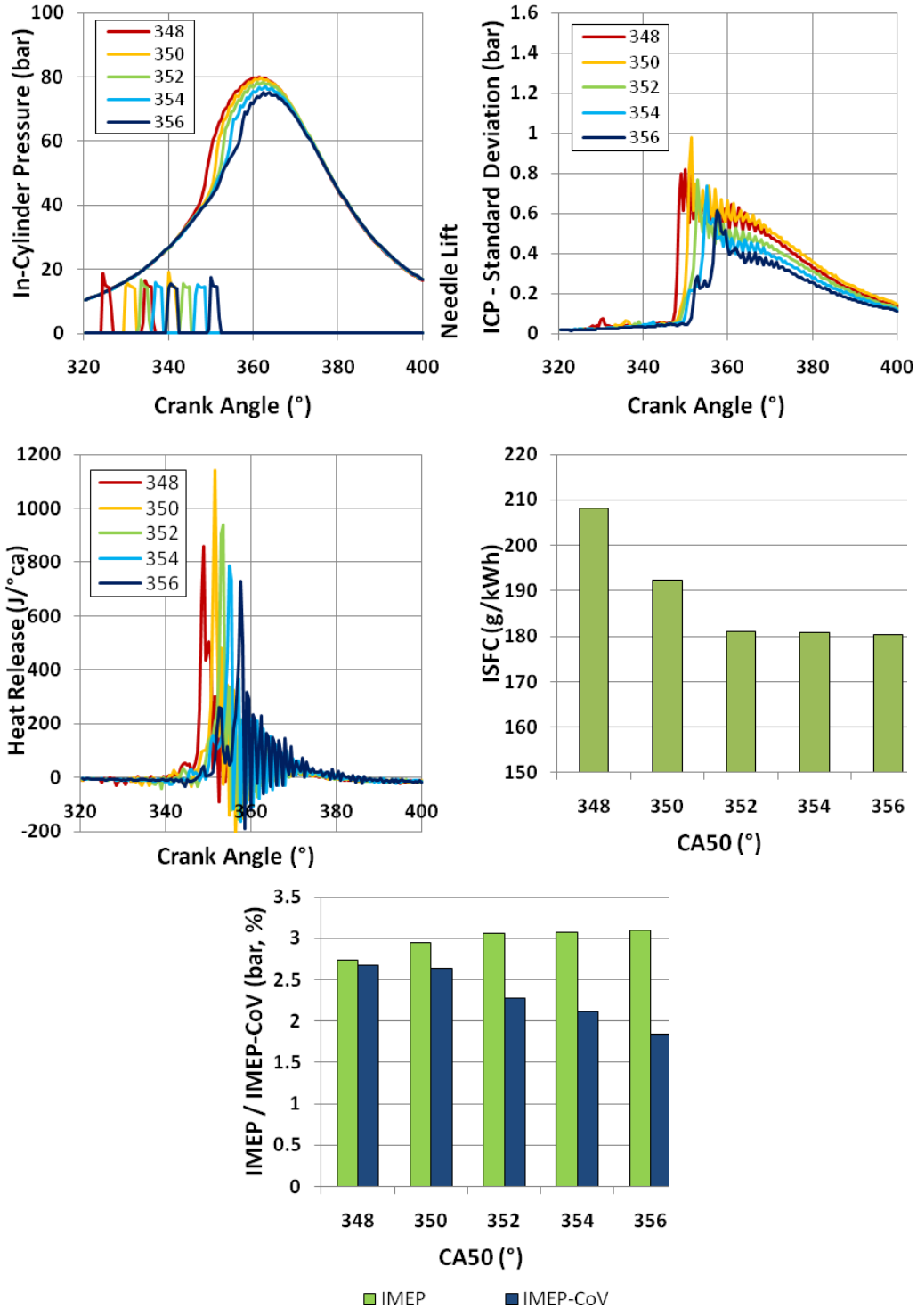

Figure 9-24: G30 LTC 10° Split injection 700 bar

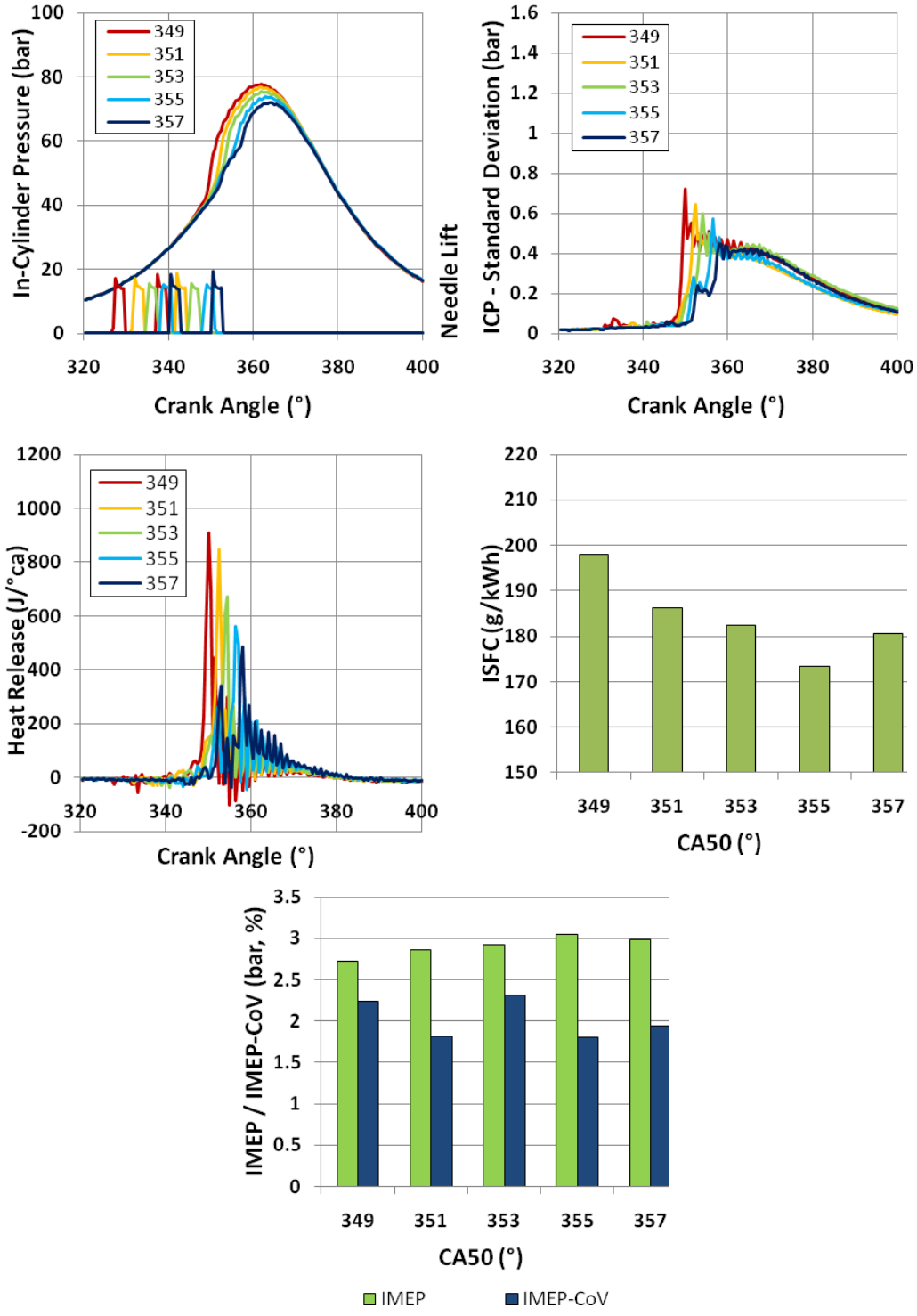

Figure 9-25: G50 LTC 10° Split injection 600 bar

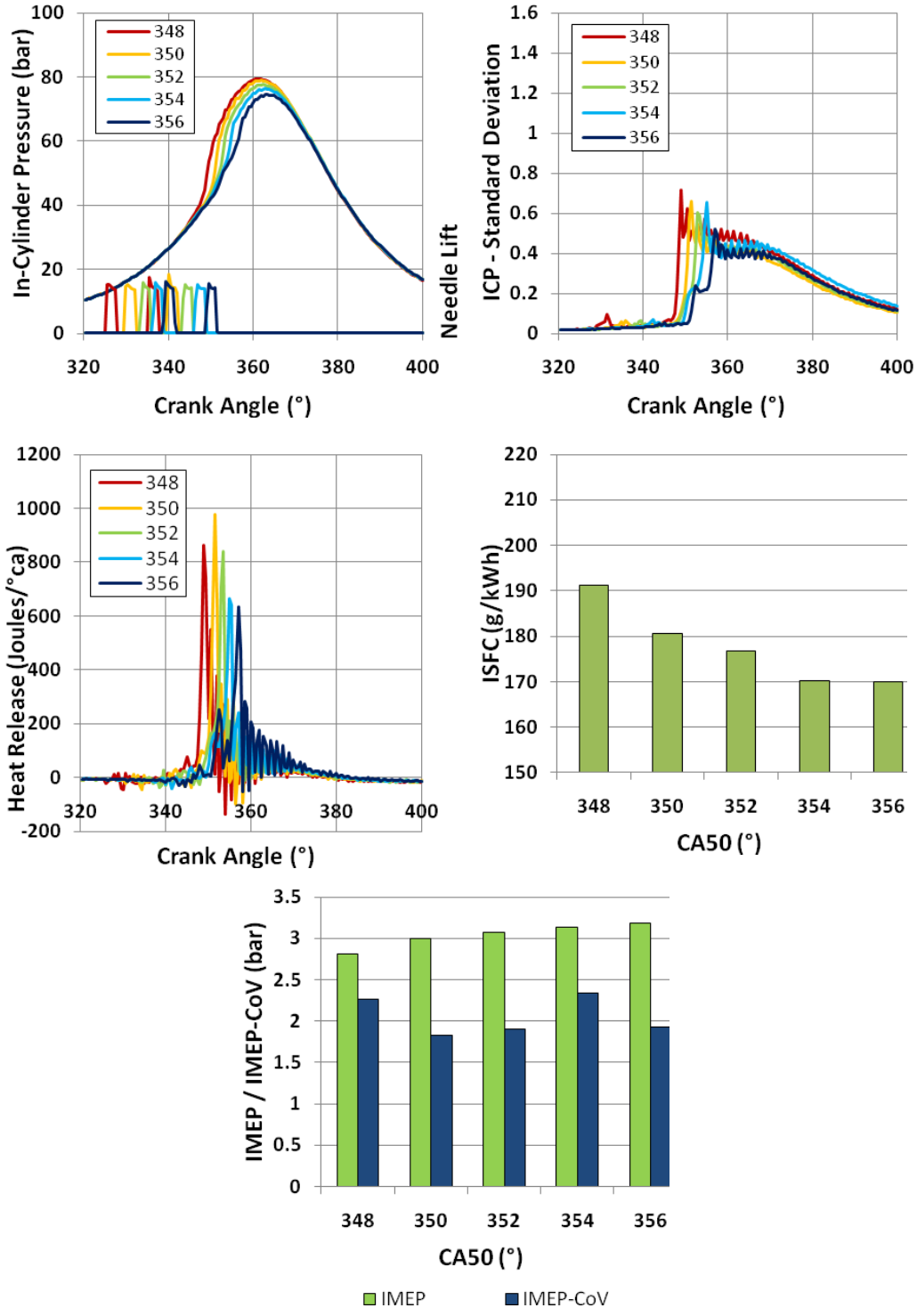

Figure 9-26: G50 LTC 10° Split injection 700 bar

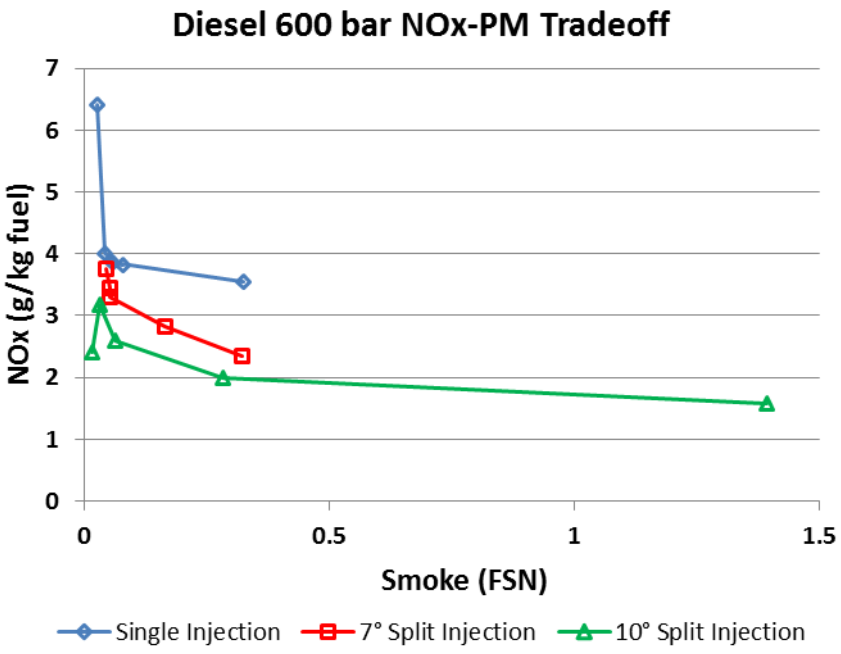
Diesel 600 bar NOx-PM Tradeoff
NOx (g/kg fuel)
Smoke (FSN)
0
1
2
3
4
5
6
7
0
0.5
1
1.5
Single Injection
7° Split Injection
10° Split Injection

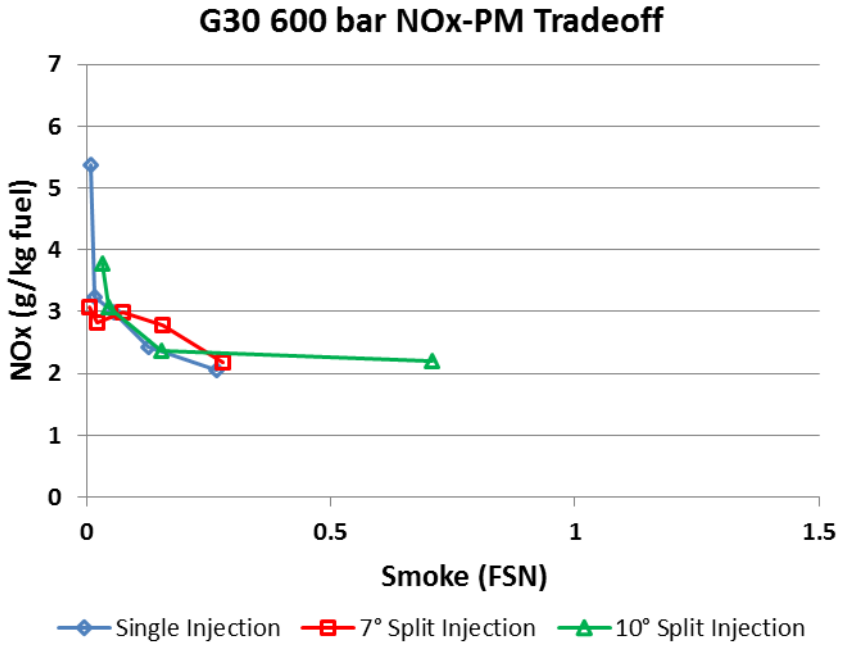
G30 600 bar NOx-PM Tradeoff
NOx (g/kg fuel)
Smoke (FSN)
0
1
2
3
4
5
6
7
0
0.5
1
1.5
Single Injection
7° Split Injection
10° Split Injection

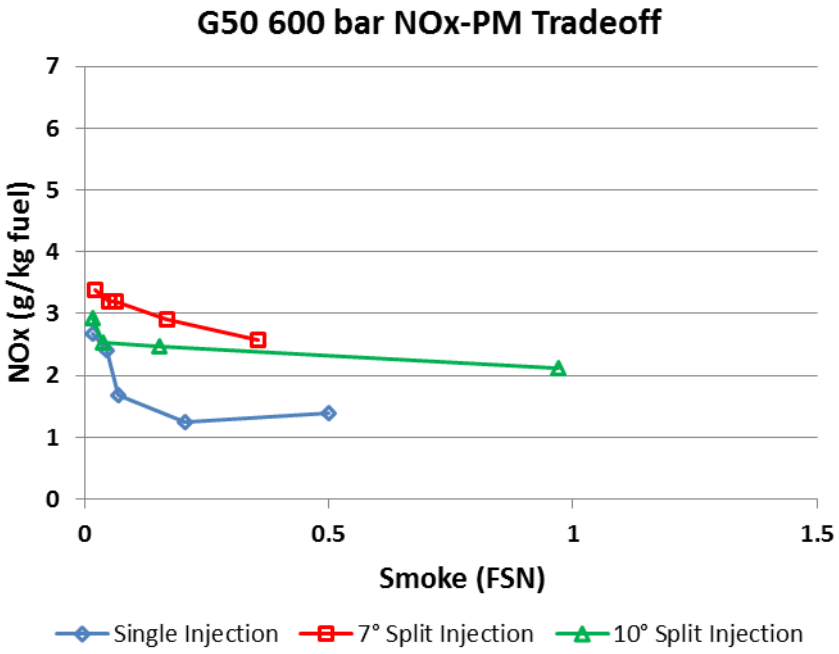

Figure 9-27: NO_x-PM trade-off for Diesel, G30 & G50 in LTC

10 References

Akihama K, Takatori Y, Inagaki K, Sasaki S, Dean A. M., 2001, “Mechanism of the Smokeless Rich Diesel Combustion by Reducing Temperature”, SAE 2001-01-0655, 2001

Aligrot C., Champoussin J-C., et al. A Correlative Model to Predict Autoignition Delay of Diesel Fuels. SAE 970638, 1997

Alrikson M., Denbratt I. G., “Low Temperature Combustion in a Heavy Duty Diesel Engine Using High Levels of EGR” SAE 2006-01-0075, 2006

Ando, H., Takemura, J., and Koujina, E., “A Knock Anticipating Strategy Basing on the Real-Time Combustion Mode Analysis,” SAE 890882, 1989

Assanis, D. N., Filipi, Z. S., Fiveland, S. B., and Syrimis, M., “A PredictiveIgnition Delay Correlation Under Steady-State and Transient Operation of a Direct Injection Diesel Engine,” ASME J. Eng. Gas Turbines Power, Vol. 125, 2003

AVL “Current and Future Exhaust Emissions Legislation”, AVL List GmbH, 2007

Azetsu A., Sato Y., Wakisaka Y., “Effects if Aromatic Components in Fuel on Flame Temperature and Soot Formation in Intermittent Spray Combustion” SAE 2003-01-1913, 2003

Badami M., Nuccio P., Trucco G., “Influence of Injection Pressure on the Performance of a DI Diesel Engine with a Common Rail Fuel Injection System”, SAE 1999-01-0193, 1999

Badami M., Mallamo F., Millo F., Rossi E., “Experimental Investigation on the Effect of Multiple Injection Strategies on Emissions, Noise and Brake Specific Fuel Consumption of an Automotive Direct Injection Common-Rail Diesel Engine”, International Journal of Engine Research 4(4): 299-314, 2003

Barton, R. K., Lestz, S. S., and Duke, L. C., 1970, “Knock Intensity as a Function of Engine Rate of Pressure Change,” SAE 700061

Bobba M. K., Genzale C. L., Musculuse P. B., “Effect of Ignition Delay on In-Cylinder Soot Characteristics of a Heavy Duty Diesel Engine Operating at Low Temperature Conditions”, SAE 2009-01-0946, 2009

Boger T., Tilgner I. C., Shen M., Jiang Y., “Oxide Based Particulate Filters for Light-Duty Diesel Applications – Impact of the Filter Length on the Regeneration and Pressure Drop Behavior”, SAE 2008-01-0485, 2008

Bosch Automotive Handbook, 8th Edition, SAE International, ISBN 978-0-7680-4851-3

Borthwick R. P., Farrell P. V., “Fuel Injection Spray and Combustion Chamber Wall Impingement in Large Bore Diesel Engines”, SAE 2002-01-0496, 2002

Checkel, M. D., and Dale, J. D., “Computerized Knock Detection from Engine Pressure Record,” SAE 860028, 1986

Chen S. K., 2000, “Simultaneous Reduction of NOx and Particulate Emissions by Using Multiple Injections in a Small Diesel Engine”, SAE 2000-01-3084, 2000

Christensen M., Johansson B., B. “Influence of Mixture Quality on Homogeneous Charge Compression-ignition”, SAE 982454, 1998

Christensen M., Johansson B., Ameneus P., Maus F., “Supercharged Homogeneous Charge Compression-ignition” SAE 980787, 1998

Cong S., McTaggart-Cowan G.P., Garner C.P., "Measurement of residual gas fraction in a single cylinder HSDI diesel engine through skip-firing", SAE 2009-01-1961, 2009

Cong S., “An Experimental Study of Low Temperature Combustion in a Diesel Engine”, PhD Thesis, Loughborough University, Loughborough, UK, 2009.

Cong S., McTaggart-Cowan G. P., Garner C. P., “Effects of Fuel Injection Parameters on Low Temperature Diesel Combustion Stability”, SAE 2010-01-0611, 2010

Costa M., Siano D., Allocca L., Montanaro A., F.Bozza, “Light Duty Diesel Engine: Optimization of Performances, Noxious Emission and Radiated Noise”, SAE 2009-2032-0105, 2009

Dec J. E., "A Conceptual Model of DI Diesel Combustion Based on Laser-Sheet Imaging", SAE 970873, 1997

Dec J. E., “Advanced Compression-Ignition Engines – Understanding the In-Cylinder Process”, Proc. Combust. Inst. (2009), doi:10.1016/jproci.2008.08.08

Dec J. E., Sjöberg M., “A Parametric Study of HCCI Combustion - the Sources of Emissions at Low Loads and the Effects of GDI Fuel Injection”, SAE 2003-01-0752, 2003

Dec J. E., Hwang W., Sjöberg M., “An Investigation of Thermal Stratification in HCCI Engines Using Chemiluminescence Imaging”, SAE 2006-01-1518, 2006

Delphi, “Worldwide emissions standards, Passenger cars & Light Duty Vehicles”, Delhi Corp., 2010-2011.

Deng J., Li C., Hu Z., et al., “Spray Characteristics of Biodiesel and Diesel fuels Under High Injection Pressure with a Common Rail System”, SAE 2010-01-2268, 2010

Direction production et energies durables (DEPD) “Life Cycle Assessments Applied to First Generation Biofuels used in France”, 2010

Dronniou N., Lejeune M., Balloul I., and Higelin P., “Combination of High EGR Rates and Multiple Injection Strategies to Reduce Pollutant Emissions,” SAE 2005-01-3726, 2005

Ekoto I. W., Colban W. F., Miles P. C., Park S. W., et al., “UHC and CO Emissions Sources from a Light-Duty Diesel Engine Undergoing Dilution-Controlled Low-Temperature Combustion” SAE International Journal of Engines 2, pp411-430, 2009

Eng J. A., “Characterization of Pressure Waves in HCCI combustion”, SAE 2002-01-2859, 2002

EU, *REGULATION (EC) No 715/2007 OF THE EUROPEAN PARLIAMENT AND OF THE COUNCIL, 2007*

Fang T., Lee C., Coverdill R., White R., “Effects of Injection Pressure on Low-sooting Combustion in an Optical HSDI Diesel Engine Using a Narrow Angle Injector”, SAE 2010-01-0339, 2010

Fenimore C. P., "Studies of Fuel-Nitrogen Species in Rich Flame Gases", 17th Symposium (Intl.) on Combustion, The Combustion Institute, USA, Pittsburgh, PA, 1979, pp. 661-670

Fenimore C. P., "Formation of Nitric Oxide in Premixed Hydrocarbon Flames", 13th Symposium (Intl.) on Combustion, The Combustion Institute, USA, Pittsburgh, PA, 1970, pp.373-380

Fischer S., Stein J. O., “Investigation on the Effect of Very High Fuel Injection Pressure on Soot-NOx Emissions at High Load in a Passenger Car Diesel Engine”, SAE 2009-01-1930, 2009

Fukumoto M., Oguma M., Goto S., “Experimental Investigation of Lubricity Improvement of Gas-to-liquid (GTL) Fuels with Additives for Low Sulphur Diesel Fuel”, SAE 2003-01-1948, 2003

Ganser M. A., “Common Rail Injectors for 2000 bar and Beyond”, SAE 2000-01-0706, 2000

Gardner T., Yetkin A., Shotwell R., Kotrba A., et al., “Evaluation of a DPF Regeneration System and DOC Performance Using Secondary Fuel Injection”, SAE 2009-01-2884, 2009

Ge-qun S., Hai-quiao W., Rui H., “The Transfer Function of CombustionNoise in DI-Diesel Engine”, SAE 2005-01-2486, 2005

Han M., Assanis D. N., Bohac S. V., "Sources of Hydrocarbon Emissions from Low-Temperature Premixed Compression-ignition Combustion from a Common Rail Direct Injection Diesel Engine", Combustion Science and Technology 181(3): pp.496-517

Habchi C., Verhoeven D., Hyun Huu C., Lambert L., et al. “Modeling Atomization and Break Up in High-Pressure Diesel Sprays”, SAE 970881, 1997

Hassaneen A. E., “Fuel Economy and Emission Characteristics of Gas-to-Liquid (GTL) and Rapseed Methyl Ester (RME) as alternative fuels for diesel engines”, Fuel, doi:10.1016/j.fuel.2012,01,077, 2012

Heywood J. B., “Internal Combustion Engines Fundamentals”, McGraw-Hill, New York, 1988

Holman J. P., “Experimental Methods for Engineers”, 7th edition, 1998

Horiba Instruction Manual MEXA-7100, 2001

Hsu B. D., "Practical Diesel-Engine Combustion Analysis", Society of Automotive Engineers: Warrendale, 2002

Huhtala K., Vilenius M., “Study of a Common Rail Fuel Injection System”, SAE 2001-01-3184, 2001

Husberg T., Denbratt I., and Karlsson A., “Analysis of Advanced Multiple Injection Strategies in a Heavy-Duty Diesel Engine using Optical Measurements and CFD Simulations,” SAE 2008-01-1328, 2008

IPCC Fourth Assessment Report: Climate Change 2007 Vol. 2010, 2007

Ishida M., Chen Z. L., Luo G. F., Ueki H., “The Effect of Pilot Injection on Combustion in a Turbocharged D. I. Diesel Engine”, SAE 941692, 1994

Johnson T. V., “Diesel Emissions in Review”, SAE 2011-01-0304, 2011

Jung D. W., Jeong J. H., Lim O.T., “Influence of Pilot Injection on Combustion Characteristics and Emissions in a DI Diesel Engine Fuelled with Diesel and DME”, SAE, 2011-01-1958, 2011

Juttu S., Thispe S. S., Marathe N. V., Babu M. K. G., “Homogeneous Charge Compression-ignition (HCCI): A New Concept for Near Zero NOx and Particulate Matter (PM) from Diesel Engine Combustion”, SAE 2007-26-020, 2007

Kanda H., Okubo M., Yonezawa T., “Analysis of Noise Sources and Their Transfer Paths in Diesel Engines”, SAE 900014, 1990

Katrašnik T., Trenc F., Rodman Oprešnik S., “A new Criterion to Determine the Start of Combustion in Diesel Engines”, Journal of Engineering for Gas Turbines and Power, Oct Vol. 128., 2006

Kitamura Y., Mohammad A., Ishiyama T., Shioji M., "Fundamental Investigation of NOx Formation in Diesel Combustion under Supercharged and EGR Conditions, SAE 2005-01-0364, 2005

Kitano K., Sakata I., Clark R., “Effects of GTL Fuel Properties on DI Diesel Combustion”, SAE 2005-01-3763, 2005

Kobori, S., Kamimoto, T., and Aradi, A. A., “A Study of Ignition Delay of Diesel Fuel Sprays,” International Journal of Engine Research, 2000

Koci C.P., Ra Y., Krieger R., Andrie M., Foster D.E., Siewert R.M*., et al. “*Detailed Unburned Hydrocarbon Investigations in a Highly-Dilute Diesel Low Temperature Combustion Regime” SAE 2009-01-0928, 2009

Kuo K. K., *Principles of Combustion*. Second edn. John Wiley & Sons: New Jersey, 2005 Lee S, Shin D, Lee J, Sung N (2004). Soot Emission from a Direct Injection Diesel Engine. SAE Paper: 2004-01-0927

Ladommatos N., Abdelhalim S., Zhao H., "The Effects of Exhaust Gas Recirculation on Diesel Combustion and Emissions", International Journal of Engine Research, vol.1, no.1, pp.107-126, 2000

Lee S., Shin D., Lee J., Sung N., "Soot Emission from a Direct Injection Diesel Engine", SAE 2004-01-0927, 2004

Li Y., Tian G., Xu H., "Comparative Experimental Study on Microscopic SprayCharacteristics of RME, GTL and Diesel", SAE 2010-01-2284, 2010

Mendez S., Kashdan J. T., Bruneaux G., Thirouard B., Vangraefshepe F., "Formation of Unburned Hydrocarbons in Low Temperature Diesel Combustion", SAE Internal Journal of Engines 2(2) pp.205-225

Mendez S., Thirouard B., "Using Multiple Injection Strategies in Diesel Combustion: Potential to Improve Emissions, Noise and Fuel Economy Trade-Off in Low CR Engines", SAE 2008-01-1329, 2008

Merkel S., Eckert P., Wagner U., Velji A., Spicher U., "Investigation of a New injection Strategy for Simultaneous Soot and NOx Reduction in a Diesel Engine with Direct Injection", SAE 2009-01-1790, 2008

Michael, S., Shigahara, K., Assanis, D. N., "Correlation Between Knock Intensity and Heat Transfer Under Light and Heavy Knocking Conditions in a Spark Ignition Engine," SAE 960495, 1996

Miller J. A., "Bowman C. T., "Mechanism and Modelling of Nitrogen Chemistry in Combustion", Prog. in Energy and Comb. Sci., 15, 287-338, 1989

Minami T., Takeouchi K., Shimazaki N., "Reduction of Diesel Engine NOx using Pilot Injection" SAE 950611, 1995

Mitsuharu, O., Shinichi, G., Kazuya, O, Kouseki, S., Makihiko, M., "The Possibility of Gas to Liquid (GTL_ as a Fuel of Direct Injection Diesel Engine", SAE 2002-01-1706, 2002

Mitsuharu, O., Shinichi, G., 2004, “Fuel Characteristics Evaluation of GTL for DI Diesel engine”, SAE 2004-01-0088, 2004

Mizuno K., Usui S., et al. “Fuel Rail with Integrated Damping Effect”, SAE 2002-01-0853, 2002

Mizuno K., Imura I., Tsuchiya H., “A development of a fuelrail, for an electronic fuel injection type gasoline engine, which reduces fuel-pressure- pulsation in a rail”, SAE 2001-08-0069, 2001

Montgomery D. T., Reitz R. D., “Effects of Multiple Injections and Flexible Control of Boost and EGR on Emissions and Fuel Consumption of a Heavy-Duty Diesel Engine”, SAE 2001-01-0195, 2001

Moon G., Lee Y., Choi K., Jeong D., “Emission Characteristics of Diesel, GTL and biodiesel-blended fuels in a diesel engine for passenger cars”, Fuel 89 (2010) 3840-3846, 2010

Muench J., Leppelt R., Dotzel R., “Extruded Zeolite Based Honeycomb Catalyst for NOx Removal from Diesel Exhaust”, SAE 2008-01-1024, 2008

Musculus M. P. B., Thierry L, Pickett L. M., Idicheria C. A., “End-of-Injection Over-Mixing and Unbudned Hydrocarbon Emissions in Low-Temperature-Combustion Diesel engines”, SAE 2007-01-0907, 2007

Neely G. D., Sasaki S., Huang Y., Leet J.A., Stewart D.W., “New Diesel Emission Control Strategy to Meet US Tier 2 Emissions Regulations” SAE 2005-01-1091, 2005

Nehmer D. A., Reitz R. D., “Measurement of the Effect of Injection Rate and Split Injections on Diesel Engine Soot and NOx Emissions”, SAE 940668, 1994

Nishina T., “Introduction and Future Prospects of Substitute Fuels for Vehicles”, JSAE Vol.53 No.5, 1999

Nishida M., Nakahira T., Komori M. et al. “Observation of High Pressure Fuel Spray with Laser Light Sheet Method”, SAE 1992-02-01, 1992

Northrop W., F., Bohac S. V., Assanis D. N., “Premixed Low Temperature Combustion of Biodiesel and Blends in a High Speed Compression-ignition Engine” SAE 2009-01-0133, 2009

Northrop W. F., Assanis D., Bohac S., “Evaluation of Diesel Oxidation Catalyst Conversion of Hydrocarbons and Particulate Matter from Premixed Low Temperature Combustion of Biodiesel”, SAE 2011-01-1186, 2001

Oguma M., Goto M., Konno M., Sugiyama K, Mori M., “Experimental Study of Direct Injection Diesel Engine fuels with two types of Gas to Liquid Fuels”, SAE 2002-01-2691, 2002

Oguma M., Goto M., Kinoshita K., “Performance and Exhaust Characteristics of Diesel Engines fuelled with GTL”, Proceedings of 17th Internal Combustion Engine Symposium, Japan, pp.44-46, 2002

Oguma M., Goto M., Kinoshita K., “Engine Performance and Emission Characteristics of DI Diesel Engines Fueled with GTL”, JSAE Vol.56 No.10 pp.84-89, 2002

Oguma M., Goto S., Oyama K., et al. “The Possibility of Gas-To-Liquid (GTL) as a Fuel of Direct Injection Diesel Engine”, SAE 2002-01-1706, 2002

Payri F., Benajes J., Pastor J.V., Molina S., “Influence of the Post-Injection Pattern on Performance, Soot and NOx Emissions in a HD Diesel Engine,” SAE 2002-01-0502, 2002

Pesant L., Forti L., Jeuland N., “Effect of Fuel Characteristics on the Performances and Emissions of an Early-injection LTC / Diesel Engine”, SAE 2008-01-2408, 2008

Pierpont D. A., Montgomery D. T., Reitz R. D., “Reducing Particulate and NOx Using Multiple Injections and EGR in a D.I. Diesel”, SAE 950217, 1995

Sarangi A. K., “Diesel Low Temperature Combustion: An Experimental Study”, PhD thesis, Loughborough University, Loughborough UK, 2012

Sarangi A.K., McTaggart-Cowan G.P., Garner C.P., “The Effects of Intake Pressure on High EGR Low Temperature Diesel Engine Combustion”, SAE 2010-01-2145, 2010

Schaberg, P., Botha, J., Schnell, M., Hermann, H-O., Pelz, N., Maly, R., 2005, “Emissions Performance of GTL Diesel Fuel with Blends with Optimised Engine Calibrations”, SAE 2005-01-2187, 2005

Schwab S. D., Bennett J. J., Dell S. J., et al. “Internal Injector Deposits in High-Pressure Common Rail Diesel Engines”, SAE 2010-01-2242, 2010

Shayler P. J., Brooks T. D., Pugh G. J., Gambrill R., “The Influence of Pilot and Split-Main Injection Parameters on Diesel Emissions and Fuel Consumption” SAE 2005-01-0375, 2005

Sjöberg M., Dec J. E., “Influence of Fuel Autoignition Reactivity on the High Load Limits of HCCI Engines”, SAE 2008-01-0054, 2008

Skiba S., Melbert J., “Dosing Performance of Piezo Injectors and Sensorless Closed-Loop Controlled Solenoid Injectors for Gasoline Direct Injection”, SAE 2012-01-0932, 2012

Smith J., Szekely G., Solomon A., parrish S., “A Comparisson of Spray-Guided Stratified Charge Combustion Performance With Outwardly-Opening Piezo and Multi-Hole Solenoid Injectors”, SAE 2011-01-1217, 2011

Southward B. W. L., Basso S., Pfeifer M., “On the Development of Low PGM Content Direct Soot Combustion Catyalysts for Diesel Particulate Filters”, SAE 2010-01-0558, 2010

Stone R., "Introduction to Internal Combustion Engines", third edition, Plagrave, New York, 1999

Terry, B., McCormick, R. L., Natarajan, M., 2006, “Impact of Biodiesel Blends on Fuel System Component Durability”, SAE 2006-01-3279, 2006

Tow T. C., Pierpont D. A., Reitz R. D., “Reducing Particulate and NOx Emissions by Using Multiple Injections in a Heavy Duty D.I. Diesel Engine”, SAE 940897, 1994

Van Basshuysen R., Schäfer F., "Internal Combustion Engine Handbook," SAE International, 2004

Warnatz J., Maas U., Dibble R. W., “Combustion - Physical and Chemical Fundamentals, Modelling and Simulation, Experiments, Pollutant Formation” Second edn. Springer: Berlin, 1999

Yun H., Sellnau M., Milovanovic N., Zuelch S. “Development of Premixed Low-Temperature Diesel Combustion in a HSDI Diesel Engine”, SAE: 2008-01-0639, 2008

Yun H., Sun Y., Reitz R.D., “An Experimental and Numerical Investigation on the Effect of Post Injection Strategies on Combustion and Emissions in the Low-Temperature Diesel Combustion Regime”, ASME Internal Combustion Engine Division 2005 Spring Technical Conference

Zarling D.D., Pipho M. J., Kittelson D. B., “Measurement of Cyclic Variability in a Diesel Engine Using a Single Cycle Sampler”, SAE 930602, 1993

Zel'Dovich Y. B., "The Oxidation of Nitrogen and Combustion Explosives", Acta Physicochim, USSR, 21, 577, 1946

Zhao F., Asmus T. W., Assanis D. N., Dec J. E., Eng J. A., Najit P. M. “Homogeneous Charge Compression-ignition (HCCI) Engines: Key research and Development Issues”, Society of Automotice Engineers, Warrnedale, PA, USA, 2003

Zhong L., Singh I. P., Han J., Lai M-C., Henein N. A., Bryzik W.,2003, “Effect of Cycle-to-Cycle Variation in the Injection Pressure in a Common Rail Diesel Injection System on Engine Performance”, SAE 2003-01-0699, 2003